DOCTORAL THESIS

Out of the Shadows: Reconstructing Mammoth Paleoecology from Underrepresented Regions of the Western Siberian Plain and Estonia, Eastern Europe

Ivan Krivokorin

TALLINNA TEHNIKAÜLIKOOL
TALLINN UNIVERSITY OF TECHNOLOGY
TALLINN 2025

TALLINN UNIVERSITY OF TECHNOLOGY
DOCTORAL THESIS
88/2025

Out of the Shadows: Reconstructing Mammoth Paleoecology from Underrepresented Regions of the Western Siberian Plain and Estonia, Eastern Europe

IVAN KRIVOKORIN

TAL TECH PRESS

TALLINN UNIVERSITY OF TECHNOLOGY
School of Science
Department of Geology
This dissertation was accepted for the defence of the degree PhD in Earth Sciences 03/11/2025

Supervisor: Dr. Leeli Amon
School of Science
Tallinn University of Technology, Tallinn, Estonia

Co-supervisors: Prof. Siim Veski
School of Science
Tallinn University of Technology, Tallinn, Estonia

Dr. Laura Arppe
Finnish Museum of Natural History LUOMUS
University of Helsinki, Helsinki, Finland

Scientific advisor: Prof. Sergey Leshchinskiy
Laboratory of Mesozoic and Cenozoic Continental Ecosystems
Tomsk State University, Tomsk, Russia

Opponents: Dr hab. Piotr Wojtal
Institute of Systematics and Evolution of Animals
Polish Academy of Science, Kraków, Poland

Dr. Lembi Lõugas
Department of Archaeobiology and Ancient Technology
Tallinn University, Tallinn, Estonia

Defence of the thesis: 08/12/2025, Tallinn

Declaration:
Hereby I declare that this doctoral thesis, my original investigation and achievement, submitted for the doctoral degree at Tallinn University of Technology, has not been submitted for a doctoral or equivalent academic degree.

Ivan Krivokorin

---
signature

European Union
European Regional Development Fund

Investing in your future

Copyright: Ivan Krivokorin, 2025
ISSN 2585-6898 (publication)
ISBN 978-9916-80-413-1 (publication)
ISSN 2585-6901 (PDF)
ISBN 978-9916-80-414-8 (PDF)
DOI https://doi.org/10.23658/taltech.88/2025

Krivokorin, I. (2025). *Out of the Shadows: Reconstructing Mammoth Paleoecology from Underrepresented Regions of the Western Siberian Plain and Estonia, Eastern Europe* [TalTech Press]. https://doi.org/10.23658/taltech.88/2025

TALLINNA TEHNIKAÜLIKOOL
DOKTORITÖÖ
88/2025

Varjust välja: mammutite paleokeskkonna rekonstrueerimine Lääne-Siberi tasandikul ja Ida-Euroopas asuvate vähemuuritud piirkondade põhjal

IVAN KRIVOKORIN

TAL TECH
KIRJASTUS

Contents

List of publications

The list of author's publications, on the basis of which the thesis has been prepared:

I Krivokorin, I., Amon, L., Leshchinskiy, S. V., & Arppe, L. (2024). Oxygen isotope studies of the largest West Siberian mammoth sites and implications for last glacial maximum climate reconstruction. Quaternary Science Reviews, 343, 108938. https://doi.org/10.1016/j.quascirev.2024.108938

II Krivokorin, I., Poska, A., Vassiljev, J., Veski, S., & Amon, L. (2025). Environment of European Last Mammoths: Reconstructing the Landcover of the Eastern Baltic Area at the Pleistocene/Holocene Transition. Land, 14(1), 178. https://doi.org/10.3390/land14

III Krivokorin, I., Amon, L., Leshchinskiy, S. V., & Arppe, L. (2025). Mammoths at the margins: new δ13C and δ15N isotope data from the southeast of the Western Siberian plain. Quaternary Science Reviews, 369, 109645. https://doi.org/10.1016/j.quascirev.2025

Author's Contribution to the Publications

Contribution to the papers in this thesis are:

I The author of this Dissertation is the first author in this article. The author was responsible for fieldwork and sample collection. The author contributed to the conceptualisation of the study, the development of the methodology, and the investigation. The author carried out oxygen, carbon and nitrogen isotopic analysis. The author prepared the original draft of the manuscript and contributed to the review and editing of the text. The author was responsible for the visualisation of the results.

II The author of this Dissertation is the first author in this article. The author was responsible for fieldwork and sample collection. The author carried out plant macrofossil analysis, carbon and nitrogen isotopic analysis. The author prepared the original draft of the manuscript and contributed to the review and editing of the text, and contributed to the visualisation of the results.

III The author of this Dissertation is the first author in this article. The author was responsible for fieldwork and sample collection. The author contributed to the conceptualisation of the study, the development of the methodology, and the investigation. The author carried out oxygen, carbon and nitrogen isotopic analysis. The author prepared the original draft of the manuscript and contributed to the review and editing of the text, and was responsible for the visualisation of the results.

Abbreviations

SEWS	Southeast of Western Siberia
SH	Shestakovo
KK	Krasnoyarskaya Kurya
VG	Volchia Griva

Symbols

$\delta^{13}C$	Carbon isotope value
$\delta^{15}N$	Nitrogen isotope value
$\delta^{18}O$	Oxygen isotope value
$\delta^{18}Ow$	Oxygen isotope value of paleowaters

Preservation-related terms and indices

Hydroxyapatite	A naturally occurring mineral form of calcium apatite (Ca10(PO4)6(OH)2) (J. A. Lee-Thorp et al., 1989)
Bioapatite	Contains carbonate ions ($CO3^{2-}$) substituted in the PO43− position or OH− position (J. A. Lee-Thorp et al., 1989)
A-type carbonates	When the hydroxyl group OH^- substitutes the $CO3^{2-}$ group along the c-axis in the crystal structure (Grunenwald et al., 2014)
B-type carbonates	When the hydroxyl group OH^- substitutes for the phosphate group $PO3^{4-}$ along the c-axis in the crystal structure (Grunenwald et al., 2014)
C/P	Shows the ratio of B-type carbonates V3 $CO3^{2-}$ to V3 $PO4^{3-}$. C/P values falling out of the established range (0.08–0.2 for enamel and 0.05–0.3 for dentin) will indicate loss or addition of carbonate and/or phosphate from the bioapatite (France et al., 2020)
IRSF (infrared splitting factor)	Shows pronounced V4 PO^{3-} peaks divided by the intermediary valley. According to France et al. (2020), the IRSF falling out of the established range (3.1–4.0 for enamel; and 3.1–4.0 for dentin) can indicate a sign of recrystallisation in the analysed bioapatite, but based on the results of **Paper I**, we used IRSF as a sign of the loss of the carbonate component from the bioapatite.
ATR-FTIR or FTIR	Attenuated Total Reflectance-Fourier Transform Infrared Spectroscopy. A vibrational spectroscopy method that generates unique spectra for molecules present in biological tissues.

Geochronological context and terms

EH — Early Holocene	11.7–11.3 ka cal BP (Rasmussen et al., 2014)
GS-1—Greenland stadial 1	12.85–11.7 ka cal BP (corresponding to Younger Dryas) (Rasmussen et al., 2014)
GI-1—Greenland interstadial 1	14.6–12.85 ka cal BP (corresponding to Bølling–Allerød Interstadial) (Rasmussen et al., 2014)
The "Voka" stage	38–32 ka cal BP (Molodkov et al., 2007; Molodkov & Bolikhovskaya, 2022)
LGM — Last Glacial Maximum	27,200–23,500 ka cal BP (cal BP) (Hughes & Gibbard, 2015)
Pre-LGM	50–27 ka cal BP (and older)
Post-LGM	23–12 ka cal BP

Introduction

Woolly mammoth (*Mammuthus primigenius*, Blumenbach, 1799) played a key role in a mammoth steppe ecosystem—a distinctive, herbaceous plant-dominated biome, an emblem of the Quaternary period that stretched from Ireland to the Northern Yukon in North America—between approximately 110,000 and 12,000 years ago (R. D. Guthrie, 1968; R. D. Kahlke, 1999; Koch & Barnosky, 2006). Even though the woolly mammoth went extinct a long time ago, it continues to captivate the minds of scientists around the world. Studies of past mass extinctions provide us with crucial insights into the consequences of contemporary species loss. The changes in the diversity and population sizes of large mammals can modify terrestrial ecosystems substantially (Bocherens, 2015; Stivrins et al., 2019). Mammoth research offers a framework to understand the complex relationship between extinct herbivorous megafauna, environmental and ecosystem dynamics. By investigating sub-fossil remains of woolly mammoths, we can establish their ecological niche, determine their role within past ecosystems. Moreover, because the proboscidean remains are linked with humans over a broad temporal and geographical scales, they can tell us of the activities and environmental contexts of ancient humans and provide insights into the behavioural patterns of human populations inhabiting these regions (Metcalfe, 2017; Schwartz-Narbonne et al., 2015).

Numerous glaciation events during the Pleistocene significantly influenced the distribution and migration patterns of biota in the Northern Hemisphere, and the transition into the Holocene was marked by the extinction of several large herbivores, such as the woolly mammoth and woolly rhinoceros (Barnosky et al., 2004; D. R. Guthrie, 2006; Stuart & Lister, 2012). The reasons for these extinctions, whether they are ecological, climatic, environmental, or anthropogenic, are still in debate. There is a strong link between vegetation dynamics and climate, and between vegetation and herbivorous fauna (Koch, 2007). Therefore, it is essential to use methods capable of reconstructing both the environmental conditions and dietary habits. While vegetation change can be inferred through traditional palaeobotanical proxies such as pollen and plant macrofossils preserved in sediments, retrieving information about past mammoth living environments, diets, and mobility patterns from mammoth remains and the surrounding sedimentary context requires different methodologies.

This research focused on reconstructing different aspects of mammoths' ecology, including their living environments, dietary patterns, and the climatic context. Particular attention was given to the temporal and regional context of the studied samples—determining what is currently known and unknown about these regions, establishing the chronological framework of the analysed material, sample quality assessment for isotope studies which included testing the FTIR-IRSF method to assess the preservation of bioapatite and evaluating the fitness of the samples for palaeoenvironmental reconstructions, and assessing the availability of reference data for comparative purposes. Throughout this dissertation, these factors were examined to evaluate their implications for mammoth palaeoecology and the broader understanding of past environmental changes. This study integrates multiple analytical approaches to demonstrate how various proxies can improve our understanding of mammoth environments in Europe and Siberia. The stable isotope analyses are one of the main methods in modern palaeoecological research and the main method used for this dissertation. However, this research project also incorporates more classical palaeoecological approaches and utilises plant macrofossil and pollen analyses to provide a broader interpretative framework.

The primary objective of this PhD research project was to contribute to a comprehensive understanding of mammoth palaeoecology during the Last Glacial Maximum (LGM) in the southeast of Western Siberia (SEWS) and the late Pleistocene in the Baltics (particularly in Estonia), Eastern Europe, by:

(1) Thoroughly assessing the preservation of all mammoth samples from SEWS and the Eastern Baltics to determine whether the mammoth remains have been subject to post-depositional diagenetic alteration in the burial environment, and if they have, identify the cause of such alteration. Additionally, evaluating whether enamel from SEWS mammoths, which were not preserved under permafrost conditions, can provide reliable oxygen isotope data suitable for palaeoenvironmental reconstructions.
(2) Presenting the palaeoclimatic and palaeoecological reconstructions from SEWS by analysing oxygen isotopes from 29 mammoth enamel and tusk samples and horse and deer enamel samples, and reconstructing $\delta^{18}O$ of water ($\delta^{18}Ow$) values for 28–22 ka cal BP.
(3) Reporting the carbon and nitrogen isotopic composition of woolly mammoth (*Mammuthus primigenius*) remains from Shestakovo, Krasnoyarskaya Kurya, and Volchia Griva for 28–22 ka cal BP by analysing 29 mammoth dentine samples, alongside dentine from one horse and one deer.
(4) Compiling a comprehensive dataset consisting of all available pollen and plant macrofossil records and mammoth finds from the Eastern Baltics and a new pollen and plant macrofossil record from Lake Kaatsjärv in central Estonia and comparing the landcover changes during the 14.3–11.3 ka cal BP period with the landcover changes during the pre-LGM period (50–27 ka cal BP) to assess whether environmental changes were indeed the reason for the decline of mammoths in the Eastern Baltics during the late Pleistocene.
(5) Overall, contributing to a better, more comprehensive understanding of the late Pleistocene palaeoecology in Eurasia.

Scope of the study

The thesis presented here is built upon three individual papers developed during this PhD project. The primary objective of this synthesis is to provide an overview of all the work that has been done over the past four years and summarise the findings from the individual publications, rather than to present a step-by-step account of every result obtained. Regarding the use of pronouns: "I" is used when referring to work done solely by the author of this synthesis, whereas "we" is used to indicate collaborative effort undertaken with co-authors of the three published papers discussed herein.

Papers I and **III** are based on the same sample set of mammoth remains from three geographical sites in the southeast of the Western Siberian Plain: Shestakovo, Krasnoyarskaya Kurya and Volchia Griva (Figure 1), and focus on different aspects of their palaeoenvironment. **Paper I** uses oxygen isotope analysis to examine regional climatic changes during the Last Glacial Maximum, while **Paper III** uses carbon and nitrogen isotope analyses to reconstruct the dietary patterns and local environmental conditions.

Paper II shifts the focus to the last mammoths in Eastern Europe, investigating the environmental factors that may have contributed to their extinction. This study primarily uses plant macrofossils and pollen analyses as main proxies to reconstruct past vegetation dynamics, providing insights into the habitat changes that likely influenced mammoth populations in the region. However, we integrate carbon and nitrogen isotopic analysis to complement the results achieved using pollen and plant macrofossil results.

Figure 1. Map showing the general location of the investigated sites, along with other locations of mammoth sites discussed in the text. The dotted line shows the 127 E meridian. Basemap: Biomes and Ecoregions, 2017 Esri, Maxar, Earthstar Geographics, and the GIS User Community.

1 Scientific background

1.1 Pleistocene megafauna and climate in the Northern Hemisphere

The Northern Hemisphere during the Pleistocene epoch was characterised by a unique and extensive ecosystem known as the Mammoth Steppe with *Mammuthus–Coelodonta* faunal complex (Kahlke, 1994) supporting a diverse megafauna and consisting of mammoths (*Mammuthus primigenius*), woolly rhinoceros (*Coelodonta antiquitatis*), musk ox (*Ovibos moschatus*) and reindeer (*Rangifer tarandus*), saiga (*Saiga borealis*), and bison (*Bison bonasus*) (Guthrie, 1968, 1982; Kahlke, 1999; Stuart, 2005; Drucker, 2022). Mammoth steppe was a non-analogue productive ecosystem, cold and dry (R. D. Guthrie, 1982; Yurtsev, 2001), having high insolation and low humidity (Guthrie, 2001). Fast turnover of nutrients and carbon in the upper soil levels, as well as high light exposure, supported a productive vegetation and, by extension, a large grazing community (Reinecke et al., 2021). The Pleistocene epoch was characterised by a general trend of global cooling and increasing aridification across Eurasia (Kahlke, 2014). In Northern Siberia, the latter half of the Middle Weichselian period (34–24 ka BP) was characterised by cooler summers compared to the period of 52–40 ka BP (Wetterich et al., 2021).

The Last Glacial Maximum (LGM) (ca. 27.2–23.5 ka cal BP) and the Pleistocene to Holocene (ca. 11,700 cal BP) transition are the key time periods for the extinction of a large part of the Mammoth Steppe species (Cooper et al., 2015), and most of the survivors show a decline in their genetic diversity after the LGM (e.g., Lorenzen et al. (2011). The causes of the late Quaternary extinctions have been explained by various reasons: climatic change and human impact, either as separate factors or as a combined effect (e.g., Koch & Barnosky, 2006). The loss of a high proportion of the largest herbivores caused major changes to the landscape and functioning of ecosystems (e.g., Johnson 2009). During the LGM, the climate in northern Europe was extremely cold and dry, with reconstructed annual mean temperatures 8–24°C lower and modelled surface temperatures 10–20°C lower than at present (Bartlein et al., 2011; Feurdean et al., 2014; Kageyama et al., 2006; Pollard & Barron, 2003; Tarasov et al., 1999; Wu et al., 2007). Continuous permafrost (Kitover et al., 2016) extended as far south as 45°N in Germany and Poland (Huijzer & Vandenberghe, 1998). In Northern Siberia, the modelling studies indicate a global summer cooling of approximately 6°C during the period 23–19 ka BP compared to the previous period (Tierney et al., 2020). According to pollen records and climate models, the Eastern Siberia had higher summer temperature anomalies and moisture levels similar to modern conditions during the LGM (Weitzel et al., 2022). Fossil insects at the Laptev Sea Coast in Northeastern Siberia show the persistence of tundra steppe with warmer summers and colder winters than today (Sher et al., 2005). Pollen-based reconstructions (Cleator et al., 2020; Tarasov et al., 1999; Wu et al., 2007) also show higher summer temperatures at high latitudes compared to mid-latitude Central Siberia, despite overall cold and dry conditions during the LGM (Bush, 2004; Kageyama et al., 2001; Schirrmeister et al., 2002; Tarasov et al., 1999).

The accelerated loss of megafauna during the Last Glacial Period happened worldwide and was quite severe in Eurasia and North America (Bergman et al., 2023; Seersholm et al., 2020; Stewart et al., 2021; Stuart, 2005; Zimov et al., 2012). Mammoths disappeared from northern and north-eastern Europe between 22 and 18 ka, likely due to the extremely harsh climatic and environmental conditions near the Scandinavian Ice Sheet (SIS) margin (Ukkonen et al., 2011). The transition from the Pleistocene to the Holocene around 11,700 years ago was marked by abrupt warming events (Birks & Birks, 2008; Drucker,

2022; Engels et al., 2022; Seddon et al., 2015). This period saw increased ground moisture due to precipitation and snowfall, along with the widespread proliferation of shrubs and trees (Rey-Iglesia et al., 2021). Although the extinction of mammoths at the end of the Pleistocene is well established, the timing of woolly mammoths' disappearance varied across different regions. On mainland Asia and North America, woolly mammoths vanished between 14,000 and 13,200 years ago, although some mainland populations might have persisted until around 10,500 years ago (Graham et al., 2016). The final regional extinction in northern Europe occurred during the Younger Dryas (Greenland Stadial 1; GS1) at about 12 ka cal BP, correlating with the decline of open biomes, such as steppe-tundra rapid reforestation during the Younger Dryas–Holocene boundary warming (Lõugas et al., 2002; Ukkonen et al., 2011). Notably, rare mammoth populations survived well into the Middle Holocene on isolated islands: on Wrangel Island (northeast Siberia) until approximately 4,000 cal BP (3,730 14C years BP) (Arppe et al., 2019; Zimov et al., 2012), and on St. Paul Island (Bering Sea, Alaska) until about 6,500 cal BP (5,700 14C years BP) (Graham et al., 2016).

1.2 Regional setting and geochronological context of the finds

1.2.1 Southeast of the Western Siberian Plain (SEWS)

The climate in the southeast of the Western Siberian Plain is extremely continental-cyclonic, having short hot summers and long cold winters (Rutkovskaya, 1979, 1996) and the landscapes of the region alternate between forest-steppe, mixed small-leaved forests and southern taiga. Summers are warm and humid, with an average July temperature of +18.5°C in the southern part of the area. Winters in the region are moderately severe, with an average January temperature of –19.1°C. There are 246 days per year when the temperature is above 0°C. The average yearly precipitation is 420–600 mm (Lapshina, 2003; Rutkovskaya, 1979). From 1977 to 1986, the average annual temperature was 0.4°C, whereas between 2018 and 2021, it was 1.5°C, indicating a temperature increase of over 1°C in the area since 1986 (Blyakharchuk et al., 2025).

In SEWS, the most prominent late Pleistocene sites discovered thus far in Eurasia, especially in regarding the abundance of mammoth findings (S. Leshchinskiy, 2015) are Shestakovo, Krasnoyarskaya Kurya and Volchia Griva (Figures 1 and 2). Shestakovo has yielded over 4500 remains belonging to at least 18 woolly mammoths since 1975 (Derevianko et al., 2000, 2003). Krasnoyarskaya Kurya have yielded 5600 woolly mammoth bones and teeth, skeletal fragments from at least 35 individuals (Lazarev & Leshchinskiy, 2011; Leshchinskiy et al., 2014; Seuru et al., 2017). Volchia Griva is possibly the largest site in Northern Asia where woolly mammoth remains are preserved in situ. Volchia Griva has yielded over 7000 fragments, whole bones, and teeth from at least 80 woolly mammoths on an area of more than 550 m^2 since 1957 (Leshchinskiy et al., 2023; Leshchinskiy & Burkanova, 2022). Human presence at all three sites has also been proven by the presence of palaeolithic artefacts at all three sites (Derevianko et al., 2000; Leshchinskiy et al., 2021; Vasyukova & Leshchinskiy, 2011).

Due to the substantial amount of mammoth fauna material buried at Shestakovo, Krasnoyarskaya Kurya and Volchia Griva, the uniqueness of these sites and the potential of holding valuable isotopic records, these sites were chosen as study sites specifically, and the time interval (ca. 27.5–22 ka cal BP) of the selected materials from SEWS covered the peak of LGM in the southeast of Western Siberia. Published oxygen isotope data for Siberia are limited, particularly for the LGM (e.g. Fox et al., 2007; Iacumin et al., 2010)

and are absent in the δ^{18}Ow reconstructions for the southeast of Western Siberia (Genoni et al., 1998). The only available comparative reconstructed δ^{18}Ow values near Shestakovo, Kranoyarskaya Kurya and Volchia Griva are primarily based on post-LGM reindeer samples (Genoni et al., 1998). Outside of SEWS, the nearest low-latitude mammoth-based δ^{18}Ow values relevant for comparison are located in the European Plain. For carbon and nitrogen isotopes, Beringia is currently one of the best-documented areas regarding stable carbon and nitrogen isotope data derived from woolly mammoth (Szpak et al., 2010) conducted a comprehensive study of 58 mammoth bone samples from both Eastern Beringia (Alaska and Yukon) and Western Beringia (Siberia), although only five samples out of 58 came from LGM. (Arppe et al., 2019) reported δ^{13}C, δ^{15}N, and δ^{34}S from 77 mammoth specimens from the last known mammoth refugia, Wrangel Island (Zimov et al., 2012). Approximately 12% of these samples were dated to the LGM. (Iacumin et al., 2000) reported δ^{13}C and δ^{15}N values from mammoth teeth and bones of post-LGM European Plain samples, reindeer and deer from south-central Siberia, and mammoth remains from the Taymyr Peninsula and Yakutia, many of which were not radiocarbon-dated. In contrast, isotopic data from SEWS, remain sparse. Leshchinskiy and Burkanova, 2022 provided the first δ^{13}C and δ^{15}N data from ten post-LGM mammoth bones recovered at Volchia Griva.

1.2.2 Eastern Baltics

The Eastern Baltic region is located in a transitional climate that ranges from maritime influences in the west to a more continental climate in the east. The landscape is predominantly flat, covered with mixed forests. In Estonia, the mean temperature in July is 16–17°C, while in February, the coldest month of the year, it ranges from –2.5°C to –7°C (Estonian Environment Agency, 2024). In Latvia, the mean temperature in July is 17.4°C, and in February, it averages –3.7°C (World Bank Group, 2024). The region receives an annual precipitation of approximately 550–700 mm.

Pollen-based reconstructions and macrofossil records from the eastern Baltics indicate that the climate warming during the GI-1 (14,650–12,850 cal yr BP) was modest due to proximity of region to retreating continental ice. The climate was generally cool, with long winters, persistent ice cover, and brief summers (Veski et al., 2012, 2015, Bakumenko et al, 2025, in press). Around 12,850 cal yr BP, the climate cooled again, though gradually in the southern Baltic-Belarus region (Heikkilä et al., 2009; Veski et al., 2012, 2015). During the Younger Dryas, dry conditions persisted (Goslar et al., 1999; Wohlfarth et al., 2006), though short warmer episodes with brief summers were also likely (Grafenstein et al., 1999; Isarin & Renssen, 1999; Lane et al., 2013; Liiv et al., 2019; Schenk et al., 2018; Schmidt et al., 2002; Schwark et al., 2002). Younger Dryas ended with abrupt warming, marking the onset of the Holocene.

The study of mammoths and their palaeoenvironment in the Eastern Baltics during the late Pleistocene is a relatively under-researched topic that has the potential for expanding our knowledge of the region's mammoth fauna. Despite the significant role that mammoths played in the ecosystems of this period, there are still large gaps in our understanding of their distribution, behaviour, and interaction with the environment in this region. The discovery of mammoth remains in Estonia can be traced back to 1874 (Grewingk, 1874). Since 1874 to 1960s, a total of 24 samples, including 13 molars and 11 tusks, were recovered from various locations such as riverbanks, lake and seashores, construction sites, and glaciofluvial gravels. However, over time, some of these findings have been lost, and the remaining ones are unusable because there is no contextual

information or locations available for these finds (Lõugas et al., 2002) argue that most mammoth discoveries in Estonia have been redeposited into younger sediments due to glaciofluvial processes.

Published isotopic data for the Eastern Baltics are even more scarce than for the SEWS. This is not only due to the small number of studies focused specifically on the region, but also because the existing studies often include isotopic information from the Eastern Baltics mammoth samples as part of broader European datasets aimed at addressing large-scale questions like reconstructing the climate of northern Europe during the Middle to late Weichselian or reconstructing the woolly mammoths' habitat in Europe (e.g Arppe et al., 2011; Arppe & Karhu, 2010). One of the most detailed studies on the mammoths in Estonia was done by (Lõugas et al., 2002), where the authors reported $\delta^{13}C$ values for 11 dated molar, tusk and bone mammoth samples from Estonia and western Russia. The largest catalogue of dated mammoth finds in the Eastern Baltics can be found in Ukkonen et al. (2011). Furthermore, there is no distinct site with a large accumulation of mammoth remains in the Eastern Baltics, such as, for example, Volchia Griva, where the material is preserved in a clear geological context that allows for a detailed taphonomic analysis and accurate dating.

1.3 Sampling sites

1.3.1 Shestakovo

Shestakovo site (55°54'31.0"N, 87°57'07.0"E) (Figures 1 and 2) is located in the Kemerovo region, approximately 1 km downstream from the village of Shestakovo, on the high right bank of the Kiya River. The bone-bearing horizon is situated at an altitude of approximately 160–170 m, with some areas reaching higher elevations. The site was particularly attractive to large herbivores due to the presence of a "beast solonetz," a term used in Russian scientific literature to describe a geochemical landscape enriched with Ca, Mg and Na (Derevianko et al., 2000, 2003). A beast solonetz contains high concentrations of macro- and microelements, offering a broader interpretation than terms such as "salt lick," "mineral lick," or "mineral source." Within these areas, animals engage in lithophagy (soil and rock consumption) and drink mineral-rich water from springs to maintain physiological homeostasis (Leshchinskiy, 2015). Samples from the Shestakovo site come from geological layers V and VI, which are the main bone-bearing horizon (Derevianko et al., 2000, 2003). The age of the samples from the Shestakovo site falls within the period of ca. 28–27 ka cal BP.

1.3.2 Krasnoyarskaya Kurya

Krasnoyarskaya Kurya (coordinates: 54°39'48.4"N, 80°19'47.6"E; surface elevation is 123 m) (Figures 1 and 2) is situated in the southeastern region of the West Siberian Plain, within the Chulym River Valley. The site is located 148 km to the north of Shestakovo. Krasnoyarskaya Kurya samples come from the bone-bearing horizon's middle and lower levels. The age of the samples from Krasnoyarskaya Kurya falls within ca. 25–23 ka cal BP (Boiko et al., 2005; Derevianko et al., 2003) and (Seuru et al., 2017).

1.3.3 Volchia Griva

Volchia Griva (translated to "Wolf's Ridge" or "Wolf's Mound") (coordinates: 54°39'48.4"N, 80°19'47.6"E; surface elevation approximately 148 m) (Figures 1 and 2) is a mound in "Mamontovoe" village, Kargat district of the Novosibirsk region, east of the Baraba

Lowland. It occupies the northeastern section of an elongated, sloping mound bearing the same name, which extends approximately 11 km in length and 0.5–1 km in width. The site is 500 km southwest of Shestakovo and 535 km southwest of Krasnoyarskaya Kurya.

Since its discovery in 1957, Volchia Griva has been recognised as a large mammoth cemetery and one of the last mammoths refugia. (Leshchinskiy & Burkanova, 2022) state that large mammal remains have accumulated at this site from the Last Glacial Maximum (LGM) to the end of the Pleistocene. Similarly to Shestakovo, Volchia Griva was attractive to large herbivores because of the salt lick (S. V. Leshchinskiy, 2018). The age of the samples from Volchia Griva falls within ca. 24–22 ka cal BP (Kuzmin et al., 2024).

1.3.4 Lake Kaatsjärv

We have compiled a comprehensive dataset consisting of all available pollen and plant macrofossil records and mammoth finds from the Eastern Baltics and a new pollen and plant macrofossil record from Lake Kaatsjärv in central Estonia. Lake Kaatsjärv (Figure 3) is a small lake in central Estonia (59.1318 N; 25.3141 E) (Figures 1 and 3), surrounded by a mixed pine forest. The area of the lake is 1 ha, the elevation is 68.5 m above sea level (a.s.l.), and the maximum water depth is 6 m. We selected this lake because of its central location in Estonia, the fact that it had not been sampled before, and its potential to complement existing palaeoenvironmental records from the region. More detailed information on the coring of Kaatsjärv is presented in **Paper II**.

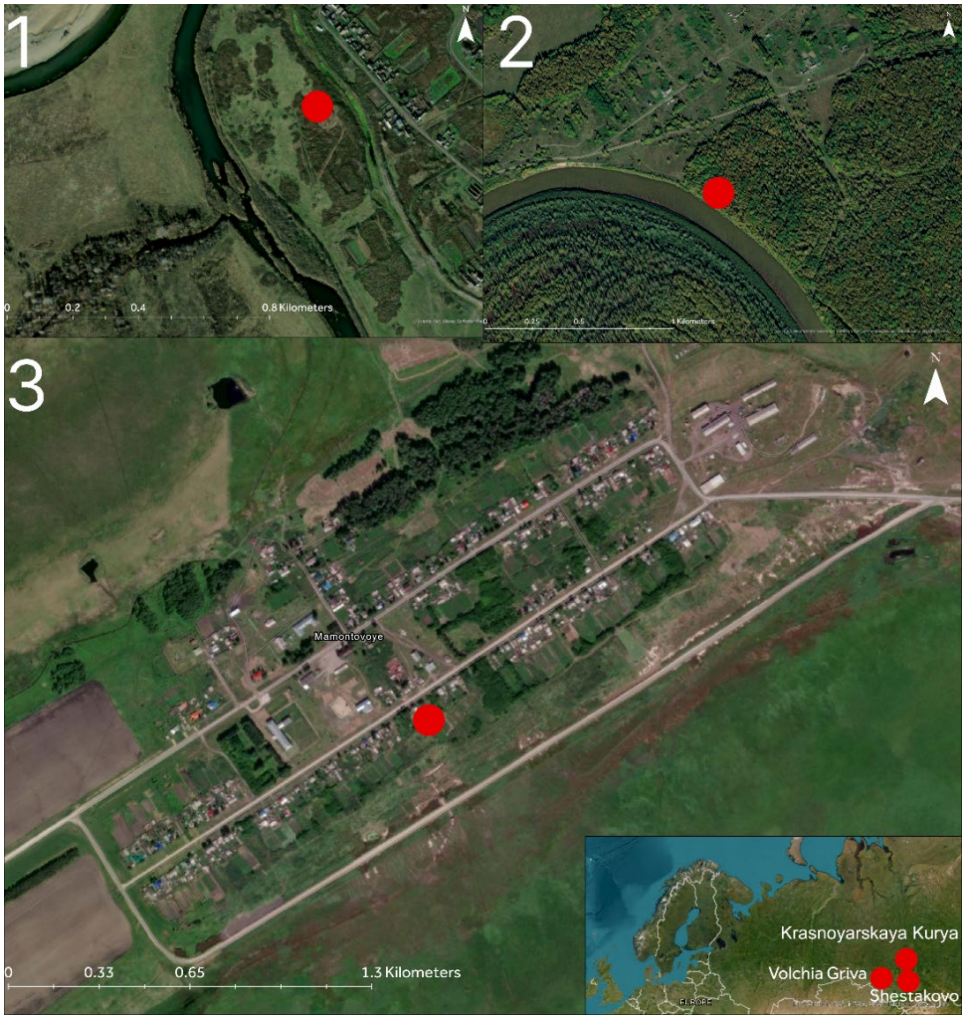

Figure 2. Map showing satellite images of 1) Shestakovo, 2) Krasnoyarskaya Kurya, and 3) Volchia Griva sites and their location on a larger map of Eurasia. Basemap: Esri, Maxar, Earthstar Geographics, and the GIS User Community.

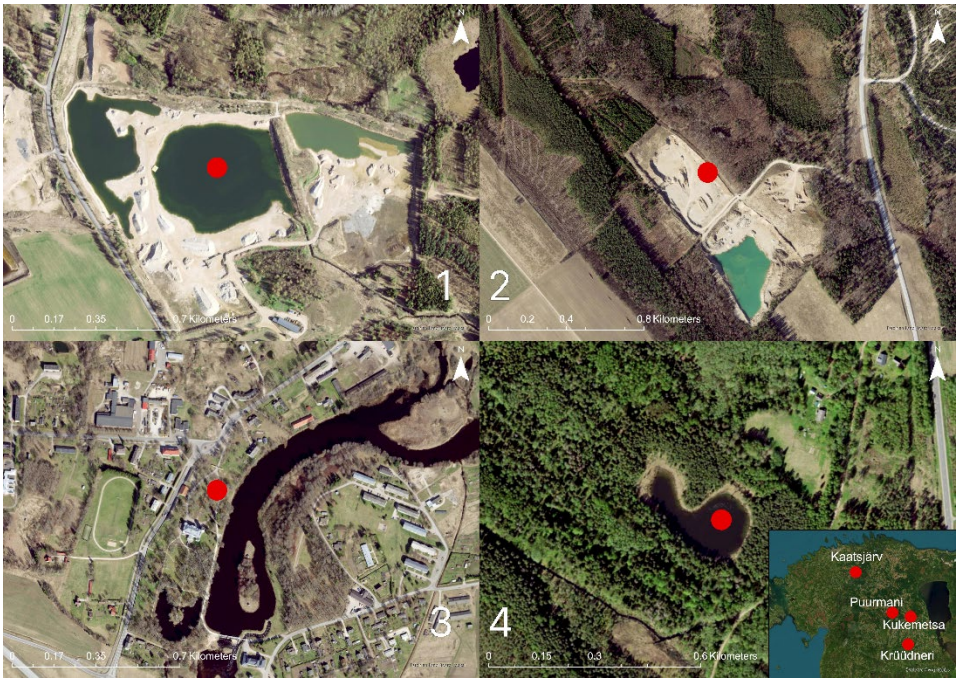

Figure 3. Map showing the satellite image of 1) Krüüdneri; 2) Kukemetsa, 3) Puurmani and 4) Lake Kaatsjärv sites and their location on a map of Estonia. Basemap: Esri, Maxar, Earthstar Geographics, and the GIS User Community.

2 Methodology

2.1 Mammoth sample selection

For **Papers I** and **III**, we took 31 samples from the Laboratory of Mesozoic and Cenozoic Continental Ecosystems at Tomsk State University, Russia: 29 samples were from woolly mammoths, and two were from a deer and a horse. Samples from the southeast of Western Siberia included tooth enamel and tusks. For **Paper II**, we collected four Estonian mammoth tooth samples, two from the Puurmani site (TAM G441:47 and TAM G441:48), one from Kukemetsa (KUK) and one from Krüüdneri (KRÜ) sites. The specimens were cut using a Dremel 300 drill. All samples were photographed, stored in zip-lock bags, and labelled accordingly. In further text, Shestakovo will be referred to as "SH," Krasnoyarskaya Kurya as "KK," and Volchia Griva as "VG".

2.2 Stable isotopes

The use of stable isotope analysis of skeletal remains in palaeoecology offers several significant benefits. It is often the only option available to study the foraging ecology of extinct animals (Ben-David & Flaherty, 2012) because we often do not have access to soft tissues such as blood, muscle, or hair, which would enable more precise dietary reconstructions (Bocherens, 2015). Stable isotopes allow to investigate how individual species respond to changes in habitat, food availability, competition, predation and how these responses influence reproductive success and survival, emerging population dynamics, and community and ecosystem processes (Ben-David & Flaherty, 2012). Stable isotope analysis, alongside other methods, can inform modern conservation efforts and policy decisions, helping to identify current risks to species by providing detailed understanding of past megafaunal extinctions (Ben-David & Flaherty, 2012). Therefore, choosing isotopic analysis as the primary method for our research was the most appropriate. This method is particularly effective when one has an abundance of teeth and bones, and a lack of access to soft tissues.

Stable isotopic data in this dissertation text is reported as delta value, a per mill difference from the international reference standards based on the following formula: $\delta = (R_{sample}/R_{standard} - 1) \times 1000$. VSMOW (Vienna Standard Mean Ocean Water) standard is used for oxygen, VPDB (Vienna Peedee Belemnite) for carbon and atmospheric nitrogen called AIR is used as a standard for nitrogen isotopes.

2.2.1 Oxygen isotopes

Oxygen isotopes (general). Several studies (Daniel Bryant et al., 1994, 1996; Genoni et al., 1998; Iacumin et al., 2004) showed that stable oxygen isotope compositions in mammoth enamel, dentin, and bone, provide valuable insights into past climatic conditions.

The isotopic composition of body water determines the oxygen isotope composition of mammalian apatite. In turn, the magnitude and composition of oxygen fluxes influence the body water (Longinelli, 1984; Luz et al., 1984). Because the mineralised tissues of large mammals form at a near constant body temperature of 37°C, the composition of body water causes variability in their apatite's oxygen isotope composition. The oxygen isotope composition of body water is sensitive to the oxygen isotope composition of meteoric water, as large mammals obtain most of their water through drinking from surface water reservoirs (Daniel Bryant & Froelich, 1995; Longinelli, 1984). In addition, annual $\delta^{18}O$ mean of precipitation and annual mean surface air temperatures for

mid- and high northern latitudes are closely related (Dansgaard, 1964; Rozanski et al., 1992). As a result, $\delta^{18}O$ values obtained from animal tissues reflect temporal changes in humidity, aridity, relative air temperature and the climate (Metcalfe, 2017; Tütken et al., 2007). Because of the connection between the $\delta^{18}O$ values of mammal bioapatite ($\delta^{18}Oap$) and the ingested meteoric waters ($\delta^{18}Ow$), the $\delta^{18}O$ values from mammal skeletal remains can be used for palaeoclimatological investigations.

Oxygen isotopes (study-specific). Oxygen isotope analysis was conducted at the Laboratory of Chronology, Finnish Museum of Natural History. The sample preparation protocols were also performed at the same laboratory. The oxygen isotope data for both phosphate and carbonate are presented as delta values ($\delta^{18}O$) in per mil against to the VSMOW standard. Carbonate $\delta^{18}O$ values were calibrated to the VSMOW scale using the conversion equation: $\delta^{18}O(VSMOW) = \delta^{18}O(VPDB) * 1.03092 + 30.92$ (Sharp, 2017). Oxygen carbonate results are provided in the Supplementary Data of **Paper I**.

2.2.2 Carbon and nitrogen isotopes

Carbon and nitrogen isotopes (general). Stable carbon and nitrogen isotope compositions of mammoth skeletal remains, such as dentin and bone, are used to extract information about mammoths' diet and the surrounding vegetation (Ayliffe et al., 1992; Kohn & Cerling, 2002). Carbon isotope analysis ($\delta^{13}C$) provides valuable insights into an animal's dietary habits, palaeoecology, and climatic conditions by reflecting the isotopic signatures of consumed plants, which, as a result, can help differentiate between C_3 and C_4 vegetation in the diet (Arppe et al., 2011; Fox-Dobbs et al., 2008; Kuitems et al., 2015; Szpak et al., 2010). Most trees, shrubs, herbs, grasses and sedges use the C_3 photosynthetic pathway (the Calvin cycle). These plants usually have $\delta^{13}C$ values ranging between –35‰ and –22‰, with an average of –27‰ (Cerling et al., 1999; O'Leary, 1988). Plants that follow the C_4 pathway (the Hatch-Slack cycle), are mostly tropical grasses and some species of sedges. Their $\delta^{13}C$ values range from –15‰ to –10‰, with an average of 13‰. Succulents that grow in dry environments use a mechanism called crassulacean acid metabolism (CAM). This photosynthetic mechanism combines features of both the C_3 and C_4 pathways, and usually plants with CAM type have their $\delta^{13}C$ values between the other two types.

Nitrogen isotope analysis ($\delta^{15}N$) is used to reconstruct trophic relationships and detect nutritional stress. The $\delta^{15}N$ values in bone collagen are directly correlated to the $\delta^{15}N$ composition of dietary protein (Deniro & Epstein, 1981; Schoeninger & DeNiro, 1984). Because nitrogen isotopic composition varies among food sources, analysing $\delta^{15}N$ values from mammoth remains provides key insights into the dietary preferences of the analysed animals and the ecological conditions of the sites where they were found (Deniro & Epstein, 1981). The application of $\delta^{15}N$ analysis, therefore, contributes to understanding trophic structures within past ecosystems and reconstructing dietary patterns of extinct herbivores.

Carbon and nitrogen isotopes (study-specific). Collagen extraction for carbon and nitrogen isotope analysis was carried out using the protocol F outlined by Cersoy et al. (2017). The extracted collagen was placed in tin foil capsules, packed, and analysed using a Thermo-Finnigan Delta V Plus mass spectrometer coupled with a Thermo Flash 1112 elemental analyser at Tartu University. The mean values and standard deviations (SD) of the two replicates for each sample are provided in Table 1, and detailed information for each duplicate is available in the Supplementary Data of **Paper III**. The $\delta^{13}C$ and $\delta^{15}N$ values are reported relative to the "Vienna" equivalent of the Belemnite PeeDee Formation (VPDB) and atmospheric nitrogen (AIR) standards, respectively.

2.3 Statistical analysis and isotopic data comparison

The $\delta^{18}O$ isotopic values from Shestakovo, Krasnoyarskaya Kurya, and Volchia Griva were compared using statistical methods. The mean values for these three sites were calculated as unweighted means. Statistical analysis was performed in Python (version 3.11.4), using the pandas (McKinney, 2010), NumPy (Harris et al., 2020), and SciPy (Virtanen et al., 2020) libraries. The Python code used for these analyses is provided in the Supplementary Data. We used the Shapiro-Wilks test to assess the normality of the data distribution. Non-parametric Kruskal-Wallis test was applied for non-normally distributed data. Differences in carbon and nitrogen isotopic values between Shestakovo, Krasnoyarskaya Kurya and Volchia Griva were tested using RStudio (version R 3.6.0). The means for the three distinct sites were calculated as averages. The code is available in the Supplementary Data. RStudio (version R 3.6.0) was used to test the differences in isotopic values between Shestakovo, Krasnoyarskaya Kurya and Volchia Griva. The means for the three distinct sites were calculated as averages.

2.4 Isotopic data processing: calibration equations

For the mammoth enamel and tusk samples, the calibration equation for elephants (Ayliffe et al., 1992) was used to convert $\delta^{18}O$ values of phosphate ($\delta^{18}Op$) to estimates of $\delta^{18}O$ in water ($\delta^{18}Ow$), under the assumption that mammoths shared broadly similar ecological behaviours, dietary patterns, physiological traits, and metabolic rates with modern elephants (Haynes, 1991; Olivier, 1982). Previous studies have successfully employed this equation to calculate environmental water values (e.g., Arppe & Karhu, 2010; Tütken et al., 2007)). For the horse sample, the calibration equation for wild horses (Delgado Huertas et al., 1995) was applied, and for the deer sample, the calibration equation for reindeer (Longinelli et al., 2003) was used. Error calculations and propagation for $\delta^{18}Ow$ values followed the formulas outlined in Pryor et al., (2014).

2.5 Preservation evaluation

Preservation evaluation (general). Among skeletal tissues, tooth enamel has demonstrated the highest resistance to diagenetic alteration and is, therefore, usually a preferred material for isotope analysis (Kohn & Cerling, 2002; Metcalfe & Longstaffe, 2012). Well-preserved specimens of mammoth tusks can also provide highly detailed records of both climate fluctuations and individual life histories (e.g. Rowe et al. (2024)). However, the preservation and the isotopic integrity of skeletal remains vary largely depending on site-specific environmental conditions (J. Lee-Thorp & Sponheimer, 2003). Unlike North Siberian permafrost sites, which have yielded well-preserved enamel and bone suitable for oxygen isotope analysis (e.g. Arppe et al., (2019); Fox et al., (2007); Iacumin et al., (2010)), the sites examined here are not under permafrost conditions. Consequently, carefully and methodically assessing the extent of post-depositional diagenetic alteration of the materials from permafrost-free sites is necessary.

In studies of extinct megafauna, the selection of well-preserved samples is understandably prioritised, as the quality of preservation directly affects both the accuracy of isotopic results and the reliability of subsequent palaeoclimatic interpretations. However, in mammoth research, sometimes it is not possible to consistently obtain well-preserved samples. Although working with well-preserved material is more straightforward, this approach risks excluding significant portions of data, particularly

from underrepresented regions such as the ones discussed in this synthesis, the southeast of the Western Siberian Plain (SEWS) and the Eastern Baltics. Isotopic data from these areas are important for developing a more comprehensive understanding of past mammoth-related climatic and ecological conditions across Eurasia, and limiting analyses to Arctic Siberia alone, for example, paints only part of the picture. While future studies will need to place greater emphasis on assessing preservation in such contexts, the potential value of data obtained from less ideal or previously overlooked sites is immense. These data can serve as important reference points for both future investigations and paleogeographic reconstructions. Our study sties, SEWS and the Eastern Baltics differ widely in geographic location and chronology, but they are united by their historical "neglect" in isotopic research, largely due to uncertainties surrounding the preservation of the discovered mammoth remains. Therefore, regions such as SEWS and Eastern Baltics deserve more attention and a willingness to take some risks. Despite the additional effort required for preservation assessment and the more cautious interpretation of data, it is very important to include such samples in isotopic studies in order to achieve a more complete understanding of mammoth paleoecology and the environmental dynamics of the late Pleistocene in Eurasia.

2.5.1 Visual preservation evaluation

Each selected samples was categorised according to its condition ("very good", "good", or "acceptable") based on visual and tactile inspections, paying particular attention to the colour and translucence of the enamel, as well as its hardness and brittleness. We intentionally selected samples representing the full spectrum of preservation conditions at SEWS sites. When deciding which materials to select for our analysis, we considered the typical preservation state of materials from these sites. Photographs of the samples are included in the Supplementary Data of **Papers I** and **III**.

2.5.2 Mineral and organic fractions

Mammoth teeth consist of two fractions: the organic fraction, collagen, and the inorganic fraction, which is bioapatite. In this study, oxygen isotopes were extracted from the bioapatite ($Ca10(PO4)6(OH)2$), while carbon and nitrogen isotopes were extracted from collagen ($C102H152N30O31$). Both fractions require thorough preservation evaluation, as it is possible that within one sample, one fraction remains intact while the other degrades. We used various established methods described below to assess the preservation of each fraction. Detailed descriptions of the methodologies can be found in **Papers I, II**, and **III**.

$\delta^{18}O$ CO_3-PO_4 Equilibrium (mineral fraction). We assessed the preservation of the expected equilibrium between the $\delta^{18}O$ values of the structural carbonate and phosphate components of bioapatite to determine whether the oxygen isotope compositions had been altered by diagenetic processes (Daniel Bryant et al., 1996; Iacumin et al., 1996). The oxygen isotope composition of the phosphate and structural carbonate within bioapatite is formed in isotopic equilibrium, derived from the same oxygen source—body water—at a consistent temperature (approximately 37°C for mammals). As a result, there is a strong linear relationship between the $\delta^{18}Op$ and $\delta^{18}Oc$ values (Iacumin et al., 1996). When plotting $\delta^{18}Op$ values against $\delta^{18}Oc$, the data points should align closely with the linear relationship line representing well-preserved isotope values, exhibiting a mutual offset within the acceptable range of 7.2–10.6‰ (Martin et al., 2008).

Fourier Transform Infrared Spectroscopy Analysis (mineral fraction). We used Fourier Transform Infrared Spectroscopy (ATR-FTIR or FTIR) to gain further insight into the preservation status of the samples. ATR-FTIR is a vibrational spectroscopy method that generates unique spectra for molecules present in biological tissues. This technique is based on the premise that changes in the chemical or structural properties of bioapatite can provide valuable information about the conditions and processes the remains have experienced since the death of the animal, as well as the degree of substitution of bioinorganic materials (Diez et al., 2021).

To indicate good preservation status, the following ranges were considered: infrared splitting factor (IRSF) (3.1–4.0) and carbonate/phosphate (C/P) (0.08–0.2) for enamel; and IRSF (3.1–4.0) and C/P (0.05–0.3) for dentin (tusk). According to recommendations by France et al. (2020), C/P index was paid more attention than other indices because it is the most informative to distinguish poor general preservation for pre-treated samples. C/P index shows the ratio of B-type carbonates to V3 PO43− and the deviations from the established range will suggest loss or addition of carbonate and/or phosphate from the bioapatite. IRSF index was also calculated and used to assess the degree of mineral recrystallisation or matrix loss during diagenesis (France et al., 2020). The infrared absorption spectrum of each sample was recorded using an FTIR spectrometer IRTracer-100 (Shimadzu), equipped with a diamond attenuated total reflectance (ATR) device. FTIR spectroscopy was performed at the Laboratory of Chemical Analysis at Tallinn University of Technology, Tallinn, Estonia. Typical enamel FTIR spectra and spectra for all analysed samples are included in the Supplementary Data of **Paper I**.

C:N ratio (organic fraction). The elemental carbon to nitrogen (C:N) ratio served as the primary criterion for assessing preservation both for Siberian samples and Eastern Baltic samples; however, we additionally considered collagen yields and the total carbon and nitrogen content (weight-% C, weight-% N). According to Ambrose, (1990); DeNiro, (1985); DeNiro & Weiner, (1988); Sealy et al., (2014); van Klinken, (1999), C:N ratios between 2.9 and 3.6 are considered indicative of well-preserved collagen. We also explored the option of applying a stricter C:N range of 3.1–3.3 suggested by (Guiry & Szpak, 2021). The following elemental content criteria were used: C > 13% and N > 4.8% (Ambrose, 1990).

Collagen yield. Well-preserved bone and dentine typically show collagen yields around 20% (van Klinken, 1999), with collagen concentrations greater than 0.5–2% generally considered sufficient for identifying adequately preserved collagen in ancient bones and teeth (Ambrose, 1990; DeNiro & Weiner, 1988; Dobberstein et al., 2009; van Klinken, 1999). Collagen yields were closely monitored in our sample set, and samples with low collagen yields were excluded from the main dataset.

2.6 Plant macrofossil method (background and limitations)

Plant macrofossil method (general). Plant macrofossil analysis, first developed by W.A. Watts in the United States (Birks & Birks, 1980; Watts & Winter, 1966), is one of the most important methods in palaeoecological research (Birks, 2008). Macrofossils include various plant remains such as fruits, seeds, leaves, cuticles, buds, anthers, flower parts, rhizomes, twigs, wood, bark, and other vegetative components. In addition, mosses, sporangia, megaspores, lichens, seaweeds, and Characeae oospores are commonly identified. Plant macrofossil remains vary in size, typically ranging from 0.5 mm to several centimetres, and in case of large woody fragments, they are referred to as “megafossils”

(MacDonald, 2013). Due to their relatively large size and weight, plant macrofossils are usually deposited near the parent plant.

Macrofossil assemblages are interpreted using the ecological tolerances of identified taxa, and they often serve as indicators of past environmental conditions. This approach is applied in palaeoecological and archaeobotanical contexts, where plant remains may be associated with anthropogenic activity rather than natural vegetation (Birks & Birks, 1980). The ecological interpretation becomes stronger when macrofossil assemblages are considered analogues to modern vegetation communities.

Plant macrofossil analysis becomes more effective when combined with pollen analysis as part of a multiproxy approach. While pollen data provide broader regional signals, macrofossils often reflect more local vegetation and can give more detailed palaeoecological records in case of taxa that are challenging to distinguish using pollen analysis such as *Larix*, *Populus*, Cupressaceae and *Juncus*. Furthermore, macrofossils can often be identified at a more precise taxonomic level than pollen, which can usually be identified to the family or genus level. Therefore, they can offer a deeper insight into forest and other vegetational successions (Birks et al., 2000; Birks & Birks, 2003). This integrative approach provides a more comprehensive reconstruction of both aquatic and terrestrial vegetation histories than either method alone (Aarnes et al., 2012; Eide et al., 2006; Gaillard & Birks, 2013; Jackson et al., 2014; Waller & Early, 2015).

Plant macrofossil analysis (study-specific). A total of 35 sediment samples were processed to assess plant macrofossil content. The preparation of these samples followed the methodology outlined by Birks (2002). Plant macrofossils were identified using atlases, reference collections, and pertinent literature (Cappers et al., 2009; Katz et al., 1977).

2.7 Pollen analysis

Pollen analysis was conducted by Prof. Siim Veski from the Department of Geology at Tallinn University of Technology. In total, seven samples were analysed. Pollen identification followed the key by Fægri & Iversen (1989) and Beug (2004). A minimum of 500 terrestrial pollen grains per sample were counted and identified to the lowest possible taxonomic level using pollen identification keys, the reference pollen collection at the Department of Geology at Tallinn University of Technology, and additional literature sources (Beug, 2004; Reille, 1992).

Pollen-based vegetation reconstructions were obtained using REVEALS modelling performed by Dr. Anneli Poska from the Department of Geology, Tallinn University of Technology. Maps and dating calibrations were made by Dr. Jüri Vassiljev from the Department of Geology, Tallinn University of Technology. We compiled data from 27 pollen records and 8 plant macrofossil records from across the region to study vegetation changes and reconstruct the habitats of Europe's last mammoths in Estonia and Latvia during the transition from the Pleistocene to the Holocene. All selected sites are radiocarbon-dated and provide information on vegetation development between 14.3 and 11.3 ka cal BP. In addition, the well-dated pollen sequence from the Voka section (59.4144 N, 27.5981 E) (Molodkov et al., 2007; Molodkov & Bolikhovskaya, 2022) was used to reconstruct pre-LGM land cover for 500-year intervals centred around 33, 34, 35, 36, and 37 ka cal BP.

2.8 Chronological control

For SEWS, it was not possible to directly radiocarbon date the analysed samples. As a results, the temporal framework for the samples was established using the chronological data of the geological layers from which the specimens were collected. We identified the stratigraphic layers of origin for each sample and used published radiocarbon dates to determine the earliest and latest ages within those layers. The age range of each sample was then estimated accordingly, while also considering possible redeposition affecting the stratigraphy.

Selected samples from Shestakovo come from geological layers V and VI, which are the main bone-bearing horizon of the site. In layer V, four mammoth bone samples were dated, and in layer VI, nine samples, including mammoth teeth and bones, horse and deer bones, charcoal, and burnt bones, were dated (Derevianko et al., 2000, 2003). The chronological boundaries for the selected samples are defined by a mammoth bone dated to ca. 27.5 ka cal BP (23,330 ±110 14C yr BP (GrA-13235)), and a mammoth bone dated to ca. 26.7 ka cal BP (22,340 ±180 14C yr BP (GrA-13240)). Thus, the estimated age range for the Shestakovo samples is approximately 28–27 ka cal BP.

Krasnoyarskaya Kurya samples were obtained from the middle and lower levels of the bone-bearing horizon. Several finds were dated at this site: a mammoth humerus/or pelvis (ca. 23.5 ka cal BP (19,670 ±120 14C yr BP (GIN-12876))), an ulna/or humerus (ca. 23.8 ka cal BP (19,780 ±180 14C yr BP (GIN-12877))) (Boiko et al., 2005; Maschenko, 2010) and pelvis (24.3–23.9 ka cal BP (20,020 ±80 14C yr BP (Beta-426078))); Seuru et al., 2017). Overall, the age range for samples from Krasnoyarskaya Kurya is within the period of ca. 25–23 ka cal BP.

At Volchia Griva, selected samples come from the lower level of the bone-bearing horizon in the central assemblage. The earliest radiocarbon date from charcoal in this layer indicates that accumulation at Volchia Griva began around 24 ka cal BP (19,790 ±70 ^{14}C yr BP, RICH-29414.1.1), while the most recent charcoal date suggests the end of accumulation occurred around 22 ka cal BP (18,230 ±70 ^{14}C yr BP, IGANAMS-8485) (Kuzmin et al., 2024). Direct radiocarbon dating of the SEWS samples in future research would be largely beneficial, as there will be an opportunity to track the changes of carbon, nitrogen and oxygen isotopes of the mammoths from SEWS through time.

For the Eastern Baltics, radiocarbon dates for mammoth samples were taken from published literature. Radiocarbon ages for the Puurmani specimens were taken from Lõugas et al. (2002), and the information about other dates mammoth samples in the Eastern Baltics was taken from Ukkonen et al. (2011), while the dates for the Krüüdneri and Kukemetsa samples were provided by Professor Siim Veski of the Department of Geology at Tallinn University of Technology. Radiocarbon dates for plant macrofossil remains from Kaatsjärv lake were done in the Poznan´ Radiocarbon Laboratory, Poland.

2.9 Radiocarbon dating

All radiocarbon dates related to the studied mammoth sites were calibrated using OxCal v.4.4.4 (Bronk Ramsey, 2009; Ramsey, 2008) and the InCal20 calibration curve (Reimer et al., 2020) and median calibrated years (ka cal BP, were 0 = 1950CE) at 95.4% probability were used below/in the discussion.

3 Results

3.1 ATR-FTIR Spectral analysis

The ATR-FTIR spectra of all enamel samples exhibit features typical for enamel, except for sample VG 30, which also failed during the Ag3PO4 extraction and δ^{18}Oc analysis (Supplementary Data of **Paper I**). The ATR-FTIR spectra of the tusk samples similarly show characteristics of pretreated dentine spectra reported by (France et al., 2020) (Supplementary Data).

The calculated C/P ratios and IRSF values for each sample are presented in Table 1. The C/P ratio values for 24 enamel and tusk samples fall within the well-preserved ranges as defined by (France et al., 2020). However, five samples (VG 18, VG 29, VG 30, VG 31, and KK 66), the majority of which are tusk samples, have C/P values outside the recommended range (Figure 4).

For the IRSF index 13 enamel samples exhibit values within the recommended range, while six samples (SH 55, VG 17, VG 18, VG 31, VG 32, KK 59) show elevated IRSF values (Figure 4). VG 18 has an exceptionally high IRSF ratio of 8.058 and a negative C/P ratio of –0.009. In contrast to the enamel samples, all tusk samples, except for KK 60, display IRSF values above the prescribed range for well-preserved dentine samples.

There is a negative correlation between the IRSF and C/P values (Figure 4), indicating that higher IRSF values are strongly associated with lower C/P values. The coefficient of determination (r^2) is 0.68, suggesting that approximately 68% of the variability in IRSF values can be explained by changes in C/P values.

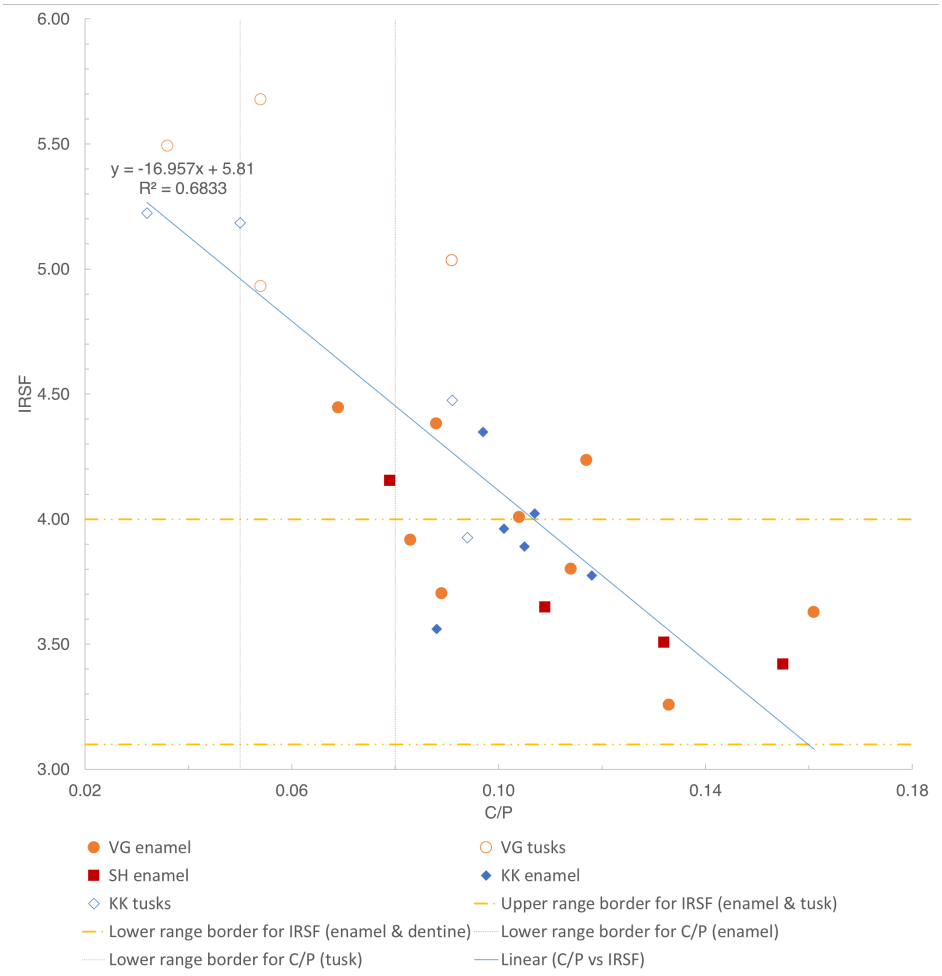

Figure 4. The relationship between IRSF values and C/P values. A strong negative correlation suggests that the elevated IRSF values are linked to loss of carbonate.

3.2 $\delta^{18}O$ Values

Table 1 presents the isotopic values for all analysed samples. In total, 29 $\delta^{18}O_p$ values and 30 $\delta^{18}Oc$ values were obtained. The range of $\delta^{18}O_p$ values across the entire dataset spans from +6.9‰ to +11.9‰, while the $\delta^{18}Oc$ values range from +16.3‰ to +22.5‰. Specifically, the $\delta^{18}O_p$ values for Shestakovo vary from +6.9‰ to +8.8‰, for Krasnoyarskaya Kurya from +8.1‰ to +9.8‰, and for Volchia Griva from +8.2‰ to +11.9‰. Regarding the carbonate component, $\delta^{18}Oc$ values for Shestakovo range from +16.3‰ to +17.5‰, for Krasnoyarskaya Kurya from +17.7‰ to +19.1‰, and for Volchia Griva from +18.7‰ to +22.5‰.

3.2.1 Oxygen Isotope CO_3-PO_4 Equilibrium (mineral fraction preservation)

The variation range of $\Delta^{18}O$ CO_3-PO_4 offsets for the entire dataset spans from +7.4‰ to +11.7‰, which is the same as the range of $\Delta^{18}O$ CO_3-PO_4 offsets for the Volchia Griva samples. The samples from Shestakovo and Krasnoyarska Kurya show narrower ranges of $\Delta^{18}O$ CO_3-PO_4 offsets, specifically from +8.7‰ to +10.4‰ and from +8.1‰ to +10.1‰, respectively (Table 1). Compared to the regression line representing the best fit through the modern animal data pairs, 25 samples show $\Delta^{18}O$ CO_3-PO_4 offsets that fall within the range suggested by Martin et al. (2008) for good isotopic preservation of samples (Figure 5). However, four samples fall outside the envelope defined by well-preserved modern sample data, indicating isotopic disequilibrium: VG 23 ($\Delta^{18}O$ CO_3-PO_4 offset 11.1‰), VG 25 (10.7‰), VG 29 (11.3‰), and VG 33 (11.7‰). These four samples were excluded from the dataset used to calculate $\delta^{18}Ow$ values for past ingested environmental waters. The quality control data for $\delta^{18}O_p$ indicates a reproducibility of approximately ±0.3‰ for $\delta^{18}O_p$ and ±0.2‰ for $\delta^{18}Oc$. Therefore, it is possible that some of the discarded samples (e.g., VG 25) may potentially have intact $\delta^{18}O_p$ values. However, for consistency, we adhered to the range of +7.2‰ – +10.6‰ (Martin et al., 2008) as the permissible $\Delta^{18}O$ CO_3-PO_4 offset range for inclusion.

After excluding the specimens with disequilibrium offsets, the ranges of $\delta^{18}O_p$ values remained unchanged. The mean $\delta^{18}O_p$ value for all accepted samples is +9.6 ±1.2‰. The site-specific mean $\delta^{18}O_p$ values for isotopically preserved samples are +7.8 ±0.9‰ for Shestakovo, +9.0 ±0.6‰ for Krasnoyarska Kurya, and +10.5 ±0.9‰ for Volchia Griva. Statistical analysis revealed that $\delta^{18}O_p$ and $\delta^{18}Oc$ values significantly differ among the sites (Kruskal-Wallis test, $p < 0.05$). According to Tukey's Honestly Significant Difference (HSD) test, there is a statistically significant difference in $\delta^{18}O_p$ values between the Volchia Griva site and both the Krasnoyarska Kurya site (mean difference = 1.1971, $p < 0.05$ for $\delta^{18}O_p$) and the Shestakovo site (mean difference = 2.2704, $p < 0.05$ for $\delta^{18}O_p$). No significant difference in $\delta^{18}O_p$ values was observed between the Krasnoyarska Kurya and Shestakovo sites (mean difference = –1.0732, $p = 0.1517$ for $\delta^{18}O_p$).

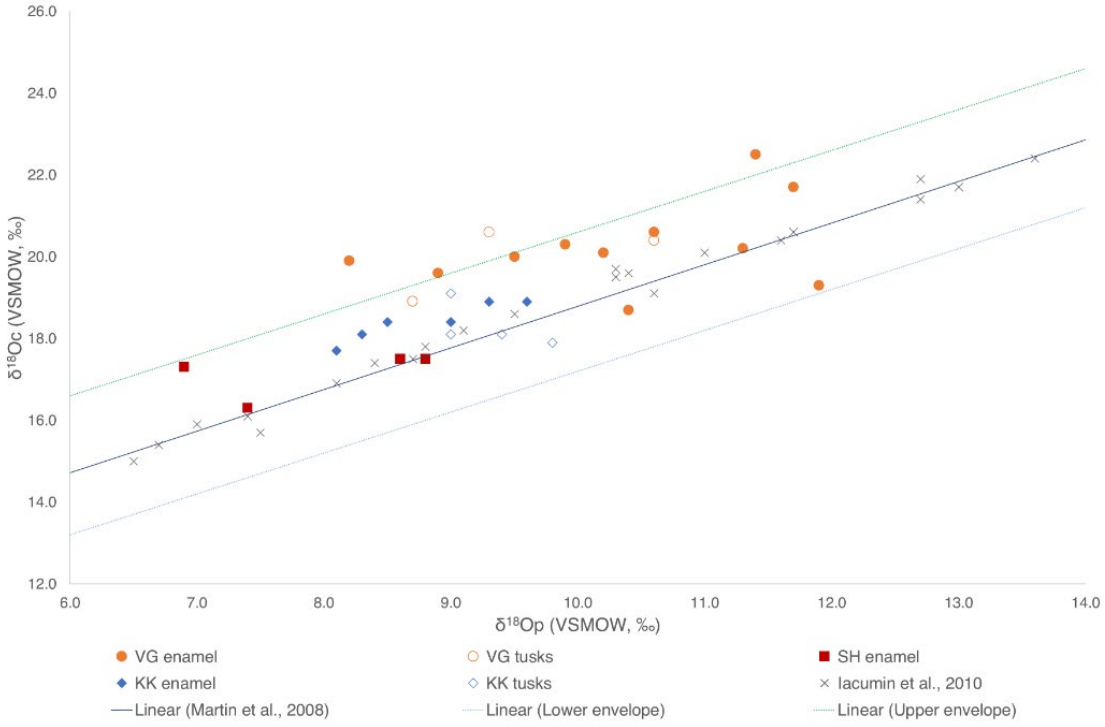

Figure 5. The relationship between oxygen isotope compositions of carbonate ($\delta^{18}Oc$) and phosphate ($\delta^{18}Op$) of bioapatite in mammoth dental samples from SEWS. The solid line $\delta^{18}Oc = 1.037 (\pm 0.026)\ \delta^{18}Op + 8.57 (\pm 0.504)$, with $r = 0.98$ ($p < 0.0001$) represents isotopic equilibrium between $\delta^{18}Oc$ and $\delta^{18}Op$ according to Martin et al. (2008), along with the dotted lines representing the upper and lower envelopes for the acceptable range of $\delta^{18}Oc$ - $\delta^{18}Op$ offsets from 7.4 to 10.6. In addition to the (Martin et al., 2008) dataset, the graph shows 23 mammoth and bison bone samples from northern Siberia with well-preserved isotopic values from (Iacumin et al., 2010) to compare with our dataset.

3.2.2 δ^{18}Ow values

Following the assessment of $\Delta^{18}O$ CO_3-PO_4 offsets, 25 samples were retained to reconstruct environmental water δ^{18}Ow values. This subset of 25 samples will be called the "new southeastern West Siberian (SEWS) dataset" in the following sections. The reconstructed δ^{18}Ow values for each sample and reconstruction errors associated with them are provided in Table 1. The δ^{18}Ow values of the horse and deer samples from Shestakovo were significantly lower than those of the mammoth specimens from the same site. For the purpose of presenting the mean values, only the mammoth specimens were used due to the constraints imposed by the error propagation method and to ensure comparability between the sites. The mean δ^{18}Ow value for all accepted mammoth samples is –14.6 ±1.1‰ (Table 1). The site-specific mean δ^{18}Ow values for isotopically preserved mammoth samples are –16.6 ±1.6‰ (n = 2) for Shestakovo, –15.2 ±1.2‰ (n = 11) for Krasnoyarska Kurya, and –13.6 ±1.0‰ (n = 11) for Volchia Griva (Table 1).

3.3 Carbon and nitrogen isotopes

3.3.1 The preservation of mammoth samples in SEWS and Eastern Baltics

The collagen yields varied significantly between 0.03% and 53%. Excluding two outliers with exceptionally high yields of 40.1% (VG 26) and 53.3% (VG 27), the average yield across the entire dataset was 0.5%. These high collagen yield values are likely due to the errors made during the weighting process. Despite this variability, sufficient collagen was extracted from all samples to obtain reliable IRMS measurements.

Out of the 29 samples analysed, 13 were excluded from the dataset. Some of the rejected samples displayed very low collagen yields, such as KK 60 (0.04%) and VG 22 (0.03%) (see Supplementary Data of **Paper III**). The full dataset, including reasons for rejection, is available in the Supplementary Data of **Paper III**. Sixteen samples remained in the final dataset, all considered to retain their original isotopic values (Table 1).

Although the accepted samples had C > 13% and N > 4.8% (Ambrose, 1990), well-preserved collagen should typically have nitrogen content ranging from 11% to 17% (Ambrose, 1990; Sealy et al., 2014; van Klinken, 1999). Five of the 16 accepted samples had N concentrations below 11%. For carbon content, (van Klinken, 1999) reported a mean C% of 34.8 ±8.8 in a large collection of well-preserved collagens, while higher values ranging from 41% to 47% were suggested by (Ambrose, 1990) and (Sealy et al., 2014). In our dataset, all C% values of the accepted sample met van Klinken's criteria but did not reach the higher values proposed by (Ambrose, 1990) and (Sealy et al., 2014).

The C:N ratios for the accepted and rejected samples varied widely, from 3.3 to 24.3 (Table 1). Among the accepted samples, the C:N ratios fell within higher end of the acceptable range (2.9–3.6) (Ambrose, 1990), with values ranging from 3.3 to 3.6. One of the rejected samples, SH 54, had an acceptable C:N ratio of 3.6 but was excluded due to extremely low collagen yield (0.07%), decreased C% (16.6%) and N% (5.4%) values, and a high δ^{13}C value (–18.8‰) compared to other samples from the same site. The remaining 12 rejected samples exhibited C:N ratios above 3.6, ranging from 3.6 to 24.4, suggesting contamination by carbon or loss of nitrogen. The highest C:N ratios were observed in KK 60 (24.4) and VG 18 (15.9) (see Supplementary Data of **Paper III**), indicating the presence of carbon contamination and/or nitrogen loss. Additionally, KK 60 and VG 18 exhibited lower δ^{13}C values (–25.6‰ and –23.6‰, respectively) and δ^{15}N values (+5.4‰ and +5.6‰, respectively) than the other samples.

Samples TAM G441:47 and TAM G441:48 exhibited C:N ratios of 4.1 and 2.7, respectively, which fall outside the generally accepted range. In contrast, the samples KRÜ and KUK displayed acceptable C:N ratios of 3.1 and 3.3, respectively.

3.3.2 $\delta^{13}C$ and $\delta^{15}N$ Values of SEWS

The overall ranges of $\delta^{13}C$ and $\delta^{15}N$ values for both accepted and rejected samples span from –25.6‰ to –14.5‰ and from +3‰ to +15‰, respectively (Supplementary Data of **Paper III**). The broad range of $\delta^{13}C$ values reflects the alteration and contamination effects in poorly preserved samples, while the $\delta^{15}N$ range corresponds to taxon-specific ecological differences. Amongst the rejected samples, KK 60 and VG 18 exhibited the lowest $\delta^{13}C$ values (–25.6‰ and –23.6‰, respectively) and the lowest $\delta^{15}N$ values for mammoth samples (5.4‰ and 5.6‰, respectively). These distinctive $\delta^{13}C$ and $\delta^{15}N$ values were associated with low carbon (C%) values (< 10%) and nitrogen (N%) values (< 1%) (Supplementary Data). Additionally, VG 21 exhibited the highest $\delta^{13}C$ value in the dataset (–14.5‰), which was also associated with lower C% (12.03%) and N% (2.07%) values, similar to KK 60 and VG 18 (Supplementary Data of **Paper III**).

Table 1 presents the $\delta^{13}C$ and $\delta^{15}N$ values for the accepted samples, along with their site-specific ranges, means, and the overall range and mean for the accepted dataset. The results of the statistical analysis are provided in Table 1. In summary, the $\delta^{13}C$ and $\delta^{15}N$ values for Shestakovo and Krasnoyarskaya Kurya are similar, while Volchia Griva exhibits distinct $\delta^{13}C$ and $\delta^{15}N$ values. Given the small number of accepted samples from Shestakovo and their statistically similar isotopic values compared to Krasnoyarskaya Kurya, as well as the relatively close proximity of these two sites, we treated the values from Shestakovo and Krasnoyarskaya Kurya as a single dataset for further comparison. The combined averages are $\delta^{13}C$: –21.1‰ ±0.05 and $\delta^{15}N$: 8.0‰ ±0.07, while Volchia Griva has an average of $\delta^{13}C$: –20.3‰ ±0.06 and $\delta^{15}N$: 13.2‰ ±0.06. The average values and standard deviations for Shestakovo and Krasnoyarskaya Kurya exclude SH 53, as it is a horse molar.

3.3.3 $\delta^{13}C$ and $\delta^{15}N$ Values of Eastern Baltics

KRÜ yielded a $\delta^{15}N$ value of +9.8‰ and a $\delta^{13}C$ value of −21.1‰; KUK had a $\delta^{15}N$ value of +10.1 ±0.02‰ and a $\delta^{13}C$ value of −20.6 ±0.05‰; TAM G441:47 yielded a $\delta^{15}N$ value of +7.4 ±0.09‰ and a $\delta^{13}C$ value of −20.2 ±0.4‰. TAM G441:48 had a $\delta^{15}N$ value of +6.5 ±0.9‰ and a $\delta^{13}C$ value of −21.2 ±0.9‰.

Table 1. Studied SEWS mammoth samples with oxygen isotope and FTIR results. M in the table stands for Mammoth, H for Horse, D for Deer. Orange colour shows the values of the inorganic fraction outside of the acceptable range, pink colour shows the values of the organic fraction outside of the acceptable range, green colour shows that the samples have been accepted, red colour shows that the samples has been rejected. The IDs of samples rejected from both datasets used for paleoclimatic reconstruction are shown in square brackets and separated from the accepted dataset with a line. The calculated δ^{18}Ow values (see Methods for equations) are given with the associated reconstruction error based on (Pryor et al., 2014). FTIR indices (C/P and IRSF) that fall out of the acceptable range recommended by (France et al., 2020) are shown in italics. VG 18 and 30 failed to yield any Ag_3PO_4 crystal.

Sample ID	Tissue type	Visual inspection	C/P	IRSF	δ^{18}Op (VSMOW, ‰)	δ^{18}Oc (VSMOW, ‰)	Δ^{18}O CO3-PO4	δ^{18}Ow	δ^{15}N (‰, AIR) ± SD	δ^{13}C (‰, V-PDB)	C:N	Paper I | Paper III	
SH 53	H enamel	Acceptable	0.155	3.42	+8.8 ± 0.09	+17.5	+8.7	- 19.4 ± 2.9	+3.0 ± 0.02	-20.3	3.6		
SH 54	D enamel	Acceptable	0.109	3.648	+7.4 ± 0.03	+16.3 ± 0.20	+8.9	- 21.4 ± 2.7	+6.4 ± 0.13	-18.8 ± 0.24	3.4		**Low collagen yield**
SH 55	M enamel	Good	*0.079*	*4.155*	+6.9 ± 0.08	+17.3	+10.4	-17.4 ± 2.0	+6.1 ± 0.04	-21.0 ± 0.01	3.4		
SH 56	M enamel	Good	0.132	3.508	+8.6 ± 0.03	+17.5 ± 0.21	+8.9	-15.6 ± 1.8	+8.8 ± 0.09	-20.5 ± 0.06	3.4		
Min.					*+6.9*	*+16.3*	*+8.7*	*- 21.4*	*+6.1 (mammoth)*	*-21.0 (mammoth)*			
Max.					*+8.8*	*+17.5*	*+10.4*	*-15.6*	*+8.8 (mammoth)*	*-20.5 (mammoth)*			
Average					*+7.8*	*+17.4*	*+9.7*	*-16.5*	*+7.5 (mammoth)*	*-20.7 (mammoth)*			
KK 57	M enamel	Good	0.105	3.891	+8.5 ± 0.14	+18.4 ± 0.03	+9.9	-15.7 ± 1.8	+8.3 ± 0.01	-20.1 ± 0.11	3.6		
KK 58	M enamel	Good	0.107	4.023	+9.6 ± 0.55	+18.9 ± 0.17	+9.3	-14.6 ± 1.8	+7.8 ± 0.02	-21.4 ± 0.12	3.5		
KK 59	M enamel	Good	0.097	*4.348*	+8.3 ± 0.02	+18.1 ± 0.05	+9.8	-16.0 ± 1.9	+8.6 ± 0.17	-21.5 ± 0.06	3.4		
KK 60	M tusk	Acceptable	0.094	3.927	+9.0 ± 0.22	+18.1 ± 0.14	+9.1	-15.2 ± 1.8	*+5.4*	*-25.6*	*24.4*		**Low collagen yield + C:N + C% + N%**
KK 61	M tusk	Acceptable	0.091	*4.475*	9.4	+18.1 ± 0.17	+8.7	-14.8	+7.1 ± 0.02	-21.9 ± 0.0	3.6		
KK 62	M enamel	Good	0.118	3.775	+8.1 ± 0.13	+17.7 ± 0.05	+9.6	-16.2 ± 1.9	-	-	-		**No δ^{15}N and δ^{13}C values**
KK 63	M enamel	Good	0.101	3.962	+9.0 ± 0.12	+18.4 ± 0.26	+9.4	-15.2 ± 1.8	+8.0 ± 0.26	-21.9 ± 0.03	*4.6*		

KK 64	M enamel	Very good	0.088	3.561	+9.3 ± 0.04	+18.9	+9.6	-14.9 ± 1.8	+9.4 ± 0.12	-21.1 ± 0.01	3.3		
KK 65	M tusk	Very good	*0.05*	*5.184*	+9.8 ± 0.14	+17.9	+8.1	-14.4 ± 1.8	+8.1 ± 0.08	-21.6 ± 0.03	3.3		
KK 66	M tusk	Acceptable	*0.032*	*5.223*	+9.0 ± 0.21	+19.1 ± 0.19	+10.1	-15.2 ± 1.8	-	-	-		
Min.					*+8.1*	*+17.7*	*+8.1*	*-16.2*	*+7.1*	*-21.9*			
Max.					*+9.8*	*+19.1*	*+10.1*	*-14.4*	*+9.4*	*-20.1*			
Average					*+9.0*	*+18.4*	*+9.4*	*-15.2*	*+8.2*	*-21.3*			
VG 16	M enamel	Acceptable	0.083	3.917	+9.5 ± 0.03	+20.0	+10.5	-14.7 ± 1.8	+12.6 ± 0.06	-20.8 ± 0.04	3.3		
VG 17	M enamel	Acceptable	0.117	*4.236*	+11.9 ± 0.02	+19.3	+7.4	-12.1 ± 1.6	+14.0 ± 0.17	-21.0 ± 0.54	*5.4*		**Elevated C:N**
VG 19	M tusk	Acceptable	0.054	*5.678*	+10.6 ± 0.05	+20.4	+9.8	-13.5 ± 1.7	+11.4 ± 0.21	*-18.4 ± 0.04*	*9.3*		**Elevated C:N**
VG 20	M tusk	Acceptable	0.091	*5.034*	+8.7 ± 0.13	+18.9	+10.2	-15.5 ± 1.8	+11.5	-22.7 ± 1.40	*5.6*		**Elevated C:N + C% + N%**
VG 22	M enamel	Good	0.153	3.406	+10.2	+20.1	+9.9	-13.9	+13.1 ± 0.18	*-15.5 ± 0.59*	*5.6*		**Low collagen yield + elevated C:N + N%**
VG 24	M enamel	Acceptable	0.114	3.801	+10.4 ± 0.21	+18.7 ± 0.07	+8.7	-13.7 ± 1.7	+14.9 ± 0.08	-19.0 ± 0.08	*3.7*		**Low collagen yield + elevated C:N**
VG 26	M enamel	Very good	0.084	4.068	+10.6 ± 0.08	+20.6 ± 0.10	+10	-13.5 ± 1.7	+14.9 ± 0.03	-19.0 ± 0.23	3.5		
VG 28	M tusk	Very good	0.054	*4.931*	+10.6 ± 0.03	+20.4 ± 0.05	+9.8	-13.5 ± 1.7	+15.0	-19.4	*6.5*		**Low collagen yield + elevated C:N + N%**
VG 31	M enamel	Acceptable	0.069	*4.446*	+11.3 ± 0.51	+20.2 ± 0.13	+8.9	-12.8 ± 1.7	+11.3 ± 0.02	-20.5 ± 0.0	3.4		
VG 32	M enamel	Acceptable	0.088	*4.382*	+11.7 ± 0.48	+21.7 ± 0.20	+10.0	-12.3 ± 1.6	+11.8 ± 0.07	-20.6 ± 0.10	3.5		
VG 34	M enamel	Acceptable	-	-	+9.9	+20.3 ± 0.21	+10.4	-14.3	+14.0 ± 0.13	-20.8 ± 0.04	3.3		

Min.					***+8.7***	***+18.7***	***+7.4***	***-15.5***	***+11.3***	***-20.9***			
Max.					***+11.9***	***+21.7***	***+10.5***	***-12.1***	***+14.9***	***-19.0***			
Average					***+10.5***	***+20.1***	***+9.6***	***-13.6***	***+13.2***	***-20.3***			
[VG 18]	M tusk	Acceptable	***-0.009***	***8.058***	-	+22.2	-	-	***+5.6 ± 1.79***	***-23.6 ± 0.03***	***15.9***	**Disequilibrium**	**Elevated C:N + C% + N%**
[VG 23]	M enamel	Good	0.161	3.627	+11.4	+22.5	***+11.1***	-	+12.6 ± 0.02	-20.0 ± 0.09	***3.8***	**Disequilibrium**	**Low collagen yield + elevated C:N**
[VG 25]	M enamel	Good	0.133	3.258	+8.9	+19.6	***+10.7***	-	-	-	-	**Disequilibrium**	**No $\delta^{15}N$ and $\delta^{13}C$ values**
[VG 29]	M tusk	Good	***0.036***	***5.492***	+9.3 ± 0.13	+20.6	***+11.3***	-	-	-	-	**Disequilibrium**	**No $\delta^{15}N$ and $\delta^{13}C$ values**
[VG 30]	M enamel	Good	0.624	3.672	-	-	-	-	+14.5 ± 0.16	-19.6 ± 0.14	***4.0***	**Disequilibrium**	**Low collagen yield + elevated C:N**
[VG 33]	M enamel	Acceptable	-	-	+8.2 ±0.09	+19.9	***+11.7***	-	+13.3	-20.7	***3.4***	**Disequilibrium**	**Low collagen yield**

3.4 Land cover reconstruction

Maps illustrating land cover proportions based on pollen data and plant macrofossil presence/absence were made for Estonia and Latvia, depicting open (represented by herbs and shrubs) and forested (represented by tree taxa) land cover across three distinct time periods: GI-1 (14.6–12.85 ka cal BP), GS-1 (12.85–11.7 ka cal BP), and EH (11.7–11.3 ka cal BP) (Figure 6).

GI-1 (14.6–12.85 ka cal BP) (Figure 6). During this period, the Baltic Ice Lake covered half of Estonia, with its northern boundary defined by the glacier (Rosentau et al., 2009; Vassiljev & Saarse, 2013). The dominant vegetation consisted primarily of herbaceous plants, indicating a cold, open environment with limited tree cover. Pollen data show the presence of trees in northern and southern Estonia and central Latvia. In contrast, plant macrofossils suggest predominantly open landscapes with no tree cover in central and northern Estonia, and a mixture of open and forested areas in southern Estonia and central Latvia.

GS-1 (12.85–11.7 ka cal BP) (Figure 6). Pollen data show a decline in forest cover across central Estonia, resulting in an open landscape, while northern and southern Estonia retained some tree cover. Plant macrofossils support the dominance of open landscapes in Estonia, with trees present only in central Latvia.

EH (11.7–11.3 ka cal BP) (Figure 6). Pollen data indicate a predominantly open landscape in eastern Estonia, while forests dominated the northern, western, and southern regions of Estonia and southern Latvia. Plant macrofossil evidence shows the establishment of trees in northern Estonia and their continued presence in central Latvia, whereas in central and southern Estonia, trees began to establish during this period.

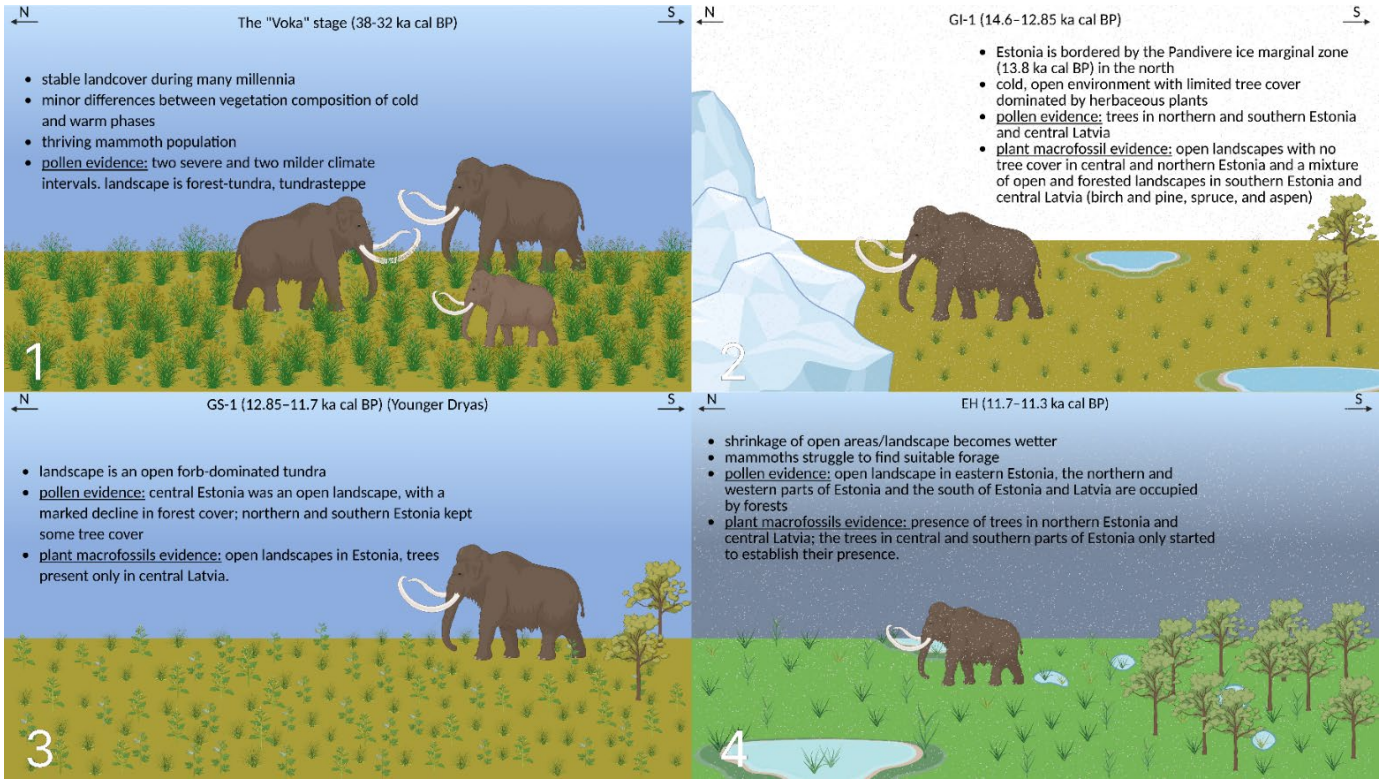

Figure 6. 1) Scheme illustrating the "Voka" stage in Estonia. The scheme is designed based on the pollen analysis done by Molodkov et al., (2007); Molodkov & Bolikhovskaya, (2022) and the isotopic analysis of mammoth tusks from Krüüdneri and Kukemetsa in ***Paper II****. 2) Scheme of the GI-1 stage in Estonia. The scheme is designed based on the landcover reconstruction in* ***Paper II****, the timing of the ice marginal zones after Rosentau et al., (2009); Vassiljev & Saarse, (2013) and supported by Amon et al., (2012); Veski et al., (2012). 3) Scheme of the Younger Dryas stage in Estonia. The scheme is designed based on the landcover reconstruction in* ***Paper II*** *and supported by (Amon et al., 2012; Veski et al., 2012). 4) Scheme of the Early Holocene stage in Estonia. The scheme is designed based on the landcover reconstruction in* ***Paper II*** *and supported by Amon et al., (2012); Veski et al., (2012).*

4 Discussion

4.1 Sample preservation

Compared to samples from high northern latitudes buried in permafrost conditions (Kohn and Cerling, 2002; Metcalfe and Longstaffe, 2012), the SEWS samples have poorer preservation overall. Notably, tusks from Krasnoyarskaya Kurya and Volchia Griva showed signs of carbonate loss and accompanying structural changes based on the elevated IRSF values and low C/P ratios. Nevertheless, the majority of their $\delta^{18}O$ values have remained intact and can be used for palaeoclimatic reconstructions.

Low collagen yields in the studied material suggest that collagen loss occurred, which is common for subfossil finds and which can serve as a sign of general degradation (van Klinken, 1999). The samples from all three SEWS sites may have degraded. In **Paper I**, we suggested that microbial heterotrophy potentially compromised the oxygen isotope integrity of the mineral part of some of the samples, and we also suggest that the same factor could have contributed to collagen deterioration as well. Moreover, the formation conditions of Volchia Griva, which included shifts between dry and wet phases (Leshchinskiy, 2018), could also create an environment favourable for the physical deterioration of the samples. It should be noted, however, that low collagen yields do not definitively suggest interactions with exogenous molecules, and the fact that degradation occurred does not mean that the isotopic integrity has also been compromised (van Klinken, 1999).

The preservation of the mammoth tooth samples from the Eastern Baltics was not ideal as well. While based on the oxygen isotopic results, the mineral fraction of the Puurmani seems to have remained intact (see Arppe & Karhu, (2010)), the C% and N% values and the C:N ratio of the samples from both Puurmani mammoth samples indicated that the organic part is likely to have been altered by post-depositional processes. However, it is challenging to establish the factor that caused this alteration due to the lack of information about the burial context and the small selection of samples. The poor preservation of the two mammoth molar samples from Puurmani has posed significant challenges to our research, as the samples' condition raises concerns about the reliability of the nitrogen and carbon isotopic values as well as 14C dating.

Paper I established that the inorganic fraction of most samples from Shestakovo, Krasnoyarskaya Kurya and Volchia Griva is intact. Nevertheless, some tusk and enamel samples showed signs of post-depositional isotopic and chemical alteration. Specifically, tusks from Krasnoyarskaya Kurya and Volchia Griva experienced carbonate loss and structural changes based on the elevated IRSF values and lower C/P ratios (France et al., 2020). Unfortunately, we were unable to establish the exact cause of the loss, because it could have been due to a combination of site-specific conditions and sample pretreatment methods.

We compared the preservation assessment results of the mineral fraction from **Paper I** with our evaluation of the organic fraction to determine whether there is a connection between the alteration of the mineral and organic components in our samples (Supplementary Data of **Paper III**). While we did not find any direct correlation, we did nevertheless notice that presentation visually estimated as poor is more strongly associated with the deterioration of the collagen, than with the mineral component at the SEWS sites. We also compared collagen quality control (QC) parameters with the elevated Infrared Splitting Factor (IRSF) values to see whether there is any clear relationship between the two factors, but we did not find any. For instance, the samples

with elevated IRSF values from Shestakovo and Krasnoyarskaya Kurya had acceptable collagen yields, C% and N% values and C:N ratios (Supplementary Data of **Paper III**, T1).

The samples from Volchia Griva exhibited more clear signs of post-depositional alteration than those from Shestakovo and Krasnoyarskaya Kurya, along with a stronger correlation between the preservation of mineral and organic component. Specifically, of the 19 Volchia Griva samples analysed for phosphate $\delta^{18}O$ values, eight showed elevated IRSF values (Table 4), indicating chemical alteration of the mineral fraction. Notably, seven of these eight also displayed elevated C:N ratios, suggesting degradation of the organic component as well. In total, ten Volchia Griva samples were excluded based on high C:N ratios, six of which also had nitrogen concentrations below 3.5% and C:N ratios exceeding 3.6—characteristics associated with the presence of non-collagenous compounds such as lipids and humic acids (Guiry & Szpak, 2021). Although the link between carbonate-phosphate disequilibrium and elevated C:N ratios is not consistent across all samples, three samples from Volchia Griva with high C:N values also demonstrated carbonate-phosphate disequilibrium, a sign of bioapatite isotopic alteration (Supplementary Data of **Papers I** and **III**). Notably, all samples showing this disequilibrium came from Volchia Griva, which shows that both the organic and mineral components of specimens from this site have undergone more severe diagenetic alteration than those from Shestakovo and Krasnoyarskaya Kurya.

4.1.1 Preservation summary

Many isotopic and ancient DNA studies focus on well-preserved mammoth remains from permafrost regions in northern Siberia. While mammoth tissues are indeed better preserved under permafrost conditions, focusing on a specific geographic area limits our understanding of mammoth ecology: these creatures inhabited a large territory spanning from Ireland to Alaska (Guthrie, 1968; Kahlke, 1999; Stuart, 2005), and obtaining isotopic records from underrepresented regions such as SEWS is essential for a more detailed understanding of their dietary habits and migratory patterns. Our research demonstrates that samples not preserved under permafrost conditions can still yield reliable results for palaeoenvironmental reconstructions.

4.1.2 Environmental and climate dynamics

The calculated mean $\delta^{18}Ow$ for the SEWS sites is −14.6‰. According to the Online Isotopes in precipitation calculator (OIPC 3.1; Bowen & Revenaugh (2003)) and to a lesser extent the IAEA records (−14.6‰; GNIP, Novosibirsk meteorological station, year 1991), the present-day mean annual $\delta^{18}Ow$ values at all three sites are similar to mean value of −14.6 ‰ calculated for the LGM. Thus, we did not observe the changes in the $\delta^{18}Ow$ value of precipitation between ca. 28–22 ka cal BP the SEWS dataset and the present-day at the mean annual level. This observation is consistent with the outcomes of the Genoni et al. (1998) paper, where the authors suggest that, indeed, the mean isotopic composition of atmospheric precipitation over Southern Siberia was not significantly lower than that of modern mean annual precipitation; compared to the present day, the summers were hotter, and the winters were colder.

$\delta^{18}Ow$ values increase from the deposition of the bone-bearing layer at SH (ca. 28–27 ka cal BP) with lower $\delta^{18}Ow$ values to those of Volchia Griva (24–22 ka cal BP). According to the studies of the present day patterns of $\delta^{18}Ow$ in precipitation by Butzin et al., (2014); Kurita et al., (2004) that air temperature is the main controlling factor of the variability (ca. 80%) in $\delta^{18}Ow$ of annual precipitation in Russia, however,

the wintertime δ^{18}Ow-T correlation is the main driving factor behind this correlation. Therefore, if during glacial times, the same relationship between δ^{18}Ow and temperature existed, the SEWS δ^{18}Ow values likely reflect changes in winter air temperatures in particular and the climate warming in the region overall.

LGM is not represented in the previous δ^{18}Ow records for the southeast of Western Siberia (Genoni et al., 1998), and the only reference values suitable for comparison with SEWS consist primarily of reindeer samples and are from the post-LGM time: Afontova Gora II site with an average δ^{18}Ow value of −13.6‰ (17.2–15.5 ka cal BP) and one reindeer bone sample from the Listvenka site of −12.7‰ (16.2 ka cal BP) (Figure 4; Genoni et al., 1998). Compared to these values, the mean δ^{18}Ow values at Shestakovo and Krasnoyarskaya Kurya are lower, but the Volchia Griva's site-specific mean of −13.6 ±1 ‰ is similar to them. Since material from Volchia Griva is from the youngest layer analysed (ca. 24–22 ka cal PB), the similarity of Volchia Griva's mean value to that of post-LGM records supports the hypothesis of the temporal development of the climate in the region.

The nearest δ^{18}Ow LGM records are in the European Plain at a similar low latitude to that of the SEWS: in Khotylovo (29.2 ka cal BP); −11.6‰) and Avdeevo (27 ka cal BP; −11.8‰) (Figure 7; Genoni et al., 1998), which have a mean glacial δ^{18}Ow value of −11.6‰. The mean δ^{18}Ow values for Shetaskovo, Krasnoyarska Kurya and Volchia Griva during LGM were lower compared to those from the European Plain, which is consistent with the present-day pattern of δ^{18}O values of precipitation over Eurasia: according to (OIPC 3.1; Bowen and Revenaugh, 2003), the modern mean δ^{18}O precipitation values in SEWS (−14.6‰) are 4.6‰ lower than the annual mean δ^{18}O precipitation values for the European plain: −10.0‰ (Figure 7). **Paper I** explains that such a difference between the mean δ^{18}Ow values of the southeast of Western Siberia and the European plain shows that there was a similar gradient of the depletion of δ^{18}O in precipitation over Eurasia at this latitude and that the "continental effect" during LGM was similar to present (Rozanski et al., 1993).

The outcomes of **Paper I** align with results from previous studies, such as those by Genoni et al. (1998) and Szpak et al. (2010). For example, Szpak et al. (2010) suggested that mammoths were able to cope well with the extreme climatic conditions of the LGM. This interpretation is further supported by the phylogeographic analyses conducted by (Debruyne et al., 2008), which indicated that the LGM had only a minimal effect on the overall genetic diversity of high-latitude mammoth populations in Eurasia and North America.

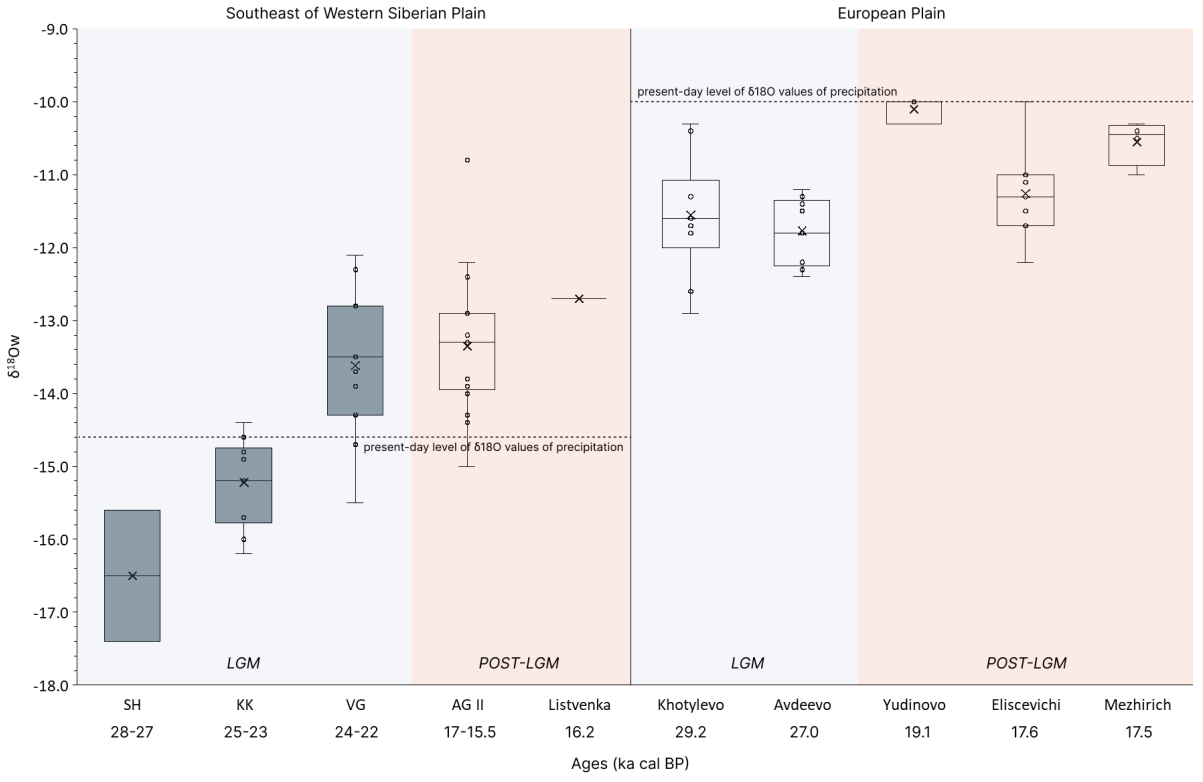

Figure 7. Comparison of δ^{18}Ow values reconstructed bioapatite δ^{18}Op values from two low-latitude areas in Eurasia: the southeast of Western Siberia based on the new SEWS dataset as well as data from (Genoni et al., 1998) for Afontova Gora (AG II) and Listvenka; and sites of the European plain (Genoni et al., 1998). Box and whisker statistics are drawn for all data with finite calibrated dates from published sources. The numbers next to the boxes and datapoints refer to calendar years in ka cal BP. Horizontal dashed lines represent the regions' present-day level of δ^{18}O values in precipitation.

4.2 Carbon and nitrogen isotopic interpretation

We used a large carbon and nitrogen isotopic dataset comprised of mammoth data from the Northern Siberian sites spanning 60–12 ka (Arppe et al., 2019) with averages for $\delta^{13}C$ (–21.7 ±0.6‰; n = 82) and $\delta^{15}N$ (9.0 ±1.8‰; n = 82) ("the Northern Siberian dataset" further in the text) as a point of comparison with our dataset consisting of carbon and nitrogen isotopic data from Shestakovo and Krasnoyarskaya Kurya ("SH+KK dataset") and Volchia Griva ("VG dataset"). Isotopic values at Volchia Griva clearly stand out from both SH+KK and Northern Siberian mammoth data, therefore the comparisons of SH+KK and VG datasets to the Northern Siberian dataset will be discussed separately below in the text.

While the $\delta^{13}C$ values of the SH+KK dataset (−21.1‰) and the Northern Siberian dataset (−21.7‰) (Figure 8) suggest that the diet of mammoths in both regions consisted predominantly of C_3 plants (Ambrose & DeNiro, 1986; van der Merwe, 1982), the average $\delta^{13}C$ value from the SH+KK dataset is higher than the Northern Siberian dataset by 0.6‰, whereas the $\delta^{15}N$ average value from the SH+KK dataset is 1.3‰ lower (Figure 8 and Table 1).

A pattern similar to the one with SH+KK site mammoths having higher $\delta^{13}C$ values and lower $\delta^{15}N$ values compared to Northern Siberia, has been reported by Szpak et al., (2010), where the authors compared the $\delta^{13}C$ and $\delta^{15}N$ values of Late Pleistocene woolly mammoths in Eastern Beringia (Alaska and Yukon) with Western Beringia (i.e. Northern Siberia). Because higher $\delta^{13}C$ and $\delta^{15}N$ values are often linked to more arid climatic conditions and higher temperatures (Amundson et al., 2003; Craine et al., 2009; Gröcke et al., 1997; Heaton, 1987; Kohn, 2010; Sealy et al., 1987; Wooller et al., 2021), the pattern of lower $\delta^{15}N$ and a higher $\delta^{13}C$ contradicts this notion. According to Szpak et al. (2010), the explanation of the contrasting $\delta^{13}C/\delta^{15}N$ responses could lie in more arid conditions being the main driver behind higher $\delta^{15}N$ values in Northern Siberian mammoths. They also suggests that variations in high arctic $\delta^{13}C$ may rather reflect regional differences in mean annual temperature than the moisture differences, which is also supported by the recent climate simulations (Extended data in Wang et al., 2021).

Paper III suggested that the contrasting $\delta^{13}C/\delta^{15}N$ responses may be explained by the environmental threshold points: plant $\delta^{15}N$ values stop responding to changing mean annual temperatures (MAT) in a linear way below –0.5°C (Craine et al., 2009), and since mean annual temperatures during LGM in the Northern Siberia were far below zero (Vandenberghe et al., 2014; Wang et al., 2021), it is highly likely plant $\delta^{15}N$ values were rather insensitive to variations in temperature. As for carbon isotopes, hypothesis of 'too wet to register differences in MAP' does not seem plausible: while the correlation between plant $\delta^{13}C$ and mean annual precipitation (MAP) flattens out in wet environments (Kohn, 2010), the mammoth steppe was generally characterised by aridity with MAPs well below 500 mm/a (Wang et al., 2021).

Paper III also suggested that other alternative/complementary factors, such as metabolic strategies for dealing with aridity and/or a diet composed primarily of nutrient-poor, protein-deficient herbaceous and graminoid vegetation (Szpak et al., 2010) could explain the more elevated $\delta^{15}N$ values in the Northern Siberian dataset. A study by Wang et al. (2021) also supports the graminoid-dominated diet of the Northern Siberia mammoths by showing that vegetation during the LGM in Northern Siberia had a larger proportion of graminoids compared to Eastern Beringia. In addition, in arid environments with plants having lower protein and nitrogen levels, the $\delta^{15}N$ values

of herbivores may be elevated due to microbial recycling of nitrogen in the digestive tract (Sealy et al., 1987) or water saving mechanisms increasing the urea concentration of urine (Ambrose & DeNiro, 1986). While there is a lack of consensus on how animal metabolic processing influences the $\delta^{15}N$ tissue (Sponheimer et al., 2003), it is nevertheless plausible that some of the nitrogen-conserving mechanisms mentioned above in the text were more commonly used by the Northern Siberian mammoths, resulting in their higher $\delta^{15}N$ values. In summary, the isotopic differences between mammoth populations in Southeast Western Siberia and Northern Siberia can be explained by the differences in regional vegetation, climate, and physiological adaptations.

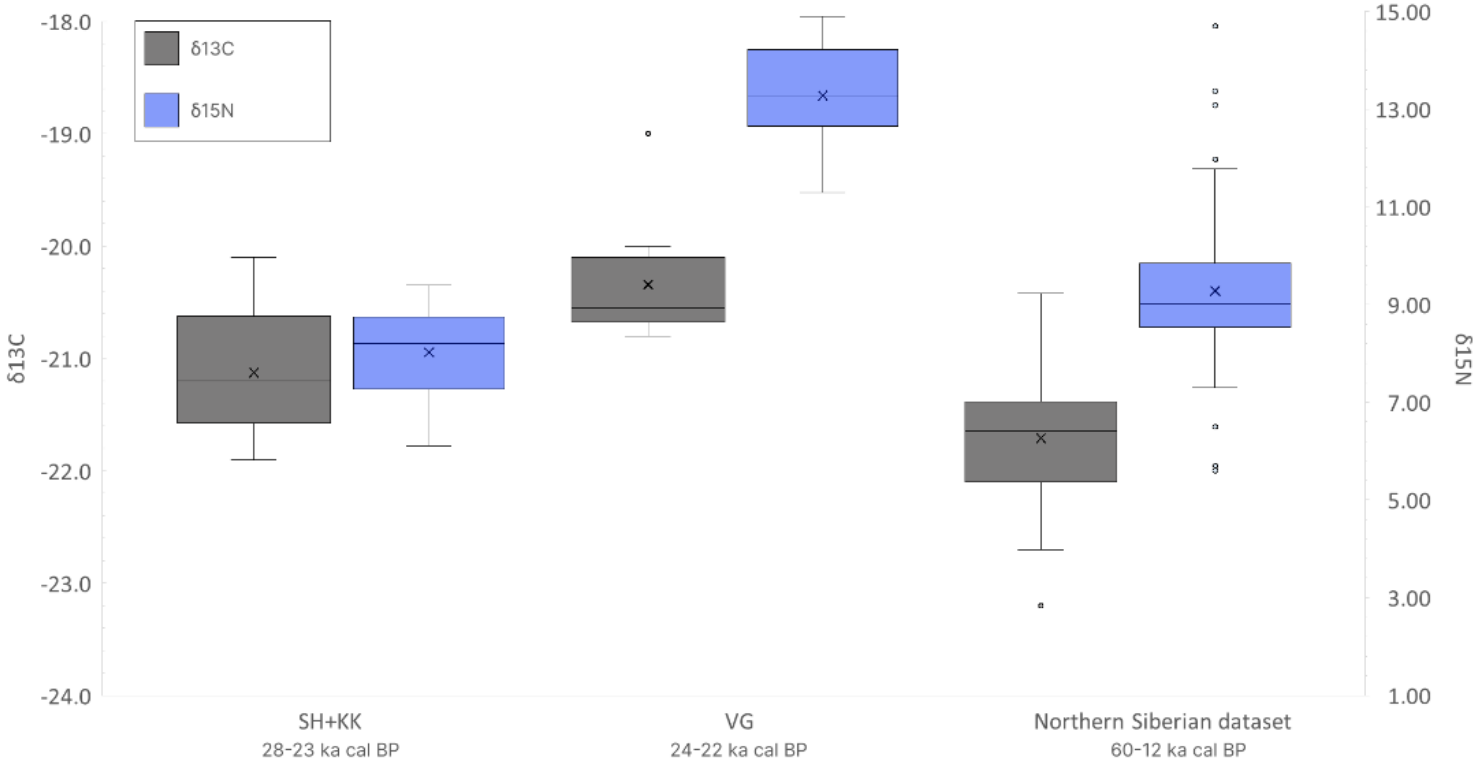

Figure 8. Comparison between the $\delta^{13}C$ and $\delta^{15}N$ values between the SH+KK, Volchia Griva and the Northern Siberian Dataset (Arppe et al., 2019; Iacumin et al., 2010; Szpak et al., 2010).

4.2.1 Unusual carbon and nitrogen isotopic values from Volchia Griva

In support of the aridity-related interpretation of the $\delta^{15}N$ data from Volchia Griva, the elevated $\delta^{13}C$ values suggest that the mammoths found there came to the area from a more arid environment, whereas their counterparts in Northern Siberia or at Shestakovo and Krasnoyarskaya Kurya came to those sites from more northern regions. This hypothesis is supported by the palynological analysis from Volchia Griva (Leshchinskiy & Burkanova, 2022), which showed an aridisation of the climate since the site's formation. The soil salinity at Volchia Griva could also contributed to the elevated $\delta^{13}C$ values (for review see van Groenigen & van Kessel (2002)). In addition, mammoths found at Volchia Griva could have supplemented their diet with C_4 plants in addition to the regular diet composed of C_3 plants: the geographical location of Volchia Griva is within the natural area of distribution of certain C_4 taxa, such as which are well adapted to saline and ruderal environments (Rakhmankulova et al., 2019; Sukhorukov et al., 2022). Pollen analysis from Volchia Griva supports the presence of such taxa at Volchia Griva: for the investigated period of 24–22 ka cal BP, Leshchinskiy & Burkanova (2022) showed the presence of Chenopodiacea, Poaceae and Asteracea pollen, families that have species that utilise the C_4-type photosynthesis (Sage, 2017).

Abnormally high $\delta^{15}N$ values of mammoths from Volchia Griva occupy a unique niche among the published isotopic records of mammoth sites globally. There are very few published samples with $\delta^{15}N$ values similar to the ones in Volchia Griva's range of 11–15‰ (e.g. Arppe et al., (2019); Bocherens et al., (1996); Iacumin et al., (2000); Kirillova et al., (2023); Metcalfe & Longstaffe, (2012); Szpak et al., (2010)). We suggest several potential factors that could have led to such high $\delta^{15}N$ values: large animal dung accumulating at mineral oases like Volchia Griva could increase plant $\delta^{15}N$ values (e.g. Szpak (2014)). Coprophagy, a common behaviour amongst mammoths, could elevate $\delta^{15}N$ values in their tissues (Clementz et al., 2009; Kuitems et al., 2015; van Geel et al., 2008, 2011). In addition, local soils at Volchia Griva are heavily salinised, which would result in high $\delta^{15}N$ values in local plants and, by extension, in local mammoths' tissues.

4.3 Eastern Baltics

Here, it is useful to shift the focus away from the southeast of Western Siberia (SEWS), as our investigation in the Eastern Baltic presents a different perspective on the mammoth history, because the investigated time period is much closer to the species' eventual disappearance in Europe.

Rapid landcover change and afforestation is considered to have largely contributed to the extinction of herbivorous megafauna in northern Europe at the end of the Pleistocene, with mammoths persisting mainly during colder stadials of post-LGM (GS-2 and GS-1) and disappearing in warmer intervals (GI-1) (Ukkonen et al., 2011). Such observation is in agreement with the results of **Paper II** and raises the question of whether a similar pattern could be observed during the earlier time periods (Veski et al., 2015). Unlike the numerous pre-LGM mammoth finds in the Eastern Baltics, well-dated sediment sequences for the period of 50–27 ka cal BP suitable for biostratigraphic analysis are rare in the region. To date, only the Voka site in northeastern Estonia, dated to 38–32 ka cal BP, provides a reliable pollen-based record for this period (Molodkov et al., 2007; Molodkov & Bolikhovskaya, 2022). The reconstructions from the pre-LGM Voka site and the GS-1 stadial show that the environment was dominated by

dry steppe-tundra, rich in forbs, with the presence of Cyperaceae, Artemisia, and Chenopodiaceae. Such landcover composition indicates that the mammoths had plenty of food sources to graze on (Guthrie, 2001). Comparison between the "Voka" stage (period of 39–32 ka cal BP) and the GS-1 stadial periods shows that while the landcover was relatively stable during pre-LGM, the post-LGM landcover was more dynamic, and the animals may have struggled to adapt to the rapid climate change-induced changes. Climate warming at the beginning of the Holocene brought tree cover expansion and the disappearance of dry steppe with tundra-like open herb communities suitable for mammoths. Plant macrofossils show the establishment of tree cover and the abrupt disappearance of *Dryas octopetala*, a key component of forb tundra, indicating that central Estonia became inhospitable for mammoths during 11.3–11.7 ka cal BP. Nitrogen isotopes obtained from Puurmani mammoth samples suggest that, in contrast to the mammoths that inhabited the Eastern Baltics during pre-LGM, post-LGM mammoths in Estonia probably had a more nitrogen-deprived diet, which aligns well with the decline of nutrient-rich herb-dominated communities and overall expansion of forests.

Additional mammoth discoveries from this period and isotopic analysis of these findings may provide more crucial insights into the trophic position of the mammoths in the Eastern Baltics. Our landcover reconstructions and isotopic results show that the rapid forestation and the limited availability of suitable nutrients significantly contributed to the decline of mammoth populations in Estonia during the late Pleistocene.

4.4 Comparison with published records

On a broader regional and chronological scale, there is an opportunity to compare the new carbon and nitrogen isotope data from SEWS and the Eastern Baltics to previously published datasets from other regions to place our results within the context of existing records. The comparative datasets and radiocarbon dates were taken from the following publications: (Arppe et al., 2019; Barbieri et al., 2008; Bocherens et al., 1994; Debruyne et al., 2008; Drucker et al., 2018; Grigoriev et al., 2017; Iacumin et al., 2000, 2010; Lõugas et al., 2002; Mann et al., 2013; Metcalfe et al., 2016; Orlova et al., 2004; Seuru et al., 2017; Szpak et al., 2010). All published carbon and nitrogen isotopic data were divided into wider geographic regions: "Eastern Baltics", "Siberia, West" (including all published carbon and nitrogen isotopic data west of 127°E meridian), "Siberia, East" (including all published carbon and nitrogen isotopic data east of 127 meridian), "East Beringia", "SEWS", "European Plain" (Figures 1 and 9; Table 2) and into three time periods: pre-LGM (before 27 ka cal BP), LGM (27–23 ka cal BP), and post-LGM (after 23 ka cal BP until 11. 7 ka cal BP) (Figure 9 and Table 2). We reported that nitrogen isotope values from Volchia Griva are among the highest reported to date in **Paper III** and above in the text, and Figure 9 shows how Volchia Griva stands out amongst other published isotopic records. Additionally, nitrogen and carbon values from Estonia and Eastern Beringia cluster closely together in the post-LGM period. This pattern may be explained by the increased wetness in both regions during post-LGM. For Eastern Beringia, this is confirmed by Szpak et al. (2010) and Wang et al. (2021), while in Eastern Baltics it is confirmed by the outcomes of **Paper II**. In general, Figure 9 shows that nitrogen values decrease in milder climates during the post-LGM. Although the comparative isotopic data available for nearby regions are sparse, and the closest comparable datasets are located thousands of kilometres away, this dissertation presents a new and substantial dataset from regions of the Eurasian mammoth steppe with scarce prior paleoenvironmental records, with extra attention given to sample preservation. Future research efforts in

southeastern Western Siberia will expand our understanding of the environmental and ecological dynamics of SEWS during the LGM.

Our study in the Eastern Baltics demonstrates that in regions where mammoth remains are rare and their geological and taphonomic context is largely lost, vegetation reconstructions based on pollen and plant macrofossil analysis can effectively complement carbon and nitrogen isotope studies. Isotopic evidence shows that the depleted $\delta^{15}N$ values observed in post-LGM mammoth samples from Estonia are consistent with those found in other European mammoth populations from the same period, indicating that these animals likely experienced a nitrogen-deficient diet. This pattern corresponds with the decline of herb-rich vegetation and the expansion of tree species less suitable for large herbivores.

Table 2. The average carbon and nitrogen isotopic values for three time periods: pre-LGM (before 27 ka cal BP), LGM (27–23 ka cal BP), and post-LGM (after 23 ka cal BP until 11. 7 ka cal BP and for Eastern Baltics, Siberia, West, Siberia, East, East Beringia, SEWS, European Plain. The comparative datasets and radiocarbon dates were taken from the following publications: Szpak et al. 2010, Iacumin et al. 2000, Arppe et al., 2019, Iacumin et al. 2010, Barbieri et al. 2008, Debruyne et al. 2008, Grigoriev et al. 2017, Mann et al. 2013, Bocherens et al. 1994, Metcalfe et al. 2016, Seuru et al. 2017, Lanoë et al. 2017, Drucker et al. 2018, Drucker et al. 2014, Orlova et al. 2004, Lõugas et al., 2002.

$\delta^{13}C$ (‰) ± SD			
Region	**Pre-LGM**	**LGM**	**Post-LGM**
Eastern Baltics	–20.9±0.3	-	–20.7±0.5
Siberia, West	–21.9±0.5	–20.9±0.0	–21.7±0.6
Siberia, East	–21.8±0.5	–21.8±0.3	–21.5±0.5
East Beringia	–20.9±0.4	–21.1±0.2	–20.8±0.3
European Plain	–20.0±0.2	-	–20.3±0.3
SEWS	-	–20.7±0.6	–21.0±0.2
$\delta^{15}N$ (‰) ± SD			
Region	**Pre-LGM**	**LGM**	**Post-LGM**
Eastern Baltics	+10.0±0.1	-	+7.0±0.5
Siberia, West	+9.0±1.3	+9.0±0.1	+9.5±1.1
Siberia, East	+9.2±1.2	+8.8±0.9	+9.1±1.7
East Beringia	+7.3±1.0	+9.0±1.1	+7.1±1.0
European Plain	+9.5±0.4	-	+5.5±1.5
SEWS	-	+11.1±2.7	+5.0±0.5

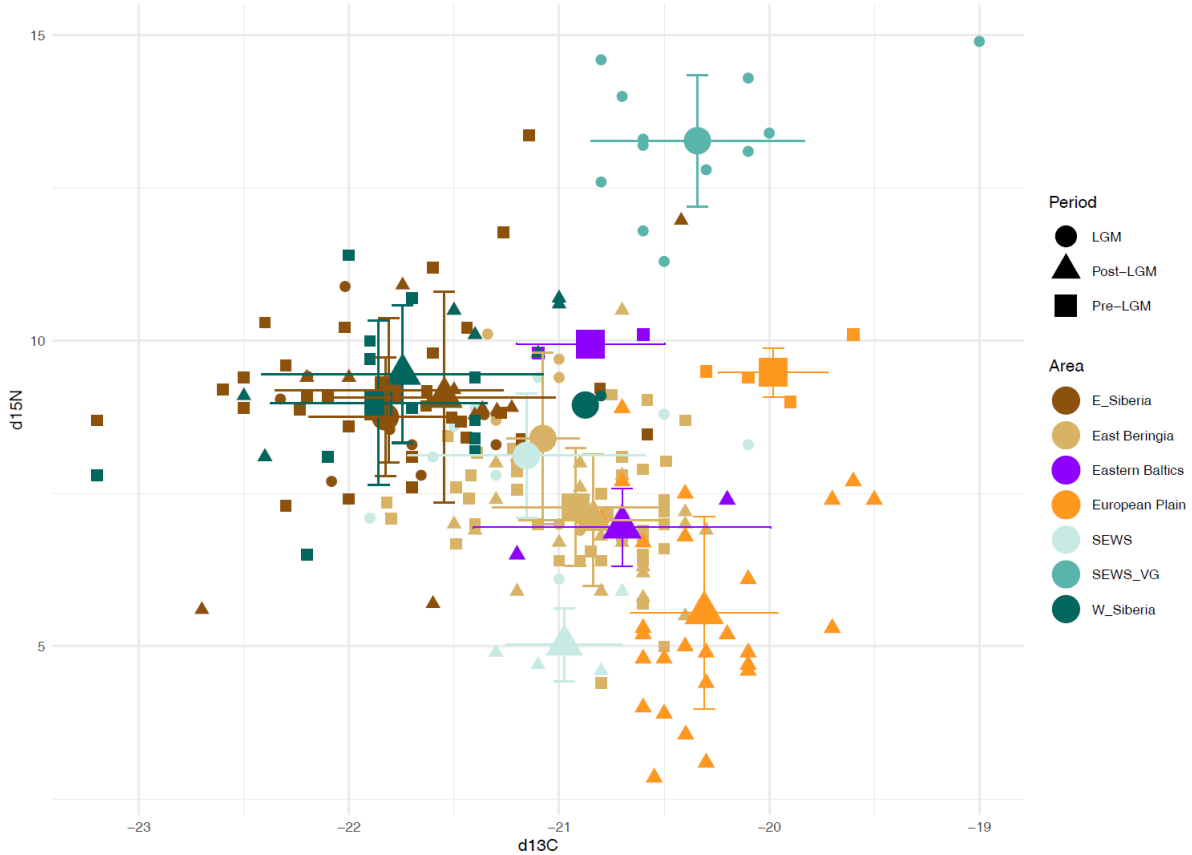

Figure 9. Comparison between the $\delta^{13}C$ values and $\delta^{15}N$ values of Eastern Baltics, Siberia, West, Siberia, East, East Beringia, SEWS, European Plain for three time periods: pre-LGM (before 27 ka cal BP), LGM (27–23 ka cal BP), and post-LGM (after 23 ka cal BP until 11. 7 ka cal BP.

In conclusion, although the two regions examined in this study—the southeast of the Western Siberian Plain and the Eastern Baltic—are geographically distant, they are connected by a shared history of being overlooked in isotopic research due to uncertainties regarding the preservation state of mammoth remains. The sites of SEWS and Eastern Baltics present challenges related to both context and preservation. Krasnoyarskaya Kurya has experienced looting in the past (Seuru et al., 2017), and Volchia Griva, despite being known since the 1950s and subjected to multiple expeditions, has also seen significant material loss (prof. Sergey Leshchinskiy, pers. comm.). Moreover, these sites are outside the permafrost zone and far from better-documented regions, complicating comparisons with existing datasets. Despite these challenges, this research took a deliberate risk in investigating samples from these underrepresented regions and from the LGM, a time period for which isotopic records in Northern Hemisphere are notably limited. Acknowledging the inherent difficulties, particularly regarding preservation, we applied rigorous evaluation methods, including the use of ATR-FTIR in **Paper I**—an approach rarely applied to evaluate enamel samples of Pleistocene age, as enamel is viewed as a generally well-preserved material. Ultimately, this study demonstrates that, with careful selection and assessment, materials from these regions can yield valuable and reliable data. It is our hope that this work will encourage future researchers to direct more attention to such sites and to further explore their potential through isotopic analysis.

5 Conclusions

This dissertation investigates the significant isotopic potential of mammoth remains from two regions that are currently underrepresented in isotopic studies: the three largest late Pleistocene sites or mammoth "cemeteries" in the southeast of the West Siberian Plain (SEWS) (Shestakovo, Krasnoyarskaya Kurya, and Volchia Griva), and the Eastern Baltics. Although substantial isotopic research has been conducted on remains from permafrost areas in Northern Siberia and Beringia, data from non-permafrost regions such as SEWS and the Eastern Baltics are still scarce.

Over the course of the PhD project, we combined stable oxygen, carbon, and nitrogen isotope analysis with pollen and plant macrofossils to reconstruct environmental conditions and mammoth diets in non-permafrost contexts. A total of 31 samples from the SEWS mammoth sites were selected and examined. The analysed specimens date to 27.5–22 ka cal BP, covering the peak of the LGM in the region. Additionally, four mammoth tooth samples from Estonia—including two from the youngest known mammoth remains in Europe—were analysed for carbon and nitrogen isotopes. Special effort was put into assessing the preservation of skeletal material, using $\delta^{18}O$ equilibrium testing and ATR-FTIR spectroscopy for bioapatite, and C:N ratios, collagen yield, and elemental composition to evaluate collagen preservation. ATR-FTIR spectroscopy is not commonly used in mammoth studies, and integrating this method to provide valuable information about post-depositional changes in the samples was an experimental step.

The preservation assessment, one of key focuses of the project, revealed that both the mineral and organic components of samples from Volchia Griva experienced post-depositional changes, possibly carbonate loss and chemical or microbial degradation. ATR-FTIR spectroscopy indicated that tusk samples from Krasnoyarskaya Kurya and Volchia Griva, in particular, were affected by carbonate loss and related structural alterations. In the Eastern Baltics, the C% and N% values, along with the C:N ratio of the youngest European mammoth samples, suggest that post-depositional processes likely altered these remains.

The oxygen isotope analysis indicated that winters during the LGM in SEWS were colder and summers warmer than present-day conditions. Within SEWS, $\delta^{18}Ow$ values increased from Shestakovo and Krasnoyarskaya Kurya (28–23 ka cal BP) to Volchia Griva (24–22 ka cal BP), pointing to a gradual warming trend. The samples from Volchia Griva were particularly outstanding in terms of their unusually high $\delta^{13}C$ and $\delta^{15}N$ values, which are the highest among other published records. Elevated $\delta^{13}C$ values suggest that mammoths that found their demise at Volchia Griva came from a more arid environment, which is supported by the palynological data indicating increasing aridity. C_4 plant consumption and local soil salinity may also have potentially influenced the $\delta^{13}C$ values of Volchia Griva's mammoths. The exceptionally high $\delta^{15}N$ values (11-15‰) could be explained by the large animal dung accumulation increasing plant $\delta^{15}N$, coprophagy and saline local soils.

In the Eastern Baltics, the disappearance of *Dryas octopetala* at the onset of the Holocene marked a shift from open to forested landscapes, making the environment unsuitable for mammoths, even in the northern parts of Estonia. The Eastern Baltics mammoths also experienced a decrease in dietary quality, which may have played a role in their regional extinction.

Integrating isotopic data with pollen and plant macrofossil records allows us to understand the environmental changes that may have influenced the extinction of

mammoth steppe megafauna more thoroughly. This research demonstrates the need for additional isotopic investigations in underrepresented areas and confirms that, when properly evaluated, non-permafrost specimens can serve as valuable sources of palaeoenvironmental data.

List of figures

List of tables

References

Aarnes, I., Bjune, A. E., Birks, H. H., Balascio, N. L., Bakke, J., & Blaauw, M. (2012). Vegetation responses to rapid climatic changes during the last deglaciation 13,500–8,000 years ago on southwest Andøya, arctic Norway. *Vegetation History and Archaeobotany*, *21*(1), 17–35. https://doi.org/10.1007/s00334-011-0320-4

Ambrose, S. H. (1990). Preparation and Characterization of Bone and Tooth Collagen for Isotopic Analysis. In *Journal of Archaeological Science* (Vol. 17). https://doi.org/https://doi.org/10.1016/0305-4403(90)90007-R

Ambrose, S. H., & DeNiro, M. J. (1986). The isotopic ecology of East African mammals. *Oecologia*, *69*(3), 395–406. https://doi.org/10.1007/BF00377062

Amon, L., Veski, S., Heinsalu, A., & Saarse, L. (2012). Timing of Lateglacial vegetation dynamics and respective palaeoenvironmental conditions in southern Estonia: evidence from the sediment record of Lake Nakri. *Journal of Quaternary Science*, *27*(2), 169–180. https://doi.org/10.1002/jqs.1530

Amundson, R., Austin, A. T., Schuur, E. A. G., Yoo, K., Matzek, V., Kendall, C., Uebersax, A., Brenner, D., & Baisden, W. T. (2003). Global patterns of the isotopic composition of soil and plant nitrogen. *Global Biogeochemical Cycles*, *17*(1). https://doi.org/10.1029/2002GB001903

Arppe, L., Aaris-Sørensen, K., Daugnora, L., Lõugas, L., Wojtal, P., & Zupiņš, I. (2011). The palaeoenvironmental δ13C record in European woolly mammoth tooth enamel. *Quaternary International*, *245*(2), 285–290. https://doi.org/10.1016/j.quaint.2010.10.018

Arppe, L., & Karhu, J. A. (2010). Oxygen isotope values of precipitation and the thermal climate in Europe during the middle to late Weichselian ice age. *Quaternary Science Reviews*, *29*(9–10), 1263–1275. https://doi.org/10.1016/j.quascirev.2010.02.013

Arppe, L., Karhu, J. A., Vartanyan, S., Drucker, D. G., Etu-Sihvola, H., & Bocherens, H. (2019). Thriving or surviving? The isotopic record of the Wrangel Island woolly mammoth population. *Quaternary Science Reviews*, *222*, 105884. https://doi.org/10.1016/j.quascirev.2019.105884

Ayliffe, L. K., Lister, A. M., & Chivas, A. R. (1992). The preservation of glacial-interglacial climatic signatures in the oxygen isotopes of elephant skeletal phosphate. *Palaeogeography, Palaeoclimatology, Palaeoecology*, *99*(3–4), 179–191. https://doi.org/10.1016/0031-0182(92)90014-V

Barbieri, M., Kuznetsova, T. V., Nikolaev, V. I., & Palombo, M. R. (2008). Strontium isotopic composition in late Pleistocene mammal bones from the Yakutian region (North-Eastern Siberia). *Quaternary International*, *179*(1), 72–78. https://doi.org/10.1016/j.quaint.2007.08.014

Barnosky, A. D., Koch, P. L., Feranec, R. S., Wing, S. L., & Shabel, A. B. (2004). Assessing the Causes of Late Pleistocene Extinctions on the Continents. *Science*, *306*(5693), 70–75. https://doi.org/10.1126/science.1101476

Bartlein, P. J., Harrison, S. P., Brewer, S., Connor, S., Davis, B. A. S., Gajewski, K., Guiot, J., Harrison-Prentice, T. I., Henderson, A., Peyron, O., Prentice, I. C., Scholze, M., Seppä, H., Shuman, B., Sugita, S., Thompson, R. S., Viau, A. E., Williams, J., & Wu, H. (2011). Pollen-based continental climate reconstructions at 6 and 21 ka: a global synthesis. *Climate Dynamics*, *37*(3–4), 775–802. https://doi.org/10.1007/s00382-010-0904-1

Ben-David, M., & Flaherty, E. A. (2012). Stable isotopes in mammalian research: a beginner's guide. *Journal of Mammalogy*, *93*(2), 312–328. https://doi.org/10.1644/11-MAMM-S-166.1

Bergman, J., Pedersen, R. Ø., Lundgren, E. J., Lemoine, R. T., Monsarrat, S., Pearce, E. A., Schierup, M. H., & Svenning, J.-C. (2023). Worldwide Late Pleistocene and Early Holocene population declines in extant megafauna are associated with Homo sapiens expansion rather than climate change. *Nature Communications*, *14*(1), 7679. https://doi.org/10.1038/s41467-023-43426-5

Beug, H. J. (2004). *Leitfaden der Pollenbestimmung fur Mitteleuropa und angrenzende Gebiete*. Publisher Verlag Friedrich Pfeil.

Birks, H. H. (2008). The Late-Quaternary history of arctic and alpine plants. *Plant Ecology & Diversity*, *1*(2), 135–146. https://doi.org/10.1080/17550870802328652

Birks, H. H., Battarbee, R. W., & Birks, H. J. B. (2000). The development of the aquatic ecosystem at Krakenes Lake, western Norway, during the late-glacial and early-Holocene - A synthesis. *Journal of Paleolimnology*, *23*(1), 91–114. https://doi.org/10.1023/A:1008079725596

Birks, H. H., & Birks, H. J. B. (2003). Reconstructing Holocene climate from pollen and plant macrofossils. In A. Mackay, R. Battarbee, J. Birks, & F. Oldfield (Eds.), *Global change in the Holocene* (pp. 342–357). London: Arnold.

Birks, H. J. B., & Birks, H. H. (1980). *Quaternary palaeoecology*.

Birks, H. J. B., & Birks, H. H. (2008). Biological responses to rapid climate change at the Younger Dryas—Holocene transition at Kråkenes, western Norway. *The Holocene*, *18*(1), 19–30. https://doi.org/10.1177/0959683607085572

Blyakharchuk, T. A., van Hardenbroek, M., Pupysheva, M. A., Kirpotin, S. N., & Blyakharchuk, P. A. (2025). Late Glacial and Holocene history of climate, vegetation landscapes and fires in South Taiga of Western Siberia based on radiocarbon dating and multi-proxy palaeoecological research of sediments from Shchuchye Lake. *Radiocarbon*, *67*(1), 1–24. https://doi.org/10.1017/RDC.2024.103

Bocherens, H. (2015). Isotopic tracking of large carnivore palaeoecology in the mammoth steppe. *Quaternary Science Reviews*, *117*, 42–71. https://doi.org/10.1016/j.quascirev.2015.03.018

Bocherens, H., Fizet, M., Mariotti, A., Gangloff, R. A., & Burns, J. A. (1994). Contribution of isotopic biogeochemistry (^{13}C, ^{15}N, ^{18}O) to the paleoecology of mammoths *(mammuthus primigenius)*. *Historical Biology*, *7*(3), 187–202. https://doi.org/10.1080/10292389409380453

Bocherens, H., Pacaud, G., Lazarev, P. A., & Mariotti, A. (1996). Stable isotope abundances (13C, 15N) in collagen and soft tissues from Pleistocene mammals from Yakutia: Implications for the palaeobiology of the Mammoth Steppe. *Palaeogeography, Palaeoclimatology, Palaeoecology*, *126*(1–2), 31–44. https://doi.org/10.1016/S0031-0182(96)00068-5

Boiko, P. V., Maschenko, E. N., & Sylerzhitskii, L. D. (2005). *A new large Late Pleistocene mammoth's locality in Western Siberia*. 22–26.

Bowen, G. J., & Revenaugh, J. (2003). Interpolating the isotopic composition of modern meteoric precipitation. *Water Resources Research*, *39*(10). https://doi.org/10.1029/2003WR002086

Bronk Ramsey, C. (2009). Bayesian Analysis of Radiocarbon Dates. *Radiocarbon*, *51*(1), 337–360. https://doi.org/10.1017/S0033822200033865

Bush, A. B. G. (2004). Modelling of late Quaternary climate over Asia: a synthesis. *Boreas*, *33*(2), 155–163. https://doi.org/10.1111/j.1502-3885.2004.tb01137.x

Butzin, M., Werner, M., Masson-Delmotte, V., Risi, C., Frankenberg, C., Gribanov, K., Jouzel, J., & Zakharov, V. I. (2014). Variations of oxygen-18 in West Siberian precipitation during the last 50 years. *Atmospheric Chemistry and Physics*, *14*(11), 5853–5869. https://doi.org/10.5194/acp-14-5853-2014

Cappers, R. T. J., Neef, R., & Bekker, R. M. (2009). *Digital Atlas of Economic Plants: Vol. Vol 1*. Barkhuis. https://doi.org/https://doi.org/10.2307/j.ctt20p56d7

Cerling, T. E., Harris, J. M., & Leakey, M. G. (1999). Browsing and grazing in elephants: the isotope record of modern and fossil proboscideans. *Oecologia*, *120*(3), 364–374. https://doi.org/10.1007/s004420050869

Cersoy, S., Zazzo, A., Lebon, M., Rofes, J., & Zirah, S. (2017). Collagen Extraction and Stable Isotope Analysis of Small Vertebrate Bones: A Comparative Approach. *Radiocarbon*, *59*(3), 679–694. https://doi.org/10.1017/RDC.2016.82

Cleator, S. F., Harrison, S. P., Nichols, N. K., Prentice, I. C., & Roulstone, I. (2020). A new multivariable benchmark for Last Glacial Maximum climate simulations. *Climate of the Past*, *16*(2), 699–712. https://doi.org/10.5194/cp-16-699-2020

Clementz, M. T., Fox-Dobbs, K., Wheatley, P. V., Koch, P. L., & Doak, D. F. (2009). Revisiting old bones: coupled carbon isotope analysis of bioapatite and collagen as an ecological and palaeoecological tool. *Geological Journal*, *44*(5), 605–620. https://doi.org/10.1002/gj.1173

Cooper, A., Turney, C., Hughen, K. A., Brook, B. W., McDonald, H. G., & Bradshaw, C. J. A. (2015). Abrupt warming events drove Late Pleistocene Holarctic megafaunal turnover. *Science*, *349*(6248), 602–606. https://doi.org/10.1126/science.aac4315

Craine, J. M., Elmore, A. J., Aidar, M. P. M., Bustamante, M., Dawson, T. E., Hobbie, E. A., Kahmen, A., Mack, M. C., McLauchlan, K. K., Michelsen, A., Nardoto, G. B., Pardo, L. H., Peñuelas, J., Reich, P. B., Schuur, E. A. G., Stock, W. D., Templer, P. H., Virginia, R. A., Welker, J. M., & Wright, I. J. (2009). Global patterns of foliar nitrogen isotopes and their relationships with climate, mycorrhizal fungi, foliar nutrient concentrations, and nitrogen availability. *New Phytologist*, *183*(4), 980–992. https://doi.org/10.1111/j.1469-8137.2009.02917.x

Daniel Bryant, J., & Froelich, P. N. (1995). A model of oxygen isotope fractionation in body water of large mammals. *Geochimica et Cosmochimica Acta*, *59*(21), 4523–4537. https://doi.org/10.1016/0016-7037(95)00250-4

Daniel Bryant, J., Koch, P. L., Froelich, P. N., Showers, W. J., & Genna, B. J. (1996). Oxygen isotope partitioning between phosphate and carbonate in mammalian apatite. *Geochimica et Cosmochimica Acta*, *60*(24), 5145–5148. https://doi.org/10.1016/S0016-7037(96)00308-0

Daniel Bryant, J., Luz, B., & Froelich, P. N. (1994). Oxygen isotopic composition of fossil horse tooth phosphate as a record of continental paleoclimate. *Palaeogeography, Palaeoclimatology, Palaeoecology*, *107*(3–4), 303–316. https://doi.org/10.1016/0031-0182(94)90102-3

Dansgaard, W. (1964). Stable isotopes in precipitation. *Tellus*, *16*(4), 436–468. https://doi.org/10.1111/j.2153-3490.1964.tb00181.x

Debruyne, R., Chu, G., King, C. E., Bos, K., Kuch, M., Schwarz, C., Szpak, P., Gröcke, D. R., Matheus, P., Zazula, G., Guthrie, D., Froese, D., Buigues, B., de Marliave, C., Flemming, C., Poinar, D., Fisher, D., Southon, J., Tikhonov, A. N., … Poinar, H. N. (2008). Out of America: Ancient DNA Evidence for a New World Origin of Late Quaternary Woolly Mammoths. *Current Biology*, *18*(17), 1320–1326. https://doi.org/10.1016/j.cub.2008.07.061

Delgado Huertas, A., Iacumin, P., Stenni, B., Sánchez Chillón, B., & Longinelli, A. (1995). Oxygen isotope variations of phosphate in mammalian bone and tooth enamel. *Geochimica et Cosmochimica Acta*, *59*(20), 4299–4305. https://doi.org/10.1016/0016-7037(95)00286-9

DeNiro, M. J. (1985). Postmortem preservation and alteration of in vivo bone collagen isotope ratios in relation to palaeodietary reconstruction. *Nature*, *317*(6040), 806–809. https://doi.org/10.1038/317806a0

Deniro, M. J., & Epstein, S. (1981). Influence of diet on the distribution of nitrogen isotopes in animals. *Geochimica et Cosmochimica Acta*, *45*(3), 341–351. https://doi.org/10.1016/0016-7037(81)90244-1

DeNiro, M. J., & Weiner, S. (1988). Use of collagenase to purify collagen from prehistoric bones for stable isotopic analysis. *Geochimica et Cosmochimica Acta*, *52*(10), 2425–2431. https://doi.org/10.1016/0016-7037(88)90299-2

Derevianko, A. P., Molodin, V. I., Zenin, V. N., Leshchinskiy, S. V., & Mashchenko, E. N. (2003). Pozdnepaleoliticheskoe Mestonakhozhdenie Shestakovo. *Novosibirsk: Izd. IAET SO RAN*.

Derevianko, A. P., Zenin, V. N., Leshchinsky, S. V., & Maschenko, E. N. (2000). Peculiarities of mammoth accumulation at Shestakovo site in West Siberia. *Archaeology, Ethnology and Anthropology of Eurasia*, *3*, 42–55.

Diez, C., Rojo, M. Á., Martín-Gil, J., Martín-Ramos, P., Garrosa, M., & Córdoba-Diaz, D. (2021). Infrared Spectroscopic Analysis of the Inorganic Components from Teeth Exposed to Psychotherapeutic Drugs. *Minerals*, *12*(1), 28. https://doi.org/10.3390/min12010028

Dobberstein, R. C., Collins, M. J., Craig, O. E., Taylor, G., Penkman, K. E. H., & Ritz-Timme, S. (2009). Archaeological collagen: Why worry about collagen diagenesis? *Archaeological and Anthropological Sciences*, *1*(1), 31–42. https://doi.org/10.1007/s12520-009-0002-7

Drucker, D. G. (2022). The Isotopic Ecology of the Mammoth Steppe. *Annual Review of Earth and Planetary Sciences*, *50*(1), 395–418. https://doi.org/10.1146/annurev-earth-100821-081832

Drucker, D. G., Stevens, R. E., Germonpré, M., Sablin, M. V., Péan, S., & Bocherens, H. (2018). Collagen stable isotopes provide insights into the end of the mammoth steppe in the central East European plains during the Epigravettian. *Quaternary Research*, *90*(3), 457–469. https://doi.org/10.1017/qua.2018.40

Eide, W., Birks, H. H., Bigelow, N. H., Peglar, S. M., & Birks, H. J. B. (2006). Holocene forest development along the Setesdal valley, southern Norway, reconstructed from macrofossil and pollen evidence. *Vegetation History and Archaeobotany*, *15*(2), 65–85. https://doi.org/10.1007/s00334-005-0025-7

Engels, S., Lane, C. S., Haliuc, A., Hoek, W. Z., Muschitiello, F., Baneschi, I., Bouwman, A., Bronk Ramsey, C., Collins, J., de Bruijn, R., Heiri, O., Hubay, K., Jones, G., Laug, A., Merkt, J., Müller, M., Peters, T., Peterse, F., Staff, R. A., … Wagner-Cremer, F. (2022). Synchronous vegetation response to the last glacial-interglacial transition in northwest Europe. *Communications Earth & Environment*, *3*(1), 130. https://doi.org/10.1038/s43247-022-00457-y

Estonian Environment Agency. (2024). *https://www.ilmateenistus.ee/*. https://www.ilmateenistus.ee/

Fægri, K., & Iversen, J. (1989). *Textbook of pollen analysis* (fourth edition). John Wiley & Sons.

Feurdean, A., Perşoiu, A., Tanţău, I., Stevens, T., Magyari, E. K., Onac, B. P., Marković, S., Andrič, M., Connor, S., Fărcaş, S., Gałka, M., Gaudeny, T., Hoek, W., Kolaczek, P., Kuneš, P., Lamentowicz, M., Marinova, E., Michczyńska, D. J., Perşoiu, I., … Zernitskaya, V. (2014). Climate variability and associated vegetation response throughout Central and Eastern Europe (CEE) between 60 and 8 ka. *Quaternary Science Reviews*, *106*, 206–224. https://doi.org/10.1016/j.quascirev.2014.06.003

Fox, D. L., Fisher, D. C., Vartanyan, S., Tikhonov, A. N., Mol, D., & Buigues, B. (2007). Paleoclimatic implications of oxygen isotopic variation in late Pleistocene and Holocene tusks of Mammuthus primigenius from northern Eurasia. *Quaternary International*, *169–170*, 154–165. https://doi.org/10.1016/j.quaint.2006.09.001

Fox-Dobbs, K., Leonard, J. A., & Koch, P. L. (2008). Pleistocene megafauna from eastern Beringia: Paleoecological and paleoenvironmental interpretations of stable carbon and nitrogen isotope and radiocarbon records. *Palaeogeography, Palaeoclimatology, Palaeoecology*, *261*(1–2), 30–46. https://doi.org/10.1016/j.palaeo.2007.12.011

France, C. A. M., Sugiyama, N., & Aguayo, E. (2020). Establishing a preservation index for bone, dentin, and enamel bioapatite mineral using ATR-FTIR. *Journal of Archaeological Science: Reports*, *33*, 102551. https://doi.org/10.1016/j.jasrep.2020.102551

Gaillard, M.-J., & Birks, H. H. (2013). PLANT MACROFOSSIL METHODS AND STUDIES | Paleolimnological Applications. In *Encyclopedia of Quaternary Science* (pp. 657–673). Elsevier. https://doi.org/10.1016/B978-0-444-53643-3.00207-7

Genoni, L., Iacumin, P., Nikolaev, V., Gribchenko, Yu., & Longinelli, A. (1998). Oxygen isotope measurements of mammoth and reindeer skeletal remains: an archive of Late Pleistocene environmental conditions in Eurasian Arctic. *Earth and Planetary Science Letters*, *160*(3–4), 587–592. https://doi.org/10.1016/S0012-821X(98)00113-7

Goslar, T., Bałaga, K., Arnold, M., Tisnerat, N., Starnawska, E., Kuźniarski, M., Chróst, L., Walanus, A., & Więckowski, K. (1999). Climate-related variations in the composition of the Late Glacial and early Holocene sediments of Lake Perespilno (eastern Poland). *Quaternary Science Reviews*, *18*(7), 899–911. https://doi.org/10.1016/S0277-3791(99)00004-9

Grafenstein, U. von, Erlenkeuser, H., Brauer, A., Jouzel, J., & Johnsen, S. J. (1999). A Mid-European Decadal Isotope-Climate Record from 15,500 to 5000 Years B.P. *Science*, *284*(5420), 1654–1657. https://doi.org/10.1126/science.284.5420.1654

Graham, R. W., Belmecheri, S., Choy, K., Culleton, B. J., Davies, L. J., Froese, D., Heintzman, P. D., Hritz, C., Kapp, J. D., Newsom, L. A., Rawcliffe, R., Saulnier-Talbot, É., Shapiro, B., Wang, Y., Williams, J. W., & Wooller, M. J. (2016). Timing and causes of mid-Holocene mammoth extinction on St. Paul Island, Alaska. *Proceedings of the National Academy of Sciences*, *113*(33), 9310–9314. https://doi.org/10.1073/pnas.1604903113

Grewingk, C. (1874). Diluviale Thierreste in Menzen (Kreis Werro, Kirchspiel Harjel). *Sitzungsberichte Der Naturforscher-Gesellschaftbei Der Universität Dorpat*, *3*, 475–477.

Grigoriev, S. E., Fisher, D. C., Obadă, T., Shirley, E. A., Rountrey, A. N., Savvinov, G. N., Garmaeva, D. K., Novgorodov, G. P., Cheprasov, M. Yu., Vasilev, S. E., Goncharov, A. E., Masharskiy, A., Egorova, V. E., Petrova, P. P., Egorova, E. E., Akhremenko, Y. A., van der Plicht, J., Galanin, A. A., Fedorov, S. E., … Tikhonov, A. N. (2017). A woolly mammoth (Mammuthus primigenius) carcass from Maly Lyakhovsky Island (New Siberian Islands, Russian Federation). *Quaternary International*, *445*, 89–103. https://doi.org/10.1016/j.quaint.2017.01.007

Gröcke, D. R., Bocherens, H., & Mariotti, A. (1997). Annual rainfall and nitrogen-isotope correlation in macropod collagen: application as a palaeoprecipitation indicator. *Earth and Planetary Science Letters*, *153*(3–4), 279–285. https://doi.org/10.1016/S0012-821X(97)00189-1

Grunenwald, A., Keyser, C., Sautereau, A. M., Crubézy, E., Ludes, B., & Drouet, C. (2014). Revisiting carbonate quantification in apatite (bio)minerals: a validated FTIR methodology. *Journal of Archaeological Science*, *49*, 134–141. https://doi.org/10.1016/j.jas.2014.05.004

Guiry, E. J., & Szpak, P. (2021). Improved quality control criteria for stable carbon and nitrogen isotope measurements of ancient bone collagen. *Journal of Archaeological Science*, *132*, 105416. https://doi.org/10.1016/j.jas.2021.105416

Guthrie, D. R. (2006). New carbon dates link climatic change with human colonization and Pleistocene extinctions. *Nature*, *441*(7090), 207–209. https://doi.org/10.1038/nature04604

Guthrie, R. D. (1968). Paleoecology of the Large-Mammal Community in Interior Alaska during the Late Pleistocene. *American Midland Naturalist*, *79*(2), 346. https://doi.org/10.2307/2423182

Guthrie, R. D. (1982). MAMMALS OF THE MAMMOTH STEPPE AS PALEOENVIRONMENTAL INDICATORS. In *Paleoecology of Beringia* (pp. 307–326). Elsevier. https://doi.org/10.1016/B978-0-12-355860-2.50030-2

Guthrie, R. D. (2001). Origin and causes of the mammoth steppe: a story of cloud cover, woolly mammal tooth pits, buckles, and inside-out Beringia. *Quaternary Science Reviews*, *20*(1–3), 549–574. https://doi.org/10.1016/S0277-3791(00)00099-8

Harris, C. R., Millman, K. J., van der Walt, S. J., Gommers, R., Virtanen, P., Cournapeau, D., Wieser, E., Taylor, J., Berg, S., Smith, N. J., Kern, R., Picus, M., Hoyer, S., van Kerkwijk, M. H., Brett, M., Haldane, A., del Río, J. F., Wiebe, M., Peterson, P., … Oliphant, T. E. (2020). Array programming with NumPy. *Nature*, *585*(7825), 357–362. https://doi.org/10.1038/s41586-020-2649-2

Haynes, G. (1991). *Mammoths, mastodonts, and elephants: biology, behavior and the fossil record*. Cambridge University Press.

Heaton, T. H. E. (1987). The 15N/14N ratios of plants in South Africa and Namibia: relationship to climate and coastal/saline environments. *Oecologia*, *74*(2), 236–246. https://doi.org/10.1007/BF00379365

Heikkilä, M., Fontana, S. L., & Seppä, H. (2009). Rapid Lateglacial tree population dynamics and ecosystem changes in the eastern Baltic region. *Journal of Quaternary Science*, *24*(7), 802–815. https://doi.org/10.1002/jqs.1254

Hughes, P. D., & Gibbard, P. L. (2015). A stratigraphical basis for the Last Glacial Maximum (LGM). *Quaternary International*, *383*, 174–185. https://doi.org/10.1016/j.quaint.2014.06.006

Huijzer, B., & Vandenberghe, J. (1998). Climatic reconstruction of the Weichselian Pleniglacial in northwestern and central Europe. *Journal of Quaternary Science*, *13*, 391–417.

Iacumin, P., Bocherens, H., Mariotti, A., & Longinelli, A. (1996). Oxygen isotope analyses of co-existing carbonate and phosphate in biogenic apatite: a way to monitor diagenetic alteration of bone phosphate? *Earth and Planetary Science Letters*, *142*(1–2), 1–6. https://doi.org/10.1016/0012-821X(96)00093-3

Iacumin, P., Di Matteo, A., Nikolaev, V., & Kuznetsova, T. V. (2010). Climate information from C, N and O stable isotope analyses of mammoth bones from northern Siberia. *Quaternary International*, *212*(2), 206–212. https://doi.org/10.1016/j.quaint.2009.10.009

Iacumin, P., Nikolaev, V., & Ramigni, M. (2000). C and N stable isotope measurements on Eurasian fossil mammals, 40 000 to 10 000 years BP: Herbivore physiologies and palaeoenvironmental reconstruction. *Palaeogeography, Palaeoclimatology, Palaeoecology*, *163*(1–2), 33–47. https://doi.org/10.1016/S0031-0182(00)00141-3

Iacumin, P., Nikolaev, V., Ramigni, M., & Longinelli, A. (2004). Oxygen isotope analyses of mammal bone remains from Holocene sites in European Russia: palaeoclimatic implications. *Global and Planetary Change*, *40*(1–2), 169–176. https://doi.org/10.1016/S0921-8181(03)00107-3

Isarin, R. F. B., & Renssen, H. (1999). Reconstructing and modelling Late Weichselian climates: the Younger Dryas in Europe as a case study. *Earth-Science Reviews*, *48*(1–2), 1–38. https://doi.org/10.1016/S0012-8252(99)00047-1

Jackson, S. T., Booth, R. K., Reeves, K., Andersen, J. J., Minckley, T. A., & Jones, R. A. (2014). Inferring local to regional changes in forest composition from Holocene macrofossils and pollen of a small lake in central Upper Michigan. *Quaternary Science Reviews*, *98*, 60–73. https://doi.org/10.1016/j.quascirev.2014.05.030

Kageyama, M., Laîné, A., Abe-Ouchi, A., Braconnot, P., Cortijo, E., Crucifix, M., de Vernal, A., Guiot, J., Hewitt, C. D., & Kitoh, A. (2006). Last Glacial Maximum temperatures over the North Atlantic, Europe and western Siberia: a comparison between PMIP models, MARGO sea–surface temperatures and pollen-based reconstructions. *Quaternary Science Reviews*, *25*(17–18), 2082–2102. https://doi.org/10.1016/j.quascirev.2006.02.010

Kageyama, M., Peyron, O., Pinot, S., Tarasov, P., Guiot, J., Joussaume, S., & Ramstein, G. (2001). The Last Glacial Maximum climate over Europe and western Siberia: a PMIP comparison between models and data. *Climate Dynamics*, *17*(1), 23–43. https://doi.org/10.1007/s003820000095

Kahlke, R. D. (1994). *"Die Entstehungs-, Entwicklungs-und Verbreitungsgeschichte-des oberpleistozänen Mammuthus-Coelodonta-Faunenkomplexes-in Eurasien (Großsäuger).*

Kahlke, R. D. (1999). *The history of the origin, evolution and dispersal of the Late Pleistocene Mammuthus-Coelodonta faunal complex in Eurasia (large mammals)*. Mammoth Site of Hot Springs.

Kahlke, R.-D. (2014). The origin of Eurasian Mammoth Faunas (Mammuthus–Coelodonta Faunal Complex). *Quaternary Science Reviews*, *96*, 32–49. https://doi.org/10.1016/j.quascirev.2013.01.012

Katz, N. J., Katz, S. V, & Skobeyeva, E. I. (1977). *Atlas rastitelnyh ostatkov v Torfah (Atlas of Plant Remains in Peat)*. Nedra.

Kirillova, I. V., Markova, E. A., Panin, A. V., Van der Plicht, J., & Titov, V. V. (2023). ON SMALL CONTINENTAL MAMMOTHS AND DWARFISM. *Зоологический Журнал*, *102*(11), 1280–1300. https://doi.org/10.31857/S0044513423100045

Kitover, D. C., van Balen, R. T., Vandenberghe, J., Roche, D. M., & Renssen, H. (2016). LGM Permafrost Thickness and Extent in the Northern Hemisphere derived from the Earth System Model *i* LOVECLIM. *Permafrost and Periglacial Processes*, *27*(1), 31–42. https://doi.org/10.1002/ppp.1861

Koch, P. L. (2007). Isotopic Study of the Biology of Modern and Fossil Vertebrates. In *Stable Isotopes in Ecology and Environmental Science* (pp. 99–154). Wiley. https://doi.org/10.1002/9780470691854.ch5

Koch, P. L., & Barnosky, A. D. (2006). Late Quaternary Extinctions: State of the Debate. *Annual Review of Ecology, Evolution, and Systematics*, *37*(1), 215–250. https://doi.org/10.1146/annurev.ecolsys.34.011802.132415

Kohn, M. J. (2010). Carbon isotope compositions of terrestrial C3 plants as indicators of (paleo)ecology and (paleo)climate. *Proceedings of the National Academy of Sciences*, *107*(46), 19691–19695. https://doi.org/10.1073/pnas.1004933107

Kohn, M. J., & Cerling, T. E. (2002). Stable Isotope Compositions of Biological Apatite. *Reviews in Mineralogy and Geochemistry*, *48*(1), 455–488. https://doi.org/10.2138/RMG.2002.48.12

Kuitems, M., van Kolfschoten, T., & van der Plicht, J. (2015). Elevated δ15N values in mammoths: a comparison with modern elephants. *Archaeological and Anthropological Sciences*, *7*(3), 289–295. https://doi.org/10.1007/s12520-012-0095-2

Kurita, N., Yoshida, N., Inoue, G., & Chayanova, E. A. (2004). Modern isotope climatology of Russia: A first assessment. *Journal of Geophysical Research: Atmospheres*, *109*(D3). https://doi.org/10.1029/2003JD003404

Kuzmin, Y. V, Leshchinskiy, S. V, Zenin, V. N., Burkanova, E. M., Zazovskaya, E. P., & Samandrosova, A. S. (2024). CHRONOLOGY OF THE VOLCHIA GRIVA MEGAFAUNAL LOCALITY AND PALEOLITHIC SITE (WESTERN SIBERIA) AND THE ISSUE OF HUMAN OCCUPATION OF SIBERIA AT THE LAST GLACIAL MAXIMUM. *Radiocarbon*, *66*(6), 1630–1642. https://doi.org/10.1017/RDC.2023.82

Lane, C. S., Brauer, A., Blockley, S. P. E., & Dulski, P. (2013). Volcanic ash reveals time-transgressive abrupt climate change during the Younger Dryas. *Geology*, *41*(12), 1251–1254. https://doi.org/10.1130/G34867.1

Lapshina, E. D. (2003). Flora of mires of south-east of West Siberia. *Tomsk University, Tomsk.*

Lazarev, S., & Leshchinskiy, S. V. (2011). Preliminary results of drilling activity on the Krasnoyarskaya Kurya mammoth site. *Trudy TSU*, *280*, 232–235.

Lee-Thorp, J. A., Sealy, J. C., & van der Merwe, N. J. (1989). Stable carbon isotope ratio differences between bone collagen and bone apatite, and their relationship to diet. *Journal of Archaeological Science*, *16*(6), 585–599. https://doi.org/10.1016/0305-4403(89)90024-1

Lee-Thorp, J., & Sponheimer, M. (2003). Three case studies used to reassess the reliability of fossil bone and enamel isotope signals for paleodietary studies. *Journal of Anthropological Archaeology*, *22*(3), 208–216. https://doi.org/10.1016/S0278-4165(03)00035-7

Leshchinskiy, S. (2015). Enzootic diseases and extinction of mammoths as a reflection of deep geochemical changes in ecosystems of Northern Eurasia. *Archaeological and Anthropological Sciences*, *7*(3), 297–317. https://doi.org/10.1007/S12520-014-0205-4/FIGURES/25

Leshchinskiy, S., Burkanova, E., Polumogina, Y., Lazarev, S., & Zenin, V. (2014). *Last Glacial Maximum mammoth fauna of the Krasnoyarskaya Kurya site (southeastern part of the West Siberian Plain)*. 105.

Leshchinskiy, S. V. (2018). Results of latest paleontological, stratigraphic and geoarchaeological research of the Volchia Griva mammoth fauna site. *Proceedings of the Zoological Institute RAS*, *322*(3), 315–384. https://doi.org/10.31610/trudyzin/2018.322.3.315

Leshchinskiy, S. V., & Burkanova, E. M. (2022). The Volchia Griva mineral oasis as unique locus for research of the mammoth fauna and the late Pleistocene environment in Northern Eurasia. *Quaternary Research*, *109*, 157–182. https://doi.org/10.1017/QUA.2022.8

Leshchinskiy, S. V., Zenin, V. N., & Bukharova, O. V. (2021). The Volchia Griva mammoth site as a key area for geoarchaeological research of human movements in the Late Paleolithic of the West Siberian Plain. *Quaternary International*, *587–588*, 368–383. https://doi.org/10.1016/j.quaint.2020.08.036

Leshchinskiy, S. V., Zenin, V. N., Burkanova, E. M., & Kuzmin, Y. V. (2023). The unique Late Paleolithic artifactual bone assemblage from the Volchia Griva site, Western Siberia. *Quaternary Research*, *114*, 93–113. https://doi.org/10.1017/qua.2023.4

Liiv, M., Alliksaar, T., Amon, L., Freiberg, R., Heinsalu, A., Reitalu, T., Saarse, L., Seppä, H., Stivrins, N., Tõnno, I., Vassiljev, J., & Veski, S. (2019). Late glacial and early Holocene climate and environmental changes in the eastern Baltic area inferred from sediment C/N ratio. *Journal of Paleolimnology*, *61*(1), 1–16. https://doi.org/10.1007/s10933-018-0041-0

Longinelli, A. (1984). Oxygen isotopes in mammal bone phosphate: A new tool for paleohydrological and paleoclimatological research? *Geochimica et Cosmochimica Acta*, *48*(2), 385–390. https://doi.org/10.1016/0016-7037(84)90259-X

Longinelli, A., Iacumin, P., Davanzo, S., & Nikolaev, V. (2003). Modern reindeer and mice: revised phosphate–water isotope equations. *Earth and Planetary Science Letters*, *214*(3–4), 491–498. https://doi.org/10.1016/S0012-821X(03)00395-9

Lorenzen, E. D., Nogués-Bravo, D., Orlando, L., Weinstock, J., Binladen, J., Marske, K. A., Ugan, A., Borregaard, M. K., Gilbert, M. T. P., Nielsen, R., Ho, S. Y. W., Goebel, T., Graf, K. E., Byers, D., Stenderup, J. T., Rasmussen, M., Campos, P. F., Leonard, J. A., Koepfli, K.-P., … Willerslev, E. (2011). Species-specific responses of Late Quaternary megafauna to climate and humans. *Nature*, *479*(7373), 359–364. https://doi.org/10.1038/nature10574

Lõugas, L., Ukkonen, P., & Jungner, H. (2002). Dating the extinction of European mammoths: new evidence from Estonia. *Quaternary Science Reviews*, *21*(12–13), 1347–1354. https://doi.org/10.1016/S0277-3791(01)00098-1

Luz, B., Kolodny, Y., & Horowitz, M. (1984). Fractionation of oxygen isotopes between mammalian bone-phosphate and environmental drinking water. *Geochimica et Cosmochimica Acta*, *48*(8), 1689–1693. https://doi.org/10.1016/0016-7037(84)90338-7

MacDonald, G. M. (2013). PLANT MACROFOSSIL METHODS AND STUDIES | Megafossils. In *Encyclopedia of Quaternary Science* (pp. 621–629). Elsevier. https://doi.org/10.1016/B978-0-444-53643-3.00205-3

Mann, D. H., Groves, P., Kunz, M. L., Reanier, R. E., & Gaglioti, B. V. (2013). Ice-age megafauna in Arctic Alaska: extinction, invasion, survival. *Quaternary Science Reviews*, *70*, 91–108. https://doi.org/10.1016/j.quascirev.2013.03.015

Martin, C., Bentaleb, I., Kaandorp, R., Iacumin, P., & Chatri, K. (2008). Intra-tooth study of modern rhinoceros enamel δ18O: Is the difference between phosphate and carbonate δ18O a sound diagenetic test? *Palaeogeography, Palaeoclimatology, Palaeoecology*, *266*(3–4), 183–189. https://doi.org/10.1016/j.palaeo.2008.03.039

Maschenko, E. N. (2010). Age profile and morphology of mammoth from the Chulym river (Teguldet locality, Tomsk region, Russia). *Proceedings of the 4th International Mammoth Conference*, 41–53.

McKinney, W. (2010). *Data structures for statistical computing in python*. 51–56.

Metcalfe, J. Z. (2017). Proboscidean isotopic compositions provide insight into ancient humans and their environments. *Quaternary International*, *443*, 147–159. https://doi.org/10.1016/j.quaint.2016.12.003

Metcalfe, J. Z., & Longstaffe, F. J. (2012). Mammoth tooth enamel growth rates inferred from stable isotope analysis and histology. *Quaternary Research*, *77*(3), 424–432. https://doi.org/10.1016/j.yqres.2012.02.002

Metcalfe, J. Z., Longstaffe, F. J., Jass, C. N., Zazula, G. D., & Keddie, G. (2016). Taxonomy, location of origin and health status of proboscideans from Western Canada investigated using stable isotope analysis. *Journal of Quaternary Science*, *31*(2), 126–142. https://doi.org/10.1002/jqs.2849

Molodkov, A., & Bolikhovskaya, N. (2022). Palaeoenvironmental changes and their chronology during the latter half of MIS 5 on the south-eastern coast of the Gulf of Finland. *Quaternary International*, *616*, 40–54. https://doi.org/10.1016/J.QUAINT.2021.10.016

Molodkov, A., Bolikhovskaya, N., Miidel, A., & Ploom, K. (2007). The sedimentary sequence recovered from the Voka outcrops, northeastern Estonia: implications for late Pleistocene stratigraphy. *Estonian Journal of Earth Sciences*, *56*(1), 47. https://doi.org/10.3176/earth.2007.09

O'Leary, M. H. (1988). Carbon Isotopes in Photosynthesis. *BioScience*, *38*(5), 328–336. https://doi.org/10.2307/1310735

Olivier, R. C. D. (1982). ECOLOGY AND BEHAVIOR OF LIVING ELEPHANTS: BASES FOR ASSUMPTIONS CONCERNING THE EXTINCT WOOLLY MAMMOTHS. In *Paleoecology of Beringia* (pp. 291–305). Elsevier. https://doi.org/10.1016/B978-0-12-355860-2.50029-6

Orlova, L. A., Kuzmin, Y. V, & Dementiev, V. N. (2004). A Review of the Evidence for Extinction Chronologies for Five Species of Upper Pleistocene Megafauna in Siberia. *Radiocarbon*, *46*(1), 301–314. https://doi.org/10.1017/S0033822200039618

Pollard, D., & Barron, E. J. (2003). Causes of model–data discrepancies in European climate during oxygen isotope stage 3 with insights from the last glacial maximum. *Quaternary Research*, *59*(1), 108–113. https://doi.org/10.1016/S0033-5894(02)00019-4

Pryor, A. J. E., Stevens, R. E., O'Connell, T. C., & Lister, J. R. (2014). Quantification and propagation of errors when converting vertebrate biomineral oxygen isotope data to temperature for palaeoclimate reconstruction. *Palaeogeography, Palaeoclimatology, Palaeoecology*, *412*, 99–107. https://doi.org/10.1016/j.palaeo.2014.07.003

Rakhmankulova, Z. F., Shuyskaya, E. V., Voronin, P. Yu., & Usmanov, I. Yu. (2019). Comparative Study on Resistance of C3 and C4 Xerohalophytes of the Genus Atriplex to Water Deficit and Salinity. *Russian Journal of Plant Physiology*, *66*(2), 250–258. https://doi.org/10.1134/S1021443719020109

Ramsey, C. B. (2008). Deposition models for chronological records. *Quaternary Science Reviews*, *27*(1–2), 42–60. https://doi.org/10.1016/j.quascirev.2007.01.019

Rasmussen, S. O., Bigler, M., Blockley, S. P., Blunier, T., Buchardt, S. L., Clausen, H. B., Cvijanovic, I., Dahl-Jensen, D., Johnsen, S. J., Fischer, H., Gkinis, V., Guillevic, M., Hoek, W. Z., Lowe, J. J., Pedro, J. B., Popp, T., Seierstad, I. K., Steffensen, J. P., Svensson, A. M., … Winstrup, M. (2014). A stratigraphic framework for abrupt climatic changes during the Last Glacial period based on three synchronized Greenland ice-core records: refining and extending the INTIMATE event stratigraphy. *Quaternary Science Reviews*, *106*, 14–28. https://doi.org/10.1016/j.quascirev.2014.09.007

Reille M. (1992). *Pollen et spores d'Europe et d'Afrique du Nord*. Laboratoire de Botanique Historique et Palynologique,CNRS.

Reimer, P. J., Austin, W. E. N., Bard, E., Bayliss, A., Blackwell, P. G., Bronk Ramsey, C., Butzin, M., Cheng, H., Edwards, R. L., Friedrich, M., Grootes, P. M., Guilderson, T. P., Hajdas, I., Heaton, T. J., Hogg, A. G., Hughen, K. A., Kromer, B., Manning, S. W., Muscheler, R., … Talamo, S. (2020). The IntCal20 Northern Hemisphere Radiocarbon Age Calibration Curve (0–55 cal kBP). *Radiocarbon*, *62*(4), 725–757. https://doi.org/10.1017/RDC.2020.41

Reinecke, J., Ashastina, K., Kienast, F., Troeva, E., & Wesche, K. (2021). Effects of large herbivore grazing on relics of the presumed mammoth steppe in the extreme climate of NE-Siberia. *Scientific Reports*, *11*(1), 12962. https://doi.org/10.1038/s41598-021-92079-1

Rey-Iglesia, A., Lister, A. M., Stuart, A. J., Bocherens, H., Szpak, P., Willerslev, E., & Lorenzen, E. D. (2021). Late Pleistocene paleoecology and phylogeography of woolly rhinoceroses. *Quaternary Science Reviews*, *263*, 106993. https://doi.org/10.1016/j.quascirev.2021.106993

Rosentau, A., Vassiljev, J., Hang, T., Saarse, L., & Kalm, V. (2009). Development of the Baltic Ice Lake in the eastern Baltic. *Quaternary International*, *206*(1–2), 16–23. https://doi.org/10.1016/J.QUAINT.2008.10.005

Rowe, A. G., Bataille, C. P., Baleka, S., Combs, E. A., Crass, B. A., Fisher, D. C., Ghosh, S., Holmes, C. E., Krasinski, K. E., Lanoë, F., Murchie, T. J., Poinar, H., Potter, B., Rasic, J. T., Reuther, J., Smith, G. M., Spaleta, K. J., Wygal, B. T., & Wooller, M. J. (2024). A female woolly mammoth's lifetime movements end in an ancient Alaskan hunter-gatherer camp. *Science Advances*, *10*(3). https://doi.org/10.1126/sciadv.adk0818

Rozanski, K., Araguás-Araguás, L., & Gonfiantini, R. (1992). Relation Between Long-Term Trends of Oxygen-18 Isotope Composition of Precipitation and Climate. *Science*, *258*(5084), 981–985. https://doi.org/10.1126/science.258.5084.981

Rutkovskaya, N. V. (1979). Climatic characteristics of seasons of Tomsk region. *Tomsk: Tomsk State University*.

Rutkovskaya, N. V. (1996). The climate of the Tomsk region and its formation. *Questions of Geography of Siberia*, *6*, 3–39.

Sage, R. F. (2017). A portrait of the C_4 photosynthetic family on the 50th anniversary of its discovery: species number, evolutionary lineages, and Hall of Fame. *Journal of Experimental Botany*, *68*(2), 4039–4056. https://doi.org/10.1093/jxb/erx005

Schenk, F., Väliranta, M., Muschitiello, F., Tarasov, L., Heikkilä, M., Björck, S., Brandefelt, J., Johansson, A. V., Näslund, J.-O., & Wohlfarth, B. (2018). Warm summers during the Younger Dryas cold reversal. *Nature Communications*, *9*(1), 1634. https://doi.org/10.1038/s41467-018-04071-5

Schirrmeister, L., Siegert, C., Kuznetsova, T., Kuzmina, S., Andreev, A., Kienast, F., Meyer, H., & Bobrov, A. (2002). Paleoenvironmental and paleoclimatic records from permafrost deposits in the Arctic region of Northern Siberia. *Quaternary International*, *89*(1), 97–118. https://doi.org/10.1016/S1040-6182(01)00083-0

Schmidt, R., van den Bogaard, C., Merkt, J., & Müller, J. (2002). A new Lateglacial chronostratigraphic tephra marker for the south-eastern Alps: The Neapolitan Yellow Tuff (NYT) in Längsee (Austria) in the context of a regional biostratigraphy and palaeoclimate. *Quaternary International*, *88*(1), 45–56. https://doi.org/10.1016/S1040-6182(01)00072-6

Schoeninger, M. J., & DeNiro, M. J. (1984). Nitrogen and carbon isotopic composition of bone collagen from marine and terrestrial animals. *Geochimica et Cosmochimica Acta*, *48*(4), 625–639. https://doi.org/10.1016/0016-7037(84)90091-7

Schwark, L., Zink, K., & Lechterbeck, J. (2002). Reconstruction of postglacial to early Holocene vegetation history in terrestrial Central Europe via cuticular lipid biomarkers and pollen records from lake sediments. *Geology*, *30*(5), 463–466.

Schwartz-Narbonne, R., Longstaffe, F. J., Metcalfe, J. Z., & Zazula, G. (2015). Solving the woolly mammoth conundrum: amino acid 15N-enrichment suggests a distinct forage or habitat. *Scientific Reports*, *5*(1), 9791. https://doi.org/10.1038/srep09791

Sealy, J. C., van der Merwe, N. J., Thorp, J. A. L., & Lanham, J. L. (1987). Nitrogen isotopic ecology in southern Africa: Implications for environmental and dietary tracing. *Geochimica et Cosmochimica Acta*, *51*(10), 2707–2717. https://doi.org/10.1016/0016-7037(87)90151-7

Sealy, J., Johnson, M., Richards, M., & Nehlich, O. (2014). Comparison of two methods of extracting bone collagen for stable carbon and nitrogen isotope analysis: comparing whole bone demineralization with gelatinization and ultrafiltration. *Journal of Archaeological Science*, *47*, 64–69. https://doi.org/10.1016/j.jas.2014.04.011

Seddon, A. W., Macias-Fauria, M., & Willis, K. J. (2015). Climate and abrupt vegetation change in Northern Europe since the last deglaciation. *The Holocene*, *25*(1), 25–36. https://doi.org/10.1177/0959683614556383

Seersholm, F. V., Werndly, D. J., Grealy, A., Johnson, T., Keenan Early, E. M., Lundelius, E. L., Winsborough, B., Farr, G. E., Toomey, R., Hansen, A. J., Shapiro, B., Waters, M. R., McDonald, G., Linderholm, A., Stafford, T. W., & Bunce, M. (2020). Rapid range shifts and megafaunal extinctions associated with late Pleistocene climate change. *Nature Communications*, *11*(1), 2770. https://doi.org/10.1038/s41467-020-16502-3

Seuru, S., Leshchinskiy, S., Auguste, P., & Fedyaev, N. (2017). Woolly mammoth and Man at Krasnoyarskaya Kurya site, West Siberian Plain, Russia (excavation results of 2014). *Bulletin de La Société Géologique de France*, *188*(1–2), 4. https://doi.org/10.1051/bsgf/2017005

Sharp, Z. (2017). *Principles of Stable Isotope Geochemistry, 2nd Edition*.

Sher, A. V., Kuzmina, S. A., Kuznetsova, T. V., & Sulerzhitsky, L. D. (2005). New insights into the Weichselian environment and climate of the East Siberian Arctic, derived from fossil insects, plants, and mammals. *Quaternary Science Reviews*, *24*(5–6), 533–569. https://doi.org/10.1016/j.quascirev.2004.09.007

Sponheimer, M., Robinson, T., Ayliffe, L., Roeder, B., Hammer, J., Passey, B., West, A., Cerling, T., Dearing, D., & Ehleringer, J. (2003). Nitrogen isotopes in mammalian herbivores: hair δ^{15}N values from a controlled feeding study. *International Journal of Osteoarchaeology*, *13*(1–2), 80–87. https://doi.org/10.1002/oa.655

Stewart, M., Carleton, W. C., & Groucutt, H. S. (2021). Climate change, not human population growth, correlates with Late Quaternary megafauna declines in North America. *Nature Communications*, *12*(1), 965. https://doi.org/10.1038/s41467-021-21201-8

Stivrins, N., Cerina, A., Gałka, M., Heinsalu, A., Lõugas, L., & Veski, S. (2019). Large herbivore population and vegetation dynamics 14,600–8300 years ago in central Latvia, northeastern Europe. *Review of Palaeobotany and Palynology*, *266*, 42–51. https://doi.org/10.1016/j.revpalbo.2019.04.005

Stuart, A. J. (2005a). The extinction of woolly mammoth (Mammuthus primigenius) and straight-tusked elephant (Palaeoloxodon antiquus) in Europe. *Quaternary International*, *126–128*, 171–177. https://doi.org/10.1016/j.quaint.2004.04.021

Stuart, A. J. (2005b). The extinction of woolly mammoth (Mammuthus primigenius) and straight-tusked elephant (Palaeoloxodon antiquus) in Europe. *Quaternary International*, *126–128*(1 SPEC.ISS.), 171–177. https://doi.org/10.1016/j.quaint.2004.04.021

Stuart, A. J., & Lister, A. M. (2012). Extinction chronology of the woolly rhinoceros Coelodonta antiquitatis in the context of late Quaternary megafaunal extinctions in northern Eurasia. *Quaternary Science Reviews*, *51*, 1–17. https://doi.org/10.1016/j.quascirev.2012.06.007

Sukhorukov, A. P., Kushunina, M., & Sennikov, A. N. (2022). A new classification of C4-Atriplex species in Russia, with the first alien record of Atriplex flabellum (Chenopodiaceae, Amaranthaceae) from North Siberia. *PhytoKeys*, *202*, 59–72. https://doi.org/10.3897/phytokeys.202.87306

Szpak, P. (2014). Complexities of nitrogen isotope biogeochemistry in plant-soil systems: implications for the study of ancient agricultural and animal management practices. *Frontiers in Plant Science*, *5*. https://doi.org/10.3389/fpls.2014.00288

Szpak, P., Gröcke, D. R., Debruyne, R., MacPhee, R. D. E., Guthrie, R. D., Froese, D., Zazula, G. D., Patterson, W. P., & Poinar, H. N. (2010). Regional differences in bone collagen δ13C and δ15N of Pleistocene mammoths: Implications for paleoecology of the mammoth steppe. *Palaeogeography, Palaeoclimatology, Palaeoecology*, *286*(1–2), 88–96. https://doi.org/10.1016/j.palaeo.2009.12.009

Tarasov, P. E., Peyron, O., Guiot, J., Brewer, S., Volkova, V. S., Bezusko, L. G., Dorofeyuk, N. I., Kvavadze, E. V., Osipova, I. M., & Panova, N. K. (1999). Last Glacial Maximum climate of the former Soviet Union and Mongolia reconstructed from pollen and plant macrofossil data. *Climate Dynamics*, *15*(3), 227–240. https://doi.org/10.1007/s003820050278

Tierney, J. E., Zhu, J., King, J., Malevich, S. B., Hakim, G. J., & Poulsen, C. J. (2020). Glacial cooling and climate sensitivity revisited. *Nature*, *584*(7822), 569–573. https://doi.org/10.1038/s41586-020-2617-x

Tütken, T., Furrer, H., & Walter Vennemann, T. (2007). Stable isotope compositions of mammoth teeth from Niederweningen, Switzerland: Implications for the Late Pleistocene climate, environment, and diet. *Quaternary International*, *164–165*, 139–150. https://doi.org/10.1016/j.quaint.2006.09.004

Ukkonen, P., Aaris-Sørensen, K., Arppe, L., Clark, P. U., Daugnora, L., Lister, A. M., Lõugas, L., Seppä, H., Sommer, R. S., Stuart, A. J., Wojtal, P., & Zupinš, I. (2011). Woolly mammoth (Mammuthus primigenius Blum.) and its environment in northern Europe during the last glaciation. *Quaternary Science Reviews*, *30*(5–6), 693–712. https://doi.org/10.1016/j.quascirev.2010.12.017

van der Merwe, N. J. (1982). “Carbon Isotopes, Photosynthesis, and Archaeology: Different Pathways of Photosynthesis Cause Characteristic Changes in Carbon Isotope Ratios That Make Possible the Study of Prehistoric Human Diets.” *American Scientist*, *70*(6), 596–606.

van Geel, B., Aptroot, A., Baittinger, C., Birks, H. H., Bull, I. D., Cross, H. B., Evershed, R. P., Gravendeel, B., Kompanje, E. J. O., Kuperus, P., Mol, D., Nierop, K. G. J., Pals, J. P., Tikhonov, A. N., van Reenen, G., & van Tienderen, P. H. (2008). The Ecological implications of a Yakutian mammoth’s last meal. *Quaternary Research*, *69*(03), 361–376. https://doi.org/10.1016/j.yqres.2008.02.004

van Geel, B., Guthrie, R. D., Altmann, J. G., Broekens, P., Bull, I. D., Gill, F. L., Jansen, B., Nieman, A. M., & Gravendeel, B. (2011). Mycological evidence of coprophagy from the feces of an Alaskan Late Glacial mammoth. *Quaternary Science Reviews*, *30*(17–18), 2289–2303. https://doi.org/10.1016/j.quascirev.2010.03.008

van Groenigen, J.-W., & van Kessel, C. (2002). Salinity-induced Patterns of Natural Abundance Carbon-13 and Nitrogen-15 in Plant and Soil. *Soil Science Society of America Journal*, *66*(2), 489–498. https://doi.org/10.2136/sssaj2002.4890

van Klinken, G. J. (1999). Bone Collagen Quality Indicators for Palaeodietary and Radiocarbon Measurements. *Journal of Archaeological Science*, *26*(6), 687–695. https://doi.org/10.1006/jasc.1998.0385

Vandenberghe, J., French, H. M., Gorbunov, A., Marchenko, S., Velichko, A. A., Jin, H., Cui, Z., Zhang, T., & Wan, X. (2014). The Last Permafrost Maximum (LPM) map of the Northern Hemisphere: permafrost extent and mean annual air temperatures, 25–17 ka BP. *Boreas*, *43*(3), 652–666. https://doi.org/10.1111/bor.12070

Vassiljev, J., & Saarse, L. (2013). Timing of the Baltic Ice Lake in the eastern Baltic. *Bulletin of the Geological Society of Finland*, *85*(1), 9–18. https://doi.org/10.17741/bgsf/85.1.001

Vasyukova, E. A., & Leshchinskiy, S. V. (2011). Petrographic analysis of Palaeolithic artifacts of the Krasnoyarskaya Kurya mammoth site. *Trudy TSU*, 207–209.

Veski, S., Amon, L., Heinsalu, A., Reitalu, T., Saarse, L., Stivrins, N., & Vassiljev, J. (2012). Lateglacial vegetation dynamics in the eastern Baltic region between 14,500 and 11,400calyrBP: A complete record since the Bølling (GI-1e) to the Holocene. *Quaternary Science Reviews*, *40*, 39–53. https://doi.org/10.1016/j.quascirev.2012.02.013

Veski, S., Seppä, H., Stančikaite, M., Zernitskaya, V., Reitalu, T., Gryguc, G., Heinsalu, A., Stivrins, N., Amon, L., Vassiljev, J., & Heiri, O. (2015). Quantitative summer and winter temperature reconstructions from pollen and chironomid data between 15 and 8 ka BP in the Baltic–Belarus area. *Quaternary International*, *388*, 4–11. https://doi.org/10.1016/J.QUAINT.2014.10.059

Virtanen, P., Gommers, R., Oliphant, T. E., Haberland, M., Reddy, T., Cournapeau, D., Burovski, E., Peterson, P., Weckesser, W., Bright, J., van der Walt, S. J., Brett, M., Wilson, J., Millman, K. J., Mayorov, N., Nelson, A. R. J., Jones, E., Kern, R., Larson, E., … Vázquez-Baeza, Y. (2020). SciPy 1.0: fundamental algorithms for scientific computing in Python. *Nature Methods*, *17*(3), 261–272. https://doi.org/10.1038/s41592-019-0686-2

Waller, M., & Early, R. (2015). Vegetation dynamics from a coastal peatland: insights from combined plant macrofossil and pollen data. *Journal of Quaternary Science*, *30*(8), 779–789. https://doi.org/10.1002/jqs.2812

Wang, Y., Pedersen, M. W., Alsos, I. G., De Sanctis, B., Racimo, F., Prohaska, A., Coissac, E., Owens, H. L., Merkel, M. K. F., Fernandez-Guerra, A., Rouillard, A., Lammers, Y., Alberti, A., Denoeud, F., Money, D., Ruter, A. H., McColl, H., Larsen, N. K., Cherezova, A. A., … Willerslev, E. (2021). Late Quaternary dynamics of Arctic biota from ancient environmental genomics. *Nature*, *600*(7887), 86–92. https://doi.org/10.1038/s41586-021-04016-x

Watts, W. A., & Winter, T. C. (1966). Plant macrofossils from Kirchner Marsh, Minnesota—a paleoecological study. *Geological Society of America Bulletin*, *77*(12), 1339–1359.

Weitzel, N., Hense, A., Herzschuh, U., Böhmer, T., Cao, X., & Rehfeld, K. (2022). *A state estimate of Siberian summer temperature and moisture availability during the Last Glacial Maximum combining pollen records and climate simulations*. https://doi.org/10.31223/X59P9H

Wetterich, S., Meyer, H., Fritz, M., Mollenhauer, G., Rethemeyer, J., Kizyakov, A., Schirrmeister, L., & Opel, T. (2021). Northeast Siberian Permafrost Ice-Wedge Stable Isotopes Depict Pronounced Last Glacial Maximum Winter Cooling. *Geophysical Research Letters*, *48*(7). https://doi.org/10.1029/2020GL092087

Wohlfarth, B., Tarasov, P., Bennike, O., Lacourse, T., Subetto, D., Torssander, P., & Romanenko, F. (2006). Late Glacial and Holocene Palaeoenvironmental Changes in the Rostov-Yaroslavl' Area, West Central Russia. *Journal of Paleolimnology*, *35*(3), 543–569. https://doi.org/10.1007/s10933-005-3240-4

Wooller, M. J., Bataille, C., Druckenmiller, P., Erickson, G. M., Groves, P., Haubenstock, N., Howe, T., Irrgeher, J., Mann, D., Moon, K., Potter, B. A., Prohaska, T., Rasic, J., Reuther, J., Shapiro, B., Spaleta, K. J., & Willis, A. D. (2021). Lifetime mobility of an Arctic woolly mammoth. *Science*, *373*(6556), 806–808. https://doi.org/10.1126/science.abg1134

World Bank Group. (2024). *Climate Change Knowledge Portal*. https://climateknowledgeportal.worldbank.org/country/latvia/climate-data-historical

Wu, H., Guiot, J., Brewer, S., & Guo, Z. (2007). Climatic changes in Eurasia and Africa at the last glacial maximum and mid-Holocene: reconstruction from pollen data using inverse vegetation modelling. *Climate Dynamics*, *29*(2–3), 211–229. https://doi.org/10.1007/s00382-007-0231-3

Zimov, S. A., Zimov, N. S., Tikhonov, A. N., & Chapin, F. S. (2012). Mammoth steppe: a high-productivity phenomenon. *Quaternary Science Reviews*, *57*, 26–45. https://doi.org/10.1016/j.quascirev.2012.10.005

Acknowledgements

This PhD journey has been one of the most challenging things I have ever experienced in my life, and I certainly would not have been able to do it all on my own. There are so many people I would like to thank.

I would first like to express my deepest gratitude to my supervisor, Dr. Leeli Amon, for her immense support and patience, for always believing in me and encouraging my ideas, for providing a variety of educational opportunities, and for offering guidance both within and beyond academic studies.

My sincere thanks also go to my co-supervisor, Prof. Siim Veski, whose response to my very first email inquiring about potential PhD positions changed the course of my life. I am grateful for his calm presence, his willingness to share his experience, his sense of humour, and his continuous advice and support throughout this journey.

I am very thankful to my co-supervisor, Dr. Laura Arppe, for her patience, for working through multiple edits and drafts of texts with me, and for always being creative and insightful. Her valuable knowledge, experience, and unwavering support were indispensable to this dissertation.

I also wish to sincerely thank my co-supervisor, Prof. Sergey Leshchinsky, for his contagious passion for science, optimism, and resilience. I am especially grateful for his encouragement, his support, and for providing me with the opportunity to participate in some of the most memorable and inspiring fieldwork of my life.

My warmest thanks go to Dr. Anneli Poska for her contributions to my PhD journey, for always being ready to help, and for generously sharing her vision and innovative ideas. Her input has been highly valuable to this work.

I am also grateful to my colleagues at the Department of Geology, Dr. Jüri Vassiljev, Prof. Atko Heinsalu, and Dr. Merlin Liiv, for their constant support and encouragement during my studies. I also wish to thank the head of the department, Dr. Olle Hints, for being immensely helpful and supportive, not only as a head of department but also as a colleague and a person.

I would like to thank my fellow PhD students, Varvara Bakumenko, Anna Lanka, and Eliise Poolma, for their company, countless chats, coffees, board games, computer games, and shared activities. Without you, completing this project would have been far more difficult.

Special thanks go to my friend Alexey Makarov for being there through everything, for sharing endless conversations, countless songs, and for supporting me through the most difficult times.

I would also like to express my special thanks to Mikhail Khatkov, the best wingman and teammate I could ever ask for, for spending so much time playing games with me, helping me stay afloat, and keeping me sane during this journey. I am equally grateful to the other members of our Counter-Strike crew, with whom I shared some of the most enjoyable moments that helped me get through this period tremendously.

Finally, I owe my deepest gratitude to my parents, my mother and father, for their constant support, encouragement, and guidance throughout this challenging time.

This work was supported by ESF projects PRG1993, TK 215 and the Doctoral School of Earth Sciences and Ecology, and the European Union, European Regional Development Fund (ASTRA “TTÜ arenguprogramm aastateks 2016–2022”).

Abstract

Out of the shadows: reconstructing mammoth paleoecology from underrepresented regions of the Western Siberian Plain and Estonia, Eastern Europe

This dissertation explores the immense isotopic potential of mammoth remains from two regions underrepresented in terms of isotopic data: the three largest Late Pleistocene sites/mammoth "cemeteries" in the southeast of the West Siberian plain (SEWS) (Shestakovo, Krasnoyarskaya Kurya and Volchia Griva) and the Eastern Baltic. Despite the extensive isotopic research conducted in permafrost in Northern Siberia and Beringia, isotopic data from non-permafrost regions such as SEWS and the Eastern Baltic remain scarce.

This study integrates stable oxygen, carbon, and nitrogen isotope analysis with palaeobotanical proxies (plant macrofossils and pollen) to reconstruct environmental conditions and mammoth diet in non-permafrost contexts. In total, 31 samples from mammoth sites in the southeast of Western Siberia were selected and analysed. The time interval (ca. 27.5–22 ka cal BP) of the samples from SEWS covers the peak of LGM in the southeast of Western Siberia. In addition, four Estonian mammoth tooth samples, two from the youngest mammoth find in Europe, were collected and analysed for carbon and nitrogen isotopes. Special attention was given to the preservation of skeletal remains: using $\delta^{18}O$ equilibrium and ATR-FTIR spectroscopy of bioapatite, and C:N ratios, collagen yield, and elemental content to check the preservation of collagen. ATR-FTIR spectroscopy is not a standard method for evaluating the preservation of bioapatite in mammoth research, but it can provide detailed insights into the post-depositional history of the samples.

The main outcomes of this research project are:

- Thorough preservation assessment, which was one of the most important aspects of the project, showed that the mineral and the organic part of samples from Volchia Griva have suffered from post-depositional alteration, potentially carbonate loss, chemical and microbial degradation. Using ATR-FTIR spectroscopy helped us to identify that tusk specimens from Krasnoyarskaya Kurya and Volchia Griva specifically had suffered from carbonate loss and accompanying structural changes.
- In the Eastern Baltics, the C% and %N values and the C:N ratio of the samples from the European youngest mammoths indicated that the samples are likely to have been altered by post-depositional processes.
- Oxygen isotopic results showed that winters during the Late Pleistocene were colder and summers warmer than today. Within SEWS, oxygen isotope data show increasing $\delta^{18}Ow$ values from Shestakovo and Krasnoyarskaya Kurya (ca. 28–23 ka cal BP) to Volchia Griva (ca. 24–22 ka cal BP), suggesting gradual warming in the region.
- Samples from Volchia Griva exhibited unusually high $\delta^{15}N$ values in the range of 10–15‰, possibly the highest nitrogen values reported for mammoth remains so far. We hypothesise that local environmental conditions, such as saline soils, trampling, and possibly coprophagy, could have contributed to such high $\delta^{15}N$ values.
- In the Eastern Baltics, at the beginning of the Holocene, the landscape shifted from an open to a forested one, making the environment inhospitable for mammoths even in northernmost Estonia. The mammoths in the Eastern Baltic experienced a decline in the nutritional value of their diet, contributing to their demise in the Eastern Baltic.

- Combining isotopic methods with pollen and macrofossil analysis offers a more comprehensive understanding of the environmental changes that may have contributed to megafaunal extinction.
- This work demonstrates the need for further isotopic studies in underrepresented regions and confirms that non-permafrost materials, when carefully screened, can be a valuable source of paleoenvironmental information.

Lühikokkuvõte

Varjust välja: mammutite paleokeskkonna rekonstrueerimine Lääne-Siberi tasandikul ja Ida-Euroopas asuvate vähemuuritud piirkondade põhjal

Käesolevas väitekirjas uuritakse mammutileidude isotoopanalüüside märkimisväärset potentsiaali kahes piirkonnas, mis on isotoop-geokeemiliste andmete poolest alaesindatud: kolm suurimat hilispleistotseeni leiukohta/mammutite „kalmistut" Lääne-Siberi tasandiku kaguosas (SEWS) (Šestakovo, Krasnojarskaja Kurja ja Volchia Griva) ning Ida-Baltikumi alal. Vaatamata arvukatele igikeltsast pärinevate leidude uuringutele Põhja-Siberis ja Beringias, on isotoopandmed igikeltsata piirkondadest, nagu SEWS ja Ida-Baltikumi piirkond, endiselt vähesed.

Käesolevas uuringus kombineeritakse stabiilse hapniku, süsiniku ja lämmastiku isotoopide analüüs paleobotaaniliste andmestikega (taimede makrofossiilid ja õietolm), et rekonstrueerida keskkonnatingimusi ja mammutite toitumist igikeltsata aladel. Kokku valiti ja analüüsiti 31 proovi mammutite leiukohtadest Lääne-Siberi kaguosas. SEWS-i proovide vanusevahemik (*ca* 27,5–22 ka cal BP) hõlmab viimase jäätumise maksimumi Lääne-Siberi kaguosas. Lisaks koguti ja analüüsiti süsiniku ja lämmastiku isotoopide tarvis neli Eesti mammutihamba proovi, sealhulgas neist kaks pärinevad Euroopa noorimast mammutileiust.

Erilist tähelepanu pöörati luuleidude säilivusele: bioapatiidi säilimise kontrollimiseks kasutati $\delta^{18}O$ tasakaalu ja ATR-FTIR spektroskoopiat ning C:N suhet, kollageeni saagist ja elementide sisaldust. ATR-FTIR spektroskoopia ei ole mammutite uurimisel bioapatiidi säilimise hindamise standardmeetod, kuid see võimaldab saada üksikasjalikku teavet proovide mattumisjärgse ajaloo kohta.

Selle uurimisprojekti peamised tulemused on:

- Põhjalik luuleidude säilivuse hindamine, üks projekti olulisemaid aspekte, näitas, et Volchia Griva proovide mineraalne ja orgaaniline osa on kannatanud nii mattumisjärgse muutuse, võimaliku karbonaatse osise kao, kui keemilise ja mikrobioloogilise lagunemise all. ATR-FTIR spektroskoopia abil suutsime kindlaks teha, et Krasnojarskaja Kurja ja Volchia Griva leidusid mõjutas karbonaatse osise kadu, mis tõi kaasa struktuurilisi muutuseid.
- Ida-Baltikumi piirkonnas viitasid Euroopa noorimate mammutite proovide C% ja %N väärtused ning C:N suhe, et leiud on tõenäoliselt olnud mõjutatud mattumisjärgsetest protsessidest.
- Hapniku isotoopanalüüsi tulemuste põhjal võib väita, et hilispleistotseeni talved SEWS piirkonnas olid külmemad ja suved soojemad kui tänapäeval. Hapniku isotoopide $\delta^{18}Ow$ väärtused olid suuremad Shestakovo ja Krasnojarskaja Kurja (umbes 28–23 ka cal BP) leiukohtades kui nooremas, Volchia Griva (u 24–22 ka cal BP) leiukohas, mis viitab piirkonna järkjärgulisele soojenemisele.
- Volchia Griva proovid sisaldasid ebatavaliselt kõrgeid $\delta^{15}N$ väärtusi vahemikus 10–15‰, mis on tõenäoliselt kõrgeimad seni mammutileidudest mõõdetud lämmastiku väärtused. Meie hüpotees on, et kõrgete $\delta^{15}N$ väärtuste tekkimisele võisid kaasa aidata kohalikud keskkonnatingimused, nagu sooldunud pinnas, tallamine ja võimalik, et ka koprofaagia.
- Holotseeni perioodi alguses muutus Ida-Baltikumi maastik avatud maastikust metsaseks, muutes keskkonna mammutitele ebasobivaks isegi Eesti põhjapoolseimas

osas. Ida-Baltikumi mammutite sööda toiteväärtus langes, mis oli põhjuseks nende väljasuremisele Ida-Balti piirkonnas.

- Isotoopmeetodite kombineerimine õietolmu ja taimsete makrofossiilide analüüsiga annab põhjalikuma ülevaate keskkonnamuutustest, mis võisid viia Pleistotseeni megafauna väljasuremiseni.
- Uurimus tõstatab vajaduse täiendavate isotoopuuringute järgi vähemuuritud piirkondades ja tõestab, et hoolikalt valitud igikeltsata piirkonna leiud võivad olla väärtuslikuks teabeallikaks mineviku keskkonnamuutuste kohta.

Appendix 1 (Paper I)

Krivokorin, I., Amon, L., Leshchinskiy, S. V., & Arppe, L. (2024). Oxygen isotope studies of the largest West Siberian mammoth sites and implications for last glacial maximum climate reconstruction. Quaternary Science Reviews, 343, 108938. https://doi.org/10.1016/j.quascirev.2024.108938

Quaternary Science Reviews 343 (2024) 108938

Contents lists available at ScienceDirect

Quaternary Science Reviews

journal homepage: www.elsevier.com/locate/quascirev

Oxygen isotope studies of the largest West Siberian mammoth sites and implications for last glacial maximum climate reconstruction

Ivan Krivokorin [a,*], Leeli Amon [a], Sergey V. Leshchinskiy [b,c], Laura Arppe [d]

[a] Tallinn University of Technology, Department of Geology, Ehitajate tee 5, 12616, Tallinn, Estonia
[b] Laboratory of Mesozoic and Cenozoic Continental Ecosystems, Tomsk State University, Lenin Ave. 36, Tomsk, 634050, Russia
[c] Museum of Nature and Man, Mira st. 11, Khanty-Mansiysk, 628011, Russia
[d] Finnish Museum of Natural History LUOMUS, P.O. Box 64, 00014, University of Helsinki, Helsinki, Finland

ARTICLE INFO

Handling Editor: Mira Matthews

Keywords:
LGM
West Siberian plain
Mammoth fauna
Paleoecology
Paleogeography
Oxygen isotopes
Fourier Transform infrared spectroscopy

ABSTRACT

This study examines the isotopic potential of mammoth remains from three paleontological sites in the southeast of the West Siberian Plain (SEWS): Shestakovo, Krasnoyarskaya Kurya, and Volchia Griva. We analysed oxygen isotopes from 29 mammoth enamel and tusk samples and horse and deer enamel samples. We verified sample preservation using ATR-FTIR and obtained δ^{18}Op, δ^{18}Oc, and reconstructed δ^{18}Ow values for 28-22 ka cal BP. Preservation assessments revealed variable preservation conditions. Our findings indicate an increase of 1.4‰ in reconstructed δ^{18}Ow values from glacial levels at 28-23 ka to late-glacial conditions at ca. 17–15.5 ka, likely reflecting climatic warming at the end of the Pleistocene. The extensive fossil material at these sites offers significant potential for further Last Glacial Maximum studies.

1. Introduction

Woolly mammoth (*Mammuthus primigenius*, Blumenbach, 1799) was a key species in "mammoth steppe", a unique ecosystem dominated by herbaceous plants that covered almost all northern parts of Eurasia from Ireland in Europe to Northern Yukon in North America (Guthrie, 1968; Kahlke, 1999; Stuart, 2005) during ca. 110,000–12,000 years ago (Koch and Barnosky, 2006). At the end of the Pleistocene, Northern Hemisphere megafauna that had included mastodons, mammoths, cave bears, woolly rhinoceroses, and other species decreased by 36% in Eurasia and 72% in North America (Barnosky et al., 2004). This study focuses on the isotopic study potential of the mammoth fauna skeletal remains from the three largest Late Pleistocene sites/mammoth "cemeteries" in the southeast of West Siberian plain: Shestakovo, Krasnoyarskaya Kurya and Volchia Griva (Fig. 1). These sites are unique due to the substantial amount of mammoth fauna material buried at these locations. Shestakovo covers an area of more than 125,000 m^2 and has yielded over 4500 remains belonging to at least 18 woolly mammoths since 1975 (Derevianko et al., 2000, 2003). Krasnoyarskaya Kurya covers an area of more than 5000 m^2. Approximately 5600 woolly mammoth remains from at least 35 individuals have been found at this site, including bones and teeth, skeletal fragments (Lazarev and Leshchinskiy, 2011; Leshchinskiy et al., 2014; Seuru et al., 2017). Volchia Griva covers an area of more than 20,000 m^2 and is considered to be one of the youngest mammoth refugia in Eurasia. In terms of the numbers of finds, it is possibly the largest site in Northern Asia where woolly mammoth remains are preserved in situ. Since 1957, researchers at Volchia Griva have found over 7000 of fragments, whole bones, and teeth from at least 80 woolly mammoths on an area > 550 m^2 (Leshchinskiy and Burkanova, 2022; Leshchinskiy et al., 2023). Palaeolithic artefacts indicating human presence have been discovered at all three sites (Derevianko et al., 2000; Leshchinskiy et al., 2005, 2021; Vasyukova and Leshchinskiy, 2011; Zenin, 2002). These three sites align well with some of the most prominent Late Pleistocene sites discovered thus far in Eurasia, especially in regarding the abundance of mammoth findings (Leshchinskiy, 2015). For example, other Siberian sites of Lugovskoye and Berelyokh have yielded ca. 5500 and 7200 remains of mostly woolly mammoth (Leshchinskiy, 2006, 2017). In Europe, they can be compared to the significance of Kraków Spadzista Street in Poland and Milovice I and Předmostí sites in the Czech Republic, containing ca. 23,000 and ca. 44,000, and probably over 100,000 mammoth remains, respectively (Brugère and Fontana, 2009; Krzemińska and Wędzicha, 2015;

* Corresponding author.
E-mail address: ivan.krivokorin@taltech.ee (I. Krivokorin).

https://doi.org/10.1016/j.quascirev.2024.108938
Received 17 June 2024; Received in revised form 1 August 2024; Accepted 27 August 2024
Available online 3 September 2024
0277-3791/© 2024 Elsevier Ltd. All rights are reserved, including those for text and data mining, AI training, and similar technologies.

Leshchinskiy, 2012; Wojtal, 2004; Wojtal and Sobczyk, 2005) (Fig. 1).

It has been well-established that stable isotope compositions of mammoth skeletal remains like enamel, dentin and bone contain information about past climatic conditions including estimates of atmospheric temperatures in terrestrial environments and isotopic composition of palaeowater (Bryant et al., 1994, 1996; Genoni et al., 1998; Hedges et al., 2004; Iacumin et al., 2004). The oxygen isotope composition of mammalian apatite is determined by the isotopic composition of body water, which, in turn, is influenced by the magnitude and composition of oxygen fluxes to and from the body water (Longinelli, 1984; Luz et al., 1984). Large mammals' mineralized tissues form at a near constant body temperature, which means that the composition of body water is the determining source of variation in their apatite's oxygen isotope composition. In large mammals that generally obtain the bulk of their water through drinking, the oxygen isotope composition of body water is sensitive to the oxygen isotope composition of meteoric water (Bryant and Froelich, 1995; Longinelli, 1984). Surface water reservoirs are the primary source of drinking water, and the oxygen isotope composition of drinking water is mainly influenced by meteoric water, with adjustments made through evaporative enrichment in $\delta^{18}O$ and local hydrological processes (Bryant and Froelich, 1995; Kohn, 1996). There is a close relation between annual $\delta^{18}O$ mean of precipitation and annual mean surface air temperatures for mid- and high northern latitudes (Dansgaard, 1964; Rozanski et al., 1992). Consequently, $\delta^{18}O$ values derived from animal tissues reflect temporal changes in relative air temperature, humidity, aridity and subsequently the climate (Metcalfe, 2017; Tütken et al., 2007). The connection between the $\delta^{18}O$ values of mammal bioapatite ($\delta^{18}Oap$) and the ingested meteoric waters ($\delta^{18}Ow$) allows the use of $\delta^{18}O$ values from mammal skeletal remains for palaeoclimatological investigations. The oxygen in the phosphate component ($\delta^{18}Op$) and the oxygen in the structural carbonate ($\delta^{18}Oc$) are often used in palaeoclimatological research. For example, a study by Arppe and Karhu (2010), used $\delta^{18}Op$ and $\delta^{18}Oc$ values of mammoth tooth enamel and published isotopic records on palaeogroundwater to reconstruct the geographic variation of $\delta^{18}O$ values of glacial precipitation across a large area of Europe. The results showed a remarkable agreement between enamel-derived long-term mean glacial $\delta^{18}Ow$ values and local glacial palaeogroundwater oxygen isotope levels in various European locations. This lends credibility to using mammoth enamel as a proxy for long-term $\delta^{18}Op$ values of precipitation.

To conduct valid paleoclimatic reconstructions, the in vivo isotopic compositions of the analysed skeletal tissues must remain uncompromised by diagenetic alteration in the burial environment. Due to low porosity, high density and the highest degree of mineralization, tooth enamel is most resistant to diagenesis and thus, it is the preferred tissue for oxygen isotope analyses (Kohn and Cerling, 2002; Metcalfe and Longstaffe, 2012). In the right depositional conditions supporting tissue preservation, tusks have been shown to provide a reliable climatic record as well (e.g., Fox et al., 2007), and well-preserved tusks can yield remarkably detailed information about climate and the life history of the animals themselves (e.g. Rowe et al., 2024). The preservation potential and isotopic integrity of skeletal remains can highly vary according to the environmental conditions of the site (e.g., Lee-Thorp and Sponheimer, 2003). Unlike many of the North Siberian mammoth sites that have yielded well enough preserved enamel and bone materials for oxygen isotope analyses (e.g., Arppe et al., 2019; Fox et al., 2007; Iacumin et al., 2010), Volchia Griva, Shestakovo and Krasnoyarska Kurya are not under constant permafrost conditions, calling for an evaluation of post-depositional diagenetic alteration of the finds prior to utilising oxygen isotopic data. The massive long-term accumulations of mammoth skeletal remains at Volchia Griva, Shestakovo and Kransoyarskaya Kurya contain a highly valuable archive of isotopic values representing past environmental conditions.

In this paper, we report on the oxygen isotope analyses of 29 mammoth molar enamel and tusk dentine samples, one deer enamel sample and one horse enamel sample from late Pleistocene, ca. 27.5–22 ka cal BP, to explore the potential of the mammoth remains for climatic reconstruction using the $\delta^{18}O$ values of the phosphate component recorded in the bioapatite and provide a unique insight into climatic changes at the southeast of Western Siberia during the peak of Last Glacial Maximum (LGM). According to Hughes and Gibbard (2015), LGM spans from 27 to 23 ka cal BP as it is defined in the NGRIP Greenland ice-core stratigraphy, although based on existing relative sea level (RSL), LGM could also be limited to 26.5–19.0 ka cal BP (Clark et al., 2009). Therefore, our chosen time interval (ca. 27.5–22 ka cal BP) covers the peak of LGM in the southeast of Western Siberia. We used the oxygen isotope equilibrium between the two oxygen-bearing components of bioapatite to assess whether the original δ18Op values had been preserved and visual inspection and FTIR analysis to carefully investigate the preservation of the samples and use well-preserved material to estimate δ18O of precipitation during LGM in the southeast of Western Siberia. Western Siberia is underrepresented in terrestrial compilations of LGM climate reconstructions, as the majority of studies have focused on northern Siberia; therefore, our newly obtained isotopic record will contribute valuable data to the underresearched region and time period.

2. Regional setting, geological and geochronological context

2.1. Shestakovo

Shestakovo (55°54′31.0″N, 87°57′07.0″E; the bone bearing horizon altitude is approximately 160–170 m and higher in some areas) is located in Kemerovo region 1 km downstream from the village of Shestakovo on the high right bank of the Kiya River (Fig. 1). The site was attractive for large herbivores because there was formed a "beast solonetz" on the Ca-Mg-Na geochemical landscape (Derevianko et al., 2000, 2003). «*The beast solonetz is the Russian term for a ground surface area characterized by a high content of certain macro- and microelements; as such it has a broader interpretation than "salt lick", "mineral lick" and "mineral source". Within the confines of the beast solonetz, animals eat soil and rocks and drink mineralized water from springs to maintain homeostasis*» (Leshchinskiy, 2015, p. 298).

The selected samples from the Shestakovo site come from the main bone-bearing horizon – geological layers V and VI. Four mammoth bone samples from layer V and nine samples including mammoth teeth and bones, horse and deer bones, charcoal, burnt bones from layer VI have been dated (Derevianko et al., 2000, 2003). The earliest and latest dates defining this horizon come from a mammoth bone dated to ca. 27.5 ka cal BP (23,330 ± 110 ^{14}C yr BP (GrA-13235)), and a mammoth bone dated to ca. 26.7 ka cal BP (22,340 ± 180 ^{14}C yr BP (GrA-13240)). Therefore, we estimate that the age of the samples from the Shestakovo site falls roughly within the period of ca. 28-27 ka cal BP. Throughout the text, all the mammoth site related radiocarbon dates discussed in calendar years (cal BP) were calibrated using OxCal v.4,4.4 (Ramsey, 2009) and calibration curve InCal20 (Reimer et al., 2020).

2.2. Krasnoyarskaya Kurya

Krasnoyarskaya Kurya (54°39′48.4″N, 80°19′47.6″E; the surface altitude is approximately 123 m) is located in the south-eastern part of the West Siberian Plain, in the Chulym River Valley (Fig. 1). The site is located 148 km north of Shestakovo.

Samples from Krasnoyarskaya Kurya come from the middle and lower levels of the bone-bearing horizon. Three mammoth bones were dated: a humerus/or pelvis was dated to ca. 23.5 ka cal BP (19,670 ± 120 ^{14}C yr BP (GIN-12876)), an ulna/or humerus to ca. 23.8 ka cal BP (19,780 ± 180 ^{14}C yr BP (GIN-12877)) (Boiko et al., 2005; Mashchenko, 2010) and pelvis to 24.3–23.9 ka cal BP (20,020 ± 80 ^{14}C yr BP (Beta-426078); Seuru et al., 2017). Overall, despite the low number of dated samples, we estimate that the age of the samples from Krasnoyarskaya Kurya falls within the period of ca. 25 - 23 ka cal BP.

Fig. 1. Map showing the general location of Volchia Griva, Shestakovo and Krasnoyarskaya Kurya sites along with other locations of mammoth sites discussed in the text. Basemap: Esri, Maxar, Earthstar Geographics, and the GIS User Community.

2.3. Volchia Griva

Volchia Griva (Wolf's Ridge or Wolf's Mound) (54°39′48.4″N, 80°19′47.6″E; the surface altitude is approximately 148 m) is located in the village Mamontovoe, Kargat district of the Novosibirsk region on the east of the Baraba lowland and is confined to the north-eastern part of an elongated sloping mound of the same name (length ~ 11 km, width 0.5–1 km). The site is 500 km south-west from Shetakovo and 535 km south-west from Krasnoyarskaya Kurya. The site has been known as a large mammoth cemetery since 1957. According to Leshchinskiy and Burkanova (2022) the remains of large mammals were accumulating at Volchia Griva during the wide interval from LGM to the end of the Pleistocene. The authors suggest that mammoths and other animals used Volchia Griva as a source of mineral replenishment to compensate for the mineral deficiency. By the end of the Pleistocene, the large herbivorous animals of Siberia suffered from a chronic deficiency of calcium and other essential elements, which is proven by a palaeoecological analysis of more than 1500 mammoth remains from ~13 to 12 ka BP found at the Berelyokh site (Leshchinskiy, 2017). The observed osteodystrophy was caused by the strong acidification of geochemical landscapes in the Northern Eurasian region, which began after 30 ka BP (Leshchinskiy, 2009, 2015). This is why a high concentration of alkaline-earth and alkaline metals (primarily, Ca, Mg and Na) in the groundwater and pore water sediments that form the geochemical landscape of Volchia Griva was so attractive for the mammoth steppe megafauna: the animals were able to find "mud pits", forage and drinking water with vital chemical elements (Leshchinskiy, 2018).

At Volchia Griva, bone layers have accumulated from 24 to 12.5 ka cal BP potentially providing a unique opportunity to track changes in climatic development from the latest Pleistocene through the LGM into the Holocene at a single site (Kuzmin et al., 2023). Samples from Volchia Griva that were selected for analysis in this study come from the lower level of the bone-bearing horizon in the central assemblage, where the earliest direct radiocarbon charcoal date places the beginnings of accumulation at ca. 24 ka cal BP (19,790 ± 70 ^{14}C yr BP, RICH-29414.1.1) with the latest charcoal date being 22 ka cal BP (18,230 ± 70 ^{14}C yr BP, IGAN$_{AMS}$-8485) (Kuzmin et al., 2023). Information on the current climate and temperature at Shestakovo, Krasnoyarskaya Kurya and Volchia Griva are included in the Supplementary data.

3. Materials and Methods

3.1. Material collection

The samples, listed in Table 1, were selected from the collection of the Laboratory of Mesozoic and Cenozoic Continental Ecosystems, Tomsk State University, Russia. Most of them were woolly mammoth (n = 29), with single exceptions for horse and deer samples. We collected samples from tooth enamel and tusks to compare their δ^{18}Op data and see whether the isotopic data from tusks would be consistent with the isotopic data from tooth enamel and, thus, support also the use of tusk (dentine) tissue for δ^{18}Op based reconstructions at these sites. The specimens were sampled using a Dremel 300 drill with a diamond blade. A total number of 31 samples were collected, photographed, and placed in zip packages. Samples from Shestakovo were marked as "SH", samples from Krasnoyarskaya Kurya were marked as "KK", and samples from VG were marked as "VG". Photographs of the samples are included in the Supplementary data.

3.2. Evaluation of preservation

To evaluate whether the oxygen isotope compositions had been compromised by diagenetic alteration, we relied on the preservation of the expected equilibrium of δ^{18}O values between the structural carbonate and the phosphate components of bioapatite (Bryant et al., 1996; Iacumin et al., 1996). Additional insight into the general preservation

Table 1
Studied samples with oxygen isotope and FTIR results. M in the table stands for Mammoth, H for Horse, D for Deer. The IDs of samples rejected from the dataset used for paleoclimatic reconstruction are shown in square brackets and separated from the accepted dataset with a line. The calculated δ^{18}Ow values (see Methods for equations) are given with the associated reconstruction error based on Pryor et al. (2014). FTIR indices that fall out of the acceptable range recommended by France et al. (2020) are shown in bold italics. VG 18 and 30 failed to yield any Ag3PO4 crystals.

Sample ID	Tissue type	Visual inspection	C/P	IRSF	δ^{18}Op (VSMOW, ‰)	δ^{18}Oc (VSMOW, ‰)	Δ^{18}O CO3-PO4	δ^{18}Ow
SH 53	H enamel	Acceptable	0.155	3.42	+8.8 ± 0.09	+17.5	+8.7	−19.4 ± 2.9
SH 54	D enamel	Acceptable	0.109	3.648	+7.4 ± 0.03	+16.3 ± 0.20	+8.9	−21.4 ± 2.7
SH 55	M enamel	Good	***0.079***	***4.155***	+6.9 ± 0.08	+17.3	+10.4	−17.4 ± 2.0
SH 56	M enamel	Good	0.132	3.508	+8.6 ± 0.03	+17.5 ± 0.21	+8.9	−15.6 ± 1.8
Min.					+6.9	+16.3	+8.7	−21.4
Max.					+8.8	+17.5	+10.4	−15.6
Average					+7.8	+17.4	+9.7	−16.5
KK 57	M enamel	Good	0.105	3.891	+8.5 ± 0.14	+18.4 ± 0.03	+9.9	−15.7 ± 1.8
KK 58	M enamel	Good	0.107	4.023	+9.6 ± 0.55	+18.9 ± 0.17	+9.3	−14.6 ± 1.8
KK 59	M enamel	Good	0.097	***4.348***	+8.3 ± 0.02	+18.1 ± 0.05	+9.8	−16.0 ± 1.9
KK 60	M tusk	Acceptable	0.094	3.927	+9.0 ± 0.22	+18.1 ± 0.14	+9.1	−15.2 ± 1.8
KK 61	M tusk	Acceptable	0.091	***4.475***	9.4	+18.1 ± 0.17	+8.7	−14.8
KK 62	M enamel	Good	0.118	3.775	+8.1 ± 0.13	+17.7 ± 0.05	+9.6	−16.2 ± 1.9
KK 63	M enamel	Good	0.101	3.962	+9.0 ± 0.12	+18.4 ± 0.26	+9.4	−15.2 ± 1.8
KK 64	M enamel	Very good	0.088	3.561	+9.3 ± 0.04	+18.9	+9.6	−14.9 ± 1.8
KK 65	M tusk	Very good	***0.05***	***5.184***	+9.8 ± 0.14	+17.9	+8.1	−14.4 ± 1.8
KK 66	M tusk	Acceptable	***0.032***	***5.223***	+9.0 ± 0.21	+19.1 ± 0.19	+10.1	−15.2 ± 1.8
					+8.1	+17.7	+8.1	−16.2
					+9.8	+19.1	+10.1	−14.4
					+9.0	+18.4	+9.4	−15.2
VG 16	M enamel	Acceptable	0.083	3.917	+9.5 ± 0.03	+20.0	+10.5	−14.7 ± 1.8
VG 17	M enamel	Acceptable	0.117	***4.236***	+11.9 ± 0.02	+19.3	+7.4	−12.1 ± 1.6
VG 19	M tusk	Acceptable	0.054	***5.678***	+10.6 ± 0.05	+20.4	+9.8	−13.5 ± 1.7
VG 20	M tusk	Acceptable	0.091	***5.034***	+8.7 ± 0.13	+18.9	+10.2	−15.5 ± 1.8
VG 22	M enamel	Good	0.153	3.406	+10.2	+20.1	+9.9	−13.9
VG 24	M enamel	Acceptable	0.114	3.801	+10.4 ± 0.21	+18.7 ± 0.07	+8.7	−13.7 ± 1.7
VG 26	M enamel	Very good	0.084	4.068	+10.6 ± 0.08	+20.6 ± 0.10	+10	−13.5 ± 1.7
VG 28	M tusk	Very good	0.054	***4.931***	+10.6 ± 0.03	+20.4 ± 0.05	+9.8	−13.5 ± 1.7
VG 31	M enamel	Acceptable	0.069	***4.446***	+11.3 ± 0.51	+20.2 ± 0.13	+8.9	−12.8 ± 1.7
VG 32	M enamel	Acceptable	0.088	***4.382***	+11.7 ± 0.48	+21.7 ± 0.20	+10.0	−12.3 ± 1.6
VG 34	M enamel	Acceptable	–	–	+9.9	+20.3 ± 0.21	+10.4	−14.3
Min.					+8.7	+18.7	+7.4	−15.5
Max.					+11.9	+21.7	+10.5	−12.1
Average					+10.5	+20.1	+9.6	−13.6
[VG 18]	M tusk	Acceptable	***−0.009***	***8.058***	–	+22.2	–	–
[VG 23]	M enamel	Good	0.161	3.627	+11.4	+22.5	***+11.1***	–
[VG 25]	M enamel	Good	0.133	3.258	+8.9	+19.6	***+10.7***	–
[VG 29]	M tusk	Good	***0.036***	***5.492***	+9.3 ± 0.13	+20.6	***+11.3***	–
[VG 30]	M enamel	Good	0.624	3.672	–	–	–	–
[VG 33]	M enamel	Acceptable	–	–	+8.2 ± 0.09	+19.9	***+11.7***	–

status was obtained using attenuated total reflectance Fourier Transformed Infrared Spectroscopy (ATR-FTIR), with the idea that changes detected in the chemical or structural properties of the bioapatite could help us better understand the conditions and processes the remains have undergone since the death of the animal and evaluate the degree of substitution of bioinorganic materials (Diez et al., 2021).

In addition, we assigned each sample into an initial condition category (very good/good/acceptable condition) based on a visual and tactile inspection of the specimens, where attention was paid to the colour and translucence of enamel as well as the 'feel' of the sample (hardness, brittleness). We intentionally selected samples that represented the full spectrum of different condition categories to determine whether future, more extensive studies should include all materials or restrict themselves to the best-preserved ones. We collected these samples for several reasons: the general, typical preservation condition of finds in these sites, the limited availability of enamel samples in the collection, and the potential for useable results from samples that might not look appealing.

3.2.1. *Oxygen isotope CO3-PO4 equilibrium*

A way to monitor possible diagenetic alteration of skeletal bioapatite is through the analysis of co-existing carbonate and phosphate in biogenic apatite. We note that this approach, despite its limitations to determine which of the components is the cause of disequilibrium, is the only screening method able to flag signs of *isotopic* changes – which is the most important aspect for the purposes of this study. The oxygen isotope composition of both the phosphate and the structural carbonate within bioapatite is formed together in isotopic equilibrium with the same oxygen source, body water, at the same temperature (ca. 37 °C for mammals), and there is a strong linear relationship between the δ^{18}Op and δ^{18}Oc values (Iacumin et al., 1996). When the δ^{18}Op values are plotted against δ^{18}Oc, the points should lie close to the line of established well-preserved isotope values and exhibit a mutual offset near ~9‰ (Bryant et al., 1996; Iacumin et al., 1996). A more recent and extensive compilation of the expected offset between the δ^{18}O values of carbonate and phosphate (Δ^{18}O CO3-PO4) in well-preserved bioapatite, highlighting significant natural variability possibly stemming from physicochemical factors that influence enamel formation and hydroxyapatite crystallization, has since expanded the range of offsets considered acceptable (Martin et al., 2008) to 7.2–10.6‰. Here, we've compared our δ^{18}O value pairs to the dataset presented by Martin et al. (2008), who used modern carbonate shells (Lecuyer et al., 1998; Longinelli and Nuti, 1973), modern *Equus* (Bryant et al., 1996), *Gazella gazella* (Shahack-Gross et al., 1999), *Hippopotamus amphibius* (Zazzo, 2001) and several modern mammals (Iacumin et al., 1996).

3.2.2. *ATR-FTIR Spectral analysis*

To gain more insight into the general condition and preservation of

the specimens at the study sites, ATR-FTIR was used. ATR-FTIR is a vibrational spectroscopy technique that is used to provide unique spectra for molecules in biological tissues. Skeletal tissue is comprised of different mineral and organic components that experience different molecular vibrations. ATR-FTIR analysis provides information about the chemical composition, the structural differences, and the degree of substitution of bioinorganic materials (Dal Sasso et al., 2018; Diez et al., 2021). The low amount of required sample needed for the analysis (~1–2 mg), the speed of the analytical procedure and its non-destructive nature make this method very advantageous (Cersoy et al., 2017; Dal Sasso et al., 2018).

During the assessment of sample preservation, we used criteria outlined in France et al. (2020), presenting various acceptance ranges based on sample pretreatment and sampled bioapatite tissue. As our samples were already pretreated, we utilized the following ranges to indicate good preservation status: infrared splitting factor (IRSF) (3.1–4.0) and carbonate/phosphate (C/P) (0.08–0.2) for enamel; and IRSF (3.1–4.0) and C/P (0.05–0.3) for dentin (tusk) (Fig. 3). As recommended by France et al. (2020), we looked at the C/P index more than other indices as the most informative index for distinguishing poor general preservation for pre-treated samples. C/P is calculated as a ratio of B-type carbonates to V3 $PO4^{3-}$ and therefore any deviations from the established range will indicate loss or addition of carbonate and/or phosphate from the bioapatite.

In addition, we calculated the IRSF index. Despite its limitations (Dal Sasso et al., 2018), IRSF is a useful index for assessing the degree of mineral recrystallisation or matrix loss during diagenesis (France et al., 2020), which can have bearing also on the isotopic integrity. Even if the mineral matrix has not been contaminated by additions of diagenetically precipitated new phosphate or carbonate and the proportions of $CO3^{2-}$ and $PO4^{3-}$ are acceptable according to the C/P index, isotope exchange may happen due to recrystallisation. This is why deviations from the recommended IRSF range also call for an evaluation of the $\delta^{18}O$ values. Signs of significant recrystallisation may indicate that the bioapatite exhibits isotopic values altered by exchange with the surrounding burial environment. While usually the $CO3^{2-}$ component can more easily with the oxygen from the environment, in situations of high microbial catalytic activity, the usually resistant $PO4^{3-}$ oxygen can be altered as well (Zazzo et al., 2004a), and therefore the isotopic values cannot be used for paleoclimatic reconstructions.

It is important to note that the study by France et al. (2020) was designed to make the pre-screening of bioapatite alteration in archaeological mammal and human remains more precise for chemical and structural studies of bioapatite and consequently does not address the implications of any possible chemical/structural changes to isotopic alteration, making the findings suggestive when applied to isotopic studies. Nevertheless, the study by France et al. (2020) offers the most comprehensive data regarding the acceptable ranges of diverse ATR-FTIR indices in various contexts, and their criteria were valuable in evaluating the general preservation state of our samples.

The infrared (FTIR) absorption spectrum of the test substance was obtained using a FTIR spectrometer IRTracer-100 (Shimadzu) equipped with diamond attenuated total reflectance (ATR) device. An aliquot of the pretreated sample powder was loaded onto the ATR surface and absorbance (%A) spectrum was recorded in the range 400–4000 cm-1 with a resolution of 4 cm-1 having accumulations of 24 scans. Out of 33 samples, FTIR spectroscopy was carried out for the set of 31 samples by The Laboratory of Chemical Analysis of Tallinn University of Technology, Tallinn, Estonia because there was not enough material left to analyse the two remaining samples, VG 33 and VG 34. The C/P index was calculated as absorbance peak at 1415 cm-1 divided by the absorbance peak at 1035 cm-1. IRSF index was calculated as the sum of absorbance peaks at 565 cm-1 and 605 cm-1 divided by the absorbance peak at 590 cm-1. Typical enamel FTIR spectra, as well as FTIR spectra for all analysed samples, are available in the Supplementary data.

3.3. Oxygen isotope analyses

Oxygen isotope analysis was performed at the Laboratory of Chronology, Finnish Museum of Natural History. The samples were divided into three batches for different stages of the process. During the pretreatment stage, we weighed approximately 10 mg of enamel and approximately 15 mg of dentine for their respective batches. The pretreatment of the samples followed the modified procedure outlined in Bocherens et al. (1997): at first, the samples were treated with a 2.5% NaOCl solution for approximately 17 h, allowing them to react at room temperature. The following day, the NaOCl solution was removed through centrifugation, and the samples were washed 4 times with MilliQ water. Afterwards, the samples underwent treatment with a buffer solution of 1 M Ca acetate, followed by another round of centrifugation and MilliQ water washes. After drying in a thermal cabinet at +40 °C overnight, the samples were homogenized, weighed to calculate mass loss, and prepared for further analysis. The subsequent analysis of carbonate $\delta^{18}O$ values is based on the classical method by McCrea (1950), which involves using anhydrous phosphoric acid to release CO_2 from the carbonate samples. The analytical procedure is based on the modified procedure after Revesz et al. (2001). We weighed approximately 2.5 mg of the material for both the original and duplicate samples. The samples were placed in borosilicate glass Exetainer vials (Labco Ltd, UK), sealed with rubber septum screw caps, and flushed with helium to remove air. Anhydrous >100% H3PO4 is added to initiate the acid reaction, and the vials are then placed in the sample block of an automated GasBench II preparation peripheral at 25 °C for 18 h to react and equilibrate. The resulting CO_2 gas is analysed for $\delta^{18}O$ values using continuous flow gas isotope ratio mass spectrometry, with the Thermo Scientific Delta V Advantage isotope ratio mass spectrometer coupled to the GasBench II preparation device. Isotope data were normalized using NBS-18 (−23.01‰ ($\delta^{18}O$) and −5.01‰ ($\delta^{13}C$)) and NBS-19 (−2.2‰ ($\delta^{18}O$) and −1.95‰ ($\delta^{13}C$)). The runs additionally included replicates of an in-house calcite material from the Vimpeli quarry ("VIM"; n = 15) and a mammoth tooth enamel powder from Wrangel Island ("J-5"; n = 3). The precision indicated by replicates of all the reference materials analysed with the unknowns was ±0.2‰. Due to analytical challenges one of the two replicate analyses was rejected for altogether 14 samples (see Supplementary data). The mean standard deviation of duplicates for the unaffected samples (n = 16) was 0.14‰. The mean value and SD of the two replicates for each sample, when both are available, are presented in Table 1.

The $\delta^{18}O$ value of skeletal phosphate was analysed as Ag3PO4. The precipitation of Ag3PO4 followed the modified procedure outlined in Wiedemann-Bidlack et al. (2008) with a longer precipitation time of 48 h to ensure full precipitation. We weighed approximately 0.5 mg of enamel and 0.8 mg of dentine for both the original and duplicate samples. After the pretreatment, the samples were dissolved in HNO3 for 20 h. Meanwhile, precipitation vials were prepared, and the required amount of AgNO3 was weighed out in a beaker. The dissolved sample solution was added to the precipitation vials, which were then placed in a water bath at 50 °C 48 h. Throughout this time, the crystallization and evaporation of the solution were monitored, with MilliQ water added as necessary. Once the precipitation was complete, the crystals were inspected under microscope for colour and habit. The liquid was extracted, and MilliQ washes were performed. Finally, the Ag3PO4 crystals were transferred to silver cups. The dried crystals were then pyrolyzed at 1400 °C, and the resulting CO gas's $\delta^{18}O$ value was analysed using a Thermo Scientific Flash IRMS TCEA coupled to a Delta V Plus isotope ratio mass spectrometer. To normalise to the VSMOW scale, several known $\delta^{18}O$ values were utilized, including ANU sucrose (IAEA-CH6; (+36.4‰ for $\delta^{18}O$; −10.4‰ for $\delta^{13}C$) (Coplen et al., 2006), and two Ag3PO4 reference materials: AGPO-SCRI (+14.5‰; Halas et al., 2011) and an in-house apatite powder from Siilijärvi quarry SJ-1 (+5.5 ± 0.1‰; calibrated against USGS-80 (+13.1‰) and USGS-81 (+35.4‰) at the USGS Reston Stable isotope laboratory). NBS-120c phosphate rock

material and an in-house mammoth enamel material "J-5″ were used as quality controls throughout the analysis, and were extracted, analysed, and normalized alongside the unknowns. The NBS-120c yielded a mean value of +21.8 ± 0.10‰ (n = 8), while replicates of the J-5 enamel material gave a SD of 0.21‰ (n = 9). The external precision was determined to be better than ±0.3‰ through repeats of Ag3PO4 reference materials and samples. Altogether, 31 samples were analysed in duplicate, two samples did not yield results. The mean value and SD of the two replicates for each sample are presented in Table 1. For three samples, one of the two replicates was rejected due to a reduced Ag3PO4 yield and low signal intensity in IRMS analysis. The mean standard deviation for all successful duplicates was 0.14‰. Duplicates for three samples showed elevated standard deviations of >0.3‰.

The oxygen isotope data for both phosphate and carbonate are presented as delta values in per-mil against the VSMOW standard. The $\delta^{18}O$ values of carbonate were translated to the VSMOW scale using $\delta^{18}O(VSMOW) = \delta^{18}O(VPDB)*1.03092 + 30.92$ (Brand et al., 2014) (). The raw results for carbonates are available in the Supplementary data.

3.4. Data analyses

Differences in isotopic values between Shestakovo, Krasnoyarskaya Kurya and Volchia Griva were tested using statistical methods. The averages for the three aforementioned sites were calculated as unweighted means. Statistical analysis was performed in Python (version 3.11.4), using the pandas (Pandas Development Team, 2023), NumPy (Harris et al., 2020), and SciPy (Virtanen et al., 2020) libraries. The Python code used for statistical analyses is available in the Appendix. The Shapiro-Wilks test was used to test for normality of data distribution. The test indicated the data are not drawn from a normally distributed population, and therefore, the Kruskal-Wallis test recommended for non-normal data was performed.

For mammoth enamel and tusk samples, we used the calibration equation of elephants (Ayliffe et al., 1992) to convert $\delta^{18}Op$ values to $\delta^{18}Ow$ estimates assuming that mammoths exhibited similar ecological behaviours, dietary patterns, physiological characteristics, and metabolic rates to those of modern elephants (Olivier, 1982; Haynes, 1991). This equation has been successfully implemented to calculate environmental water values in other studies (e.g., Arppe and Karhu, 2010; Tütken et al., 2007). For the horse sample, we used the calibration equation of wild horses (Huertas et al., 1995) and for the deer sample, we used the calibration equation of reindeer (Longinelli et al., 2003). For error calculation and propagation of the $\delta^{18}Ow$ values, we used formulas from Pryor et al., (2014).

4. Results

4.1. ATR-FTIR spectral analysis

All enamel ATR-FTIR spectrograms display a spectrum typical for enamel, except VG 30 (Supplementary data), which also failed in Ag3PO4 extraction and $\delta^{18}Oc$ analysis. The ATR-FTIR spectrograms of the tusk samples also display spectrums similar to those of pretreated dentine from France et al. (2020) (Supplementary data).

The calculated C/P ratios, and the IRSF values for each sample are reported in Table 1. The C/P ratio values for 24 enamel and tusk samples fall within the well-preserved ranges as defined in France et al. (2020). Five samples have C/P values outside of the prescribed range: VG 18, VG 29, VG 30, VG 31, and KK 66, the clear majority being tusks (Fig. 3).

The IRSF ratio values for 13 enamel samples fall within the recommended range, whereas six samples, SH 55, VG 17, VG 18, VG 31, VG 32, KK 59, show elevated IRSF values (Fig. 3). Out of all samples, VG 18 stands out particularly because it has an abnormally high IRSF ratio of 8.058 and a negative C/P ratio of −0.009. In stark contrast to the enamels, all tusk samples except one, KK 60, exhibit IRSF values above the prescribed range defining well-preserved dentine samples.

There is a negative correlation between the IRSF index values and C/P values (Fig. 3), i.e. more elevated IRSF values are strongly associated with diminished C/P. The coefficient of determination r^2 stands at 0.68, implying that approximately 68% of the variability in IRSF values can be explained by the changes in C/P values.

4.2. $\delta^{18}O$ values

Table 1 displays the isotope values for all analysed samples. Altogether, 29 $\delta^{18}Op$ values and 30 $\delta^{18}Oc$ values were obtained. The range of variation of $\delta^{18}Op$ for the full dataset is +6.9‰ – +11.9‰, and +16.3‰ – +22.5‰ for $\delta^{18}Oc$. The range of variation of $\delta^{18}Op$ values for Shestakovo is from +6.9‰ to +8.8‰, from +8.1‰ to +9.8‰ for Krasnoyarskaya Kurya and from +8.2‰ to +11.9‰ for Volchia Griva. For the carbonate component, $\delta^{18}Oc$ values for Shestakovo range from +16.3‰ to +17.5‰, while the range of variation is from +17.7‰ to +19.1‰ for Krasnoyarskaya Kurya, and for Volchia Griva the range is from +18.7‰ to +22.5‰.

4.3. Oxygen isotope CO3-PO4 equilibrium

The range of variation of $\Delta^{18}O$ CO3-PO4 offsets for the full dataset is +7.4‰ – +11.7‰, which at the same time equals the range of $\Delta^{18}O$ CO3-PO4 offset values for Volchia Griva. The samples from Shestakovo and Krasnoyarska Kurya show narrower ranges of $\Delta^{18}O$ CO3-PO4 offsets: from +8.7‰ to +10.4‰, and from +8.1‰ to +10.1‰, respectively (Table 1). When compared to the regression line representing the best fit through the modern animal data pairs, 25 samples show $\Delta^{18}O$ CO3-PO4 offsets within the range suggested by Martin et al. (2008) to characterise good isotopic preservation of samples (Fig. 2 and 3). Four samples fall outside the envelope defined by the full scope of the well-preserved modern sample data and suggest isotopic disequilibrium: VG 23 ($\Delta^{18}O$ CO3-PO4 offset 11.1‰), VG 25 (10.7‰), VG 29 (11.3‰), and VG 33 (11.7‰). These four samples are omitted from the dataset used to calculate $\delta^{18}Ow$ values of past ingested environmental waters. We note that because the quality control data for δ18Op indicates a reproducibility of approximately ±0.3‰ and ±0.2 for the $\delta^{18}Oc$ values, it is possible that some of the discarded samples (e.g. VG 25) actually have intact $\delta^{18}Op$ values. However, for clarity we here adhered to the use of +7.2 – +10.6‰ (Martin et al., 2008) as a permissible range for the $\Delta^{18}O$ CO3-PO4 offset values as an unequivocal criterion for acceptance.

After the rejection of the specimens that exhibited disequilibrium offsets, the ranges of variation of $\delta^{18}Op$ values are not changed. The mean $\delta^{18}Op$ value of all the accepted samples is +9.6 ± 1.2‰. The site-specific $\delta^{18}Op$ means of isotopically preserved samples are +7.8 ± 0.9‰, +9.0 ± 0.6‰ and +10.5 ± 0.9‰ for Shestakovo, Krasnoyarska Kurya and Volchia Griva, respectively. Statistical analyses revealed that the $\delta^{18}Op$ and $\delta^{18}Oc$ values are statistically significantly different among the sites (Kruskal-Wallis test, $p < 0.05$). According to Tukey's Honestly Significant Difference (HSD), there is a statistically significant difference in $\delta^{18}Op$ and $\delta^{18}Oc$ values between the VG site and both the KK site (mean difference = 1.1971, $p < 0.05$ (for $\delta^{18}Op$), mean difference = 1.8869, $p < 0.05$ (for $\delta^{18}Oc$)) and the SH site (mean difference = 2.2704, $p < 0.05$ (for $\delta^{18}Op$), mean difference = 2.8931, $p < 0.05$ (for $\delta^{18}Oc$)). There was no significant difference in $\delta^{18}Op$ values between the KK and SH sites (mean difference = −1.0732, p = 0.1517 (for $\delta^{18}Op$), mean difference = −1.0062, p = 0.1004 (for $\delta^{18}Oc$)).

4.4. $\delta^{18}Ow$ values

Based on the $\Delta^{18}O$ CO3-PO4 offsets we left 25 samples in the dataset to be used for the reconstruction of environmental water $\delta^{18}Ow$ values. This dataset of 25 samples will be referred to in the further text as the "new southeastern West Siberian (SEWS) dataset". The reconstructed $\delta^{18}Ow$ values for individual samples and their associated reconstruction errors are listed in Table 1. The horse and deer samples from Shestakovo

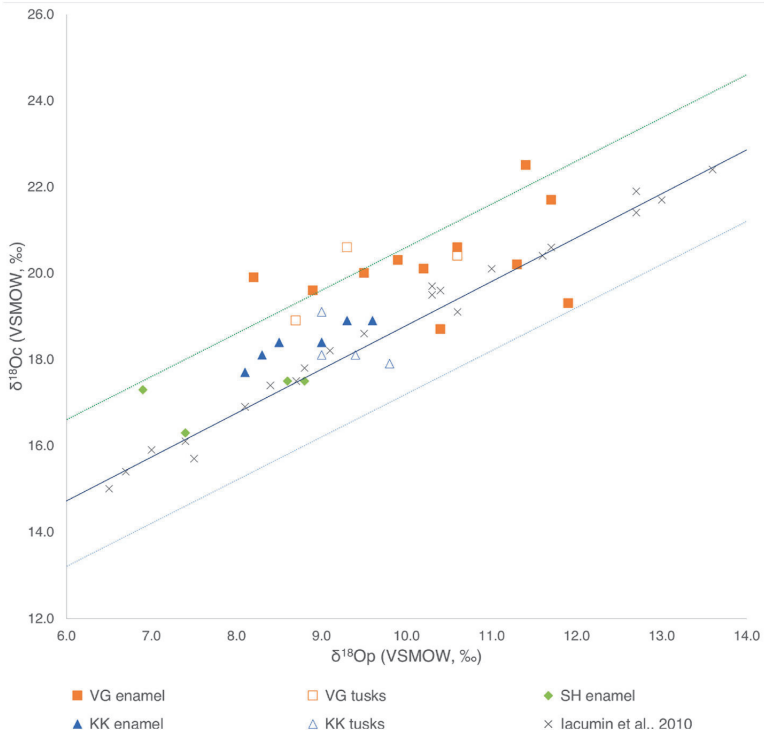

Fig. 2. The relationship between oxygen isotope compositions of carbonate (δ^{18}Oc) and phosphate (δ^{18}Op) of bioapatite. The solid line δ^{18}Oc = 1.037 (±0.026) δ^{18}Op+8.57 (±0.504), with r = 0.98 (p < 0.0001) represents isotopic equilibrium between δ^{18}Oc and δ^{18}Op according to Martin et al. (2008), along with the dotted lines representing the upper and lower envelopes for the acceptable range of δ^{18}Oc-δ^{18}Op offsets from 7.4 to 10.6. In addition to the Martin et al. (2008) dataset, the graph shows 23 mammoth and bison bone samples from northern Siberia with well-preserved isotopic values from Iacumin et al. (2010) to compare with our dataset.

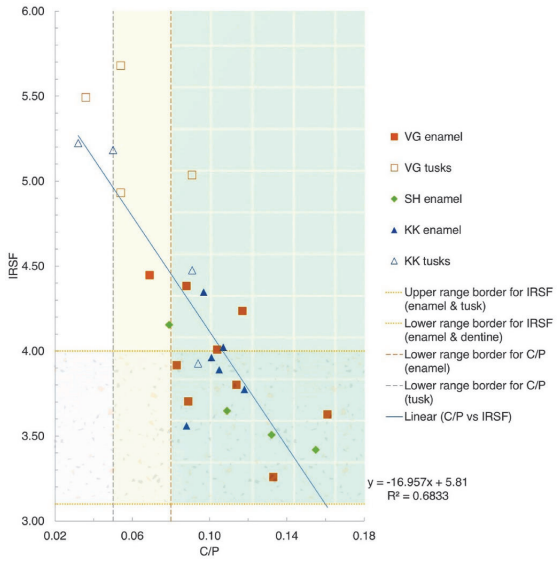

Fig. 3. The relationship between IRSF values and C/P values. A strong negative correlation suggests that the elevated IRSF values are linked to loss of carbonate (see Discussion).

yielded calculated δ^{18}Ow values clearly lower than the mammoth specimens from the site. For the mean values given here, only the mammoth specimens are used due to constraints set by the error propagation method, and for best between-site comparability. The mean δ^{18}Ow value and the associated reconstruction error (Pryor et al., 2014) of all the accepted mammoth samples is −14.6 ± 1.1‰ (Table 1). The site-specific δ^{18}Ow means of isotopically preserved mammoth samples are −16.6 ± 1.6‰ (n = 2), −15.2 ± 1.2‰ (n = 11) and −13.6 ± 1.0‰ (n = 11) for Shestakovo, Krasnoyarska Kurya and Volchia Griva, respectively (Table 1).

5. Discussion

5.1. ATR-FTIR spectral analysis

Thirteen samples, the majority of them being tusks (eight specimens), originating from all three sites showed IRSF values above the values characteristic of well-preserved samples according to France et al. (2020). The IRSF can increase with the degree of mineral recrystallisation, which could be of concern to the integrity of the in vivo δ^{18}Op values. However, the IRSF has been shown to significantly increase due to the removal of carbonate substitutions during pretreatment (France et al., 2020) which we performed on our set of samples. The high IRSF values in our samples are often associated with lowered C/P values which results in a strong negative correlation between C/P and IRSF parameters (Fig. 3). Lowered C/P values can indicate that either carbonate loss took place, or that phosphate was added to the sample. We suggest that the most parsimonious explanation to the observed

correlation reflects the previously reported association of the carbonate content and the crystallinity of apatite, whereby the removal of carbonate phases, lowering the C/P ratios, decreases the defects and increases order in the crystal structure (France et al., 2020; Pucéat et al., 2010; Snoeck and Pellegrini, 2015). Therefore, the increased IRSF indices are likely a result of some loss of the carbonate component from the bioapatite rather than a sign of recrystallisation, which might have also altered the original δ^{18}Op values.

There is a distinction between the two material types as regarding their IRSF values: out of the nine tusks analysed altogether, all but one showed IRSF values elevated above the value prescribed for well-preserved samples. At the same time, a clearly lower proportion of five out of fifteen enamels showed elevated IRSF values. Thus, the tusks appear to have been deteriorated more by post-depositional alteration and as a consequence, were more susceptible to carbonate loss during the acid pretreatment to a larger extent than enamel. This is not unexpected, as in addition to their overall superior density and mineralization level, enamel sheets are more protected by the surrounding mass of cementum and dentine of the molars. While we assume that the carbonate loss took place during acid pretreatment, we note that we cannot exclude the possibility that the material had experienced carbonate loss already at the site of burial. The preservation conditions of the materials from the investigated sites are indeed more challenging than those at the high-latitude sites of northern Siberia with permafrost. Volchia Griva stands out for the high proportion of discarded material. The materials from Volchia Griva were initially buried in subaerial conditions; subsequently, some of them were covered by lacustrine sediments (Leshchinskiy and Burkanova, 2022), and therefore the remains were influenced by the alteration of sedimentological and environmental conditions. Other causes that affect the preservation can also include chemical and microbial degradation due to post-mortem weathering or even intravital changes during geochemical stress/mineral starvation when the composition of bone and dental tissue changes (Leshchinskiy, 2012, 2015, 2017).

5.2. Oxygen isotope CO3-PO4 equilibrium

We can assess the overall dispersion of Δ^{18}O CO3-PO4 offsets in our dataset by comparing them to the dataset of well-preserved bioapatite of 23 woolly mammoth and bison (*Bison priscus*) bone samples from Iacumin et al. (2010) collected at two northern Siberian sites, the mouth of the delta of the Lena River, and the Bol'shoy Lyakhovsky Island (Fig. 1). When plotted on the Δ^{18}O CO3-PO4 diagram (Fig. 2), all the data points of the North Siberian material lie very close to the regression line of well-preserved isotope values (Martin et al., 2008). Their largest departure from the original expected offset of ~9‰ is 1‰, whereas for our new SEWS dataset the number is 1.6‰. Compared to Iacumin et al. (2010), our datapoints are more scattered, suggesting more variable preservation in general, and that the samples from the southeast of Western Siberia have a poorer overall preservation than samples from high northern latitudes buried in permafrost conditions.

The four discarded samples had Δ^{18}O CO3-PO4 offsets higher, not lower, than the upper limit of 10.6‰ (Martin et al., 2008). Therefore, the process responsible for the observed isotopic disequilibrium had lowered the δ^{18}Op values or raised the δ^{18}Oc values. Generally, the structural carbonate is more susceptible to post-depositional alteration (Iacumin et al., 1996), and thus the more likely candidate as the cause for the observed disequilibrium. However, a calculation of the expected δ^{18}Oc value of diagenetic carbonate using the carbonate-water fractionation equation by Kim & O'Neil (1997) ($1000\ln\alpha_{(Calcite\text{-}H20)} = 18.03\ (10^3\ T^{-1})$ - 32.42), and the present-day mean annual values of δ^{18}O of precipitation (−14.6‰; GNIP, Novosibirsk meteorological station, year 1991) and air temperature (0.8 °C; Arhiv klimaticheskih dannyh, 2023) for the region, yields a value of +18.7‰, which is lower than the average δ^{18}Oc value for the discarded samples (+20.9‰). Thus, the incorporation of such diagenetic carbonate would not increase the δ^{18}Oc values as needed to explain the elevated offset values.

The phosphate component of bioapatite is resistant to oxygen exchange under inorganic conditions at low temperatures because the exchange rate between phosphate and water is relatively slow and because P–O chemical bonds are strong (Zazzo et al., 2004a; Martin et al., 2008). However, the phosphate fraction may also experience diagenetic change: altered δ^{18}Op values can be a result from isotopic exchange under microbially mediated reactions (Zazzo et al., 2004a; 2004b). Additionally, the massive subaerial accumulation of megafaunal remains in a limited area over a relatively short period of time, as occurred at Shestakovo and Volchia Griva, can create a more favourable environment for microorganisms, that enhances the potential for microbially mediated alteration of phosphate-oxygen (Salesse et al., 2014).

Following the same line of reasoning as above, we calculated the expected δ^{18}Op value of diagenetic phosphate that would precipitate under ambient conditions in the study region using the phosphate-water fractionation equation by Chang and Blake (2015) ($1000\ \ln\alpha_{(PO4\text{-}H2O)} = 14.43(\pm0{,}39)1000/T(K) - 26.54(\pm1.33)$. The resulting value, +11.5‰, is higher than the δ^{18}Op values of the samples exhibiting isotopic disequilibrium and would not have acted to lower the δ^{18}Op value of the in vivo bioapatite of the samples in question.

However, we note that a diagenetic lowering of δ^{18}Op values would be possible in a scenario with clearly higher than current mean annual temperatures, e.g. during the summer season, but still low δ^{18}O values of environmental waters. Summer temperatures in Siberia during the LGM were likely as high or even higher than today (Bakker et al., 2020), but naturally the summertime environmental water δ^{18}Ow values are unknown. One could hypothesise, that possibly more severe winters and the expanded extent of permafrost down to 50°N (e.g. Kitover et al., 2016) might have kept also summer δ^{18}Ow values in the soil relatively lower than today. However, the data on permafrost at these latitudes does not have an exact temporal basis (Aubekerov and Gorbunov, 1999; Vandenberghe et al., 2014). Obtaining a diagenetic δ^{18}Op value of +8.2 ‰, the lowest δ^{18}Op value of the four discarded samples, would require a diagenetic fluid (soil water) with a δ^{18}Ow value at −13.7‰, ca. 1 ‰ higher than the δ^{18}O value of present-day mean annual precipitation in the area. We note that this value is very close to the site specific mean reconstructed δ^{18}Ow value for Volchia Griva (−13.6 ± 1.0‰).

Summarizing the above discussion on sample preservation at Shestakovo, Krasnoyarska Kurya and Volchia Griva, the majority of samples from all three sites had acceptable isotopic preservation, but there were both tusk and even enamel samples that showed signs of post-depositional isotopic and/or chemical (cf. FTIR data) alteration. As previously recognised, the potential of tusks to offer valuable insights into both climatic conditions and the life history of mammoths is significant (e.g. Fox et al., 2007; Rowe et al., 2024), but many of the tusk specimens from Krasnoyarskaya Kurya and Volchia Griva exhibited clear evidence of carbonate loss and accompanying structural changes reflected as elevated IRSF values and associated lower C/P ratios. The precise cause of the loss remains uncertain, as it could be attributed to site-specific conditions, sample pretreatment methods, or a combination of both factors. While most of the tusk samples exhibited signs of carbonate loss, their δ^{18}O values appear to have remained intact and thus, can serve as material for future δ^{18}O studies. However, the prevalence of carbonate loss may indicate that the general condition of tusk specimens at these sites is less than optimal, which may have a bearing on e.g. preservation status of the organic component commonly used for δ^{13}C and δ^{15}N studies.

5.3. Paleoclimatic reconstruction

Western Siberia (Fig. 1) is underrepresented in terrestrial compilations of LGM climate reconstructions, as the majority of studies have focused on northern Siberia. The latter half of the Middle Weichselian period (34–24 ka) in Siberia was characterised by summers cooler than

during the earlier part of MIS 3 (52-40 ka yr BP) (Wetterich et al., 2021). Modelling studies suggest a global-scale summer cooling of approximately 6 °C during the LGM 23 - 19 ka yr BP (Tierney et al., 2020). Pollen records and the modelling efforts of LGM summer temperatures around 21 kyr BP in Eastern Siberia (Fig. 1) reveal a consistent pattern of higher summer temperature anomalies compared to other high-latitude regions, along with moisture availability levels similar to present-day levels (Weitzel et al., 2022). Fossil insect evidence from East Siberian Arctic regions supports the existence of a tundra-steppe biome sustained by a continental climate with warmer summers and colder winters than the present environment (Sher et al., 2005). Pollen-based reconstructions by Tarasov et al. (1999), Wu et al., 2007, and Cleator et al., 2020 indicate higher summer temperature anomalies at high latitudes than at mid-latitudes in Central Siberia. Based on pollen and plant macrofossil analysis, consistently cold and dry conditions characterised the LGM in the Northern and Central Siberia (Bush, 2004; Kageyama et al., 2001; Schirrmeister et al., 2002; Shin et al., 2003; Tarasov et al., 1999). Palynological analysis of bone-bearing sediments of layer V at Shestakovo shows an open landscape with Cyperacea, Papaveracea and Poaceae dominating in the grass cover. The overlying sediments of layer VI were formed under conditions of relative climate warming (Derevianko et al., 2000, 2003). According to pollen data from Volchia Griva, from the start of the site's formation, the climatic conditions gradually shifted to more arid but the data does not show extreme cooling (Leshchinskiy and Burkanova, 2022).

We can use the oxygen isotopic records from the three studied sites to investigate the climatic context of the LGM period in the southeast of Western Siberia and compare that to the patterns in Western Siberia reported earlier. Fig. 4 illustrates the site-specific reconstructed δ^{18}Ow values of the SEWS dataset during the LGM, and the mean values are as follows: Shestakovo (ca. 28-27 ka cal BP) −16.6 ± 1.6‰ (n = 2), Krasnoyarskaya Kurya (ca. 25 - 23 ka cal BP) −15.2 ± 1.2‰ (n = 11), and Volchia Griva (ca. 24-22 ka cal BP) −13.6 ± 1.0‰ (n = 11). The mean δ^{18}Ow for all three investigated sites is −14.6‰. In the present day, the mean annual δ^{18}Ow values suggested by the Online Isotopes in precipitation calculator (OIPC 3.1; Bowen and Revenaugh, 2003) at all three sites are similar with a mean value of −14.6 ‰ for all three sites. This estimate also compares well to the present-day mean annual values of δ^{18}O of precipitation indicated by the IAEA records, albeit being very limited in extent (−14.6‰; GNIP, Novosibirsk meteorological station, year 1991). Thus, when considering the mean δ^{18}Ow value of all three sites, the SEWS dataset suggests no change in the δ^{18}Ow value of precipitation between ca. 28-22 ka cal BP and the present-day at the mean annual level. This is consistent with Genoni et al. (1998) suggesting that during the Late Pleistocene and early Holocene, the mean isotopic composition of atmospheric precipitation over Southern Siberia was not significantly lower than that of modern mean annual precipitation and that during Late Pleistocene, the winters were colder, and the summers were hotter compared to the present day.

The comparison between the sites, however, reveals a pattern: the increasing δ^{18}Ow values from Shestakovo and Krasnoyarskaya Kurya to Volchia Griva may reflect a warming trend from the deposition of the bone-bearing layer at SH (ca. 28–27 ka cal BP) with lower δ^{18}Ow values to that of Volchia Griva (24–22 ka cal BP) with higher δ^{18}Ow values in the region. Because there are only two mammoth samples from Shestakovo and at the same time, the δ^{18}Ow values from Shestakovo and Krasnoyarskaya Kurya are statistically similar (see Materials and Methods), the δ^{18}Ow values from these sites can be combined as one dataset with a mean at −15.2 ± 1.8‰ which is statistically different from the Volchia Griva δ^{18}Ow mean value (mean difference = 1.5997, $p < 0.05$). Therefore, our isotopic record captures a shift from glacial conditions with low δ^{18}Ow at time periods corresponding to the accumulation of the Shestakovo and Krasnoyarska Kurya bone layers to higher δ^{18}Ow levels similar to those of late glacial levels (Fig. 4) at Volchia Griva. Studies of the present day patterns of δ^{18}Ow in precipitation (Kurita et al., 2004; Butzin et al., 2014) indicate that air temperature is the main controlling factor of the variability (ca. 80%) in δ^{18}Ow of annual precipitation in Russia, and at the same time, much of the correlation is driven by the strong wintertime δ^{18}Ow-T correlation. If the same relationship between δ^{18}Ow and temperature in general, and

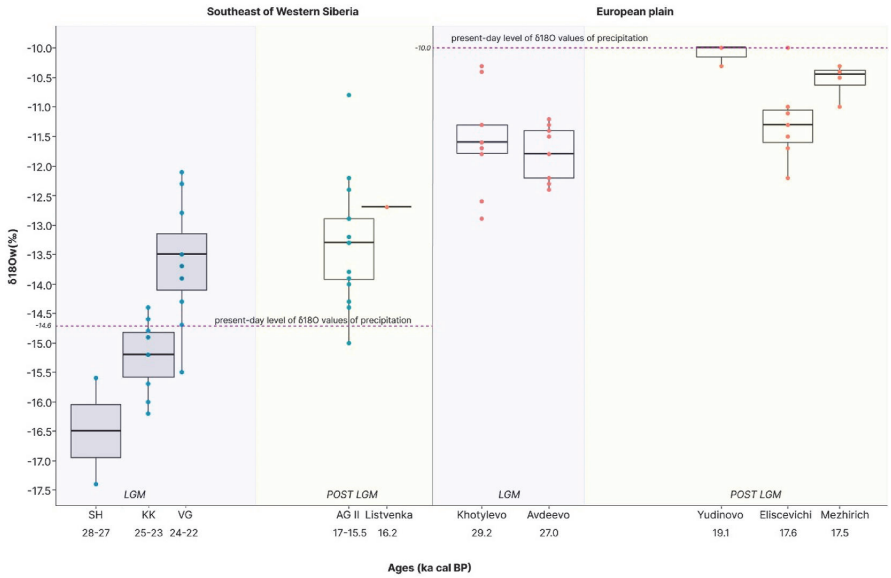

Fig. 4. Comparison of δ^{18}Ow values reconstructed bioapatite δ^{18}Op values from two low-latitude areas in Eurasia: the southeast of Western Siberia based on the new SEWS dataset as well as data from Genoni et al., 1998 for Afontova Gora (AG II) and Listvenka; and sites of the European plain (Genoni et al., 1998). Box and whisker statistics are drawn for all data with finite calibrated dates from published sources. The numers next to the boxes and datapoints refer to calendar years in ka cal BP. Purple horizontal dashed lines represent the regions' present-day level of δ^{18}O values in precipitation.

that of seasonal systematics prevailed also during glacial times, the mammoth-derived SEWS δ^{18}Ow values likely reflect changes in air temperature, winter temperatures in particular. We suggest that the temporal development, i.e. warming, of climate is the main explanation for the increase in the δ^{18}Ow values from the layer dates of ca. 28–23 (SH and KK) to ca. 24–22 ka cal BP (VG), but we treat the temporal context of this hypothesis cautiously because the 14C dates constrain the approximate ages of layers instead of the actual individual samples analysed here for oxygen isotope values. However, we chose to avoid applying quantitative temperature conversions for our study because of the many factors that can complicate the calculations, namely any changes that might have occurred in the humidity, temperature and the isotopic composition of the source conditions and the seasonality of precipitation (e.g. Alley and Cuffey, 2001; Fricke and O'Neil, 1999).

Published oxygen isotopic data in Siberia are scarce overall, and LGM, in particular, forms a gap in oxygen isotopic records in northern Siberia (e.g., Fox et al., 2007; Iacumin et al., 2010) and the period is not represented in the previous δ^{18}Ow records for the southeast of Western Siberia (Genoni et al., 1998). The only reference values available that are close to our investigated sites, consist primarily of reindeer samples and are from the post-LGM time. We note that we are excluding the four specimen from Kashtanka in the SEWS (Genoni et al., 1998) due to ambiguity in its possible age (Bokarev and Martynovich, 1992; Drozdov et al., 1992). In the southeast of Western Siberia, the Afontova Gora II site yielded an average δ^{18}Ow value of −13.6‰ for 17.2–15.5 ka cal BP, and one reindeer bone sample from Listvenka site yielded a δ^{18}Ow value of −12.7‰ for 16.2 ka cal BP (Fig. 4; Genoni et al., 1998). These values are clearly higher than the mean δ^{18}Ow values at Shestakovo and Krasnoyarskaya Kurya but similar to the site-specific mean of −13.6 ± 1 ‰ at Volchia Griva. Given the fact that the material from Volchia Griva comes from the youngest layer analysed (ca. 24–22 ka cal PB), the difference between the post-LGM records and those from Shestakovo and Krasnoyarskaya Kurya, and the similarity with Volchia Griva supports the hypothesis of the temporal development of the climate in the region.

Much further to the west, another area with mammoth based δ^{18}Ow values available at a similar low latitude to that of the SEWS dataset is the European Plain (Fig. 1). There, the mean δ^{18}Ow values from Khotylovo (29.2 ka cal BP); −11.6‰) and Avdeevo (27 ka cal BP; −11.8‰) (Fig. 4; Genoni et al., 1998) give a mean glacial δ^{18}Ow value of −11.6‰. Compared to the samples from the European Plain, the mean δ^{18}Ow values for Shetaskovo, Krasnoyarska Kurya and Volchia Griva during LGM were lower, particularly the samples from SH and KK show non-overlapping ranges compared to the Avdeevo and Khotylevo δ^{18}Ow values. The per mill difference between Shestakovo (28–27 ka) and Khotylevo/Avdeevo (29–27 ka) is ~5‰. The lower δ^{18}Ow values for the SEWS dataset are consistent with the present-day pattern of δ^{18}O values of precipitation over Eurasia, where the mean δ^{18}O precipitation values in our study area (−14.6‰) are 4.6 ‰ lower than the annual mean δ^{18}O precipitation values for the European plain: −10.0‰ (OIPC 3.1; Bowen and Revenaugh, 2003) (Fig. 4). The per mill difference observed in mean δ^{18}Ow values between the southeast of Western Siberia and the European plain, with the latter exhibiting higher values, both for LGM and for present day suggests a similar gradient of the depletion of δ^{18}O in precipitation over Eurasia at this latitude and shows that the "continental effect" during LGM was similar to present day (Rozanski et al., 1993). The similarity of the geographical δ^{18}Ow pattern between these two regions both during the LGM time period and the present day then implies that the total shift in the δ^{18}Ow values of precipitation from glacial to modern conditions was similar, approximately 1.5–2‰.

For the post-LGM period in the European plain, the mean δ^{18}Ow value from Yudinovo (19.1 ka cal BP) is −10.1‰, from Mezhirich (17.5 ka cal BP) it is −10.5‰ and from Elisevichi (17.6 ka cal BP) it is −11.3‰, giving a combined post-LGM mean δ^{18}Ow value at −10.8 ± 0.4 ‰. Compared to these values, the mean δ^{18}Ow values for the two late glacial sites in SEWS Afontova Gora II and Listvenka (−13.2‰) is again clearly lower, yet not at the ca. 5 ‰ difference level as seen for the present-day and LGM period. Compared to a noticeable shift in the δ^{18}Ow values in the southeast of Western Siberia from the age of the SH and KK layers at ca. 28-23 ka cal BP to the dates associated with Afontova Gora/Listvenka at ca. 17–15.5 ka, the changes in the δ^{18}Ow values in the European Plain from approximately the same time interval are much smaller: the earliest δ^{18}Ow value for Shestakovo samples (−16.6‰) is 3.4‰ lower than the latest post-LGM δ^{18}Ow value from Afontova GoraII/Listvenka (−13.2‰), whereas the mean LGM δ^{18}Ow values from Khotylovo/Avdeevo (−11.6‰) is only 0.3‰ lower than the latest post-LGM value from European plain site Elisevichi (−11.3‰) respectively. Based on our isotopic records, these comparisons suggest that the southeast of Western Siberia experienced a more pronounced climatic change from 28 to 23 to the late glacial level than the European plain. This is associated with the fact that the reconstructed late-glacial δ^{18}Ow levels for SEWS are actually ca. 1 ‰ above the present-day level of δ^{18}Ow values in precipitation, whilst, on the European Plain, they remained ca. 0.8‰ below the present-day levels. We further note that the reconstructed δ^{18}Ow values for Volchia Griva are already on par with the SEWS late-glacial values, suggesting that the shift to ameliorated conditions occurred relatively early in this region.

Numerous studies have suggested that the LGM was an unfavourable period for mammoth existence, with some suggesting that temperatures were as low as −10 °C (e.g., Nikolayev and Mikhalev, 1995), making it particularly inhospitable for both large fauna and humans. However, our isotope data works in support of the notion that mammoth fauna could not only inhabit but also potentially thrive in the SEWS during the LGM. Despite the observed shift in temperature during the LGM in SEWS, our comparison between LGM, post LGM and present-day values indicates that the climatic conditions were not unbearable for mammoth fauna.

6. Conclusions

We analysed 29 mammoth enamel and tusk samples, deer and horse enamel samples from three geographical sites in the southeast of Western Siberia: Shestakovo, Krasnoyarskaya Kurya and Volchia Griva, checked their preservation using ATR-FTIR, obtained δ^{18}Op and δ^{18}Oc values, assessed their isotopic integrity using oxygen isotope CO3-PO4 equilibrium and reconstructed δ^{18}Ow values for the time period ca. 28 - 22 ka cal BP.

We propose that the temporal development of the climate in the SEWS primarily explains the increase in δ^{18}Ow values from 28 to 23 to ca. 24-22 ka cal BP, and that changes in air temperature likely played a significant role in causing the isotopic changes. The observed per mill difference in mean δ^{18}Ow values between the SEWS and the European plain suggests a consistent gradient of δ^{18}O depletion in precipitation over Eurasia at this latitude, indicating that the "continental effect" during the LGM was similar to the present day. Isotopic records show that SEWS experienced more pronounced climatic changes transitioning from glacial conditions (ca. 29 to 23 ka) to the lateglacial (ca. 17 to 15.5 ka) than the European plain. The transition from the LGM to warmer conditions occurred relatively early, already at 24-22 ka, in the southeast of Western SIberia. Despite differences in local isotopic values, the comparison between past and modern values reveals that the isotopic shift from the LGM mean δ^{18}Ow values to the present day is similar for both regions, ca. 1.5–2‰.

The potential of the Volchia Griva, Shestakovo and Krasnoyarskaya Kurya sites for investigating the Late Glacial Maximum in SEWS is enormous due to the large amount of fossil material buried there. In the future, direct dating of the selected samples would allow us to understand their chronological positioning within LGM more precisely. Our study demonstrates the significance of carefully assessing the preservation of fossil material not under permafrost conditions. The preservation of the studied material is variable compared to more well-preserved material from North-Eastern Siberia, possibly due to different preservation conditions at all three sites. The difference in

preservation is especially apparent between the enamel and tusk material for all three sites. Four out of 31 analysed samples, including enamel and tusks, have exhibited isotopic disequilibrium and were excluded from the original dataset. Additionally, thirteen out of 31 samples, mainly tusks, are likely to have experienced carbonate loss.

Our findings challenge using enamel samples from suboptimal preservation conditions without checking for isotopic integrity, as three of the four discarded samples exhibiting disequilibrium offsets were enamel specimens. Given this observation, we advocate carefully evaluating the isotopic preservation of all skeletal tissue types, including enamel, in the context of our three study sites and generally for all the sites not under permafrost conditions. FTIR analysis may provide more insights into the properties and deposition histories of the samples, but the method does not allow us to identify isotopic alteration nor, in our case, at least, to firmly associate any detected isotopic disequilibrium to a process that has affected the samples. Of course, one can make an argument that it is less complicated to work with the fossil remains from permafrost where the samples are most likely to be preserved in best conditions, rather than working with samples whose condition must be carefully evaluated. However, for the whole southeast of Western Siberia, there are very few published paleoclimatic studies and even fewer δ^{18}Ow records, and all of them refer to earlier or later time periods. Thus, data from this region are extremely important because we cannot fully understand past climatic changes in Siberia by only analysing the values obtained from the material in Arctic Siberia. Although future studies will have to put more work and care into evaluating the preservation status, the potential of the information contained in these sites is tremendous.

The information presented in this article can be used as a reference point for future studies as well as paleogeographic reconstructions that involve comparing the oxygen isotope values of mammoth remains in the southeast of Western Siberia and Eurasia in general.

CRediT authorship contribution statement

Ivan Krivokorin: Software, Formal analysis, Investigation, Writing – original draft, Writing – review & editing, Visualization. **Leeli Amon:** Resources, Writing – review & editing, Supervision, Project administration. **Sergey V. Leshchinskiy:** Conceptualization, Resources, Writing – review & editing, Supervision, Project administration. **Laura Arppe:** Conceptualization, Methodology, Validation, Resources, Writing – review & editing, Supervision.

Declaration of competing interest

The authors declare that they have no known competing financial interests or personal relationships that could have appeared to influence the work reported in this paper.

Data availability

Data will be made available on request.

Acknowledgements

We want to thank the individuals who assisted us throughout the course of this project. Special thanks are due to Igor Shevchuk and Hanna Turunen at the Laboratory of Chronology, LUOMUS, for IRMS analytics, Maria Kulp and the Laboratory of Chemical Analysis at Tallinn University of Technology for conducting FTIR analysis, Mikko Kytökari for his expertise in FTIR interpretation, Jüri Vassiljev for C14 calibration, Varvara Bakumenko for her contributions to the statistical analysis, Elena Burkanova, Vasiliy Zenin, Artur Dzhumanov, Aleksandra Samandrosova, Aleksey Klimov, and Dmitriy Kadochnikov for their assistance in acquiring the samples. The research was funded by ESF projects PRG1993,TK 215 and the Doctoral School of Earth Sciences and Ecology, supported by the European Union, European Regional Development Fund (ASTRA "TTÜ arenguprogramm aastateks 2016–2022").

Appendix A. Supplementary data

Supplementary data to this article can be found online at https://doi.org/10.1016/j.quascirev.2024.108938.

References

Alley, R.B., Cuffey, K.M., 2001. Oxygen-and hydrogen-isotopic ratios of water in precipitation: beyond paleothermometry. Rev. Mineral. Geochem. 43, 527–554.
Arppe, L., Karhu, J.A., 2010. Oxygen isotope values of precipitation and the thermal climate in Europe during the middle to late Weichselian ice age. Quat. Sci. Rev. 29 (9–10), 1263–1275.
Arppe, L., Karhu, J.A., Vartanyan, S., Drucker, D.G., Etu-Sihvola, H., Bocherens, H., 2019. Thriving or surviving? The isotopic record of the Wrangel Island woolly mammoth population. Quat. Sci. Rev. 222, 105884.
Aubekerov, B., Gorbunov, A., 1999. Quaternary permafrost and mountain glaciation in Kazakhstan. Permafr. Periglac. Process. 10, 65–80.
Ayliffe, L.K., Lister, A.M., Chivas, A.R., 1992. The preservation of glacial-interglacial climatic signatures in the oxygen isotopes of elephant skeletal phosphate. Palaeogeogr. Palaeoclimatol. Palaeoecol. 99 (3–4), 179–191.
Bakker, P., Rogozhina, I., Merkel, U., Prange, M., 2020. Hypersensitivity of glacial summer temperatures in Siberia. Clim. Past 16 (1), 371–386.
Barnosky, A.D., Koch, P.L., Feranec, R.S., Wing, S.L., Shabel, A.B., 2004. Assessing the causes of Late Pleistocene extinctions on the continents. Science 306, 70–75.
Bocherens, H., Billiou, D., Patou-Mathis, M., Bonjean, D., Otte, M., Mariotti, A., 1997. Paleobiological implications of the isotopic signatures (13C, 15N) of fossil mammal collagen in Scladina Cave (Sclayn, Belgium). Quaternary research 48 (3), 370–380.
Boiko, P.V., Maschenko, E.N., Sylerzhitskii, L.D., 2005. A new large Late Pleistocene mammoth's locality in Western Siberia. September. In: Short Papers and Abstracts, 2nd International Congress the World of Elephants, vol. 4. Mammoth Site of Hot Springs, SD, pp. 22–26.
Bokarev, A.A., Martynovich, N.V., 1992. Prichinnost raspolozheniya Kashtankovskoi gruppy pozdnepaleoliticheskikh mestonakhozhdenyi (k strategii osvoeniya drevnim chelovekom Severo-Minusinskoi kotloviny) [The causality of location of the Kashtanka cluster of Upper Palaeolithic localities (to the strategy of ancient humans settling of the Northern Minusinsk depression)]. In: Derevianko, A.P., Drozdov, N.I., Akimova, E.V., Chekha, V.P. (Eds.), Paleoekologiya I Rasselenie Drevnego Cheloveka V Severnoi Azii I Amerike [The Palaeoecology and Dispersal of Ancient Humans in Northern Asia and America], Institute of Archaeology & Ethnography: Krasnoyarsk, pp. 22–26 (in Russian).
Bowen, G.J., Revenaugh, J., 2003. Interpolating the isotopic composition of modern meteoric precipitation. Water resources research 39 (10).
Brand, W.A., Coplen, T.B., Vogl, J., Rosner, M., Prohaska, T., 2014. Assessment of international reference materials for isotope-ratio analysis (IUPAC Technical Report). Pure and Applied Chemistry 86 (3), 425–467.
Brugère, A., Fontana, L., 2009. Origin and exploitation patterns of mammoth at Milovice (area G excepted). Milovice: site of the mammoth people below the Pavlov hills: the question of mammoth bone structures 27, 51–105.
Bryant, J.D., Froelich, P.N., 1995. A model of oxygen isotope fractionation in body water of large mammals. Geochem. Cosmochim. Acta 59 (21), 4523–4537.
Bryant, J.D., Koch, P.L., Froelich, P.N., Showers, W.J., Genna, B.J., 1996. Oxygen isotope partitioning between phosphate and carbonate in mammalian apatite. Geochem. Cosmochim. Acta 60 (24), 5145–5148.
Bryant, J.D., Luz, B., Froelich, P.N., 1994. Oxygen isotopic composition of fossil horse tooth phosphate as a record of continental paleoclimate. Palaeogeogr. Palaeoclimatol. Palaeoecol. 107 (3–4), 303–316.
Bush, A.B., 2004. Modelling of late Quaternary climate over Asia: a synthesis. Boreas 33 (2), 155–163.
Butzin, M., Werner, M., Masson-Delmotte, V., Risi, C., Frankenberg, C., Gribanov, K., Jouzel, J., Zakharov, V.I., 2014. Variations of oxygen-18 in West Siberian precipitation during the last 50 years. Atmospheric Chemistry and Physics 14 (11), 5853–5869.
Cersoy, S., Zazzo, A., Lebon, M., Rofes, J., Zirah, S., 2017. Collagen extraction and stable isotope analysis of small vertebrate bones: a comparative approach. Radiocarbon 59 (3), 679–694.
Chang, S.J., Blake, R.E., 2015. Precise calibration of equilibrium oxygen isotope fractionations between dissolved phosphate and water from 3 to 37 C. Geochem. Cosmochim. Acta 150, 314–329.
Clark, P.U., Dyke, A.S., Shakun, J.D., Carlson, A.E., Clark, J., Wohlfarth, B., Mitrovica, J. X., Hostetler, S.W., McCabe, A.M., 2009. The last glacial maximum. science 325 (5941), 710–714.
Cleator, S.F., Harrison, S.P., Nichols, N.K., Prentice, I.C., Roulstone, I., 2020. A new multivariable benchmark for Last Glacial Maximum climate simulations. Climate of the Past 16 (2), 699–712.
Coplen, T.B., Brand, W.A., Gehre, M., Gröning, M., Meijer, H.A., Toman, B., Verkouteren, R.M., 2006. New guidelines for δ 13C measurements. Analytical chemistry 78 (7), 2439–2441.
Dal Sasso, G., Asscher, Y., Angelini, I., Nodari, L., Artioli, G., 2018. A universal curve of apatite crystallinity for the assessment of bone integrity and preservation. Sci. Rep. 8 (1), 12025.

Dansgaard, W., 1964. Stable isotopes in precipitation. Tellus 16 (4), 436–468.
Derevianko, A.P., Molodin, V.I., Zenin, V.N., Leshchinskiy, S.V., Mashchenko, E.N., 2003. Pozdnepaleoliticheskoe Mestonakhozhdenie Shestakovo. Institute of Archeology and Ethnography. Siberian Branch of the Russian Academy of Sciences, Novosibirsk.
Derevianko, A.P., Zenin, V.N., Leshchinsky, S.V., Maschenko, E.N., 2000. Peculiarities of mammoth accumulation at Shestakovo site in west Siberia. Archaeol. Ethnol. Anthropol. Eurasia (3), 42–55.
Diez, C., Rojo, M.Á., Martín-Gil, J., Martín-Ramos, P., Garrosa, M., Córdoba-Diaz, D., 2021. Infrared spectroscopic analysis of the inorganic components from teeth exposed to psychotherapeutic drugs. Minerals 12 (1), 28.
Drozdov, N.I., Chekha, V.P., Davis, R., Koltsova, V.G., Martynovich, N.V., Bokarev, A.A., Artemiev, E.V., Demidenko, G.A., Orlova, L.A., Sulerzhitsky, L.D., 1992. Pozdnepaleoliticheskaya stoyanka Kashtanka [the upper palaeolithic site of Kashtanka]. In: Drozdov, N.I., Chekha, V.P. (Eds.), Arkheologiya, Geologiya I Paleogeografiya Palaeolithicheskikh Pamyatnikov Yuga Srednei Sibiri [Archaeology, Geology and Palaeogeography of Palaeolithic Sites in the South of Central Siberia], Derevianko AP. Institute of Archaeology & Ethnography: Krasnoyarsk, pp. 94–109 (in Russian).
Fox, D.L., Fisher, D.C., Vartanyan, S., Tikhonov, A.N., Mol, D., Buigues, B., 2007. Paleoclimatic implications of oxygen isotopic variation in late Pleistocene and Holocene tusks of Mammuthus primigenius from northern Eurasia. Quat. Int. 169, 154–165.
France, C.A., Sugiyama, N., Aguayo, E., 2020. Establishing a preservation index for bone, dentin, and enamel bioapatite mineral using ATR-FTIR. J. Archaeol. Sci.: Reports 33, 102551.
Fricke, H.C., O'Neil, J.R., 1999. The correlation between 18O/16O ratios of meteoric water and surface temperature: its use in investigating terrestrial climate change over geologic time. Earth Planet Sci. Lett. 170 (3), 181–196.
Genoni, L., Iacumin, P., Nikolaev, V., Gribchenko, Y., Longinelli, A., 1998. Oxygen isotope measurements of mammoth and reindeer skeletal remains: an archive of Late Pleistocene environmental conditions in Eurasian Arctic. Earth Planet Sci. Lett. 160 (3–4), 587–592.
Guthrie, R.D., 1968. Paleoecology of the large-mammal community in interior Alaska during the late Pleistocene. Am. Midl. Nat. 346–363.
Halas, S., Skrzypek, G., Meier-Augenstein, W., Pelc, A., Kemp, H.F., 2011. Inter-laboratory calibration of new silver orthophosphate comparison materials for the stable oxygen isotope analysis of phosphates. Rapid Commun. Mass Spectrom. 25 (5), 579–584.
Harris, C.R., Millman, K.J., Van Der Walt, S.J., Gommers, R., Virtanen, P., Cournapeau, D., Wieser, E., Taylor, J., Berg, S., Smith, N.J., Kern, R., 2020. Array programming with NumPy. Nature 585 (7825), 357–362.
Haynes, G., 1991. Mammoths, Mastodonts, and Elephants: Biology, Behavior and the Fossil Record. Cambridge University Press.
Hedges, R.E., Stevens, R.E., Richards, M.P., 2004. Bone as a stable isotope archive for local climatic information. Quat. Sci. Rev. 23 (7–8), 959–965.
Huertas, A.D., Iacumin, P., Stenni, B., Chillón, B.S., Longinelli, A., 1995. Oxygen isotope variations of phosphate in mammalian bone and tooth enamel. Geochem. Cosmochim. Acta 59 (20), 4299–4305.
Hughes, P.D., Gibbard, P.L., 2015. A stratigraphical basis for the last glacial maximum (LGM). Quat. Int. 383, 174–185.
Iacumin, P., Bocherens, H., Mariotti, A., Longinelli, A., 1996. Oxygen isotope analyses of co-existing carbonate and phosphate in biogenic apatite: a way to monitor diagenetic alteration of bone phosphate? Earth Planet Sci. Lett. 142 (1–2), 1–6.
Iacumin, P., Di Matteo, A., Nikolaev, V., Kuznetsova, T.V., 2010. Climate information from C, N and O stable isotope analyses of mammoth bones from northern Siberia. Quat. Int. 212 (2), 206–212.
Iacumin, P., Nikolaev, V., Ramigni, M., Longinelli, A., 2004. Oxygen isotope analyses of mammal bone remains from Holocene sites in European Russia: palaeoclimatic implications. Global Planet. Change 40 (1–2), 169–176.
Kageyama, M., Peyron, O., Pinot, S., Tarasov, P., Guiot, J., Joussaume, S., Ramstein, G., 2001. The Last Glacial Maximum climate over Europe and western Siberia: a PMIP comparison between models and data. Clim. Dynam. 17, 23–43.
Kahlke, R.D., 1999. The history of the origin, evolution and dispersal of the Late Pleistocene Mammuthus-Coelodonta faunal complex in Eurasia (large mammals). Mammoth Site of Hot Springs.
Kim, S.T., O'Neil, J.R., 1997. Equilibrium and nonequilibrium oxygen isotope effects in synthetic carbonates. Geochem. Cosmochim. Acta 61 (16), 3461–3475.
Kitover, D.C., Van Balen, R.T., Vandenberghe, J., Roche, D.M., Renssen, H., 2016. LGM permafrost thickness and extent in the Northern Hemisphere derived from the Earth System Model iLOVECLIM. Permafr. Periglac. Process. 27 (1), 31–42.
Koch, P.L., Barnosky, A.D., 2006. Late Quaternary extinctions: state of the debate. Annu. Rev. Ecol. Evol. Syst. 37 (1), 215–250.
Kohn, M.J., Cerling, T.E., 2002. Stable isotope compositions of biological apatite. Rev. Mineral. Geochem. 48 (1), 455–488.
Kohn, M.J., 1996. Predicting animal $\delta^{18}O$: accounting for diet and physiological adaptation. Geochem. Cosmochim. Acta 60 (23), 4811–4829.
Krzemińska, A., Wędzicha, S., 2015. Pathological changes on the ribs of woolly mammoths (Mammuthus primigenius). Quat. Int. 359, 186–194.
Kurita, N., Yoshida, N., Inoue, G., Chayanova, E.A., 2004. Modern isotope climatology of Russia: A first assessment. Journal of Geophysical Research: Atmospheres 109 (D3).
Kuzmin, Y.V., Leshchinskiy, S.V., Zenin, V.N., Burkanova, E.M., Zazovskaya, E.P., Samandrosova, A.S., 2023. Chronology of the Volchia Griva megafaunal locality and paleolithic site (western Siberia) and the issue of human occupation of Siberia at the last glacial maximum. Radiocarbon 1–13.
Lazarev, S., Leshchinskiy, S., 2011. Preliminary results of drilling activity on the Krasnoyarskaya Kurya mammoth site. Trudy TSU, Tomsk 280, 232–235, 2011.
Lecuyer, C., Grandjean, P., Barrat, J.A., Nolvak, J., Emig, C., Paris, F., Robardet, M., 1998. δ18O and REE contents of phosphatic brachiopods: a comparison between modern and lower Paleozoic populations. Geochem. Cosmochim. Acta 62 (14), 2429–2436.
Lee-Thorp, J., Sponheimer, M., 2003. Three case studies used to reassess the reliability of fossil bone and enamel isotope signals for paleodietary studies. J. Anthropol. Archaeol. 22 (3), 208–216.
Leshchinskiy, S., 2015. Enzootic diseases and extinction of mammoths as a reflection of deep geochemical changes in ecosystems of Northern Eurasia. Archaeological and Anthropological Sciences 7, 297–317.
Leshchinskiy, S.V., 2006. Lugovskoye: environment, taphonomy, and origin of a paleofaunal site. Archaeol. Ethnol. Anthropol. Eurasia 25 (1), 33–40.
Leshchinskiy, S.V., 2009. Mineral deficiency, enzootic diseases and extinction of mammoth of Northern Eurasia. Dokl. Biol. Sci. 424 (1), 72–74.
Leshchinskiy, S.V., 2012. Paleoecological investigation of mammoth remains from the Kraków Spadzista Street (B) site. Quat. Int. 276, 155–169.
Leshchinskiy, S.V., 2017. Strong evidence for dietary mineral imbalance as the cause of osteodystrophy in Late Glacial woolly mammoths at the Berelyokh site (Northern Yakutia, Russia). Quat. Int. 445, 146–170.
Leshchinskiy, S.V., 2018. Results of latest paleontological, stratigraphic and geoarchaeological research of the Volchia Griva mammoth fauna site. Proceedings of the Zoological Institute 322, 315–332.
Leshchinskiy, S.V., Burkanova, E.M., Luneva, D.E., Ivantsov, S.V., Zenin, I.V., Akhteryakova, A.B., 2005. – Predvaritelnye rezultaty issledovaniy mestonahozhdenia mamontovoy fauny i paleolita "Krasnoyarskaya kurya" (Zapadno-Sibirskaya ravnina). In: Podobina, V.M. (Ed.), Evolution of Life on the Earth. – Proceedings of the III International Symposium. Tomsk State University, Tomsk, pp. 352–356 (in Russian).
Leshchinskiy, S., Burkanova, E., Polumogina, Y., Lazarev, S., Zenin, V., 2014. Last glacial maximum mammoth fauna of the Krasnoyarskaya kurya site (southeastern part of the West Siberian Plain). SCIENTIFIC ANNALS OF THE SCHOOL OF GEOLOGY SPECIAL 102, 105.
Leshchinskiy, S.V., Burkanova, E.M., 2022. The Volchia Griva mineral oasis as unique locus for research of the mammoth fauna and the late Pleistocene environment in Northern Eurasia. Quaternary Research 109, 157–182.
Leshchinskiy, S.V., Zenin, V.N., Bukharova, O.V., 2021. The Volchia Griva mammoth site as a key area for geoarchaeological research of human movements in the Late Paleolithic of the West Siberian Plain. Quat. Int. 587, 368–383.
Leshchinskiy, S.V., Zenin, V.N., Burkanova, E.M., Kuzmin, Y.V., 2023. The unique late paleolithic artifactual bone assemblage from the Volchia Griva site, western Siberia. Quaternary Research 114, 93–113.
Longinelli, A., 1984. Oxygen isotopes in mammal bone phosphate: a new tool for paleohydrological and paleoclimatological research? Geochem. Cosmochim. Acta 48 (2), 385–390.
Longinelli, A., Nuti, S., 1973. Revised phosphate-water isotopic temperature scale. Earth Planet Sci. Lett. 19 (3), 373–376.
Longinelli, A., Iacumin, P., Davanzo, S., Nikolaev, V., 2003. Modern reindeer and mice: revised phosphate–water isotope equations. Earth Planet Sci. Lett. 214 (3–4), 491–498.
Luz, B., Kolodny, Y., Horowitz, M., 1984. Fractionation of oxygen isotopes between mammalian bone-phosphate and environmental drinking water. Geochem. Cosmochim. Acta 48 (8), 1689–1693.
Martin, C., Bentaleb, I., Kaandorp, R., Iacumin, P., Chatri, K., 2008. Intra-tooth study of modern rhinoceros enamel $\delta^{18}O$: is the difference between phosphate and carbonate $\delta^{18}O$ a sound diagenetic test? Palaeogeogr. Palaeoclimatol. Palaeoecol. 266 (3–4), 183–189.
Mashchenko, E.N., 2010. Age profile and morphology of mammoth from the Chulym river (Teguldet locality, Tomsk region, Russia). In: Lazarev, P.A. (Ed.), Proc 4th Int Mammoth Conf. Yakutsk, pp. 41–53.
McCrea, J.M., 1950. On the isotopic chemistry of carbonates and a paleotemperature scale. J. Chem. Phys. 18 (6), 849–857.
Metcalfe, J.Z., 2017. Proboscidean isotopic compositions provide insight into ancient humans and their environments. Quat. Int. 443, 147–159.
Metcalfe, J.Z., Longstaffe, F.J., 2012. Mammoth tooth enamel growth rates inferred from stable isotope analysis and histology. Quaternary Research 77 (3), 424–432.
Nikolayev, V.I., Mikhalev, D.V., 1995. An oxygen-isotope paleothermometer from ice in Siberian permafrost. Quaternary Research 43 (1), 14–21.
Olivier, R.C., 1982. Ecology and behavior of living elephants: bases for assumptions concerning the extinct woolly mammoths. In: Paleoecology of Beringia. Academic Press, pp. 291–305.
Pandas Development Team, 2023. Pandas: powerful data analysis tools for Python [Online] Available at:, Version 1.4.0. https://pandas.pydata.org/. (Accessed 10 December 2023).
Pryor, A.J., Stevens, R.E., O'Connell, T.C., Lister, J.R., 2014. Quantification and propagation of errors when converting vertebrate biomineral oxygen isotope data to temperature for palaeoclimate reconstruction. Palaeogeogr. Palaeoclimatol. Palaeoecol. 412, 99–107.
Pucéat, E., Joachimski, M.M., Bouilloux, A., Monna, F., Bonin, A., Motreuil, S., Morinière, P., Hénard, S., Mourin, J., Dera, G., Quesne, D., 2010. Revised phosphate–water fractionation equation reassessing paleotemperatures derived from biogenic apatite. Earth Planet Sci. Lett. 298 (1–2), 135–142.
Ramsey, C.B., 2009. Bayesian analysis of radiocarbon dates. Radiocarbon 51 (1), 337–360.
Reimer, P.J., Austin, W.E., Bard, E., Bayliss, A., Blackwell, P.G., Ramsey, C.B., Butzin, M., Cheng, H., Edwards, R.L., Friedrich, M., Grootes, P.M., 2020. The IntCal20 Northern

Hemisphere radiocarbon age calibration curve (0–55 cal kBP). Radiocarbon 62 (4), 725–757.
Revesz, K.M., Landwehr, J.M., Keybl, J.E., 2001. Measurement of ([delta] 13C and [delta] 18O) Isotopic Ratios of CaCO3 Using a Thermoquest Finnigan GasBench II Delta Plus XL Continuous Flow Isotope Ratio Mass Spectrometer with Application to Devils Hole Core DH-11 Calcite. US Department of the Interior, US Geological Survey, pp. 1–257.
Rowe, A.G., Bataille, C.P., Baleka, S., Combs, E.A., Crass, B.A., Fisher, D.C., Ghosh, S., Holmes, C.E., Krasinski, K.E., Lanoë, F., Murchie, T.J., 2024. A female woolly mammoth's lifetime movements end in an ancient Alaskan hunter-gatherer camp. Sci. Adv. 10 (3), eadk0818.
Rozanski, K., Araguas-Araguas, L., Gonfiantini, R., 1992. Relation between long-term trends of oxygen-18 isotope composition of precipitation and climate. Science 258 (5084), 981–985.
Rozanski, K., Araguás-Araguás, L., Gonfiantini, R., 1993. Isotopic patterns in modern global precipitation. Climate change in continental isotopic records 78, 1–36.
Salesse, K., Dufour, E., Lebon, M., Wurster, C., Castex, D., Bruzek, J., Zazzo, A., 2014. Variability of bone preservation in a confined environment: the case of the catacomb of Sts Peter and Marcellinus (Rome, Italy). Palaeogeogr. Palaeoclimatol. Palaeoecol. 416, 43–54.
Schirrmeister, L., Siegert, C., Kuznetsova, T., Kuzmina, S., Andreev, A., Kienast, F., Meyer, H., Bobrov, A., 2002. Paleoenvironmental and paleoclimatic records from permafrost deposits in the Arctic region of northern Siberia. Quat. Int. 89, 97–118.
Seuru, S., Leshchinskiy, S., Auguste, P., Fedyaev, N., 2017. Woolly mammoth and man at Krasnoyarskaya kurya site, West Siberian plain, Russia (excavation results of 2014). Bull. Soc. Geol. Fr. 188 (1–2), 1–13.
Shahack-Gross, R., Tchernov, E., Luz, B., 1999. Oxygen isotopic composition of mammalian skeletal phosphate from the Natufian Period, Hayonim Cave, Israel: diagenesis and paleoclimate. Geoarchaeology: Int. J. 14 (1), 1–13.
Sher, A.V., Kuzmina, S.A., Kuznetsova, T.V., Sulerzhitsky, L.D., 2005. New insights into the Weichselian environment and climate of the East Siberian Arctic, derived from fossil insects, plants, and mammals. Quat. Sci. Rev. 24 (5–6), 533–569.
Shin, S.-I., Liu, Z., Otto-Bliesner, B., Brady, E.C., Kutzbach, J.E., Harrison, S.P., 2003. A simulation of the Last Glacial Maximum climate using the NCAR-CCSM. Clim. Dynam. 20, 127–151.
Snoeck, C., Pellegrini, M., 2015. Comparing bioapatite carbonate pre-treatments for isotopic measurements: Part 1—impact on structure and chemical composition. Chem. Geol. 417, 394–403.
Stuart, A.J., 2005. The extinction of woolly mammoth (Mammuthus primigenius) and straight-tusked elephant (Palaeoloxodon antiquus) in Europe. Quat. Int. 126, 171–177.
Tarasov, P.E., Peyron, O., Guiot, J., Brewer, S., Volkova, V.S., Bezusko, L.G., Dorofeyuk, N.I., Kvavadze, E.V., Osipova, I.M., Panova, N.K., 1999. Last Glacial Maximum climate of the former Soviet Union and Mongolia reconstructed from pollen and plant macrofossil data. Clim. Dynam. 15, 227–240.
Tierney, J.E., Zhu, J., King, J., Malevich, S.B., Hakim, G.J., Poulsen, C.J., 2020. Glacial cooling and climate sensitivity revisited. Nature 584 (7822), 569–573.
Tütken, T., Furrer, H., Vennemann, T.W., 2007. Stable isotope compositions of mammoth teeth from Niederweningen, Switzerland: implications for the Late Pleistocene climate, environment, and diet. Quat. Int. 164, 139–150.
Vandenberghe, J., French, H.M., Gorbunov, A., Marchenko, S., Velichko, A.A., Jin, H., Cui, Z., Zhang, T., Wan, X., 2014. The Last Permafrost Maximum (LPM) map of the Northern Hemisphere: permafrost extent and mean annual air temperatures, 25–17 ka BP. Boreas 43, 652–666.
Vasyukova, E.A., Leshchinskiy, S.V., 2011. Petrographic Analysis of Palaeolithic Artifacts of the Krasnoyarskaya Kurya Mammoth Site. Trudy TSU, pp. 207–209.
Virtanen, P., Gommers, R., Oliphant, T.E., Haberland, M., Reddy, T., Cournapeau, D., Burovski, E., Peterson, P., Weckesser, W., Bright, J., Van Der Walt, S.J., 2020. SciPy 1.0: fundamental algorithms for scientific computing in Python. Nat. Methods 17 (3), 261–272.
Weitzel, N., Hense, A., Herzschuh, U., Böhmer, T., Cao, X., Rehfeld, K., 2022. A State Estimate of Siberian Summer Temperature and Moisture Availability during the Last Glacial Maximum Combining Pollen Records and Climate Simulations (unpublished manuscript).
Wetterich, S., Meyer, H., Fritz, M., Mollenhauer, G., Rethemeyer, J., Kizyakov, A., Schirrmeister, L., Opel, T., 2021. Northeast Siberian permafrost ice-wedge stable isotopes depict pronounced last glacial maximum winter cooling. Geophys. Res. Lett. 48 (7), e2020GL092087.
Wiedemann-Bidlack, F.B., Colman, A.S., Fogel, M.L., 2008. Phosphate oxygen isotope analysis on microsamples of bioapatite: removal of organic contamination and minimization of sample size. Rapid Commun. Mass Spectrom.: An International Journal Devoted to the Rapid Dissemination of Up-to-the-Minute Research in Mass Spectrometry 22 (12), 1807–1816.
Wojtal, P., 2004. New excavations at Kraków Spadzista Street (B). In: Svoboda, J.A., Sedláčkova, L. (Eds.), The Gravettian along the Danube, the Dolní Vestonice Studies, vol. 11, pp. 180–185.
Wojtal, P., Sobczyk, K., 2005. Man and woolly mammoth at the Kraków Spadzista Street (B) - taphonomy of the site. J. Archaeol. Sci. 32, 193–206.
Wu, H., Guiot, J., Brewer, S., Guo, Z., 2007. Climatic changes in Eurasia and Africa at the last glacial maximum and mid-Holocene: reconstruction from pollen data using inverse vegetation modelling. Climate Dynamics 29, 211–229.
Zazzo, A., 2001. Validation méthodologique de l'utilisation des compositions isotopiques (13C, 18O) des bioapatites fossiles pour les reconstitutions des paléoenvironnements continentaux, vol. 6. Thèse de doctorat de l'université Pierre et Marie Curie, Paris [in French].
Zazzo, A., Lécuyer, C., Mariotti, A., 2004a. Experimentally-controlled carbon and oxygen isotope exchange between bioapatites and water under inorganic and microbially-mediated conditions. Geochem. Cosmochim. Acta 68 (1), 1–12.
Zazzo, A., Lécuyer, C., Sheppard, S.M., Grandjean, P., Mariotti, A., 2004b. Diagenesis and the reconstruction of paleoenvironments: a method to restore original δ18O values of carbonate and phosphate from fossil tooth enamel. Geochem. Cosmochim. Acta 68 (10), 2245–2258.
Zenin, V.N., 2002. Major stages in the human occupation of the West Siberian Plain during the paleolithic. Archaeol. Ethnol. Anthropol. Eurasia 4 (12), 22–44.
Arhiv klimaticheskih dannyh, 2023. http://climatebase.ru/. (Accessed 2 August 2023).

Appendix 2 (Paper II)

Krivokorin, I., Poska, A., Vassiljev, J., Veski, S., & Amon, L. (2025). Environment of European Last Mammoths: Reconstructing the Landcover of the Eastern Baltic Area at the Pleistocene/Holocene Transition. Land, 14(1), 178. https://doi.org/10.3390/land14

land

MDPI

Article

Environment of European Last Mammoths: Reconstructing the Landcover of the Eastern Baltic Area at the Pleistocene/Holocene Transition

Ivan Krivokorin [1,*], Anneli Poska [1,2], Jüri Vassiljev [1], Siim Veski [1] and Leeli Amon [1]

[1] Department of Geology, Tallinn University of Technology, Ehitajate tee 5, 12616 Tallinn, Estonia; anneli.poska@taltech.ee (A.P.); jyri.vassiljev@taltech.ee (J.V.); siim.veski@taltech.ee (S.V.); leeli.amon@taltech.ee (L.A.)
[2] Department of Physical Geography and Ecosystem Science, Lund University, 223 62 Lund, Sweden
* Correspondence: ivan.krivokorin@taltech.ee; Tel.: +372-556-12114

Abstract: The Eastern Baltic area stands out as a unique location due to the finds of Europe's youngest dated mammoth remains (12.6–11.2 ka cal BP). Our study explores the drastic climate and landcover changes during the extinction of these gigantic herbivores at the Pleistocene/Holocene boundary. We used macrofossil analysis to determine the major contemporary terrestrial plant genera present in the area and used corresponding pollen taxa for REVEALS model-based landcover reconstructions. Our results indicate that these last mammoths utilised the open landcover of the Eastern Baltic, which developed as the continental ice sheet retreated during the termination of the last glaciation. Due to climate warming during the initial stages of the Holocene interglacial, the Eastern Baltic became speedily populated by birch and pine forests. The abrupt disappearance of typical forb-dominated tundra indicators, such as *Dryas octopetala*, and the fast increase in tree birch marked a shift from an open, tundra-like landscape to a forested one, making the environment inhospitable for mammoths even in northernmost Estonia by the beginning of the Holocene. A comparison between the isotopic values of nitrogen ($\delta^{15}N$) and carbon ($\delta^{13}C$) obtained from mammoths' molars from 14.3 and 11.3 to 43.5 and 39.1 ka cal BP showed that mammoths experienced a decline in the nutritional value of their diet, resulting in their demise in the Eastern Baltic.

Keywords: pollen; plant macrofossils; woolly mammoth; LRA REVEALS; Estonia; Latvia

check for updates

Academic Editor: Mark Altaweel

Received: 18 December 2024
Revised: 7 January 2025
Accepted: 14 January 2025
Published: 16 January 2025

Citation: Krivokorin, I.; Poska, A.; Vassiljev, J.; Veski, S.; Amon, L. Environment of European Last Mammoths: Reconstructing the Landcover of the Eastern Baltic Area at the Pleistocene/Holocene Transition. *Land* **2025**, *14*, 178. https://doi.org/10.3390/land14010178

Copyright: © 2025 by the authors. Licensee MDPI, Basel, Switzerland. This article is an open access article distributed under the terms and conditions of the Creative Commons Attribution (CC BY) license (https://creativecommons.org/licenses/by/4.0/).

1. Introduction

The Eastern Baltic stands out amongst other European locations because the youngest woolly mammoth (*Mammuthus primigenius* Blumenbach) tooth remains in Europe were discovered here, dating to 12.6–11.2 ka cal BP [1]. Despite the scarcity of evidence, these and several other mammoth fossil finds suggest that these animals were present in the area during the Pleistocene/Holocene transition [1–3]. These findings raise questions about the environment these last mammoths inhabited and whether it affected their eventual extinction.

The extinction of mammoths has drawn the attention of numerous researchers globally, as these animals inhabited vast areas in Europe and North America [2,4,5] ca 110,000–12,000 years ago [6]. Different factors have been proposed as potential contributors to the extinction: landscape acidification, mineral deficiency [7], nutrient deficiency [8], large skeletal size, genetic mutations and diseases [9], climatic changes [3], and human hunting [10]. The abrupt disappearance of mammoths from Europe approximately 12,000 years

ago has been attributed to the decline of open biomes during the latter part of the Last Glacial–interglacial cycle, specifically during the Allerød and Early Holocene warming [2]. In the context of our research, certain factors, such as skeletal size, osteoporosis, or mineral deficiency, are challenging to investigate due to the limited number of samples and poor preservation of some mammoth remains. Nevertheless, we can assess the potential role of landcover change in the extinction of mammoths in the Eastern Baltic area. In contrast to a few finds dated to the termination of the last glaciation, the Eastern Baltic has an abundance of mammoth remains dated to the period prior to the Last Glacial Maximum (LGM). According to NGRIP Greenland ice core stratigraphy, the Last Glacial Maximum covers a period of 27–23 ka cal BP [11].

We focused our study on two contrasting periods: post-LGM and pre-LGM. Special attention was given to the post-LGM time interval between 14.3 and 11.3 ka cal BP because this period is crucial for understanding the environment in which the last European mammoths lived. While offering valuable insights into the past existence of mammoths, it is underrepresented in terms of pollen and plant macrofossil studies [12]. We plan to fill this critical gap in vegetational data by using plant macrofossils to determine the major contemporary terrestrial plant genera present in the Eastern Baltic and exploiting corresponding pollen taxa to make REVEALS model-based landcover reconstructions.

To determine whether the climatic and landcover changes were indeed the driving factors behind the extinction of the last European mammoths, we have compiled a comprehensive dataset consisting of all available pollen and plant macrofossil records and mammoth finds from the Eastern Baltic and a new pollen and plant macrofossil record from Lake Kaatsjärv in central Estonia. We will support the investigation by comparing the landcover changes during the 14.3–11.3 ka cal BP period with the landcover changes during the pre-LGM period (50–27 ka cal BP) to assess whether environmental changes played a definitive role in the decline of mammoths in the Eastern Baltic during the Late Pleistocene.

Furthermore, we extracted stable carbon ($\delta^{13}C$) and nitrogen ($\delta^{15}N$) isotopic values from the two Eastern Baltic's youngest molar samples found from Puurmani in central Estonia and compared the results with the published isotopic values of other mammoths that lived during the investigated time period including newly obtained isotopic values from two mammoth molar samples from the pre-LGM time period for comparison.

2. Materials and Methods

2.1. Study Area

The Eastern Baltic has a transitional climate ranging from maritime in the west to continental in the east. The area is characterised by flat terrain covered with mixed forests. In Estonia, July's mean temperature is 16–17 °C, and February's (coldest month) is −2.5 to −7 °C today [13]. In Latvia, July's mean temperature is 17.4 °C and February's mean temperature is −3.7 °C [14]. Mean annual precipitation is 550–700 mm.

The Eastern Baltic area was glaciated during the LGM. The ice retreat from the region started ~18 ka cal BP years ago [15]. The current area of Latvia became ice-free at ~15 ka cal BP [16] and Estonia at ~13 ka cal BP [17]. The Eastern Baltic geomorphology is mostly characterised by undulating low-lying glacial moraine plains, insular heights not higher than 300 m a.s.l., and drumlins and eskers consisting of deposits left by the last ice sheet [18,19].

2.2. Materials

We use data from 27 pollen and 8 plant macrofossil records across the region to investigate the vegetation changes and reconstruct the living environment of Europe's last mammoths in Estonia and Latvia at the Pleistocene/Holocene boundary (Figure 1, Table 1). All selected sites are radiocarbon-dated and contain information about vegetation

development during the time interval between 14.3 and 11.3 ka cal BP. Lake Kaatsjärv in central Estonia was sampled for pollen and plant macrofossil analysis to fill a gap in available records. The well-dated pollen record from the Voka section (59.4144 N, 27.5981 E) [20,21] (Figure 1C) was used to reconstruct the pre-LGM landcover for 500-year time windows centred around 33, 34, 35, 36, and 37 ka cal BP.

Table 1. List of studied sites. EH—Early Holocene 11.7–11.3 ka cal BP, GS-1—Greenland stadial 1 12.85–11.7 ka cal BP (corresponding to Younger Dryas), GI-1—Greenland interstadial 1 14.6–12.85 ka cal BP [22].

Site Number	Site	Longitude	Latitude	Analyses	Time Periods			Reference
					EH	GS-1	GI-1	
Post-LGM sites								
1	Ermistu	23.9829	58.3572	Pollen	+			[23]
2	Hino	27.2386	57.5831	Pollen		+		[24]
3	Imatu	27.4611	59.0997	Pollen	+			[25]
4	Järveotsa	24.1542	59.0956	Pollen	+	+		[26]
5	Kaatsjärv	25.3141	59.1318	Pollen, Macro	+	+	+	This study
6	Kahala	25.5315	59.4867	Pollen	+	+		[27]
7	Kirikumäe	27.2522	57.6830	Pollen	+	+		[28]
8	Kursi	26.0156	59.1558	Macro	+	+	+	[29]
9	Mäetilga	27.0719	57.7420	Pollen	+	+	+	[30]
10	Nakri	26.2731	57.8951	Pollen, Macro	+	+	+	[31]
11	Parika	25.7742	58.4903	Pollen		+		[32]
12	Prossa	26.5778	58.6492	Macro			+	[33]
13	Pupastvere	26.6239	58.5115	Macro	+		+	This study
14	Päidre	25.5033	58.2761	Pollen	+	+		[34]
15	Ruila	24.4297	59.1758	Pollen	+			[35]
16	Rõuge	26.905	57.7389	Pollen	+			[36]
17	Saviku	27.1940	58.4062	Pollen	+	+		[37]
18	Solova	27.4280	57.7004	Macro	+	+	+	[38]
19	Tondi	24.8533	59.4450	Pollen	+			[39]
20	Tuuljärv	27.0556	57.7056	Pollen	+	+		[40]
21	Udriku	25.9315	59.3719	Pollen, Macro	+	+	+	[41]
22	Vaskna	27.0783	57.7117	Pollen	+	+		[40]
23	Verijärv	27.0583	57.8083	Pollen	+			[42]
24	Väike_Juusa	26.5172	58.0592	Pollen		+		[43]
25	Āraiši	25.2828	57.2514	Pollen	+	+	+	[44]
26	Kurjanovas	28	56.5	Pollen	+	+	+	[45]
27	Lielais Svētiņu	27.1491	56.7591	Pollen, Macro	+	+	+	[12]

We used dates and locations of mammoth findings in the Eastern Baltic from previous publications to place these discoveries within the framework of landcover changes in the region (Table 2, Figure 1). The youngest mammoth finds in Europe come from the Puurmani site in Estonia (Table 2, Figure 1B), radiocarbon dated to 11.8 ± 0.36 and 11.9 ± 0.25 ka cal BP [1]. The youngest finds from Latvia are from the Rudzati and the Rucava sites (Table 2, Figure 1B) and are dated to 12.2 ± 0.18 and 15.4 ± 0.11 ka cal BP [3]. There is a ca 15,000-year gap in the mammoth records from the Eastern Baltic, as the area was covered in ice during the Last Glacial Maximum. This contemporaneous gap has been reported in unglaciated areas of Northern Europe as well [46]. Therefore, the second youngest

mammoth find in Estonia (Rõngu) is dated to 30.2–29.3 ka cal BP [3] and in Latvia (Veselava and Pļaviņas) from 32.8 to 29.7 ka cal BP [47] (Table 2, Figure 1C)

Table 2. C^{14} dated mammoths remains in Eastern Baltic.

	Site	Longitude	Latitude	Lab Code	^{14}C age ka BP	Calibrated Ages, ka cal BP		Description	Reference
						at 95%	Weighted Average		
	Post-LGM								
	Estonia								
1	Puurmani	26.2905	58.5758	Hela-423	10.1 ± 0.2	12.6–11.2	11.8 ± 0.36	Molar	[1]
1	Puurmani	26.2897	58.5788	Hela-425	10.2 ± 0.1	12.5–11.4	11.9 ± 0.25	Molar	[1]
	Latvia								
2	Rucava	21.1603	56.1634	LuS 7538	12.88 ± 0.07	15.6–15.2	15.4 ± 0.11	Molar	[47]
3	Rudzati	26.453	56.4171	Hela-1316	10.31 ± 0.07	12.5–11.8	12.2 ± 0.18	Scapula	[47]
	Lithuania								
4	Jiesia river	23.8963	54.8952	LuS 7529	13.8 ± 0.08	17–16.5	16.7 ± 0.14	Molar	[47]
	Pre-LGM								
	Estonia								
5	Heimtali	25.5002	58.3197	Hela-420	>37	42.1–41.7		Tusk	[1]
6	Ihasalu	25.202	59.4971	OxA 11563	46.5 ± 1	52.4–46.7	49.4 ± 1.52	Ivory	[48]
6	Ihasalu	25.202	59.4971	Hela-426	>41	44.4–43.5		Molar	[1]
7	Kallaste	26.5813	57.6105	Hela-421	>38	42.4–42.2		Molar	[1]
8	Koosa	27.0724	58.5116	OxA-12058	40.9 ± 0.6	44.8–43	43.9 ± 0.49	Tooth	[48]
9	Krüüdneri	26.6959	58.1284	Poz-118416	39.5 ± 1.3	45.5–41.9	43.5 ± 0.97	Tusk	This study
10	Kukemetsa	26.7619	58.5148	Poz-118415	34.6 ± 0.7	41.2–37.8	39.7 ± 0.84	Tusk	This study
11	Kunda	26.54	59.4613	Hela-424	>38	42.4–42.2		Tusk	[1]
12	Mooste	27.2209	58.1404	Hela-418	30.64 ± 0.83	37.1–33.4	35.2 ± 0.89	Molar	[1]
13	Rõngu	26.2442	58.1435	Poz-16733	25.63 ± 0.17	30.2–29.3	29.9 ± 0.22	Humerus	[3]
14	Taagepera	25.6921	57.982	OxA-11562	42.2 ± 0.65	46.1–44	45 ± 0.52	Molar	[3]
15	Tahkumägi	26.5375	57.5573	Hela-422	>38	42.4–42.2		Bone	[1]
16	Tudulinna	27.07	59.0377	OxA 11562	34.81 ± 0.34	40.7–39.3	40 ± 0.36	Ivory	[48]
16	Tudulinna	27.07	59.0377	Hela-414	>40	43.3–42.9		Tusk	[1]
17	Valga	26.05	57.78	OxA-11607	28.78 ± 0.16	33.8–32.3	33.2 ± 0.36	Tooth	[48]
18	Vitipalu	26.4154	58.1652	Poz-118499	38.3 ± 0.9	43.9–41.4	42.5 ± 0.56	Tooth	This study
	Latvia								
19	Aizpute	21.0562	56.539	Hela-1315	>40	43.3–42.9		Tusk	[3]
20	Jaunpils	23.013	56.731	LuS 7537	40.7 ± 0.8	45–42.7	43.8 ± 0.6	Molar	[47]
21	Ikšķile	24.4976	56.8378	LuS 7535	40.85 ± 0.75	45–42.8	43.9 ± 0.58	Molar	[47]
22	Kalni, Nigrande	22.1266	56.4466	Hela-1314	30.42 ± 0.77	36.6–33.3	35 ± 0.8	Tusk	[3]
23	Plavinas	26.195	56.496	LuS 7536	27.85 ± 0.2	32.8–31.2	31.8 ± 0.31	Molar	[47]
24	Veselava	25.398	57.279	LuS 7539	25.8 ± 0.17	30.7–29.7	30.1 ± 0.17	Molar	[47]
	Lithuania								
25	Ariogala	23.6999	55.4833	FTMC-FR-48-2	28.633 ± 0.1	33.3–32.2	32.9 ± 0.32	Incisivi	[49]
25	Ariogala	23.6999	55.4833	FTMC-FR-48-1	25.159 ± 0.09	29.8–29.2	29.4 ± 0.18	Incisivi	[49]
26	Sviraičiai	22.5315	55.9974	RICH-22970	35.415 ± 0.23	41.1–40	40.6 ± 0.27	Humerus fragment	[49]
27	Žemgrindžiai	21.29	55.77	FTMC-OZ78-1	26.579 ± 0.05	31.1–30.8	30.9 ± 0.08	Tibia	[49]
28	Žagare esker	23.2191	56.3511	KIA-55701	27.96 ± 0.23	32.9–31.4	32 ± 0.39	Incisivi	[49]
29	Kazokiškiai	24.8198	54.8076	OxA-10874	46.3 ± 1.1	52.4–46.2	49.3 ± 1.64	Incisivi	[3]
30	Jiesia	23.9282	54.858	LuS-7531	42.3 ± 1	47.1–43.2	45.2 ± 0.92	Molar	[47]
30	Jiesia	23.9282	54.858	LuS-7532	41.35 ± 0.8	45.6–43	44.3 ± 0.68	Molar	[47]
30	Jiesia	23.9282	54.858	OxA-10872	40.9 ± 0.65	44.9–42.9	43.9 ± 0.52	Incisivi	[3]
31	Jucaičiai	22.1791	55.4522	OxA-10870	40.6 ± 0.8	44.9–42.7	43.8 ± 0.59	Molar	[3]
32	Kazokiškiai	24.8198	54.8076	OxA-10875	38.05 ± 0.7	43–41.5	42.3 ± 0.36	Incisivi	[3]
32	Kazokiškiai	24.8198	54.8076	OxA-10873	33.74 ± 0.38	39.6–37.5	38.6 ± 0.59	Incisivi	[3]
33	Pilsudai	22.5133	55.4173	LuS-7533	33.65 ± 0.3	39.4–37.5	38.5 ± 0.52	Molar	[50]
34	Kruonis	24.2709	54.7805	OxA-10810	30.35 ± 0.25	35.3–34.4	34.8 ± 0.26	Incisivi	[3]
35	Turženai	24.0924	54.9838	LuS-7528	21.4 ± 0.12	26–25.4	25.7 ± 0.13	Molar	[50]
36	Olando kepure	21.0675	55.7977	Hela-3320	27.49 ± 0.25	31.9–31.1	31.5 ± 0.22	Molar	[49]
36	Olando kepure	21.0675	55.7977	LuS 7918	>43	45.8–45.1		Molar	[3]
37	Juodeliu	23.1044	54.3868	OxA-10844	>31.4	36.1–35.5		Tusk	[3]

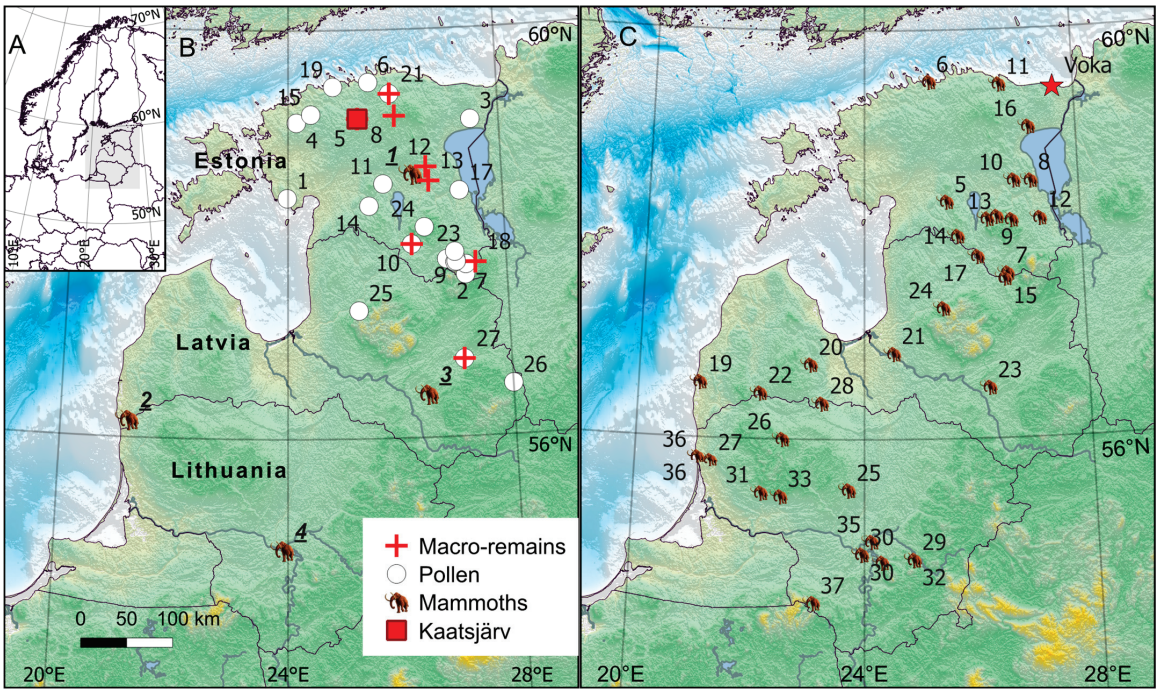

Figure 1. Overview map (**A**) and maps of the Eastern Baltic area showing post-LGM. (**B**) and pre-LGM. (**C**) known woolly mammoth finds and available plant macro remains and pollen records. Site descriptions and site numbers are given in Tables 1 and 2. Numbers in regular font refer to pollen and plant macrofossil site, underlined numbers in bold and italics refer to mammoth sites.

We have analysed two dentine samples from the youngest Estonian mammoth at Puurmani for stable carbon ($\delta^{13}C$) and nitrogen ($\delta^{15}N$) isotopes, which contain information about fauna's diet, contemporary plant cover, etc. [51,52]. In addition, we have analysed dentine samples from Krüüdneri (KRÜ) and Kukemetsa (KUK) sites (Table 2).

Possibility of abrupt changes in sedimentation rate and interruptions in sediment accumulation during the Late Glacial time [33] could impact the accuracy of the time determination and complicate establishing a chronological framework [53]. Keeping this in mind, we used only well-dated sequences to diminish possible inaccuracies and avoided interpolations beyond the dates.

2.3. Analysis of Lake Kaatsjärv Sediments

Lake Kaatsjärv (Figure 2) is a small lake in central Estonia (59.1318 N; 25.3141 E), surrounded by a mixed pine forest. The area of the lake is 1 ha, the elevation is 68.5 m above sea level (a.s.l.), and the maximum water depth is 6 m. The lake is located in front of the Pandivere (14.2 ka cal BP) ice marginal zone [17,54].

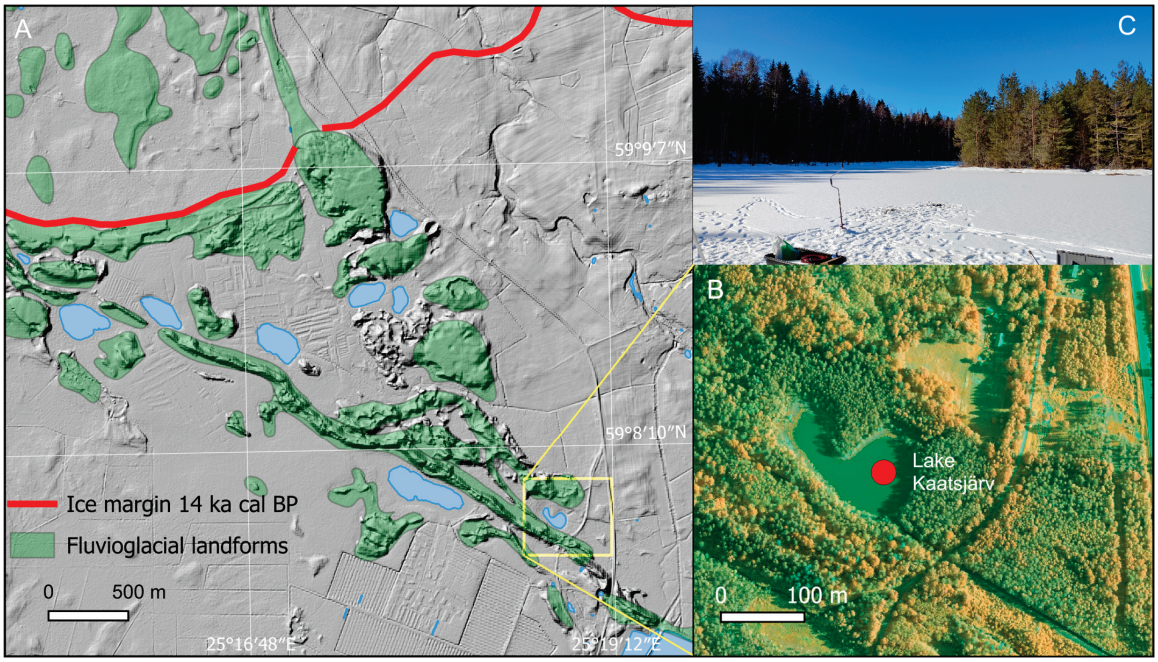

Figure 2. Shaded relief map with some geologial landforms (**A**) and false colour forestry orthophoto CIR-NGR (**B**) of the Lake Kaatsjärv area [55]. (**C**) Lake Kaatsjärv view from the coring point.

The sediment core was taken from the ice using a 1 m long and 10 cm diameter Russian corer. The retrieved cores were photographed in the field, packed into plastic tubes, and transported to the laboratory, where they were stored in a cold room at 4 °C until sampled for ^{14}C pollen and plant macrofossil analysis. The water depth at coring point was 400 cm. We analysed a 1.3 m long sediment sequence (980–1100 cm below lake water surface) covering the time period ca 11.5–13 ka cal BP. The organic matter (OM) and mineral matter (MM) content of the sediment was determined by loss on ignition (LOI) [56]. Carbonate matter content (CM) was calculated as the difference between LOI at 950 °C (for 2 h) and LOI at 550 °C, multiplied by 1.36 to express carbonates as CO_3^{2-} [56]. The noncarbonate mineral matter (MM) content was calculated by subtracting OM and CM from the total dry sample weight.

The age of the Lake Kaatsjärv sediments was determined using radiocarbon dating. Sediment samples for AMS ^{14}C dating were wet sieved through a 0.2 mm mesh; afterwards, the terrestrial plant macrofossils were selected and analysed in the Poznan radiocarbon laboratory. The age–depth model was constructed using the Oxcal 4.4.4 deposition model [57,58] and the IntCal20 calibration curve [59]. All modelled ages used in this study are given as weighted averages in calibrated years before the present (ka cal BP), where 0 = 1950 CE.

For pollen analysis, 1 cm^3 of sediment was taken. Altogether, seven samples were analysed. One *Lycopodium* spore tablet (13,911 spores per tablet; Batch No. 710961) was added to each sample before the chemical treatment to estimate the concentration of microscopic objects per cm^3 [60]. Samples were treated with 10% HCl and 10% KOH, followed by the standard acetolysis method [61,62]. Mineral matter was removed with hot 40% hydrofluoric acid [63]. The pollen identification follows Fægri and Iversen [62] and Beug [64]. A minimum of 500 terrestrial pollen grains per sample was counted and identified to the lowest possible taxonomic level using pollen keys, the reference pollen

collection at the Department of Geology at Tallinn University of Technology, and other literature sources [64,65]. The percentages of terrestrial taxa were calculated based on arboreal and non-arboreal terrestrial pollen sum, excluding sporomorphs of aquatic and wetland plants. Aquatics, spores, and non-pollen palynomorph percentages were calculated in relation to the terrestrial pollen sum [66].

For plant macrofossils analyses, ~55 cm^3 of sediment at 2 cm intervals were taken from Lake Kaatsjärv. In total, 35 sediment samples were processed for plant macrofossil content. Samples for plant macrofossil analysis were prepared following [67]. Samples were wet sieved through the mesh of 0.125 mm. Plant macrofossils and other remaining materials were examined using a stereo and light microscope. We used plant macrofossils atlases, reference collections, and relevant literature during identification [68,69].

The results of plant macrofossil analysis (expressed as the number of plant macrofossils per 100 cm^3 of sediment, i.e., concentration) and pollen (expressed as pollen percentages) analysis are presented in a combined diagram generated using TILIA v.2.0.1 [70].

2.4. Landcover Reconstructions

We have used pollen and plant macrofossil analysis results to reconstruct the composition of the terrestrial landcover, with special attention to the open versus forested conditions. Accordingly, we have included only terrestrial plant taxa and restricted the pollen records to the tree taxa and herb families represented in any of the plant macrofossil datasets confirming local presence of the taxon in order to reduce possible effects of redeposited and long-distance transported pollen (Table 3).

Plant macrofossil analysis from lake sediments represents an extra-local signal that could lead to an overrepresentation of aquatic plants and an underrepresentation of terrestrial plants. As a result, some important components of terrestrial vegetation could be missing from the records. We used presence/absence data rather than concentrations or percentages to diminish such effects to specify the terrestrial landcover type.

The cover fractions of the selected 21 tree, shrub, and herb taxa (Table 3), representing >90% of the total terrestrial pollen sum, were reconstructed from pollen data using the REVEALS (Regional Estimates of Vegetation Abundance from Large Sites) model [71]. We used the REVEALSinR function from the DISQOVER package in R [72]. The REVEALSinR parametrisation used the actual basin diameters, the Pollen Productivity Estimates (PPEs) relative to Poaceae, standard errors (SEs), and fall speeds of pollen, as shown in Table 3. The distance weighting method was set standard GPM (Gaussian Plume model) for stable conditions. The REVEALS model enables us to overcome the discrepancies between the proportions of pollen counts and vegetation cover derived from differences in pollen production and dispersal abilities of the taxa. The model is intended to estimate the vegetation proportions on a regional scale using pollen data derived from large basins. We have not strictly followed this assumption, as the data used here were derived from different-sized lakes. However, several previous investigations have shown the method's stability even when pollen records from variable-sized basins have been used [73,74]. Furthermore, the lake sizes were generally considerably larger than today during the Late Glacial period, and the contemporary landcover was sparse, suggesting that most of the recorded pollen was of regional origin regardless of the lake size.

Pollen Productivity Estimates (PPEs) and pollen fall speeds are necessary inputs for the REVEALS model. A large variety of PPE datasets is available from different locations in Northern Hemisphere [75]. Best results are usually achieved using the PPEs derived from environments like those attempted to reconstruct. We have therefore used the PPEs obtained from arctic and boreal environments of Northern Europe [76–78] and North

America [79,80] whenever available (Table 3). The PPEs for a few taxa missing from the above-mentioned sources were adopted from Europe-based sets [75].

The reconstructed cover proportions of terrestrial plant macrofossils and selected terrestrial pollen taxa (Table 3) were amalgamated into two major landcover types typical of the Late Glacial and Early Holocene environments in the Eastern Baltic area: (1) open landcover represented by different herbs, sedges (e.g., *Carex* spp., *Eriophorum* spp.), grasses (Poaceae), dwarf shrubs from heather (Ericaceae) family, and willow (*Salix* spp.); (2) forested landcover represented by typical boreal trees like birch (*Betula*), pine (*Pinus*), spruce (*Picea*), and aspen (*Populus*) (Table 3).

Many researchers do not differentiate between different birch pollen types. Therefore, it must be kept in mind that the birch pollen type used here includes pollen grains produced by both tree (*Betula pendula* and *B. pubescens*) and shrub (*B. nana* and *B. humilis*) forms of birch as the dataset was harmonised to a level obtainable for all exploited records. As birch is included here as a forest indicator, the possible addition of smaller or larger amounts of shrub-derived birch pollen could lead to an overestimation of forestation degree by reconstructions.

The pollen-based landcover reconstructions are presented as cover proportions, and macrofossils are shown based on the presence/absence of the determined landcover type indicator species. The results of landcover reconstructions are presented using QGIS 3.34 [81].

Table 3. The Pollen Productivity Estimates (PPEs) relative to Poaceae, standard errors (SE), and fall speeds of pollen grains used for calculations derived from [1] [82]; [2] [76]; [3] [80]; [4] [77]; [5] [78]; [6] [75].

Landcover Type	Taxon	PPE (SE)	Fall Speed
Open	[2] Apiaceae	0.21 (0.03)	0.042
	[6] *Artemisia*	4.33 (1.592)	0.014
	[2] Asteraceae sect. *Cichorioideae*	0.07 (0.02)	0.029
	[6] Brassicaceae	0.07 (0.04)	0.021
	[5] *Calluna*	0.3 (0.03)	0.038
	[1] Caryophyllaceae	0.6 (0.05)	0.032
	[6] Chenopodiaceae	4.28 (0.27)	0.019
	[2] Cyperaceae	0.13 (0.03)	0.035
	[1] *Equisetum*	0.09 (0.02)	0.021
	[5] Ericaceae (incl. *Empetrum nigrum* and *Vaccinum t.*)	0.09 (0.035)	0.032
	[1] *Juniperus*	1.4 (0.05)	0.016
	Poaceae	1 (0)	0.035
	[2] Ranunculaceae (incl. *R. acris t.*)	0.08 (0.02)	0.02
	[2] Rosaceae (incl. *Filipendula* and *Dryas octopetala*)	0.18 (0.04)	0.022
	[2] Rumex (incl. *R. acetosa* and *R. acetosella t.*)	0.04 (0.02)	0.018
	[5] *Salix*	0.09 (0.03)	0.022
	[6] *Urtica*	10.52 (0.31)	0.01
Forested	[4] *Betula* (incl. *B. humilis* and *B. nana)*	2.24 (0.2)	0.024
	[5] *Picea*	2.8 (0.21)	0.056
	[4] *Pinus*	8.4 (1.34)	0.031
	[3] *Populus*	0.11 (0.09)	0.026

2.5. Isotopic Analysis

Two mammoth molars found at Puurmani manor TAM G441:47 and TAM G441:48 were collected from the Estonian Museum of Natural History and sampled using a Dremel 300 drill. Two mammoth molars from Krüüdneri (KRÜ) and Kukemetsa (KUK) were sampled from the collection of the Museum of Tartu University. Collagen extraction for carbon

and nitrogen isotope analysis was conducted using Protocol F by Cersoy et al. [83] and analysed in a Thermo-Finnigan Delta V Plus mass spectrometer paired with an elemental analyser (Thermo Flash 1112) at Tartu University. The samples were analysed in duplicates, and the average of two was used.

3. Results

3.1. Lithology and Chronology of Kaatsjärv

The lithology of Kaatsjärv is presented in Figure 3. Radiocarbon dating results are given in Table 4 and Figure 3. Radiocarbon date Poz-173419 is considered to be an outlier.

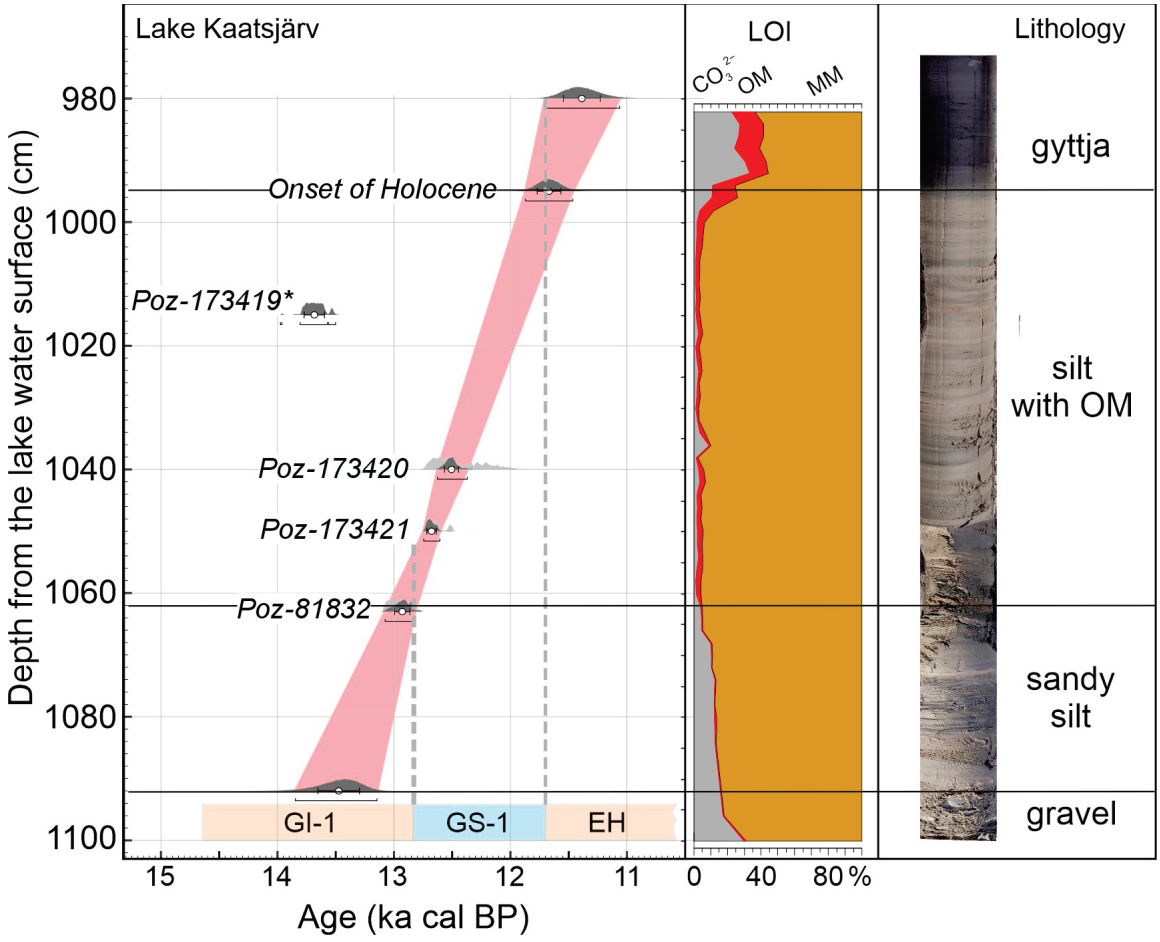

Figure 3. Lake Kaatsjärv sediment sequence age–depth model, loss on ignition (LOI) results and, lithology. The modelled ages are shown at a 95.4% probability range. The graphs on the age–depth curve show the likelihood (grey) and posterior (black) probability distribution of the calibrated radiocarbon dates. The weighted average ages are shown by white circles with associated standard errors (black lines), and an asterisk marks the outlier not used in the model. OM: organic matter, MM: mineral matter. GI-1 and GS-1: Greenland interstadial and stadial, respectively [22], EH: part of the Early Holocene.

Table 4. ^{14}C dates from Lake Kaatsjärv. OxCal deposition model results are given as modelled ages at a 95.4% probability range and corresponding weighted averages. Poz-173419 is marked with an asterisk because this date is an outlier that was not used in the age model.

Depth, from the Lake Water Surface, cm	Lab Code	^{14}C age ka BP	Modelled Ages ka cal BP		Remark	Dated Material
			At 95.4% Probability Range	Weighted Average		
1015	Poz-173419 *	11.8 ± 0.07	14.0–13.5	13.7 ± 0.09	0.3 mgC	*Dryas octopetala* leaves unidentified stems and leaves
1040	Poz-173420	10.5 ± 0.120	12.6–12.4	12.5 ± 0.06	0.08 mgC	*Dryas octopetala* leaves unidentified stems and leaves
1050	Poz-173421	10.6 ± 0.07	12.8–12.6	12.7 ± 0.04	0.18 mgC	*Dryas octopetala* leaves unidentified stems and leaves
1058–1068	Poz-81832	11 ± 0.06	13.1–12.8	12.9 ± 0.07		Bulk sediment

3.2. Kaatsjärv Plant Macrofossils and Pollen Diagram Description

The biostratigraphical material from Lake Kaatsjärv (Figure 4) was divided into three zones determined following the Greenland Ice Core Chronology (GIGC05modelext) [22].

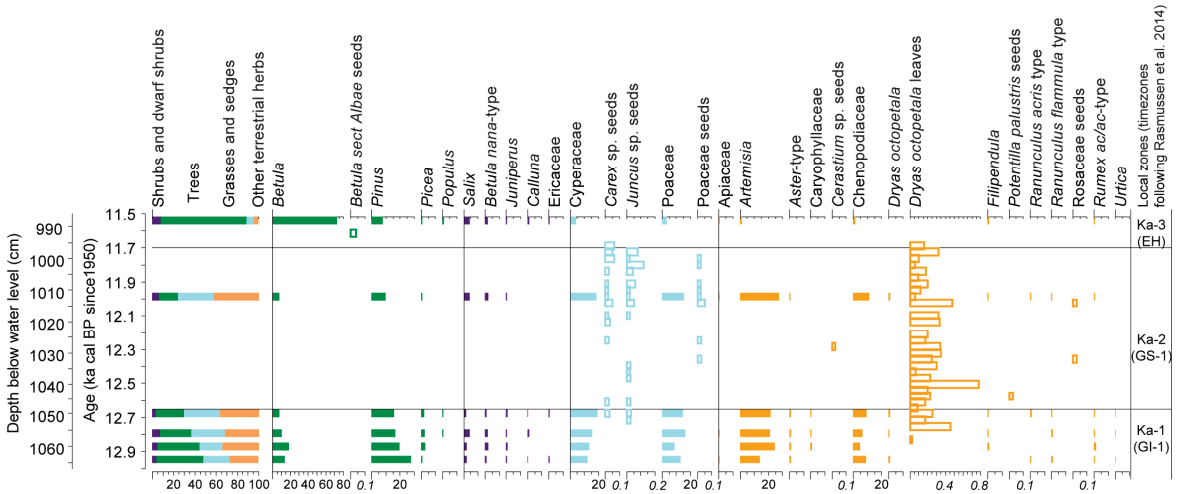

Figure 4. Combined diagram of selected taxa showing pollen percentages (filled bars) and terrestrial plant macrofossils concentrations expressed as the number of plant macrofossils per 100 cm^3 of sediment (outlined with a thick stroke).

Ka-1 (GI-1; 13.5–12.85 ka cal BP). This zone is characterised by *Pinus* domination in the pollen spectrum among tree taxa, but its part decreases by the end of the zone. *Picea* is not as prominent as *Pinus* but also increases by the end of the zone. At the same time, Cyperaceae and Poaceae increase noticeably, as does *Artemisia* and Chenopodiaceae pollen. There is a peak in Non-Arboreal Pollen (NAP) taxa at 12.8 ka cal BP. Plant macrofossil finds were very rare in this zone, mainly consisting of rare *Tomentypnum nitens* leaves.

The lowermost pollen samples from sandy silt sediments of Lake Kaatsjärv, below 1068 cm, >13.0 ka cal BP, contain redeposited pollen, making it unsuitable for our analysis. The presence of tree taxa like *Alnus*, *Ulmus,* and *Corylus* in this sequence is inconsistent with the vegetation and climate information for that period and was excluded from further analysis. The issue of redeposited pollen in the periglacial sediments is a common problem for the Eastern Baltic [12]. In addition, these samples have lower pollen concentrations and contain a high amount of corroded pollen grains.

Ka-2 (GS-1; 12.85–11.7 ka cal BP). This is the only zone where the plant macrofossils become prominent. In this zone, *Pinus* gradually decreases amongst tree pollen taxa, and *Betula* continues to decrease. *Quercus* decreases by the end of the zone. *Salix*, in contrast, increases throughout the zone. Poaceae, Cyperaceae, Chenopodiaceae, and *Artemisia* continue to increase. Plant macrofossils of KA-2 are represented by *Potentilla palustris*, *Carex,* and *Juncus* seeds. *Dryas octopetala* peaks at the depth of 12.5 ka cal BP.

The zone demonstrates a noticeable change in the vegetation composition as *Cerastium*, Rosaceae, and Poaceae seeds are present. By the end of the zone, however, Rosaceae, Poaceae, *Carex*, and *Juncus* seeds decline; *Dryas octopetala* also decreases and abruptly disappears at 11.7 ka cal BP.

Ka-3 (EH; 11.7–11.3 ka cal BP). *Pinus* increases in the pollen spectrum, but *Betula* becomes dominant in the zone among tree taxa, surpassing *Pinus*. Herbs like Poaceae, Cyperaceae, *Artemisia,* and Chenopodiaceae are decreasing. There is very little to no herb-derived macrofossil material in this zone. However, the seeds belonging to tree-type birch, *Betula* sect. *Albae* appear in this zone for the first time. The plant macrofossil assemblage instantly changes to *Betula sect. Albae* and *Potamogeton* dominated (Supplementary Materials Data).

3.3. Landcover Reconstruction

Maps encompassing Estonia and Latvia representing pollen-based landcover proportions and plant macrofossil-based presence/absence evidence of open (represented by herbs and shrubs) and forested (represented by tree taxa) landcover were generated for three time periods: GI-1 (14.6–12.85 ka cal BP), GS-1 (12.85–11.7 ka cal BP), EH (11.7–11.3 ka cal BP) (Figure 4).

GI-1 (14.6–12.85 ka cal BP). Half of Estonia's current territory was submerged by the Baltic Ice Lake and delimited by the glacier in the north [54,84]. Sparse vegetation dominated by herbaceous plants indicates a cold, open environment with limited tree cover. According to pollen data, trees were present in northern and southern Estonia and central Latvia during this period. However, plant macrofossil evidence shows open landscapes with no tree cover in central and northern Estonia and a mixture of open and forested landscapes in southern Estonia and central Latvia.

GS-1 (12.85–11.7 ka cal BP) (Younger Dryas). Pollen evidence shows that central Estonia was an open landscape, with a marked decline in forest cover, but northern and southern Estonia kept some tree cover. However, according to plant macrofossils, open landscapes dominated Estonia, and trees were present only in central Latvia.

EH (11.7–11.3 ka cal BP). Pollen evidence shows the predominantly open landscape in eastern Estonia, whereas the northern and western parts of Estonia and the south of Estonia and Latvia were predominantly occupied by forests. Plant macrofossils indicate that the trees established their presence in northern Estonia and kept their presence in central Latvia, whereas the trees in central and southern parts of Estonia only started to establish their presence.

3.4. Isotopic Results

Isotopic results are summarised in Table 5. We used the C:N atomic ratio to evaluate the extent of bone decomposition and its potential impact on the results. Following the criteria outlined by [85], C:N ratio values should fall within a range of 2.9–3.6. The acceptable nitrogen (N%) and carbon (C%) values should be higher than 1% and 3% [86]. TAM G441:47 and TAM G441:48 displayed nitrogen values of 0.5% and 0.9%, carbon values of 2.3 and 2.5, and C:N ratios of 4.1 and 2.7, respectively, outside of the ranges that are considered acceptable. KRÜ and KUK displayed acceptable C:N ratios of 3.1 and 3.3, respectively. Stricter criteria for the C:N ratio of 3.1-3.3 range suggested by Guiry and Szpak (2021) [87] also show that C:N ratios of TAM G441:47 and TAM G441:48 fall outside of the acceptable range, whereas KRÜ and KUK show acceptable C:N ratios.

Table 5. Summary of the isotopic results of four mammoth molars from three different Estonian sites.

Sample ID	Material	δ^{15}N (‰) ± SD	δ^{13}C (‰) ± SD	N	C	C:N
KRÜ	Mammoth molar	+9.8	−21.1	1.1	3.6	3.1
KUK	Mammoth molar	+10.1 ± 0.02	−20.6 ± 0.05	1.0	3.6	3.3
TAM G441:47	Mammoth molar	+7.4 ± 0.09	−20.2 ± 0.4	0.5	2.3	4.1
TAM G441:48	Mammoth molar	+6.5 ± 0.9	−21.2 ± 0.9	0.9	2.5	2.7

4. Discussion

4.1. Landcover Reconstructions

The combined effect of climate cooling and warming and changes in the extent of major water bodies and dry land created a highly variable landscape with a dynamically changing landcover for three millennia (14.6–11.3 ka cal BP) at the end of Pleistocene and the beginning of Holocene. The drastic water level changes in the Baltic basin caused by the combined effect of glacial meltwater input and glacioisostatic land uplift considerably changed the shoreline of the Eastern Baltic (Figure 5) [84]. The landscape emerged as a barren periglacial wasteland behind the retreating ice front, with continental ice cover persisting in northern Estonia until 14 ka cal BP and in southern Finland up to 11.7 ka cal BP [15]. The soil in the deglaciated region can develop in 100–1000 years [88], and shrubs and grasses can appear relatively shortly after glacier retreat according to modelling studies from Greenland [89], which shows that after the ice retreat in the Eastern Baltic, the landscape could become attractive for herbivores in a relatively short time period.

According to our pollen-based reconstructions, the area of present Estonia and Latvia was covered with sparse open landcover during a two millennia-long warmer period (GI-1, 14.6–12.85 ka cal BP) at the end of the last glaciation (Figure 5). Open dry tundra-like communities with grasses, sedges, mugworts (*Artemisia*), and members of the amaranth family (Chenopodiaceae) dominate the herb pollen assemblage at Lake Kaatsjärv (Figure 4). While such herbal vegetation composition is typical for most of the Late Glacial pollen sequences from the Eastern Baltic [12], there is no contemporary plant macrofossil evidence of mugworts or amaranth family members in the region. However, it must be kept in mind that both Artemisia and Chenopodiaceae are wind-pollinated taxa and therefore prone to be overrepresented in pollen spectra. Most pollen-based reconstructions show low (10–20%) but steady tree cover in Estonia and Latvia. However, our results of plant macrofossil analysis suggest that at least boreal trees (birch and pine, spruce, and aspen) were present in Latvia. Furthermore, there is evidence of tree birch (*Betula sect. Albae*) presence in Lithuania already around 18.7 ka cal BP, directly after ice retreat from the region [49].

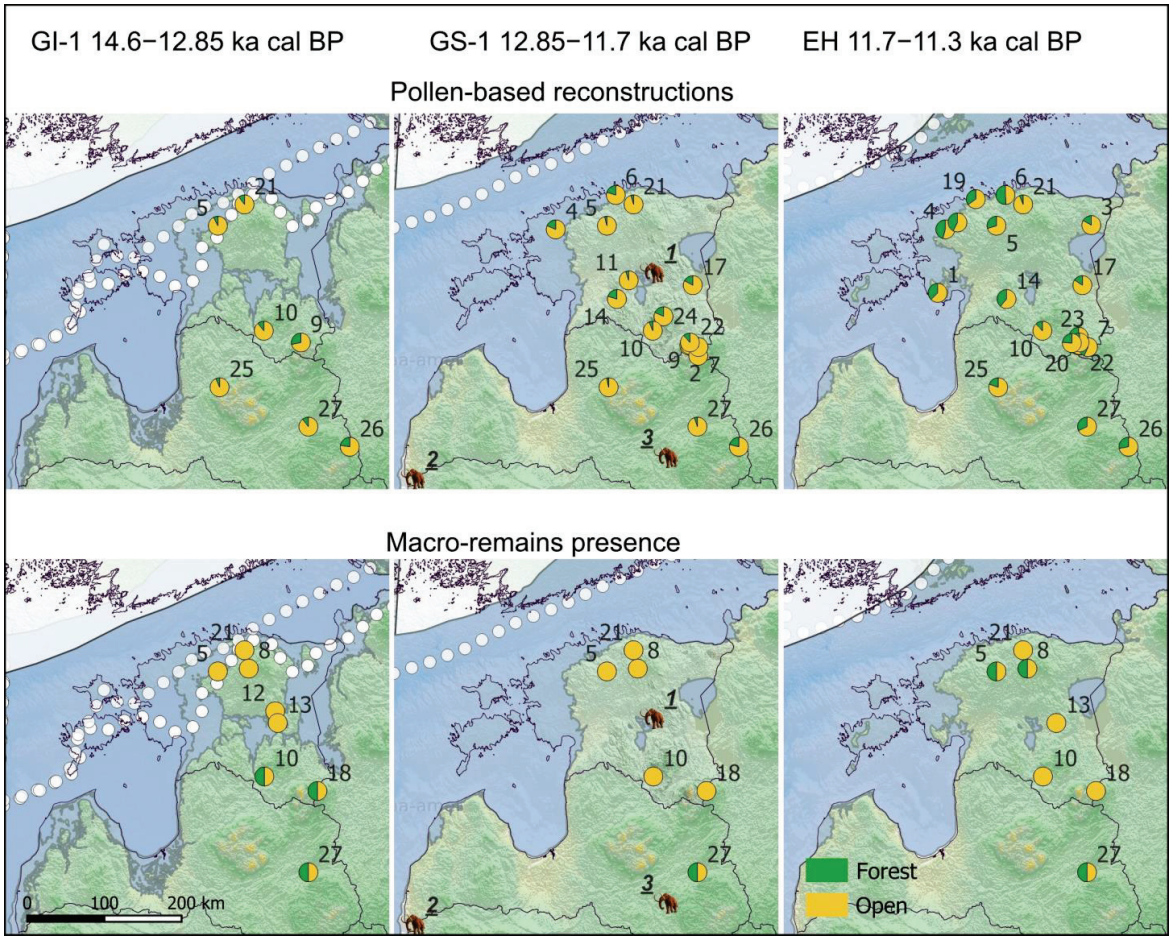

Figure 5. Palaeo-geographic maps showing pie charts representing pollen-based reconstructions of open (yellow) and forested (green) landcover proportions and the presence of herb (yellow) and tree (green) macrofossil evidence. The extent of major water bodies is shown according to [54]. Contemporary for presented time slice continental ice margin is shown with a white overlay and tentative maximum extent with dotted white lines [15,54]. Numbers in regular font refer to pollen and plant macrofossil site, underlined numbers in bold and italics refer to mammoth sites.

Our findings agree with those of earlier studies by [29,90] and indicate that the late Pleistocene mammoth populations in the Eastern Baltic area could have been trapped between the quickly developing forests in the south and the receding ice edge and meltwater lakes in the north. The contemporary plant macrofossil evidence supports the above-described pattern of vegetation cover closely following the climate changes more clearly than the pollen-based reconstructions (Figure 5). While considering pollen-based results, it should be noted that the REVEALS model cannot estimate the part of the non-vegetated ground and could, therefore, lead to gross overestimation of plant cover proportions for both open and forested landcover types for mostly barren landscapes [91]. On the other hand, the sparse vegetation cover producing low amounts of pollen could cause an overrepresentation of long-distance-derived pollen grains in pollen samples. The study on the modern forest–tundra ecotone in Scandinavia shows that the arboreal component dominates the background pollen and can contribute ca 60% of the total pollen loading in

samples from open tundra [78]. The aerobiological observations have shown that pollen produced by members of the birch and pine family can travel >1000 km distances [92,93]. The plant macrofossil-based evidence shows that the first tree-type birch (*Betula sect. alba*) and pine trees immigrated into eastern Latvia (Lake Lieliais Svetinu) ca 13.5 ka cal BP [94]. First, trees, the tree-type birch, reached the shores of Lake Nakri in southern Estonia, which was also already during GI-1 (Figure 5) [31].

The last climate cooling episode, GS-1 (12.85–11.7 ka cal BP), corresponding to the Younger Dryas climatostratigraphic episode before the current interglacial, caused considerable climate cooling, especially in the northern part of the Eastern Baltic [95,96]. Both pollen- and plant macrofossil-based evidence show a clear decrease in tree cover in Estonia and Latvia (Figure 5). Furthermore, the results of the biostratigraphic analysis from Lake Kaatsjärv, situated in the border zone between the retreating glacier and immigrating vegetation with abundant finds of *Dryas octopetala* leaves accompanied by diminishing amount of tree pollen and dominance of typical dry tundra elements as grasses, mugworts, and members of amaranth family among herb pollen, show clear evidence of prevailing open forb-dominated tundra conditions (Figure 4). However, the tree macrofossil finds from Latvia suggest that at least some tree populations, probably established already during the previous warmer period, survived the climate cooling (Figure 5). Amon et al. [94] have reported continuous finds of birch seeds, pine and spruce needles, and stomata from Lake Lielais Svetinu, Latvia.

Subsequently, by 11.7 ka cal BP, the GS-1 stadial ended abruptly with rapid climate warming [97]. The disappearance of *Dryas octopetala* and the emergence of herbs such as *Cerastium* and Rosaceae family members, along with the discovery of tree macrofossils in Lake Kaatsjärv, appear concurrently with climate warming. According to Birks and Birks [98], the annual mean temperature in northern Norway steeply rose to around 6 °C during the first 500 years of the Holocene. The formerly dominating Chenopodiaceae diminished drastically in pollen records and were replaced by a high amount of birch pollen (Figure 4). This signified a rapid transformation from a dry steppe tundra into a forested landscape, considerably reducing the shrub and herb layers.

During 11.7–11.3 ka cal BP, the pollen and plant macrofossils recorded from Lake Kaatsjärv and other parts of Estonia show the establishment of more widespread tree cover and abrupt shrinkage of the open landscapes (Figures 4 and 5). While forests were speedily advancing in Latvia and southern Estonia, northern and western Estonia was submerged by the Baltic Ice Lake [54], with the glacier front situated in southern Finland [15,99].

4.2. Mammoths and Environment

Rapid landcover change and afforestation in connection with rapid climate warming have been suggested to be one of the major factors leading to the extinction of herbivorous megafauna in Northern Europe at the end of the Pleistocene [3]. Furthermore, Ukkonen et al. [3] noted that a higher abundance of mammoth remains in Northern Europe is primarily associated with colder periods of the post-LGM, such as the GS-2 and GS-1 stadials, and are absent during warmer intervals, like GI-1 interstadial. This observation fully agrees with our results and raises the question of whether a similar pattern could be observed during the earlier time periods [96]. The pre-LGM warmer period during the last glaciation, ca 60–27 ka cal BP, led to ice-free conditions in the Eastern Baltic region (Figure 6). However, these climate oscillations were less pronounced, and the environmental conditions were more stable than those at the Late Pleistocene/Early Holocene boundary [22].

While only four mammoth molar samples have been found in Estonia and Latvia from the post-LGM period and dated between 15.4 and 11.8 ka cal BP, many more are known from the pre-LGM period, dated 50–27 ka cal BP (Figure 6, Table 2) [3]. Furthermore, it is

important to consider that the true extent of mammoth presence during this time may be heavily underrepresented due to the erosive effects of subsequent glacial advances [17]. Much of the material, including potential mammoth remains, could have been buried, eroded, or displaced, limiting our ability to capture the actual abundance and distribution of mammoth populations during the pre-LGM [1,22,100]. Due to the scarcity of the ^{14}C dated remains, it is difficult to make firm conclusions about whether a long-term coherent pattern of climate-dependent distribution of woolly mammoth exists in the Eastern Baltic region. However, the available data suggests the tendency of the mammoth appearance in connection to colder periods both during the pre- and post-LGM (Figure 6).

In contrast to the numerous pre-LGM mammoth finds known from the Eastern Baltic area, the finds of contemporary (50–27 ka cal BP) well-dated sediment sequences suitable for biostratigraphic analysis are much less frequent. To the authors' knowledge, only one site from the study area—the Voka site (Figure 1) in the northeastern part of Estonia covering 38-32 ka cal BP—is rigorously dated to this period (Figure 6) [20,21].

The Pleistocene herbivorous megafauna depended on fodder of high nutritional value [101]. Based on the mammoths' stomach content analysis, Cyperaceae and *Artemisia* were the key components of mammoths' diet [102]. Our reconstructions from the pre-LGM Voka site and our post-LGM reconstructions representing the cooler GS-1 stadial indicate an environment dominated by dry steppe-tundra communities, which are rich in forbs, graminoids, shrubs, including abundant finds of *Dryas octopetala* leaves, and pollen from Cyperaceae, *Artemisia*, and Chenopodiaceae. As steppe animals that thrived in vast, open landscapes [99], such landcover composition suggests an abundant subsistence basis with plentiful food sources for mammoths to graze on. An examination of the Voka pollen-based landcover reconstructions reveals that the landcover was notably stable during many millennia of the pre-LGM, exhibiting only minor differences between vegetation composition of cold and warm phases. The post-LGM landcover was much more dynamic, and even though the open tundra-like environment prevalent during GS-1 seems to have been suitable for mammoths, the animals may have struggled to adapt to the rapid climate change-induced shifts in landcover characteristic to the end of the last glaciation and the beginning of the Holocene (Figure 4). The volatile nature of the environmental conditions could also explain a considerably lower number of mammoth finds belonging to the post-LGM compared with the pre-LGM (Figure 6). The vegetation changes from forb-dominated, dry steppe-tundra to landcover dominated by woody plants and graminoids were shown to be concurrent with large-scale megafaunal extinction in eastern Siberia during the early Holocene [103,104]. Our results show a similar pattern for Northern Europe, with a clear connection between the rapid afforestation combined with the decline of the dry forb steppe-tundra elements coinciding with the last finds of woolly mammoth remains, leading to the ultimate extinction at the transition to the Holocene. Human activities, hunting, and the associated impacts on mammoth habitats are often considered to be among the primary factors contributing to the mammoths' demise [9,105]. However, in the Eastern Baltic, the evidence of the coexistence of woolly mammoths with local prehistoric hunter-gatherers is ambiguous. Meanwhile, the evidence from the oldest known settlement in Latvia, the Mellupite settlement (12.3 $\pm$ 0.14 ka cal BP) [106], predates the last mammoth find by 200 years, suggesting short-term co-existence and possible hunting. However, the last mammoth in Estonia predates the first known settlement, the Pulli settlement (11 $\pm$ 0.17 ka cal BP), by ca 800 years, making hunting as a course for extinction unlikely [107–109].

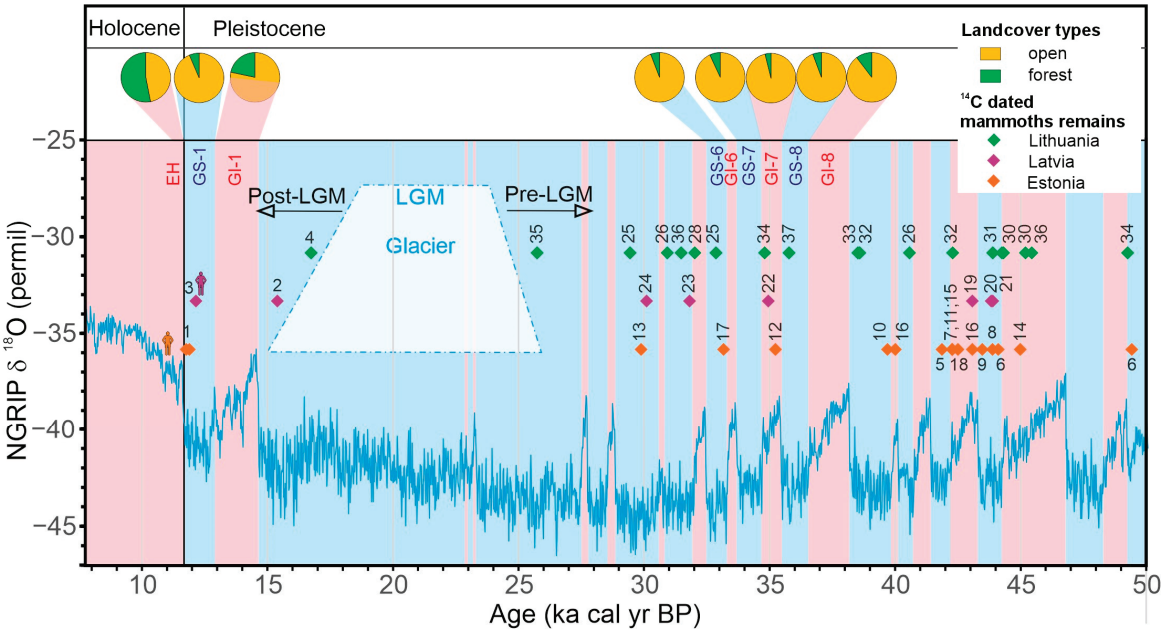

Figure 6. Radiocarbon-dated mammoth remains, NGRIP $\delta^{18}O$ curve, and pollen-based landcover reconstructions from Voka and Lake Kaatsjärv. Blue colour corresponds to the stadials (colder periods) and pink to the interstadials (warmer periods) [22]. Numbers correspond to the site numbers in Table 2.

4.3. Isotopic Evidence

Comparing palaeobotanical reconstructions based on pollen and plant macrofossil data and isotopic composition of herbivorous faunal remains has been shown to provide a deeper insight into vegetation changes in the investigated region and the diet of the tested animals, e.g., [110]. Similar to pollen data, stable isotopic records from mammoths offer a broad regional signal, with nitrogen and carbon isotope values representing an integrated summary of the dietary intake over the final years of the analysed specimen because bone collagen in adult proboscideans remodels over years and even decades, e.g., [111,112]. Isotopic data derived from dentine remains the only available tool for dietary reconstruction in this context because we do not have access to soft tissues such as blood, muscle, or hair, which would enable more precise dietary reconstructions [113]. While pollen data shows general changes in the vegetation composition, isotopic analysis provides complementary information about trophic interactions and dietary habits of the animals that inhabited the landscape. While the isotopic results from only four dentine samples are insufficient for a full-scope reconstruction, the isotopic data are still valuable for comparative purposes and to support our landcover reconstruction-based interpretation. According to [114,115], animals consuming 100% C3 plants have their collagen $\delta^{13}C$ values close to −21.5‰. Carbon ($\delta^{13}C$) isotopic values (−20.2‰ and −21.2‰) from Puurmani samples indicate a diet based on predominantly C3 plants. It has been shown that the depletion in $\delta^{13}C$ can be characteristic of plants in heavily forested areas (e.g., [116]. Occasionally, mammoths could supplement their diet with woody vegetation, resulting in lower carbon isotope values [103]. We did not observe this trend in our samples. Nevertheless, the rapid forestation of the landscape in Estonia at the end of the studied period offers the possibility that mammoths in this region may have consumed woody vegetation at certain times to compensate for the

decreased amount of suitable vegetation. Future research on mammoth dietary habits in the Eastern Baltic could explore this potential relationship in more detail.

The $\delta^{15}N$ values from Puurmani (+6.5‰ and +7.4‰) point to a low-protein, high-fibre diet and align with nitrogen values reported for other European mammoth sites, e.g., [103], who reported lower average $\delta^{15}N$ values of 5.6‰ from the Eliseevichi site (14.47 ± 0.4 ka cal BP) and 6.1‰ from Yudinovo (15.7–14.4 ka cal BP) for the European plain, both lower than the values from Puurmani. This suggests that mammoths in the European Plain were not necessarily faring better in their diet than their Estonian counterparts. In contrast, the $\delta^{15}N$ values from the Krüüdneri (9.8‰) and Kukemetsa (10.1‰) are higher and resemble isotopic values for older periods in the European plain, where [103] reported average $\delta^{15}N$ values of 9.4‰ from Khotylovo (24.9 ka cal BP) and 6.6‰ from Avdeevo (22.7 ka cal BP), indicating some regional variation in the isotopic values. Multiple studies have shown that climatic conditions, like aridity and temperature, can impact the $\delta^{15}N$ values of plants (e.g., [117]) and, as a result, impact the $\delta^{15}N$ values from mammoths' collagen. The nitrogen isotope values decrease from the environmentally more favourable pre-LGM period to the less favourable period during the post-LGM. This trend corresponds well with our landcover reconstructions. Lowered nitrogen values from the Puurmani site align with an observed general decline in $\delta^{15}N$ values around 16.0 ka cal BP noted across south-central Siberia, the European Plain [103], and Central and Western Europe [104].

More stable environmental conditions and a diet abundant in forbs (*Dryas octopetala* being one of them), sedges, and mugworts may explain the potentially larger mammoth populations in the Eastern Baltic during 38–32 ka cal BP in contrast to 14.3–11.3 ka cal BP. The presence of a thriving megafauna population could have led to significant trampling effects [118], which could, in turn, promote gap-based recruitment in vegetation [119]. This process could have favoured the proliferation of forbs as suggested by [120]. Forbs are notably more nutrient-rich than grasses [121] and more easily digestible [122], making them an optimal food source for sustaining large herbivores. Michelsen et al. [123] demonstrated that graminoids, abundant in open tundra ecosystems, typically exhibit higher $\delta^{15}N$ values than trees and shrubs. Similarly, herbs and subshrubs are more common in open environments and more isotopically enriched than vegetation associated with forested areas. Thus, the higher $\delta^{15}N$ values during interglacial periods likely reflect a grass-dominated diet, consistent with the open steppe-tundra landscapes of the time. In contrast, postglacial landscapes were characterised by the increasing dominance of forests and larger vegetation, such as trees and shrubs, leading to a dietary shift towards tree leaves and needles. This dietary change resulted in more depleted $\delta^{15}N$ values in mammoth tissues, reflecting the transition in their ecological environment.

This interpretation supports the hypothesis that a shifting environment impacted mammoth survival and dietary habits. Based on the limited isotopic records, the conditions in central Estonia at the onset of the Holocene were probably no longer as favourable for mammoths as in earlier periods: forests dominated the northern and southern regions of Estonia and central Latvia, which did not satisfy their dietary needs. $\delta^{15}N$ values from the pre-LGM Krüüdneri and Kukemetsa sites are higher than those from Puurmani, which can indicate a significant change in their diet and possibly the loss of the specialised ecological niche of these animals over time. Our observations agree with the findings of [124], who also discovered that the extinction of mammoths in the central East European plains during the Late Pleistocene was likely driven by the loss of their optimal habitat.

The C% and %N values and the C:N ratio of the samples from both Puurmani mammoth samples indicated that the samples are likely to have been altered by post-depositional processes. However, it is challenging to establish the factor that caused this alteration due to the lack of information about the burial context and the small selection of samples.

The poor preservation of the two mammoth molar samples from Puurmani has posed significant challenges to our research, as the samples' condition raises concerns about the reliability of the nitrogen and carbon isotopic values. Additional mammoth discoveries from this period and isotopic analysis of these findings may provide more crucial insights into the trophic position of the mammoths in the Eastern Baltic. Additionally, Figure 5 shows that the mammoth population in the Eastern Baltic declined since 50–33 ka cal BP. Our landcover reconstructions and isotopic results show that the rapid forestation and the limited availability of suitable nutrients significantly contributed to the decline of mammoth populations in Estonia during the Late Pleistocene.

5. Conclusions

Our analysis demonstrates considerable differences in the pre- and post-LGM landcover response to climate changes. While moderate climate changes during the pre-LGM period did not lead to considerable changes in the landcover composition, the larger climate fluctuations post-LGM led to rapid changes. The landcover reaction to intermittent colder and warmer periods was vigorous, resulting in a series of tree cover expansion and shrinkage, ending with abrupt afforestation and the disappearance of dry steppe with tundra-like open herb communities suitable for mammoths brought by rapid climate warming at the beginning of Holocene. Plant macrofossils show the progression of the tree colonisation more clearly than pollen-based reconstructions. During 11.7–11.3 ka cal BP, pollen and plant macrofossil data from Kaatsjärv show the establishment of tree cover and the abrupt disappearance of *Dryas octopetala*, a key component of forb tundra, indicating that central Estonia became inhospitable for mammoths.

We analysed four mammoth dentine samples belonging to the youngest mammoth finds in Europe (14.3–11.3 ka cal BP, 43.5 ka cal BP, and 39.1 cal BP). Although the isotopic results for carbon and nitrogen isotopic values from the Puurmani samples are not highly reliable due to the poor preservation state, and only two measured values are insufficient to draw wider conclusions about the diet of the last European mammoths, the depleted $\delta^{15}N$ isotopic values align well with those observed in other European mammoth populations from the end of the Pleistocene. Consequently, the isotopic data suggest that the investigated post-LGM mammoths probably had a suboptimal, nitrogen-deprived diet, in contrast to the mammoth that inhabited the Eastern Baltic during the pre-LGM. This aligns well with the concurrent decline in nutrient-rich, herb-dominated communities and the overall expansion of less suitable tree communities for herbivore consumption.

Supplementary Materials: The following supporting information can be downloaded at https://www.mdpi.com/article/10.3390/land14010178/s1.

Author Contributions: Conceptualization, A.P. and L.A.; Data curation, J.V.; Formal analysis, I.K. and S.V.; Funding acquisition, L.A.; Investigation, I.K.; Methodology, I.K., S.V., and L.A.; Project administration, L.A.; Software, J.V.; Supervision, S.V. and L.A.; Validation, J.V.; Visualisation, A.P. and J.V.; Writing—original draft, I.K.; Writing—review and editing, I.K., A.P., J.V., S.V. and L.A. All authors have read and agreed to the published version of the manuscript.

Funding: This research was funded by the Estonian Science Foundation Grant, grant number PRG1993, and the "Estonian Roots: Centre of Excellence for Transdisciplinary Studies on Ethnogenesis and cultural diversity", grant number TK215.

Data Availability Statement: The data presented in this study are available on request from the corresponding author.

Acknowledgments: We want to thank those who assisted us during this project. Special thanks to Karin Truuver and the Estonian Museum of Natural History for allowing us to sample mammoth molars from the Puurmani site; Rhea Kõivutalu who conducted some of the analyses for Krüüdneri

and Kukemetsa mammoth molar samples; Holar Sepp from Tartu University for conducting isotopic analysis; Anna Lanka and Varvara Bakumenko for assisting during the fieldwork; Petr Macek from the Institute of Hydrobiology at the Biology Centre of Czech Academy of Sciences for his ideas regarding the interpretation of nitrogen isotopic values.

Conflicts of Interest: The authors declare no conflicts of interest.

References

1. Lõugas, L.; Ukkonen, P.; Jungner, H. Dating the Extinction of European Mammoths: New Evidence from Estonia. *Quat. Sci. Rev.* **2002**, *21*, 1347–1354. [CrossRef]
2. Stuart, A.J. The Extinction of Woolly Mammoth (*Mammuthus primigenius*) and Straight-Tusked Elephant (*Palaeoloxodon antiquus*) in Europe. *Quat. Int.* **2005**, *126–128*, 171–177. [CrossRef]
3. Ukkonen, P.; Aaris-Sørensen, K.; Arppe, L.; Clark, P.U.; Daugnora, L.; Lister, A.M.; Lõugas, L.; Seppä, H.; Sommer, R.S.; Stuart, A.J.; et al. Woolly Mammoth (*Mammuthus primigenius* Blum.) and Its Environment in Northern Europe during the Last Glaciation. *Quat. Sci. Rev.* **2011**, *30*, 693–712. [CrossRef]
4. Guthrie, R.D. Paleoecology of the Large-Mammal Community in Interior Alaska during the Late Pleistocene. *Am. Midl. Nat.* **1968**, *79*, 346. [CrossRef]
5. Kahlke, R.D. The History of the Origin, Evolution and Dispersal of the Late Pleistocene Mammuthus-Coelodonta Faunal Complex in Eurasia (Large Mammals). *Quat. Sci. Rev.* **2014**, *96*, 32–49. [CrossRef]
6. Koch, P.L.; Barnosky, A.D. Late Quaternary Extinctions: State of the Debate. *Annu. Rev. Ecol. Evol. Syst.* **2006**, *37*, 215–250. [CrossRef]
7. Leshchinskiy, S.V. Strong Evidence for Dietary Mineral Imbalance as the Cause of Osteodystrophy in Late Glacial Woolly Mammoths at the Berelyokh Site (Northern Yakutia, Russia). *Quat. Int.* **2017**, *445*, 146–170. [CrossRef]
8. Leshchinskiy, S.V.; Burkanova, E.M. The Volchia Griva Mineral Oasis as Unique Locus for Research of the Mammoth Fauna and the Late Pleistocene Environment in Northern Eurasia. *Quat. Res.* **2022**, *109*, 157–182. [CrossRef]
9. Wojtal, P. The Woolly Mammoth (*Mammuthus primigenius*) Remains from the Upper Palaeolithic Site Kraków Spadzista Street (B). In Proceedings of the First International Congress: The World of Elephants, Rome, Italy, 16–20 October 2001.
10. Wojtal, P.; Haynes, G.; Klimowicz, J.; Sobczyk, K.; Tarasiuk, J.; Wroński, S.; Wilczyński, J. The Earliest Direct Evidence of Mammoth Hunting in Central Europe—The Kraków Spadzista Site (Poland). *Quat. Sci. Rev.* **2019**, *213*, 162–166. [CrossRef]
11. Hughes, P.D.; Gibbard, P.L. A Stratigraphical Basis for the Last Glacial Maximum (LGM). *Quat. Int.* **2015**, *383*, 174–185. [CrossRef]
12. Veski, S.; Amon, L.; Heinsalu, A.; Reitalu, T.; Saarse, L.; Stivrins, N.; Vassiljev, J. Lateglacial Vegetation Dynamics in the Eastern Baltic Region between 14,500 and 11,400calyrBP: A Complete Record since the Bølling (GI-1e) to the Holocene. *Quat. Sci. Rev.* **2012**, *40*, 39–53. [CrossRef]
13. Estonian Environment Agency. Available online: https://www.ilmateenistus.ee/ (accessed on 7 October 2024).
14. World Bank Group Climate Change Knowledge Portal. Available online: https://climateknowledgeportal.worldbank.org/country/latvia/climate-data-historical (accessed on 7 October 2024).
15. Stroeven, A.P.; Hättestrand, C.; Kleman, J.; Heyman, J.; Fabel, D.; Fredin, O.; Goodfellow, B.W.; Harbor, J.M.; Jansen, J.D.; Olsen, L.; et al. Deglaciation of Fennoscandia. *Quat. Sci. Rev.* **2016**, *147*, 91–121. [CrossRef]
16. Hughes, A.L.C.; Gyllencreutz, R.; Lohne, Ø.S.; Mangerud, J.; Svendsen, J.I. The Last Eurasian Ice Sheets—A Chronological Database and Time-slice Reconstruction, DATED-1. *Boreas* **2016**, *45*, 1–45. [CrossRef]
17. Kalm, V.; Raukas, A.; Rattas, M.; Lasberg, K. Chapter 8—Pleistocene Glaciations in Estonia. In *Quaternary Glaciations—Extent and Chronology*; Ehlers, J., Gibbard, P.L., Hughes, P.D., Eds.; Developments in Quaternary Sciences; Elsevier: Amsterdam, The Netherlands, 2011; Volume 15, pp. 95–104.
18. Rõuk, A.-M.; Raukas, A. Drumlins of Estonia. *Sediment. Geol.* **1989**, *62*, 371–384. [CrossRef]
19. Raukas, A.; Teedumäe, A. *Geology and Mineral Resources of Estonia*; Estonian Academy Publishers: Tallinn, Estonia, 1997; ISBN 9985-50-185-3.
20. Molodkov, A.; Bolikhovskaya, N. Palaeoenvironmental Changes and Their Chronology during the Latter Half of MIS 5 on the South-Eastern Coast of the Gulf of Finland. *Quat. Int.* **2022**, *616*, 40–54. [CrossRef]
21. Molodkov, A.; Bolikhovskaya, N.; Miidel, A.; Ploom, K. The Sedimentary Sequence Recovered from the Voka Outcrops, Northeastern Estonia: Implications for Late Pleistocene Stratigraphy. *Est. J. Earth Sci.* **2007**, *56*, 47. [CrossRef]
22. Rasmussen, S.O.; Bigler, M.; Blockley, S.P.; Blunier, T.; Buchardt, S.L.; Clausen, H.B.; Cvijanovic, I.; Dahl-Jensen, D.; Johnsen, S.J.; Fischer, H.; et al. A Stratigraphic Framework for Abrupt Climatic Changes during the Last Glacial Period Based on Three Synchronized Greenland Ice-Core Records: Refining and Extending the INTIMATE Event Stratigraphy. *Quat. Sci. Rev.* **2014**, *106*, 14–28. [CrossRef]

23. Veski, S. Vegetation History, Human Impact and Palaeogeography of West Estonia. Pollen Analytical Studies of Lake and Bog Sediments. *Striae* **1998**, *38*, 119.
24. Laul, S.; Kihno, K. Prehistoric Land Use and Settlement History on the Haanja Heights, Southeastern Estonia, with Special Reference to the Siksali-Hino Area. In *Environmental and Cultural History of the Eastern Baltic Region*; Miller, U., Hackens, T., Lang, V., Raukas, A., Hicks, S., Eds.; Council of Europe: Strasbourg, France, 1999; Volume 57, pp. 239–254.
25. Kimmel, A.; Pirrus, R.; Raukas, A. Holocene Deposits. In *LakePeipsi. Geology*; Sulemees Publishers: Tallinn, Estonia, 1999; pp. 42–43.
26. Poska, A. Three Pollen Diagrams from Coastal Estonia. Licentiat Thesis. *KvartärgeologiskaAvdelningen* **1994**, *170*, 40.
27. Poska, A.; Saarse, L. Holocene Vegetation and Land-Use History in the Environs of Lake Kahala, Northern Estonia. *Veg. Hist. Archaeobot.* **1999**, *8*, 185–197. [CrossRef]
28. Saarse, L.; Rajamäe, R. Holocene Vegetation and Climatic Change on the Haanja Heights, SE Estonia. *Proc. Est. Acad. Sci. Geol.* **1997**, *46*, 75. [CrossRef]
29. Amon, L.; Saarse, L.; Vassiljev, J.; Heinsalu, A.; Veski, S. Timing of the Deglaciation and the Late-Glacial Vegetation Development on the Pandivere Upland, North Estonia. *Bull. Geol. Soc. Finl.* **2016**, *88*, 69–83. [CrossRef]
30. Mäemets, H. Palynological and Radiocarbon Data on the Postglacial Vegetational History of Haanja Elevation (E.S.S.R.). In *Čelovek, Rastitelnost i Pochva*; Kurvits, Ü., Ed.; Estonian Academy of Sciences: Tartu, Estonia, 1983; pp. 98–111.
31. Amon, L.; Veski, S.; Heinsalu, A.; Saarse, L. Timing of Lateglacial Vegetation Dynamics and Respective Palaeoenvironmental Conditions in Southern Estonia: Evidence from the Sediment Record of Lake Nakri. *J. Quat. Sci.* **2012**, *27*, 169–180. [CrossRef]
32. Niinemets, E.; Poska, A.; Saarse, L. Vegetation History and Human Impact in the Parika Area, Central Estonia. *Proc. Est. Acad. Sci. Geol.* **2002**, *51*, 241. [CrossRef]
33. Kihno, K.; Saarse, L.; Amon, L. Late Glacial Vegetation, Sedimentation and Ice Recession Chronology in the Surroundings of Lake Prossa, Central Estonia. *Est. J. Earth Sci.* **2011**, *60*, 147. [CrossRef]
34. Saarse, L.; Veski, S.; Heinsalu, A.; Rajamäe, R.; Martma, T. Litho- and Biostratigraphy of Lake Päidre, South Estonia. *Proc. Est. Acad. Sci. Geol.* **1995**, *44*, 45. [CrossRef]
35. Poska, A.; Saarse, L. Biostratigraphy and 14 C Dating of a Lake Sediment Sequence on the North-West Estonian Carbonaceous Plateau, Interpreted in Terms of Human Impact in the Surroundings. *Veg. Hist. Archaeobot.* **2002**, *11*, 191–200. [CrossRef]
36. Veski, S.; Koppel, K.; Poska, A. Integrated Palaeoecological and Historical Data in the Service of Fine-resolution Land Use and Ecological Change Assessment during the Last 1000 Years in Rõuge, Southern Estonia. *J. Biogeogr.* **2005**, *32*, 1473–1488. [CrossRef]
37. Sarv, A.; Ilves, E. Über Das Alter Der Holozänen Ablagerungen Im Mündungsgebiet Des Flusses Emajogi (Saviku). *Eest. NSV Tead. Akad. Toim. Keem. Geol.* **1975**, *24*, 64. (In Russian) [CrossRef]
38. Amon, L.; Heinsalu, A.; Veski, S. Late Glacial Multiproxy Evidence of Vegetation Development and Environmental Change at Solova, Southeastern Estonia. *Est. J. Earth Sci.* **2010**, *59*, 151. [CrossRef]
39. Kimmel, K.; Rajamäe, R.; Sakson, M. The Holocene Development of Tondi Mire, Northern Estonia: Pollen, Diatom and Chronological Studies. In *Coastal Estonia. Recent Advances in Environmental and Cultural History*; Hickens, T., Hicks, S., Lang, V., Miller, U., Saarse, L., Eds.; Council of Europe: Strasbourg, France, 1996; Volume 51, pp. 85–102.
40. Ilves, E.; Mäemets, H. Results of Radiocarbon and Palynological Analyses of Coastal Depositsof Lakes Tuuljärv and Vaskna. In *Palaeohydrology of the Temperate Zone III. Mires and Lakes*; Raukas, A., Saarse, L., Eds.; Eesti NSV Teaduste Akadeemia: Tallinn, Estonia, 1987; pp. 108–130.
41. Amon, L.; Saarse, L. Postglacial Palaeoenvironmental Changes in the Area Surrounding Lake Udriku in North Estonia. *Geol. Q.* **2010**, *54*, 85–94.
42. Niinemets, E.; Saarse, L. Holocene Forest Dynamics and Human Impact in Southeastern Estonia. *Veg. Hist. Archaeobot.* **2006**, *16*, 1–13. [CrossRef]
43. Kangur, M. Spatio-Temporal Distribution of Pollen in Lake Väike-Juusa (South Estonia) Sediments. *Rev. Palaeobot. Palynol.* **2009**, *153*, 354–359. [CrossRef]
44. Stivrins, N.; Cerina, A.; Gałka, M.; Heinsalu, A.; Lõugas, L.; Veski, S. Large Herbivore Population and Vegetation Dynamics 14,600–8300 years Ago in Central Latvia, Northeastern Europe. *Rev. Palaeobot. Palynol.* **2019**, *266*, 42–51. [CrossRef]
45. Heikkilä, M.; Fontana, S.L.; Seppä, H. Rapid Lateglacial Tree Population Dynamics and Ecosystem Changes in the Eastern Baltic Region. *J. Quat. Sci.* **2009**, *24*, 802–815. [CrossRef]
46. Van Geel, B.; Van Der Plicht, J.; Kasse, C.; Mol, D. Radiocarbon Dates from the Netherlands and Doggerland as a Proxy for Vegetation and Faunal Biomass between 55 and 5 Ka Cal Bp. *J. Quat. Sci.* **2024**, *39*, 248–260. [CrossRef]
47. Arppe, L.; Karhu, J.A. Oxygen Isotope Values of Precipitation and the Thermal Climate in Europe during the Middle to Late Weichselian Ice Age. *Quat. Sci. Rev.* **2010**, *29*, 1263–1275. [CrossRef]
48. Barnes, I.; Shapiro, B.; Lister, A.; Kuznetsova, T.; Sher, A.; Guthrie, D.; Thomas, M.G. Genetic Structure and Extinction of the Woolly Mammoth, Mammuthus Primigenius. *Curr. Biol.* **2007**, *17*, 1072–1075. [CrossRef] [PubMed]

49. Satkūnas, J.; Girininkas, A.; Rimkus, T.; Daugnora, L.; Grigienė, A.; Stančikaitė, M.; Slah, G.; Skuratovič, Ž.; Uogintas, D.; Žulkus, V. New 14C Data of Megafaunal Remains from Lithuania—Implications for the Palaeoenvironmental Interpretation of the Middle Weichselian. *Geol. Q.* **2023**, *1*, 3. [CrossRef]
50. Arppe, L.; Aaris-Sørensen, K.; Daugnora, L.; Lõugas, L.; Wojtal, P.; Zupiņš, I. The Palaeoenvironmental Δ13C Record in European Woolly Mammoth Tooth Enamel. *Quat. Int.* **2011**, *245*, 285–290. [CrossRef]
51. Ayliffe, L.K.; Lister, A.M.; Chivas, A.R. The Preservation of Glacial-Interglacial Climatic Signatures in the Oxygen Isotopes of Elephant Skeletal Phosphate. *Palaeogeogr. Palaeoclimatol. Palaeoecol.* **1992**, *99*, 179–191. [CrossRef]
52. Kohn, M.J.; Cerling, T.E. Stable Isotope Compositions of Biological Apatite. *Rev. Miner. Geochem.* **2002**, *48*, 455–488. [CrossRef]
53. van der Plicht, J.; Palstra, S.W.L. Radiocarbon and Mammoth Bones: What's in a Date. *Quat. Int.* **2016**, *406*, 246–251. [CrossRef]
54. Vassiljev, J.; Saarse, L. Timing of the Baltic Ice Lake in the Eastern Baltic. *Bull. Geol. Soc. Finl.* **2013**, *85*, 9–18. [CrossRef]
55. Estonian Land Board, G.S. of E. *Geological Base Map*; 2024. Available online: https://geoportaal.maaamet.ee/eng/ (accessed on 15 September 2024).
56. Heiri, O.; Lotter, A.F.; Lemcke, G. Loss on Ignition as a Method for Estimating Organic and Carbonate Content in Sediments: Reproducibility and Comparability of Results. *J. Paleolimnol.* **2001**, *25*, 101–110. [CrossRef]
57. Bronk Ramsey, C. Deposition Models for Chronological Records. *Quat. Sci. Rev.* **2008**, *27*, 42–60. [CrossRef]
58. Bronk Ramsey, C. Bayesian Analysis of Radiocarbon Dates. *Radiocarbon* **2009**, *51*, 337–360. [CrossRef]
59. Reimer, P.J.; Austin, W.E.N.; Bard, E.; Bayliss, A.; Blackwell, P.G.; Bronk Ramsey, C.; Butzin, M.; Cheng, H.; Edwards, R.L.; Friedrich, M.; et al. The IntCal20 Northern Hemisphere Radiocarbon Age Calibration Curve (0–55 Cal KBP). *Radiocarbon* **2020**, *62*, 725–757. [CrossRef]
60. Stockmarr, J. Tables with Spores Used in Absolute Pollen Analysis. *Pollen Spores* **1971**, *13*, 615–621.
61. Berglund, B.E.; Ralska-Jasiveczowa, M. *Pollen Analysis and Pollen Diagrams. Handbook of Holocene Palaeoecology and Palaeohydrology*; Interscience: New York, NY, USA, 1986; pp. 455–484.
62. Fægri, K.; Iversen, J. *Textbook of Pollen Analysis*, 4th ed.; John Wiley & Sons: Chichester, UK, 1989.
63. Bennett, K.D.; Willis, K.J. Pollen. In *Tracking Environmental Change Using Lake Sediments*; Springer: Berlin/Heidelberg, Germany, 2002; pp. 5–32. [CrossRef]
64. Beug, H.J. *Leitfaden Der Pollenbestimmung Fur Mitteleuropa Und Angrenzende Gebiete*; Publisher Verlag Friedrich Pfeil: Munich, Germany, 2004.
65. Reille, M. *Pollen et Spores d'Europe et d'Afrique Du Nord*; Laboratoire de Botanique Historique et Palynologique, CNRS: Marseille, France, 1992.
66. Chambers, F.M.; Beilman, D.W.; Yu, Z. Methods for Determining Peat Humification and for Quantifying Peat Bulk Density, Organic Matter and Carbon Content for Palaeostudies of Climate and Peatland Carbon Dynamics. *Mires Peat* **2011**, *7*, 7.
67. Birks, H.H. Plant Macrofossils. In *Tracking Environmental Change Using Lake Sediments*; Last, W.M., Smol, J.P., Birks, H.J.B., Eds.; Kluwer: Dordrecht, The Netherlands, 2002; Volume 3, pp. 49–74.
68. Katz, N.J.; Katz, S.V.; Skobeyeva, E.I. *Atlas Rastitelnyh Ostatkov v Torfah (Atlas of Plant Remains in Peat)*; Nedra: Moscow, Russia, 1977.
69. Cappers, R.T.J.; Neef, R.; Bekker, R.M. *Digital Atlas of Economic Plants*; Barkhuis: Groningen, The Netherlands, 2009; Volume 1.
70. Grimm, E.C. Tilia and Tiliagraph. Illinois State Museum. Springfield. 1991, p. 484. Available online: https://www.neotomadb.org/apps/tilia (accessed on 14 June 2024).
71. Sugita, S. Theory of Quantitative Reconstruction of Vegetation II: All You Need Is LOVE. *Holocene* **2007**, *17*, 243–257. [CrossRef]
72. Theuerkauf, M.; Couwenberg, J.; Kuparinen, A.; Liebscher, V. A Matter of Dispersal: REVEALSinR Introduces State-of-the-Art Dispersal Models to Quantitative Vegetation Reconstruction. *Veg. Hist. Archaeobot.* **2016**, *25*, 541–553. [CrossRef]
73. Githumbi, E.; Fyfe, R.; Gaillard, M.-J.; Trondman, A.-K.; Mazier, F.; Nielsen, A.-B.; Poska, A.; Sugita, S.; Woodbridge, J.; Azuara, J.; et al. European Pollen-Based REVEALS Land-Cover Reconstructions for the Holocene: Methodology, Mapping and Potentials. *Earth Syst. Sci. Data* **2022**, *14*, 1581–1619. [CrossRef]
74. Mazier, F.; Gaillard, M.-J.; Kuneš, P.; Sugita, S.; Trondman, A.-K.; Broström, A. Testing the Effect of Site Selection and Parameter Setting on REVEALS-Model Estimates of Plant Abundance Using the Czech Quaternary Palynological Database. *Rev. Palaeobot. Palynol.* **2012**, *187*, 38–49. [CrossRef]
75. Wieczorek, M.; Herzschuh, U. Compilation of Relative Pollen Productivity (RPP) Estimates and Taxonomically Harmonised RPP Datasets for Single Continents and Northern Hemisphere Extratropics. *Earth Syst. Sci. Data* **2020**, *12*, 3515–3528. [CrossRef]
76. Hjelle, K.L. Herb Pollen Representation in Surface Moss Samples from Mown Meadows and Pastures in Western Norway. *Veg. Hist. Archaeobot.* **1998**, *7*, 79–96. [CrossRef]
77. Räsänen, S.; Suutari, H.; Nielsen, A.B. A Step Further towards Quantitative Reconstruction of Past Vegetation in Fennoscandian Boreal Forests: Pollen Productivity Estimates for Six Dominant Taxa. *Rev. Palaeobot. Palynol.* **2007**, *146*, 208–220. [CrossRef]
78. von Stedingk, H.; Fyfe, R.M. The Use of Pollen Analysis to Reveal Holocene Treeline Dynamics: A Modelling Approach. *Holocene* **2009**, *19*, 273–283. [CrossRef]

79. Bunting, M.J.; Armitage, R.; Binney, H.A.; Waller, M. Estimates of 'Relative Pollen Productivity' and 'Relevant Source Area of Pollen' for Major Tree Taxa in Two Norfolk (UK) Woodlands. *Holocene* **2005**, *15*, 459–465. [CrossRef]
80. Hopla, E.J. A New Perspective on Quaternary Land Cover in Central Alaska. Ph.D. Thesis, University of Southampton, Southampton, UK, 2017.
81. QGIS Geographic Information System 2024. Available online: https://www.qgis.org/ (accessed on 14 June 2024).
82. Bunting, M.J.; Farrell, M.; Broström, A.; Hjelle, K.L.; Mazier, F.; Middleton, R.; Nielsen, A.B.; Rushton, E.; Shaw, H.; Twiddle, C.L. Palynological Perspectives on Vegetation Survey: A Critical Step for Model-Based Reconstruction of Quaternary Land Cover. *Quat. Sci. Rev.* **2013**, *82*, 41–55. [CrossRef]
83. Cersoy, S.; Zazzo, A.; Lebon, M.; Rofes, J.; Zirah, S. Collagen Extraction and Stable Isotope Analysis of Small Vertebrate Bones: A Comparative Approach. *Radiocarbon* **2017**, *59*, 679–694. [CrossRef]
84. Rosentau, A.; Vassiljev, J.; Hang, T.; Saarse, L.; Kalm, V. Development of the Baltic Ice Lake in the Eastern Baltic. *Quat. Int.* **2009**, *206*, 16–23. [CrossRef]
85. Ambrose, S.H. Preparation and Characterization of Bone and Tooth Collagen for Isotopic Analysis. *J. Archaeol. Sci.* **1990**, *17*, 431–451. [CrossRef]
86. Ambrose, S.H. Isotopic Analysis of Paleodiet: Methodological and Interpretive Considerations, Investigation of Ancient Human Tissue: Chemical Analyses in Anthropology. *Gordon Breach* **1993**, *10*, 59–130.
87. Guiry, E.J.; Szpak, P. Improved Quality Control Criteria for Stable Carbon and Nitrogen Isotope Measurements of Ancient Bone Collagen. *J. Archaeol. Sci.* **2021**, *132*, 105416. [CrossRef]
88. Kelly, E.F.; Yonker, C.M. Factors of Soil Formation | Time. In *Encyclopedia of Soils in the Environment*; Elsevier: Amsterdam, The Netherlands, 2005; pp. 536–539.
89. Stone, E.J.; Lunt, D.J. The Role of Vegetation Feedbacks on Greenland Glaciation. *Clim. Dyn.* **2013**, *40*, 2671–2686. [CrossRef]
90. Amon, L.; Veski, S.; Vassiljev, J. Tree Taxa Immigration to the Eastern Baltic Region, Southeastern Sector of Scandinavian Glaciation during the Late-Glacial Period (14,500-11,700 Cal. b.p.). *Veg. Hist. Archaeobot.* **2014**, *23*, 207–216. [CrossRef]
91. Sun, Y.; Xu, Q.; Gaillard, M.-J.; Zhang, S.; Li, D.; Li, M.; Li, Y.; Li, X.; Xiao, J. Pollen-Based Reconstruction of Total Land-Cover Change over the Holocene in the Temperate Steppe Region of China: An Attempt to Quantify the Cover of Vegetation and Bare Ground in the Past Using a Novel Approach. *Catena* **2022**, *214*, 106307. [CrossRef]
92. Hjelmroos, M. Evidence of Long-Distance Transport of Betula Pollen. *Grana* **1991**, *30*, 215–228. [CrossRef]
93. Szczepanek, K.; Myszkowska, D.; Worobiec, E.; Piotrowicz, K.; Ziemianin, M.; Bielec-Bąkowska, Z. The Long-Range Transport of Pinaceae Pollen: An Example in Kraków (Southern Poland). *Aerobiologia* **2017**, *33*, 109–125. [CrossRef] [PubMed]
94. Amon, L.; Wagner-Cremer, F.; Vassiljev, J.; Veski, S. Spring Onset and Seasonality Patterns during the Late Glacial Period in the Eastern Baltic Region. *Clim. Past.* **2022**, *18*, 2143–2153. [CrossRef]
95. Feurdean, A.; Perşoiu, A.; Tanţău, I.; Stevens, T.; Magyari, E.K.; Onac, B.P.; Marković, S.; Andrič, M.; Connor, S.; Fărcaş, S.; et al. Climate Variability and Associated Vegetation Response throughout Central and Eastern Europe (CEE) between 60 and 8 Ka. *Quat. Sci. Rev.* **2014**, *106*, 206–224. [CrossRef]
96. Veski, S.; Seppä, H.; Stančikaite, M.; Zernitskaya, V.; Reitalu, T.; Gryguc, G.; Heinsalu, A.; Stivrins, N.; Amon, L.; Vassiljev, J.; et al. Quantitative Summer and Winter Temperature Reconstructions from Pollen and Chironomid Data between 15 and 8 Ka BP in the Baltic–Belarus Area. *Quat. Int.* **2015**, *388*, 4–11. [CrossRef]
97. Alley, R.B.; Meese, D.A.; Shuman, C.A.; Gow, A.J.; Taylor, K.C.; Grootes, P.M.; White, J.W.C.; Ram, M.; Waddington, E.D.; Mayewski, P.A.; et al. Abrupt Increase in Greenland Snow Accumulation at the End of the Younger Dryas Event. *Nature* **1993**, *362*, 527–529. [CrossRef]
98. Birks, H.J.B.; Birks, H.H. Biological Responses to Rapid Climate Change at the Younger Dryas—Holocene Transition at Kråkenes, Western Norway. *Holocene* **2008**, *18*, 19–30. [CrossRef]
99. Guthrie, R.D. Origin and Causes of the Mammoth Steppe: A Story of Cloud Cover, Woolly Mammal Tooth Pits, Buckles, and inside-out Beringia. *Quat. Sci. Rev.* **2001**, *20*, 549–574. [CrossRef]
100. Laumets, L.; Kalm, V.; Poska, A.; Kele, S.; Lasberg, K.; Amon, L. Palaeoclimate Inferred from Δ18O and Palaeobotanical Indicators in Freshwater Tufa of Lake Äntu Sinijärv, Estonia. *J. Paleolimnol.* **2014**, *51*, 99–111. [CrossRef]
101. Willerslev, E.; Davison, J.; Moora, M.; Zobel, M.; Coissac, E.; Edwards, M.E.; Lorenzen, E.D.; Vestergård, M.; Gussarova, G.; Haile, J.; et al. Fifty Thousand Years of Arctic Vegetation and Megafaunal Diet. *Nature* **2014**, *506*, 47–51. [CrossRef]
102. van Geel, B.; Fisher, D.C.; Rountrey, A.N.; van Arkel, J.; Duivenvoorden, J.F.; Nieman, A.M.; van Reenen, G.B.A.; Tikhonov, A.N.; Buigues, B.; Gravendeel, B. Palaeo-Environmental and Dietary Analysis of Intestinal Contents of a Mammoth Calf (Yamal Peninsula, Northwest Siberia). *Quat. Sci. Rev.* **2011**, *30*, 3935–3946. [CrossRef]
103. Iacumin, P.; Nikolaev, V.; Ramigni, M. C and N Stable Isotope Measurements on Eurasian Fossil Mammals, 40 000 to 10 000 Years BP: Herbivore Physiologies and Palaeoenvironmental Reconstruction. *Palaeogeogr. Palaeoclimatol. Palaeoecol.* **2000**, *163*, 33–47. [CrossRef]

104. Bocherens, H.; Drucker, D.G.; Bonjean, D.; Bridault, A.; Conard, N.J.; Cupillard, C.; Germonpré, M.; Höneisen, M.; Münzel, S.C.; Napierala, H.; et al. Isotopic Evidence for Dietary Ecology of Cave Lion (*Panthera spelaea*) in North-Western Europe: Prey Choice, Competition and Implications for Extinction. *Quat. Int.* **2011**, *245*, 249–261. [CrossRef]
105. Zimov, S.A. Pleistocene Park: Return of the Mammoth's Ecosystem. *Science* **2005**, *308*, 796–798. [CrossRef]
106. Zagorska, I. New Testimony about Reindeer Hunters in Latvia (Jauna Liecība Par Ziemeļbriežu Medniekiem Latvijā). *Latv. Vēstures Institūta Žurnāla* **2010**, *77*, 105–112.
107. Jaanits, L.; Jaanits, K. Frühmesolithische Siedlung in Pulli. *Eest. NSV Tead. Akad. Toim. Ühiskonnateadused* **1975**, *24*, 64–70. [CrossRef]
108. Lõugas, L. *Post-Glacial Development Ofvertebrate Fauna in Estonian Water Bodies*; A Palaeozoological Study; Dissertationes Biologicae Universitatis: Tartu, Estonia, 1997.
109. Poska, A.; Veski, S. Man and Environment at 9500 Bp. A Palynological Study of an Early-Mesolithic Settlement Site in South-West Estonia. *Acta Palaeobot.* **1999**, *S2*, 603–607.
110. Wooller, M.J.; Zazula, G.D.; Edwards, M.; Froese, D.G.; Boone, R.D.; Parker, C.; Bennett, B. Stable Carbon Isotope Compositions of Eastern Beringian Grasses and Sedges: Investigating Their Potential as Paleoenvironmental Indicators. *Arct. Antarct. Alp. Res.* **2007**, *39*, 318–331. [CrossRef]
111. Kilgallon, C.; Flach, E.; Boardman, W.; Routh, A.; Strike, T.; Jackson, B. Analysis of Biochemical Markers of Bone Metabolism in Asian Elephants (*Elephas maximus*). *J. Zoo Wildl. Med.* **2008**, *39*, 527–536. [CrossRef] [PubMed]
112. van der Merwe, N.J.; Thorp, J.A.L.; Bell, R.H.V. Carbon Isotopes as Indicators of Elephant Diets and African Environments. *Afr. J. Ecol.* **1988**, *26*, 163–172. [CrossRef]
113. Bocherens, H. Isotopic Tracking of Large Carnivore Palaeoecology in the Mammoth Steppe. *Quat. Sci. Rev.* **2015**, *117*, 42–71. [CrossRef]
114. van der Merwe, N.J. Carbon Isotopes, Photosynthesis, and Archaeology: Different Pathways of Photosynthesis Cause Characteristic Changes in Carbon Isotope Ratios That Make Possible the Study of Prehistoric Human Diets. *Am. Sci.* **1982**, *70*, 596–606.
115. Ambrose, S.H.; DeNiro, M.J. The Isotopic Ecology of East African Mammals. *Oecologia* **1986**, *69*, 395–406. [CrossRef]
116. van der Merwe, N.J.; Medina, E. The Canopy Effect, Carbon Isotope Ratios and Foodwebs in Amazonia. *J. Archaeol. Sci.* **1991**, *18*, 249–259. [CrossRef]
117. Amundson, R.; Austin, A.T.; Schuur, E.A.G.; Yoo, K.; Matzek, V.; Kendall, C.; Uebersax, A.; Brenner, D.; Baisden, W.T. Global Patterns of the Isotopic Composition of Soil and Plant Nitrogen. *Glob. Biogeochem. Cycles* **2003**, *17*, 31. [CrossRef]
118. Zimov, S.A.; Zimov, N.S.; Tikhonov, A.N.; Chapin, F.S. Mammoth Steppe: A High-Productivity Phenomenon. *Quat. Sci. Rev.* **2012**, *57*, 26–45. [CrossRef]
119. Owen-Smith, N. Pleistocene Extinctions: The Pivotal Role of Megaherbivores. *Paleobiology* **1987**, *13*, 351–362. [CrossRef]
120. Austrheim, G.; Eriksson, O. Recruitment and Life-History Traits of Sparse Plant Species in Subalpine Grasslands. *Can. J. Bot.* **2003**, *81*, 171–182. [CrossRef]
121. Güsewell, S. N:P Ratios in Terrestrial Plants: Variation and Functional Significance. *New Phytol.* **2004**, *164*, 243–266. [CrossRef]
122. Cornelissen, J.H.C.; Quested, H.M.; Gwynn-Jones, D.; Van Logtestijn, R.S.P.; De Beus, M.A.H.; Kondratchuk, A.; Callaghan, T.V.; Aerts, R. Leaf Digestibility and Litter Decomposability Are Related in a Wide Range of Subarctic Plant Species and Types. *Funct. Ecol.* **2004**, *18*, 779–786. [CrossRef]
123. Michelsen, A.; Quarmby, C.; Sleep, D.; Jonasson, S. Vascular Plant 15 N Natural Abundance in Heath and Forest Tundra Ecosystems Is Closely Correlated with Presence and Type of Mycorrhizal Fungi in Roots. *Oecologia* **1998**, *115*, 406–418. [CrossRef] [PubMed]
124. Drucker, D.G.; Stevens, R.E.; Germonpré, M.; Sablin, M.V.; Péan, S.; Bocherens, H. Collagen Stable Isotopes Provide Insights into the End of the Mammoth Steppe in the Central East European Plains during the Epigravettian. *Quat. Res.* **2018**, *90*, 457–469. [CrossRef]

Disclaimer/Publisher's Note: The statements, opinions and data contained in all publications are solely those of the individual author(s) and contributor(s) and not of MDPI and/or the editor(s). MDPI and/or the editor(s) disclaim responsibility for any injury to people or property resulting from any ideas, methods, instructions or products referred to in the content.

Appendix 3 (Paper III)

Krivokorin, I., Amon, L., Leshchinskiy, S. V., & Arppe, L. (Manuscript). Mammoths at the margins: new $\delta^{13}C$ and $\delta^{15}N$ isotope data from the southeast of the Western Siberian plain. Manuscript under review in: Quaternary Science Reviews

Quaternary Science Reviews 369 (2025) 109645

Contents lists available at ScienceDirect

Quaternary Science Reviews

journal homepage: www.elsevier.com/locate/quascirev

Mammoths at the margins: new $\delta^{13}C$ and $\delta^{15}N$ isotope data from the southeast of the Western Siberian plain

Ivan Krivokorin [a,*], Leeli Amon [a], Sergey V. Leshchinskiy [b,d], Laura Arppe [c]

[a] Tallinn University of Technology, Department of Geology, Ehitajate tee 5, 12616, Tallinn, **Estonia**
[b] Laboratory of Mesozoic and Cenozoic Continental Ecosystems, Tomsk State University, Lenin Ave. 36, Tomsk, 634050, **Russia**
[c] Finnish Museum of Natural History LUOMUS, P.O. Box 64, 00014, University of Helsinki, Helsinki, **Finland**
[d] Museum of Nature and Man, Mira st. 11, Khanty-Mansiysk, 628011, **Russia**

ARTICLE INFO

Handling Editor: Dr Mira Matthews

Keywords:
LGM
Paleoecology
Palaeogeography
Carbon
Nitrogen

ABSTRACT

This study investigates the carbon and nitrogen isotopic composition of woolly mammoth (Mammuthus primigenius) remains from three Late Pleistocene paleontological sites in the southeast of the Western Siberian Plain (SEWS): Shestakovo, Krasnoyarskaya Kurya, and Volchia Griva. This region and time interval (28–22 ka cal BP) remain underrepresented in isotopic records, particularly for $\delta^{13}C$ and $\delta^{15}N$ values. We analysed 29 mammoth dentine samples, alongside dentine from one horse and one deer. Preservation quality was rigorously evaluated using established criteria, including C:N atomic ratios, collagen yields, and elemental carbon and nitrogen content. Our results reveal the densest concentration of the highest mammoth $\delta^{15}N$ values reported for the Northern Hemisphere. We attribute this isotopic enrichment to the unique local environmental conditions at Volchia Griva, including saline soils and intensive trampling, which may have altered nitrogen cycling at the site.

1. Introduction

Stable carbon isotope analysis provides valuable insights into an animal's diet, local vegetation, and climate by reflecting the isotopic values of consumed plants and indicating the proportion of C_3 and C_4 forage in the diet (Arppe et al., 2011; Fox-Dobbs et al., 2008; France et al., 2007; Kuitems et al., 2015; Szpak et al., 2010). The isotopic analysis of nitrogen in collagen is instrumental in understanding trophic relationships and nutritional stress. Bone collagen nitrogen $\delta^{15}N$ values directly correlate with the $\delta^{15}N$ value of dietary protein (Deniro and Epstein, 1981; Schoeninger and DeNiro, 1984). The relationship between the $\delta^{15}N$ values of animals, tissues, and biochemical components, and the $\delta^{15}N$ value of their diet suggests that animal nitrogen isotopic compositions can provide insights into an animal's dietary preferences, particularly when potential food sources exhibit varying $\delta^{15}N$ values (Deniro and Epstein, 1981). In addition, the changes in stable carbon and nitrogen isotopes of plants can reflect the local soil characteristics (e.g. Aslam et al., 1984; van Groenigen and van Kessel, 2002), which in turn can influence the $\delta^{15}N$ values of plants and therefore affect herbivores' $\delta^{15}N$ values.

Woolly mammoth (*Mammuthus primigenius*) was a prominent species of the "mammoth steppe" ecosystem, which spanned the northern continents from Europe to North America (Guthrie, 1968; Stuart, 2005) ca. 110,000–12,000 years ago (Koch and Barnosky, 2006). The mammoth steppe resulted from the adaptation of Arctic tundra and central Asian steppe species to increased aridity, colder temperatures, and climatic fluctuations (Kahlke, 2014). This cold and drought-resistant mosaic landcover dominated the nonglaciated parts of the Northern Hemisphere, supporting diverse megafauna (Hibbert, 1982; Schweger, 1982).

The Last Glacial Maximum (LGM) ca 27 to 23 ka cal BP (Hughes and Gibbard, 2015), was the most recent period when continental ice sheets were at their maximum of extension (Drucker, 2022). LGM is considered a pivotal era in the history of mammoth megafauna because it is a key landmark for the many mammoth steppe species, as during this period, Eurasia and North America experienced a large, accelerated loss of megafauna (Cooper et al., 2015; Stuart, 2015). During 34–24 ka cal BP, environmental conditions in the North Siberian parts of the mammoth steppe were characterised by cooler summers compared to earlier periods, although temperatures were high enough to support the steppe species; this interval has been described as a relatively "cool" tundra-steppe phase (Sher et al., 2005). Overall, LGM in Northern Siberia was characterised by arid conditions (Schirrmeister et al., 2002). The existence of the mammoth steppe was maintained by a strongly

* Corresponding author. Tallinn University of Technology, Department of Geology, Ehitajate tee 5, 12616 Tallinn, **Estonia**.
E-mail address: ivakri@taltech.ee (I. Krivokorin).

https://doi.org/10.1016/j.quascirev.2025.109645
Received 4 June 2025; Received in revised form 8 September 2025; Accepted 30 September 2025
Available online 14 October 2025
0277-3791/© 2025 Elsevier Ltd. All rights are reserved, including those for text and data mining, AI training, and similar technologies.

continental climate, with summers that were either comparably warm or only slightly cooler than present, and winters significantly colder (Sher et al., 2005). Despite the harshness of this period, mammoth fauna survived in the Arctic (Sher et al., 2005).

Insight into the mammoth food sources has been gained from the isotopic compositions of megafaunal skeletal remains (e.g. Ayliffe et al., 1992; Kohn and Cerling, 2002). However, the majority of published carbon and nitrogen isotopic data on woolly mammoths have focused predominantly on the northernmost parts of the mammoth steppe, particularly Beringia, which is currently one of the best-documented areas regarding mammoth stable isotope data (Fig. 1). Szpak et al. (2010) conducted a comprehensive carbon and nitrogen isotope study of 58 mammoth bone samples from Eastern Beringia (Alaska and Yukon) and Western Beringia (Siberia), with only five samples from the LGM. They showed that before the LGM, high-latitude Siberia and the Russian Far East were colder and more arid than ecologically more diverse central Alaska and Yukon. However, during the LGM itself, Alaska and Yukon became colder and more arid than western Beringia. Arppe et al. (2019) examined $\delta^{13}C$, $\delta^{15}N$, and $\delta^{34}S$ isotopic compositions of 77 mammoth specimens from the last mammoth refugium (Zimov et al., 2012) at Wrangel Island, and Northern Siberia. Out of 77 samples, approximately 12 % are dated to the LGM. They showed that high-latitude Siberian mammoth populations existed in relatively stable environmental conditions until their extinction, suggesting that events too short-lived to have been recorded in bulk-sampled skeletal remains, e.g. a starvation event or changes in water quality, may have played a role in the eventual demise of the species. Iacumin et al. (2000) reported carbon and nitrogen isotope values of mammoth and other herbivore teeth and bones of various ages from the European plain, south-central Siberia, the Taymyr peninsula, and Yakutia, showing that mammoths in Yakutia likely experienced more significant nutritional limitations and incorporated more woody vegetation into their diet than the European Plain populations. The only comprehensive study from the southeastern Western Siberian Plain is a study by Leshchinskiy and Burkanova (2022), who reported the first $\delta^{13}C$ and $\delta^{15}N$ values from 10 post-LGM mammoth bones and several fox, wolf, bison and horse bones at Volchia Griva. In addition to isotopic records, they also provided pollen records for the site. Environmental reconstructions at Volchia Griva showed a transition from wetter conditions to open forb-grass steppes around 20-14 ka BP.

The lack of carbon and nitrogen isotope data from the LGM in the southeast of the Western Siberian plain presents a significant gap in our understanding of Late Pleistocene ecological and environmental conditions. To fill this gap, this study aims to provide new carbon and nitrogen isotope records from mammoth remains of three sites in the southeast of the Western Siberian Plain: Shestakovo, Krasnoyarskaya Kurya and Volchia Griva (Fig. 1). Each site has yielded large quantities of mammoth remains: at Shestakovo, more than 4500 skeletal remains from at least 18 individuals have been excavated (Derevianko et al., 2000, 2003). Krasnoyarskaya Kurya site has similarly produced approximately 5600 remains representing at least 35 mammoths (Lazarev and Leshchinskiy, 2011; Leshchinskiy et al., 2014; Seuru et al., 2017). Volchia Griva, discovered in the 1950s, has so far yielded over 7000 remains from at least 80 mammoths (Leshchinskiy et al., 2023; Leshchinskiy and Burkanova, 2022). Shestakovo and Volchia Griva were particularly attractive for large herbivores because both of these sites had salt licks („beast solonetz“) (Derevianko et al., 2000, 2003), where animals suffering from a chronic deficiency of calcium and other essential elements would eat rocks and soil to compensate for the mineral deficiency (Leshchinskiy, 2015, 2017). The large fossil assemblages at these sites are comparable to other Late Glacial mammoth sites in Siberia, such as Lugovskoye and Berelyokh, where approximately 5500 and 7200 woolly mammoth remains have been found, respectively (Leshchinskiy, 2006, 2017). In Europe, similarly large collections of mammoth fossils have been found at Kraków Spadzista Street in Poland, and Milovice I and Předmostí in the Czech Republic, respectively (Brugère and Fontana, 2009; Krzemińska and Wędzicha, 2015; Leshchinskiy, 2012; Wojtal, 2004; Wojtal and Sobczyk, 2005). According to radiocarbon-AMS dates of the subfossil-bearing layers, the mammoth materials date to the LGM: 28-27 ka cal BP for Shestakovo, ca. 25-23 ka cal BP for Krasnoyarskaya Kurya, and ca. 24-22 ka cal BP for Volchia Griva (Boiko et al., 2005; Derevianko et al., 2000; Kuzmin et al., 2023;

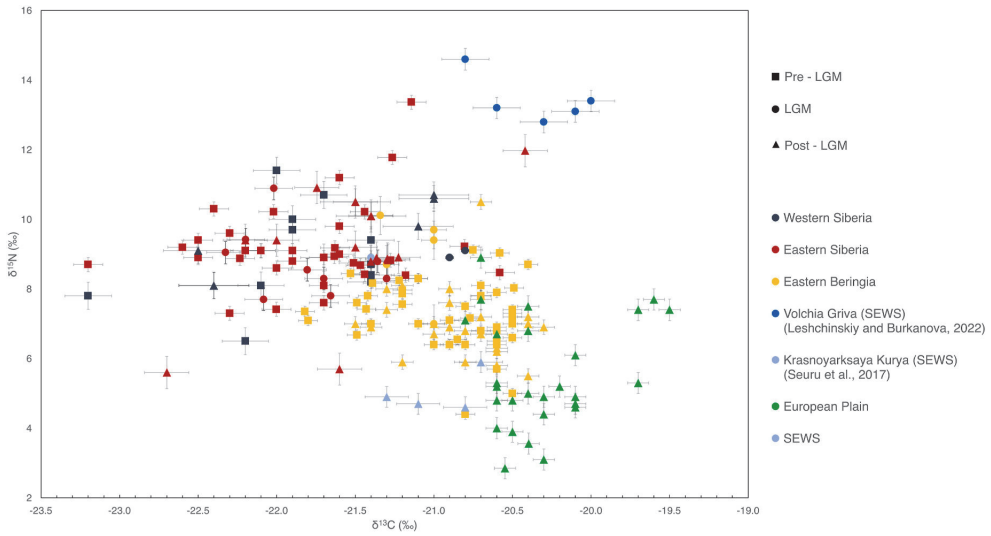

Fig. 1. Comparison between the published $\delta^{13}C$ values and $\delta^{15}N$ values of mammoths from Western Siberia, Eastern Siberia, Eastern Beringia, SEWS and European Plain for three time periods: pre-LGM (before 27 ka cal BP), LGM (27–23 ka cal BP), and post-LGM (after 23 ka cal BP until 11. 7 ka cal BP. The comparative datasets and radiocarbon dates were taken from the following publications: Szpak et al., (2010), Iacumin et al., (2000), Arppe et al. (2019), Iacumin et al., (2010), Barbieri et al., (2008), Debruyne et al., (2008), Grigoriev et al., (2017), Mann et al., (2013), Bocherens et al., (1994), Metcalfe et al. (2016), Seuru et al., (2017), Drucker et al., (2018), Drucker et al., (2014), Orlova et al., (2004).

Maschenko, 2010; Seuru et al., 2017).

In this paper, we report on the carbon and nitrogen isotope analyses of 29 megaherbivore tooth specimens, mainly representing the woolly mammoth from Shestakovo, Krasnoyarskaya Kurya and Volchia Griva l to provide unique insight into the ecology of the mammoth fauna in an underrepresented sector of the mammoth steppe, the southeast of Western Siberian Plain, significantly contributing to the limited paleoecological records in this region during the LGM. Additionally, we discuss the preservation status of the remains, and its implications for further studies of the mammoth fauna skeletal materials discovered at these sites.

2. Materials & methods

2.1. Material collection

The samples listed in Table 1 were selected from the collection of Tomsk State University. Altogether, 29 specimens belonging to woolly mammoth (*Mammuthus primigenius*, n = 27), with one horse and one deer molar were sampled using a Dremel 300 drill. The samples included: four samples from Shestakovo, eight samples from Krasnoyraskaya Kurya and 17 samples from Volchia Griva (Supplementary data, T1). Based on a visual and tactile inspection of the specimens, as well as the hardness or softness of the material, we assigned the samples to one of three categories (very good, good, or acceptable condition) (Table 1). The samples represent the full spectrum of different condition categories that reflect the typical condition of finds in these sites. Samples were photographed and placed in zip packages. Photos of the samples and their field numbers are given in the Supplementary data. For this study, we analysed one horse molar dentine sample, one deer molar dentine sample, 20 mammoth molar dentine samples and 7 mammoth molar dentine samples.

2.2. Evaluation of preservation

We used the elemental C:N ratio of the extracted collagen as the main preservation assessment criteria, with additional consideration of collagen yields and the total carbon and nitrogen content (weight-% C, weight-% N). In general C:N ratios falling within the range of 2.9–3.6 were considered indicative of well-preserved collagen (Ambrose, 1990; DeNiro, 1985; DeNiro and Weiner, 1988; Sealy et al., 2014; van Klinken, 1999). We considered a stricter C:N range of 3.1–3.3 suggested by Guiry and Szpak (2021). We used the following criteria regarding the elemental contents: C > 13 % and N > 4.8 % (Ambrose, 1990). Generally, if a sample did not meet the target set for one or more of the above criteria, we removed it from the main dataset. However, each sample was considered separately, and preservation was assessed on a case-by-case basis. Collagen yields have been calculated as the weight of extracted collagen divided by the weight of the sample and multiplied by 100 and presented as % (Table 1). Usually, well-preserved bone and dentine have collagen yields of ~20 % (van Klinken, 1999), and generally, contents larger than 0.5–2 % are considered indicative of well-enough preserved collagen for ancient bones and teeth (Ambrose, 1990; DeNiro and Weiner, 1988; Dobberstein et al., 2009; van Klinken, 1999). We did not use collagen yields as definitive criteria for rejection because collagen loss may not necessarily change the sample's isotopic composition. Consequently, the resulting C:N ratios and elemental concentrations can still meet the acceptable criteria (e.g., Dobberstein et al., 2009). Therefore, we accepted samples with collagen yields lower than 0.5 % if their C:N values, C% and N % were within the accepted range and absolute delta values were similar to the rest of the group (e.g. SH 53, SH 56, VG 32, VG 33) (Table 1). Nevertheless, we observed collagen yields in our sample set attentively and, in some cases, removed samples from the main dataset based on low collagen yields. We did not use visual preservation as a criterion for sample rejection because visually unappealing samples may still yield reliable isotopic results.

2.3. Carbon and nitrogen isotopic analysis

For isotopic analyses of carbon ($\delta^{13}C$) and nitrogen ($\delta^{15}N$) in collagen a piece of material weighing 0.5 g was cut off. Collagen extraction for carbon and nitrogen isotope analysis was conducted using the method described in Cersoy et al. (2017) (Protocol F): coarse bone powder (0.3–0.7 mm) was first treated with 1M HCl for 20 min, while being stirred continuously. The resulting solution was filtered through MF-Millipore™ membranes (mixed cellulose ester, 5.0-μm pore size,

Table 1
Carbon and nitrogen isotope values, C and N weight-% concentrations, atomic C:N ratios and collagen yields of the accepted samples. M in the table stands for Mammoth, H for Horse, SH for Shestakovo, KK for Krasnoyrskaya Kurya, VG for Volchia Griva. Bold and italics mark the values that are lower than the recommended range. Asterisk marks abnormally high yield values considered to result from weighing errors.

Sample ID	Visual inspection	Skeletal element type	$\delta^{15}N$ (‰, AIR) ± SD	$\delta^{13}C$ (‰, V-PDB)	N%	C%	C:N	Collagen yield %
SH 53	Acceptable	H molar	+3.0 ± 0.02	−20.3	10.4	32.0	3.6	***0.4***
SH 55	Good	M molar	+6.1 ± 0.04	−21.0 ± 0.01	12.5	37.0	3.4	0.6
SH 56	Good	M molar	+8.8 ± 0.09	−20.5 ± 0.06	13.0	37.7	3.4	***0.4***
		Min (mammoths)	*+6.1*	*−21.0*				
		Max (mammoths)	*+8.8*	*−20.5*				
		Average (mammoths)	*+7.5*	*−20.7*				
KK 57	Good	M molar	+8.3 ± 0.01	−20.1 ± 0.11	10.7	32.8	3.6	0.6
KK 58	Good	M molar	+7.8 ± 0.02	−21.4 ± 0.12	10.9	32.5	3.5	0.7
KK 59	Good	M molar	+8.6 ± 0.17	−21.5 ± 0.06	12.5	36.5	3.4	0.7
KK 61	Acceptable	M tusk	+7.1 ± 0.02	−21.9 ± 0.0	9.3	29.0	3.6	0.6
KK 64	Very good	M molar	+9.4 ± 0.12	−21.1 ± 0.01	13.8	39.6	3.3	1.4
KK 65	Very good	M tusk	+8.1 ± 0.08	−21.6 ± 0.03	11.7	32.9	3.3	0.5
		Min	*+7.1*	*−21.9*				
		Max	*+9.4*	*−20.1*				
		Average	*+8.2*	*−21.3*				
VG 16	Acceptable	M molar	+12.6 ± 0.06	−20.8 ± 0.04	14.2	40.5	3.3	1.0
VG 26	Very good	M molar	+14.9 ± 0.03	−19.0 ± 0.23	10.1	30.6	3.5	40.1*
VG 27	Very good	M molar	+14.3 ± 0.09	−20.1 ± 0.02	10.8	32.2	3.5	53.3*
VG 31	Acceptable	M molar	+11.3 ± 0.02	−20.5 ± 0.0	11.8	34.5	3.4	0.5
VG 32	Acceptable	M molar	+11.8 ± 0.07	−20.6 ± 0.10	10.5	31.9	3.5	***0.2***
VG 33	Acceptable	M molar	+13.3	−20.7	11.6	34.3	3.4	***0.2***
VG 34	Acceptable	M molar	+14.0 ± 0.13	−20.8 ± 0.04	13.5	38.6	3.3	0.7
		Min	*+11.3*	*−20.9*				
		Max	*+14.9*	*−19.0*				
		Average	*+13.2*	*−20.3*				

Fisher Scientific, France) and rinsed with Milli-Q water. The acid-insoluble residues were then treated with 0.1M NaOH for 20 h, followed by filtration through MF-Millipore™ membranes and rinsing with Milli-Q water. Subsequently, the alkali-insoluble residues were immersed in HCl (pH 2), and extraction was carried out at 100 °C for 17 h. The final extract was filtered once more using MF-Millipore™ membranes before collection. Approximately, 0.5 mg of extracted collagen was placed in tin foil caps, packed and analysed on a Thermo-Finnigan Delta V Plus isotope ratio mass spectrometer (IRMS) paired with an elemental analyser (Thermo Flash 1112) at Tartu University. Altogether, 29 samples were analysed in duplicates. The mean value and SD of the two replicates for each sample are presented in Table 1. Detailed information on the values for each duplicate is included in the Supplementary data, T3.

Differences in the relative content of stable isotopes of a chemical element in a substance were measured in comparison with unified international standards and denoted by the conventional unit δ (delta), which is expressed as a fraction of atoms of the heavy isotope from all atoms of the given element and converted to permille (‰) of deviation from the international standard (DeNiro, 1985). The $\delta^{13}C$ and $\delta^{15}N$ values are reported against the "Vienna" equivalent of the Belemnite PeeDee Formation (VPDB) and atmospheric nitrogen (AIR) standards, respectively. We used IAEA N-1 ($\delta^{15}N = +0.43$ ‰) (Boehlke and Coplen, 1995), IAEA N-2 ($\delta^{15}N = +20.41$ ‰) (Boehlke and Coplen, 1995) and USGS25 ($\delta^{15}N$ = -30.41 ‰) (Brand et al., 2014) reference values to normalise data to the AIR scale and IAEA-CH-3 ($\delta^{13}C$ = -24.72 ‰) (Coplen et al., 2006) and IAEA-CH-6 ($\delta^{13}C$ = -10.449 ‰) (Coplen et al., 2006) to normalise data to the VPDB scale. We used urea ($\delta^{15}N$ = -0.32 ‰; $\delta^{13}C$ = -41.30 ‰; n = 10) (Iva Analysentechnik, 2025) working standard to monitor quality. The internal precision of measurement for N was ≤0.2 ‰ and for C it was ≤0.1 ‰.

2.4. Data analysis

Differences in isotopic values between Shestakovo, Krasnoyarskaya Kurya and Volchia Griva were tested using RStudio (version R 3.6.0). The means for the three distinct sites were calculated as averages.

Throughout the text, all the mammoth site-related radiocarbon dates discussed in calendar years (cal BP) were calibrated using OxCal v.4,4.4 (Bronk Ramsey, 2009) and calibration curve InCal20 (Reimer et al., 2020).

3. Results

3.1. Sample preservation

Out of 29 analysed samples, 13 samples were removed from the dataset due to quality concerns. The full dataset with rejection reasons is available in the Supplementary data, T1. Sixteen samples remain in the main dataset and are considered to preserve the original isotopic values (Table 1).

The amount of extracted collagen was small for the whole sample set, with a highly variable yield percentage ranging between 0.03 % and 53 %. Not considering two samples with anomalously high yields at 40.1 % (VG 26) and 53.3 % (VG27), the average for the entire dataset was 0.5 %. We attribute these two high collagen yield values to an error during the weighing process. Despite the generally low yields, there was enough collagenous extract to get a reliable IRMS measurement in all cases, however, for VG 26 and VG 27 we were unable to remeasure the samples because there was no material left.

Some of the rejected samples exhibited very low collagen yields, for example, KK 60 (0.04 %) and VG 22 (0.03 %) (Supplementary data, T1). Even though the accepted samples had weight % of C > 13 % and N > 4.8 % (Ambrose, 1990), it has been shown that fresh or well-preserved collagen N contents should range from 11 % to 17 % (Ambrose, 1990; Sealy et al., 2014; van Klinken, 1999). Five of the 16 accepted samples have N contents below 11 %. Regarding carbon content, van Klinken (1999) observed a mean C% of 34.8 ± 8.8 in a substantial collection of acceptable collagens, while higher values ranging from 41 % to 47 % were suggested by Ambrose (1990) and Sealy et al. (2014). In our dataset, all C% values fall within the criteria suggested by van Klinken (1999) but do not reach the higher values proposed by Ambrose (1990) and Sealy et al. (2014). C and N weight-% concentrations in some of the rejected samples fell out of the ranges established by Ambrose (1990), Sealy et al. (2014) and van Klinken (1999) significantly. For instance, VG 18 has a C concentration of 9.94 % and N of 0.73 % (Supplementary data, T1).

The C:N range of samples was wide: 3.3–24.4. Amongst the accepted samples, the C:N ratios were all within a narrow span of the higher half of the total acceptable range of 2.9–3.6 (Ambrose, 1990), ranging from 3.3 to 3.6. Amongst the 13 rejected samples, only one sample, SH 54, had an acceptable C:N ratio of 3.6 but was removed from the main dataset due to an extremely low collagen yield (0.07 %), clearly lowered C% (16.6 %) and N% (5.4 %) and a $\delta^{13}C$ value (−18.8 ‰) that was noticeably higher than the other samples from the site. All the remaining 12 rejected samples had a C:N ratio higher than 3.6 without exception, varying from 3.6 to 24.4, indicating the presence of carbon contamination or nitrogen loss. The highest C:N ratio were shown by KK 60 (24.4) and VG 18 (15.9) (Supplementary data, T1), which, in addition, had lower $\delta^{13}C$ values (−25.6 ‰ and −23.6 ‰, respectively) and $\delta^{15}N$ values (+5.4 ‰ and +5.6 ‰, respectively) than the rest of the samples.

3.2. $\delta^{13}C$ and $\delta^{15}N$ values

While the range of $\delta^{13}C$ and $\delta^{15}N$ values for the accepted samples was −21.9 ‰ to −19.0 ‰ and from +6.1 to +14.9 ‰, respectively (Table 1), the overall range of $\delta^{13}C$ and $\delta^{15}N$ values for all analysed samples was from −25.6 ‰ to −14.5 ‰ and from +3 to +15 ‰, respectively (Supplementary data, T1). For $\delta^{13}C$, the very wide range of values is a reflection of alteration/contamination effects in poorly preserved samples, while the range for $\delta^{15}N$ is associated with taxon-specific ecological niche. Table 1 presents the $\delta^{13}C$ and $\delta^{15}N$ values of the accepted samples, their site-specific ranges and means and the range and mean for the entire accepted dataset. Given the low accepted sample number for Shestakovo and their statistically similar isotopic values in comparison to Krasnoyarskaya Kurya, as well as the relatively close proximity of these two sample sites, we treat the values from Shestakovo and Krasnoyarskaya Kurya as a single dataset referred to as SH + KK further in the text (averages $\delta^{13}C$: −21.1 ‰ ± 0.6 and $\delta^{15}N$: 8.0 ‰ ± 1.0) for further comparisons with Volchia Griva (averages $\delta^{13}C$: −20.3 ‰ ± 0.5 and $\delta^{15}N$: 13.2 ‰ ± 1.0) and other published records. The average values and standard deviations for the SH + KK dataset do not include the values of SH 53 because it is a horse molar. Originally, we included the horse and deer molars to be consistent with the $\delta^{18}O$ study by Krivokorin et al. (2024), as the set of samples used in that publication is identical to the one we are using in this study. However, in the further text, the results of horse and deer dentine samples are not discussed because the deer sample was excluded from the main dataset due to low collagen yield (see Supplementary data, T1), and the horse from Shestakovo being a singular sample not derived from mammoth in the whole dataset and being very similar to the published isotopic values of horses (e.g. Drucker et al., 2015) would not have contributed much valuable insight into the Discussion.

4. Discussion

4.1. Sample preservation

The generally low yields obtained throughout the studied material imply collagen loss, a common characteristic of subfossil finds. Low collagen yields serve as a sign of general degradation (van Klinken, 1999), when the peptide bonds between amino acids (collagen á-chains)

gradually break (Collins et al., 1995). Low yields observed in our samples suggest that the samples from all three sites have been subject to degradation and that the preservation status is less than ideal. For example, microbial heterotrophy implied as potential compromiser of the oxygen isotope integrity of the mineral part of the samples (Krivokorin et al., 2024), could have been a factor contributing to collagen deterioration. Additionally, Volchia Griva's formation conditions, which included periodic shifts between wet and dry phases (Leshchinskiy, 2018) may have created a conducive environment for the physical deterioration of the samples. Notably, low collagen yields do not immediately suggest interactions with exogenous molecules, and degradation itself does not necessarily compromise isotopic integrity (van Klinken, 1999).

According to Guiry and Szpak (2021), samples that have C:N values between 3.3 and 3.6 are all likely to carry minor level carbon contamination: according to their models, the strict induced error is within 0.5–1 ‰ from the measured value. We explored the option of applying stricter collagen quality control criteria, as suggested by Guiry and Szpak (2021). Applying the suggested stricter range of 3.1–3.3 to our dataset would reduce the number of acceptable samples from 13 to four: KK 64, KK 65, VG 16 and VG 34 ("the strict C:N dataset"). The averages in the "strict C:N″ dataset for Krasnoyarskaya Kurya ($\delta^{15}N$ +8.8.‰; $\delta^{13}C$ −21.3 ‰) and Volchia Griva ($\delta^{15}N$ +13.3 ‰; $\delta^{13}C$ −20.8 ‰) are similar to the averages for the accepted, wider C:N based Krasnoyarskaya Kurya ($\delta^{15}N$ +8.2 ‰; $\delta^{13}C$ −21.3 ‰) and Volchia Griva datasets ($\delta^{15}N$ +13.2 ‰; $\delta^{13}C$ −20.3 ‰). While the suggested strict C:N range can improve data quality (Guiry and Szpak, 2021), applying a narrower C:N range to our dataset does not influence the interpretation of our isotopic values, since the average isotopic values in the "strict C:N″ dataset do not differ from those in the main dataset. Additionally, such a small dataset would not be suitable for meaningful interpretations. Therefore, we continue relying on the C:N criteria outlined in Ambrose (1990); DeNiro (1985); DeNiro and Weiner (1988); Sealy et al. (2014); van Klinken (1999) and use the isotopic values presented in Table 1. For the purposes of this paper, i.e. a broad paleoecological interpretation and comparison to other regions, the added uncertainty level implied by the C:N ratio range 3.3–3.6 in our dataset is acceptable and taken into consideration when comparing datasets.

4.1.1. Mineral fraction vs organic fraction

In a study focusing on the $\delta^{18}O$ values of the bioapatite phosphate of the same material studied here (Krivokorin et al., 2024), found the mineral fraction of the majority of samples from Shestakovo, Krasnoyarskaya Kurya and Volchia Griva intact. Nevertheless, there were both tusk and even enamel samples that showed signs of post-depositional isotopic and/or chemical (cf. FTIR data) alteration. Many of the tusk specimens from Krasnoyarskaya Kurya and Volchia Griva displayed elevated Infrared Splitting Factor (IRSF) values and associated lower C/P ratios interpreted to reflect carbonate loss and accompanying structural changes (cf. France et al., 2020). The cause of the loss could not be established, as it could be attributed to site-specific conditions, sample pretreatment methods, or a combination of both factors (Krivokorin et al., 2024).

We compared the results of the preservation assessment of the mineral fraction from the article by Krivokorin et al. (2024) and the results of our preservation assessment of organic fraction in this study to see whether we could find a link between the alteration of the mineral and the organic parts of our samples (Supplementary data, T1). Regarding the visual preservation, some of the samples from Table 1 marked as visually "acceptable", i.e. the poorest appearance compared to other samples, yielded reliable oxygen isotope results (Krivokorin et al., 2024). However, it is notable that out of the 13 rejected samples, nine had "acceptable" visually evaluated preservation quality (Supplementary data, T1). In contrast, out of 16 accepted samples, only seven had "acceptable" preservation quality, which implies that the samples rejected based on their collagen quality properties often had worse visual preservation. The remaining accepted samples had either "good" or "very good" preservation quality. Thus, visual appearance is a more relevant clue to the preservation of the organic than the mineral, especially the phosphate component of bioapatite at these sites.

Collagen quality control parameters, including C:N ratios, nitrogen concentration, and collagen yield, did not show any clear relationship with elevated IRSF values (Supplementary data, T1), which is here used as a parameter of the general preservation status of the mineral component. Samples with elevated IRSF values from Shestakovo and Krasnoyarskaya Kurya had acceptable collagen yields, C% and N% values and C:N ratios (Supplementary data, T1).

The samples from Volchia Griva showed more pronounced signs of post-depositional alteration compared to Shestakovo and Krasnoyarskaya Kurya and more congruence between mineral and organic part preservation: regarding the mineral component, eight out of 19 VG samples analysed for phosphate $\delta^{18}O$ values showed elevated IRSF values (Supplementary data, T1). Seven out of these eight samples also demonstrated elevated C:N ratios in the organic part. Overall, ten samples from VG were excluded due to elevated C:N ratios and six out of these yielded N concentration values below 3.5 % and C:N ratios >3.6 (Supplementary data, T1), which can be considered an indicator of non-collagenous molecules like lipids and humic acids (Guiry and Szpak, 2021). Overall, it is challenging to make firm conclusions about whether there is a link between the post-depositional alteration of the organic and the mineral fraction of the samples from Shestakovo, Krasnoyarskaya Kurya and Volchia Griva. However, it is notable that three samples from Volchia Griva with elevated C:N ratios are also associated with carbonate-phosphate disequilibrium, which was used to assess the isotopic alteration of skeletal bioapatite (Supplementary data, T1). The fact that the samples with carbonate-phosphate $\delta^{18}O$ disequilibrium come exclusively from Volchia Griva further supports the evidence that the mineral and the organic part of samples from Volchia Griva have suffered from post-depositional alteration to a bigger extent than the samples from Shestakovo and Krasnoyarskaya Kurya.

4.2. Carbon and nitrogen isotope composition

There is relatively little comparative data for Eurasian mammoths from the LGM time period matching the datings of the sites analysed in this study. Altogether, 13 specimens directly dated to ca. 28-22 ka ago with published $\delta^{13}C$ and $\delta^{15}N$ isotope values are available from Northern Siberia, specifically Wrangel Island, Bykovsky peninsula, Bolchoy Lyakhovsky island, Lena Delta River and Taymyr Peninsula (Arppe et al., 2019; Iacumin et al., 2010; Szpak et al., 2010) (Fig. 2). However, their mean isotopic values (−21.6 ± 0.5 ‰ for $\delta^{13}C$ and 8.7 ± 0.9 ‰ for $\delta^{15}N$) are statistically indistinguishable from those of a much more extensive compilation of North Siberian mammoth data spanning 60-12 ka (Arppe et al., 2019) with $\delta^{13}C$ (−21.7 ± 0.6 ‰; n = 82) and $\delta^{15}N$ (9.0 ± 1.8 ‰; n = 82), and therefore, we will use the wider dataset as a point of comparison, and refer to it as the Northern Siberian dataset further in the text. A comparison between the $\delta^{13}C$ and the $\delta^{15}N$ isotopic values of SH + KK, Volchia Griva and Northern Siberian datasets is presented in Fig. 3 (see Supplementary data, T2 for full comparative data), illustrating the elevated isotope values at Volchia Griva clearly standing out from both SH + KK and Northern Siberian mammoth data.

Studies by (van der Merwe, 1982; Ambrose and DeNiro, 1986) show that animals whose diet completely consists of C_3 plants have collagen $\delta^{13}C$ values approximately around −21.5 ‰, and the average $\delta^{13}C$ values of SH + KK dataset (−21.1 ‰) and the Northern Siberian datasets (−21.7 ‰) (Fig. 3) suggest that the diet of mammoths in both regions consisted predominantly of C_3 plants. However, the SH + KK and Northern Siberian datasets are statistically different for $\delta^{13}C$ (p=0.02696) and $\delta^{15}N$ (p = 0.01054). The average $\delta^{13}C$ value from the SH + KK dataset is higher than the Northern Siberian dataset by 0.6 ‰, whereas the $\delta^{15}N$ average value from the SH + KK dataset is lower than that of the comparative dataset by 1.3 ‰ (see Fig. 3 and Table 1).

Fig. 2. Map showing the general location of Shestakovo, Krasnoyarskaya Kurya and Volchia Griva sites and other mammoth sites discussed in the text. Basemap: Esri, Maxar, Earthstar Geographics, and the GIS User Community.

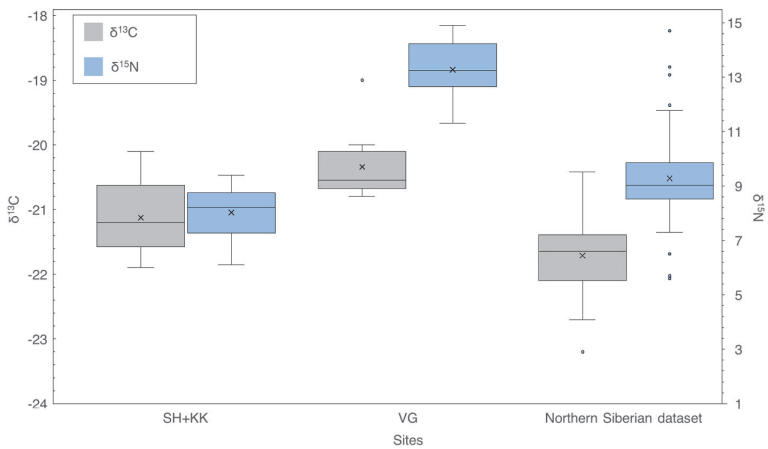

Fig. 3. Comparison between the $\delta^{1}3C$ and $\delta^{15}N$ values between the SH + KK, Volchia Griva and the Northern Siberian Dataset (Arppe et al., 2019; Iacumin et al., 2010; Szpak et al., 2010).

Firstly, the potential carbon contamination in SH + KK samples with C/N ratios >3.3 may introduce a larger error to isotopic analysis results, and thus the difference in $\delta^{13}C$ values should be considered tentative, as discussed in the "Sample preservation" section above. In contrast, the difference in $\delta^{15}N$ values is unequivocal. Despite complicating factors like season of precipitation, and edaphic conditions such as water storing capacity and rooting depth (e.g. Ehleringer, 2005; Schenk and Jackson, 2002; Farquhar et al., 1989) influencing plant isotopic values on a local scale, on a global scale, temperature, aridity and altitude are the main factors that influence $\delta^{13}C$ and $\delta^{15}N$ of plants (e.g., Amundson et al., 2003; Bocherens, 2015; Craine et al., 2009; Kohn, 2010; Körner et al., 1991; Männel et al., 2007; Sah and Brumme, 2003; Zech et al., 2011). The potentially lower $\delta^{13}C$ values in the Northern Siberian datasets compared to SH + KK can be explained by large-scale latitudinal trends in temperature and precipitation, which influence isotopic baselines at the plant level leading to lower plant $\delta^{13}C$ values at higher latitudes (Kohn, 2010; Stuiver and Braziunas, 1987; Van Klinken et al., 1994). The difference between the $\delta^{13}C$ values of the mammoths at SH + KK and the Northern Siberian dataset could also be related to differences in the makeup of their diets, with differences in the types and proportions of various plants consumed by these populations from two distant regions. For example, the mammoths in Northern Siberia could

supplement their diet with bark, twigs and mosses (Gorlova, 1982; Olivier, 1982; Vereshchagin and Baryshnikov, 1982), suggested by Iacumin et al. (2000) to lower the $\delta^{13}C$ of the mammoths' tissues. During harsh winters, the Northern Siberian mammoths may have relied on fat reserves to survive periods of food scarcity (Kubiak, 1982; Olivier, 1982). Since fat has lower $\delta^{13}C$ values relative to other nutrients, Bocherens (2003) suggested this metabolic strategy could also contribute to the lowered $\delta^{13}C$ values.

The relatively higher $\delta^{13}C$ values and lower $\delta^{15}N$ values for SH + KK site mammoths compared to Northern Siberia mirror the pattern reported by Szpak et al. (2010) for Late Pleistocene woolly mammoths of Eastern Beringia (Alaska and Yukon) in comparison to Western Beringia (i.e. Northern Siberia). The pattern of lower $\delta^{15}N$ combined with a higher $\delta^{13}C$ appears to be in conflict with plant $\delta^{13}C$ and $\delta^{15}N$ values showing parallel correlations to environmental gradients like temperature and moisture: higher $\delta^{13}C$ and $\delta^{15}N$ values are often associated with more arid climatic conditions and higher temperatures (Amundson et al., 2003; Craine et al., 2009; Gröcke et al., 1997; Heaton, 1987; Kohn, 2010; Sealy et al., 1987; Wooller et al., 2021). Szpak et al. (2010) proposed more arid conditions as the main driver of higher $\delta^{15}N$ values in Northern Siberian mammoths and suggested that variations in high arctic $\delta^{13}C$ may be insensitive to moisture differences and rather reflect regional differences in mean annual temperature, i.e. warmer conditions in Eastern Beringia. Indeed, according to recent climate simulations (Extended data in Wang et al., 2021), Eastern Beringia was more wet and had higher mean annual temperature than Western Beringia. This same line of reasoning could also explain the differences between the $\delta^{15}N$ values of SH + KK and Northern Siberian datasets. We propose that environmental threshold points may partially explain the contrasting $\delta^{13}C/\delta^{15}N$ responses. For nitrogen isotopes, Craine et al. (2009) showed that plant $\delta^{15}N$ values stop responding to changing mean annual temperatures (MAT) in a linear way below −0.5°C. Considering that mean annual temperatures during LGM in the Northern Siberia were far below zero (Vandenberghe et al., 2014; Wang et al., 2021), it is highly likely that plant $\delta^{15}N$ values were rather insensitive to variations in temperature. However, in the case of carbon isotopes, while the global C_3 plant data analysed by Kohn (2010) showed that the correlation between plant $\delta^{13}C$ and mean annual precipitation (MAP) flattens out in wet environments, the mammoth steppe was generally characterized by aridity with MAPs well below 500 mm/a (Wang et al., 2021) and thus, a hypothesis of 'too wet to register differences in MAP' doesn't seem plausible.

Alternative or complementary factors accounting for the more elevated $\delta^{15}N$ values in the Northern Siberian dataset point to involvement of metabolic strategies for dealing with aridity and/or a diet composed primarily of nutrient-poor, protein-deficient herbaceous and graminoid vegetation, as discussed in Szpak et al. (2010). Graminoid-dominated diet of the Northern Siberia mammoths is also supported by Wang et al. (2021), who showed that vegetation during LGM in Northern Siberia had a larger proportion of graminoids compared to Eastern Beringia. It has been suggested that in arid environments, where plants typically contain lower protein and nitrogen levels, herbivore $\delta^{15}N$ may be elevated due to water saving mechanisms increasing the urea concentration of urine (Ambrose and DeNiro, 1986), or microbial recycling of nitrogen in the digestive tract (Sealy et al., 1987). Overall, despite the conflicting evidence on the influence of animal metabolic processing on tissue $\delta^{15}N$ (e.g. Sponheimer et al., 2003; Ambrose, 2000; Hartman, 2011), it is plausible that the physiology and metabolism of the Northern Siberian mammoths would have additionally influenced bodily isotope levels during the LGM, a period generally thought to represent a very arid and cold time period, which could have resulted in their higher $\delta^{15}N$ values. In summary, we propose that, similarly to what has been reported for West Beringian mammoths (Szpak et al., 2010), regional vegetation, climate, and physiological adaptations all likely contributed to the isotopic differences between mammoth populations in Southeast Western Siberia and Northern Siberia.

4.2.1. Unusual isotopic values from Volchia Griva

Leshchinskiy and Burkanova (2022) published $\delta^{13}C$ and $\delta^{15}N$ values for five mammoth bone samples from Volchia Griva (age range – 22.2–23.7 ka cal BP), which are very similar to our results and are here combined with our samples from that site to yield an extended Volchia Griva dataset with mean $\delta^{13}C$ and $\delta^{15}N$ values at −20.3 ‰±0.5 and + 13.3 ‰±0.1, respectively. Mammoths had a low-protein diet and generally tended to have higher $\delta^{15}N$ values than other herbivores like horses or deer (Bocherens et al., 1996), but the mammoths from Volchia Griva occupy an outstanding position among the so far published isotopic records of mammoth sites globally due to their abnormally high $\delta^{15}N$ values. The average $\delta^{15}N$ value from Volchia Griva is 5.3 ‰ higher than the average SH + KK values and 4.3 ‰ higher than the average of the North Siberian dataset ($p < 0.05$). To the authors' knowledge, few woolly mammoth samples to date have yielded $\delta^{15}N$ values in such a high range of 11–15 ‰. For example, in the compilation of East Eurasian and Northwest North American isotope data on mammoths (Arppe et al., 2019) less than 5 % of the >350 listed samples showed $\delta^{15}N$ values ≥ 12 ‰ common for Volchia Griva mammoths, most of them from Northern Siberia (Bocherens et al., 1996; Iacumin et al., 2000; Kirillova et al., 2023; Szpak et al., 2010) and a few from Northern Yukon (Metcalfe et al., 2016). Overall, Volchia Griva potentially has the densest concentration of the highest $\delta^{15}N$ values reported for the Northern Hemisphere.

The fact that Volchia Griva has significantly higher $\delta^{13}C$ and $\delta^{15}N$ values than the SH + KK dataset is unexpected considering the relatively short distance between Shestakovo, Krasnoyarskaya Kurya and Volchia Griva. We propose that potential explanations for such differences in the isotope levels could lie in local characteristics of these sites and potentially also the likely temporal differences between the sites. We consider the elevated isotopic baselines of the Volchia Griva site as a likely relevant cause of the observed elevated $\delta^{15}N$ values, because, in addition to mammoths, for the same period of 22.2–23.7 ka cal BP, Leshchinskiy and Burkanova (2022) published elevated $\delta^{15}N$ values for a single equid (+12.3 ‰) as well as elevated $\delta^{15}N$ values for carnivores such as fox (16.2 ‰) and wolf (17.1 ‰). The other factors discussed further in the text are offered as mechanisms that can further influence the isotopic values.

Mineral salts were the primary factor attracting large herbivores to Volchia Griva (Leshchinskiy, 2018) and Shestakovo (Derevianko et al., 2000), and it also seems conceivable that there might be a connection between the elevated salinity of local soils in these areas and the nitrogen isotopic composition of local plants. High soil pH and salinity decrease NO_3^- uptake by the plants' roots (Aslam et al., 1984) and can elevate the $\delta^{15}N$ values of plants (van Groenigen and van Kessel, 2002). Therefore, it is possible that the salinisation of local soils at Volchia Griva would result in high $\delta^{15}N$ values in local plants and, by extension, in local mammoths' tissues. However, it is also worth noting that while both Shestakovo and Volchia Griva were "beast solonetz", we did not observe a similar pattern of elevated $\delta^{15}N$ values in Shestakovo samples, which may be due to the low number (n = 2) of analysed samples or other site-specific differences in soil properties, for which we do not currently hold any detailed information. This is why the high nitrogen values in samples from Volchia Griva are particularly important: there are currently no studies exploring whether such elevated nitrogen values are a general feature of salt licks. This presents a promising direction for future research.

Elevated soil salinity can also influence plant $\delta^{13}C$ values: in a manner comparable to effects of stress induced by aridity, plants tend to close their stomata due to salt stress, which reduces stomatal conductance and the within-cell partial $^{12}CO_2$ pressure. As a result, the salinity-stressed plant assimilates a larger proportion of $^{13}CO_2$, leading to less negative $\delta^{13}C$ values in the newly formed plant tissues (van Groenigen and van Kessel, 2002). In addition, although the $\delta^{13}C$ values from

Volchia Griva suggest a diet primarily composed of C_3 plants, we do not entirely rule out the inclusion of C_4 vegetation. Volchia Griva lies within the present-day native geographical distribution of certain C_4 taxa, such as *Atriplex sibirica and Atriplex tatarica* (Rakhmankulova et al., 2019; Sukhorukov et al., 2022) and these species are not only well adapted to arid climates but also well adapted to saline and ruderal environments (Rakhmankulova et al., 2019; Sukhorukov et al., 2022). The presence of such taxa at Volchia Griva is supported by the pollen analysis from Volchia Griva (Leshchinskiy and Burkanova, 2022) and suggests a minor C_4 component in mammoth diets at Volchia Griva.

As an additional local factor, large animal herds frequenting sites of mineral oases produce a lot of dung. Szpak (2014) showed that using animal dung as a fertiliser can increase plant $\delta^{15}N$ values by +2 - +8 ‰ (if cattle manure is used) and even by +10 to +40 ‰ (if pig – an omnivore - manure is used). Although reaching such an effect of elevated nitrogen values generally requires a substantial amount of dung (Bogaard et al., 2013), the presence of mammoth and other large animal populations frequenting Volchia Griva over several millennia could have led to the elevation of local soil $\delta^{15}N$ values contributing to the observed values. It is also possible that the mammoths at Volchia Griva practised coprophagy, which would, in turn, result in elevated $\delta^{15}N$ values in their tissues (Clementz et al., 2009; Kuitems et al., 2015; van Geel et al., 2008, 2011).

The elevated $\delta^{13}C$ and $\delta^{15}N$ values at Volchia Griva, compared to both the SH + KK dataset and the Northern Siberian dataset, may also suggest that the mammoths found at Volchia Griva could have subsisted in more arid conditions than their counterparts in Northern Siberia or at Shestakovo and Krasnoyarskaya Kurya, yet a difference in climatic conditions among the SEWS sites seems improbable due to their close mutual proximity. Speculatively, some kind of a permanent geographic separation in the large-scale foraging range areas between the populations frequenting VG and those discovered at SH + KK could be suggested. However, the fact that the layer dates providing the chronological context indicate the sites are not contemporaneous may play a significant role, and the isotopic differences could also reflect temporal changes in the environment. This hypothesis is further supported by the results of palynological analysis from Volchia Griva (Leshchinskiy and Burkanova, 2022), which showed a clear aridisation of the climate since the site's formation.

5. Conclusion

We analysed 29 mammoth molar dentine samples, alongside dentine from one horse and one deer molars from three Late Pleistocene paleontological sites in the southeast of the Western Siberian Plain (SEWS): Shestakovo, Krasnoyarskaya Kurya, and Volchia Griva. We assessed the preservation of these samples using C:N atomic ratios, collagen yields, and elemental carbon and nitrogen content. Our results reveal unusually high $\delta^{15}N$ values reported for mammoth remains in the Northern Hemisphere from Volchia Griva. We attribute this isotopic enrichment to the unique local environmental conditions at Volchia Griva, including saline soils and intensive trampling, which may have altered nitrogen cycling at the site. The clear difference in $\delta^{15}N$ and $\delta^{13}C$ values between Volchia Griva and the other two sites, suggests that the mammoth population represented at Volchia Griva had different foraging areas from those at Shestakovo and Krasnoyarskaya Kurya despite the geographical proximity of the sites. This could be interpreted either as restricted geographic mobility between site areas or, perhaps more likely, a reflection of the likely non-contemporanous nature of the sites, with Shestakovo and Volchia Griva displaying completely non-overlapping age ranges.

Future studies of skeletal materials from these sites should take into consideration the generally poor preservation of the organic component, resulting in low extract yields, and select samples in quantities sufficient to run initial analyses, potential reanalysis, and C14 dating. Quality screening should follow the established protocols; however, we advise considering evaluating the preservation of the samples on an individual basis. Tusks seem to have a higher rejection rate compared to molars; this trend is observed for both the mineral and organic components.

CRediT author statement

Ivan Krivokorin: Software, Formal analysis, Investigation, Writing - Original Draft, Writing - Review & Editing, Visualization; Leeli Amon: Resources, Writing - Review & Editing, Supervision, Project administration; Sergey V. Leshchinskiy: Conceptualization, Resources, Writing - Review & Editing, Supervision, Project administration; Laura Arppe: Conceptualization, Methodology, Validation, Resources, Writing - Review & Editing, Supervision.

Declaration of competing interest

The authors declare that they have no known competing financial interests or personal relationships that could have appeared to influence the work reported in this paper.

Acknowledgements

We would like to thank the individuals who assisted us throughout the course of this project. Special thanks are due to Holar Sepp from the Department of Geology at Tartu University for conducting isotopic analyses, Jüri Vassiljev for C14 calibration, Varvara Bakumenko for her contributions to the statistical analysis, Elena Burkanova, Vasiliy Zenin, Artur Dzhumanov, Aleksandra Samandrosova, Aleksey Klimov, and Dmitriy Kadochnikov for their assistance in acquiring the samples. The research was funded by ESF projects PRG 1993, TK 215 and the Doctoral School of Earth Sciences and Ecology, supported by the European Union, European Regional Development Fund (ASTRA "TTÜ arenguprogramm aastateks 2016–2022").

Appendix A. Supplementary data

Supplementary data to this article can be found online at https://doi.org/10.1016/j.quascirev.2025.109645.

Data availability

All data and/or code is contained within the submission.

References

Ambrose, S.H., 2000. Controlled diet and climate experiments on nitrogen isotope ratios of rats. In: Biogeochemical Approaches to Paleodietary Analysis. Kluwer Academic Publishers, Boston, pp. 243–259. https://doi.org/10.1007/0-306-47194-9_12.

Ambrose, S.H., 1990. Preparation and characterization of bone and tooth collagen for isotopic analysis. J. Archaeol. Sci. https://doi.org/10.1016/0305-4403(90)90007-R.

Ambrose, S.H., DeNiro, M.J., 1986. The isotopic ecology of East African mammals. Oecologia 69, 395–406. https://doi.org/10.1007/BF00377062.

Amundson, R., Austin, A.T., Schuur, E.A.G., Yoo, K., Matzek, V., Kendall, C., Uebersax, A., Brenner, D., Baisden, W.T., 2003. Global patterns of the isotopic composition of soil and plant nitrogen. Glob. Biogeochem. Cycles 17. https://doi.org/10.1029/2002GB001903.

Arppe, L., Aaris-Sørensen, K., Daugnora, L., Lõugas, L., Wojtal, P., Zupiņš, I., 2011. The palaeoenvironmental δ13C record in European woolly mammoth tooth enamel. Quat. Int. 245, 285–290. https://doi.org/10.1016/j.quaint.2010.10.018.

Arppe, L., Karhu, J.A., Vartanyan, S., Drucker, D.G., Etu-Sihvola, H., Bocherens, H., 2019. Thriving or surviving? The isotopic record of the wrangel Island woolly mammoth population. Quat. Sci. Rev. 222, 105884. https://doi.org/10.1016/j.quascirev.2019.105884.

Aslam, M., Huffaker, R.C., Rains, D.W., 1984. Early effects of salinity on nitrate assimilation in barley seedlings. Plant Physiol 76, 321–325. https://doi.org/10.1104/pp.76.2.321.

Ayliffe, L.K., Lister, A.M., Chivas, A.R., 1992. The preservation of glacial-interglacial climatic signatures in the oxygen isotopes of elephant skeletal phosphate. Palaeogeogr. Palaeoclimatol. Palaeoecol. 99, 179–191. https://doi.org/10.1016/0031-0182(92)90014-V.

Barbieri, M., Kuznetsova, T.V., Nikolaev, V.I., Palombo, M.R., 2008. Strontium isotopic composition in late Pleistocene mammal bones from the Yakutian region (North-

Eastern Siberia). Quat. Int. 179, 72–78. https://doi.org/10.1016/j.quaint.2007.08.014.
Bocherens, H., 2003. Isotopic biogeochemistry and the palaeoecology of the mammoth steppe fauna. Deinsea 9, 57–76.
Bocherens, H., 2015. Isotopic tracking of large carnivore palaeoecology in the mammoth steppe. Quat. Sci. Rev. 117, 42–71. https://doi.org/10.1016/j.quascirev.2015.03.018.
Bocherens, H., Fizet, M., Mariotti, A., Gangloff, R.A., Burns, J.A., 1994. Contribution of isotopic biogeochemistry (13 C, 15 N, 18 O) to the paleoecology of mammoths (mammuthus primigenius). Hist. Biol. 7, 187–202. https://doi.org/10.1080/10292389409380453.
Bocherens, H., Pacaud, G., Lazarev, P.A., Mariotti, A., 1996. Stable isotope abundances (13C, 15N) in collagen and soft tissues from Pleistocene mammals from Yakutia: implications for the palaeobiology of the mammoth steppe. Palaeogeogr. Palaeoclimatol. Palaeoecol. 126, 31–44. https://doi.org/10.1016/S0031-0182(96)00068-5.
Boehlke, J.K., Coplen, T.B., 1995. Interlaboratory Comparison of Reference Materials for nitrogen-isotope-ratio Measurements, pp. 51–66.
Bogaard, A., Fraser, R., Heaton, T.H., Wallace, M., Vaiglova, P., Charles, M., Jones, G., Evershed, R.P., Styring, A.K., Andersen, N.H., Arbogast, R.M., 2013. Crop manuring and intensive land management by Europe's first farmers. Proc. Natl. Acad. Sci. 110 (31), 12589–12594.
Boiko, P.V., Maschenko, E.N., Sylerzhitskii, L.D., 2005. A New Large Late Pleistocene Mammoth's Locality in Western Siberia. Short papers and Abstracts, 2nd International Congress The world of elephants. Mammoth Site of Hot Springs, SanDiego, pp. 22–26.
Brand, W.A., Coplen, T.B., Vogl, J., Rosner, M., Prohaska, T., 2014. Assessment of international reference materials for isotope-ratio analysis (IUPAC technical report). Pure Appl. Chem. 86, 425–467. https://doi.org/10.1515/pac-2013-1023.
Bronk Ramsey, C., 2009. Bayesian analysis of radiocarbon dates. Radiocarbon 51, 337–360. https://doi.org/10.1017/S0033822200033865.
Brugère, A., Fontana, L., 2009. Origin and exploitation patterns of mammoth at milovice (area G excepted). Martin oliva. Milovice: site of the mammoth people below the pavlov hills: the question of mammoth bone structures. Anthropos 27, 51–105.
Cersoy, S., Zazzo, A., Lebon, M., Rofes, J., Zirah, S., 2017. Collagen extraction and stable isotope analysis of small vertebrate bones: a comparative approach. Radiocarbon 59, 679–694. https://doi.org/10.1017/RDC.2016.82.
Clementz, M.T., Fox-Dobbs, K., Wheatley, P.V., Koch, P.L., Doak, D.F., 2009. Revisiting old bones: coupled carbon isotope analysis of bioapatite and collagen as an ecological and palaeoecological tool. Geol. J. 44, 605–620. https://doi.org/10.1002/gj.1173.
Collins, M.J., Riley, M.S., Child, A.M., Turner-Walker, G., 1995. A basic mathematical simulation of the chemical degradation of ancient collagen. J. Archaeol. Sci. 22, 175–183. https://doi.org/10.1006/jasc.1995.0019.
Cooper, A., Turney, C., Hughen, K.A., Brook, B.W., McDonald, H.G., Bradshaw, C.J.A., 2015. Abrupt warming events drove late Pleistocene holarctic megafaunal turnover. Science 349, 602–606. https://doi.org/10.1126/science.aac4315.
Coplen, T.B., Brand, W.A., Gehre, M., Gröning, M., Meijer, H.A.J., Toman, B., Verkouteren, R.M., 2006. New guidelines for δ^{13}C measurements. Anal. Chem. 78, 2439–2441. https://doi.org/10.1021/ac052027c.
Craine, J.M., Elmore, A.J., Aidar, M.P.M., Bustamante, M., Dawson, T.E., Hobbie, E.A., Kahmen, A., Mack, M.C., McLauchlan, K.K., Michelsen, A., Nardoto, G.B., Pardo, L. H., Peñuelas, J., Reich, P.B., Schuur, E.A.G., Stock, W.D., Templer, P.H., Virginia, R. A., Welker, J.M., Wright, I.J., 2009. Global patterns of foliar nitrogen isotopes and their relationships with climate, mycorrhizal fungi, foliar nutrient concentrations, and nitrogen availability. New Phytol. 183, 980–992. https://doi.org/10.1111/j.1469-8137.2009.02917.x.
Debruyne, R., Chu, G., King, C.E., Bos, K., Kuch, M., Schwarz, C., Szpak, P., Gröcke, D.R., Matheus, P., Zazula, G., Guthrie, D., Froese, D., Buigues, B., de Marliave, C., Flemming, C., Poinar, D., Fisher, D., Southon, J., Tikhonov, A.N., MacPhee, R.D.E., Poinar, H.N., 2008. Out of America: ancient DNA evidence for a new world origin of late Quaternary woolly mammoths. Curr. Biol. 18, 1320–1326. https://doi.org/10.1016/j.cub.2008.07.061.
DeNiro, M.J., 1985. Postmortem preservation and alteration of in vivo bone collagen isotope ratios in relation to palaeodietary reconstruction. Nature 317, 806–809. https://doi.org/10.1038/317806a0.
Deniro, M.J., Epstein, S., 1981. Influence of diet on the distribution of nitrogen isotopes in animals. Geochem. Cosmochim. Acta 45, 341–351. https://doi.org/10.1016/0016-7037(81)90244-1.
DeNiro, M.J., Weiner, S., 1988. Use of collagenase to purify collagen from prehistoric bones for stable isotopic analysis. Geochem. Cosmochim. Acta 52, 2425–2431. https://doi.org/10.1016/0016-7037(88)90299-2.
Derevianko, A.P., Molodin, V.I., Zenin, V.N., Leshchinskiy, S.V., Mashchenko, E.N., 2003. Pozdnepaleoliticheskoe Mestonakhozhdenie Shestakovo. Izd. IAET SO RAN, Novosibirsk.
Derevianko, A.P., Zenin, V.N., Leshchinsky, S.V., Maschenko, E.N., 2000. Peculiarities of mammoth accumulation at shestakovo site in West Siberia. Archaeol. Ethnol. Anthropol. Eurasia 3, 42–55.
Dobberstein, R.C., Collins, M.J., Craig, O.E., Taylor, G., Penkman, K.E.H., Ritz-Timme, S., 2009. Archaeological collagen: why worry about collagen diagenesis? Archaeol. Anthropol. Sci. 1, 31–42. https://doi.org/10.1007/s12520-009-0002-7.
Drucker, D.G., Bocherens, H., Péan, S., 2014. Isotopes stables (13C, 15N) du collagène des mammouths de Mezhyrich (Epigravettien, Ukraine): implications paléoécologiques. Anthropologie (Brno) 118, 504–517. https://doi.org/10.1016/j.anthro.2014.04.001.
Drucker, D.G., Stevens, R.E., Germonpré, M., Sablin, M.V., Péan, S., Bocherens, H., 2018. Collagen stable isotopes provide insights into the end of the mammoth steppe in the central East European plains during the epigravettian. Quat. Res. 90, 457–469. https://doi.org/10.1017/qua.2018.40.
Drucker, D.G., 2022. The isotopic ecology of the mammoth steppe. Annu. Rev. Earth Planet Sci. 50, 395–418. https://doi.org/10.1146/annurev-earth-100821-081832.
Drucker, D.G., Vercoutère, C., Chiotti, L., Nespoulet, R., Crépin, L., Conard, N.J., Münzel, S.C., Higham, T., van der Plicht, J., Lázničková-Galetová, M., Bocherens, H., 2015. Tracking possible decline of woolly mammoth during the gravettian in Dordogne (France) and the ach valley (Germany) using multi-isotope tracking (13C, 14C, 15N, 34S, 18O). Quat. Int. 359–360, 304–317. https://doi.org/10.1016/j.quaint.2014.11.028.
Ehleringer, J.R., 2005. The influence of atmospheric CO2, temperature, and water on the abundance of C3/C4 taxa. A History of Atmospheric CO2 and its Effects on Plants, Animals, and Ecosystems. Springer-Verlag, New York, pp. 214–231. https://doi.org/10.1007/0-387-27048-5_10.
Farquhar, G.D., Ehleringer, J.R., Hubick, K.T., 1989. Carbon isotope discrimination and photosynthesis. Annu. Rev. Plant Physiol. Plant Mol. Biol. 40, 503–537. https://doi.org/10.1146/annurev.pp.40.060189.002443.
Fox-Dobbs, K., Leonard, J.A., Koch, P.L., 2008. Pleistocene megafauna from eastern beringia: paleoecological and paleoenvironmental interpretations of stable carbon and nitrogen isotope and radiocarbon records. Palaeogeogr. Palaeoclimatol. Palaeoecol. 261, 30–46. https://doi.org/10.1016/j.palaeo.2007.12.011.
France, C.A.M., Sugiyama, N., Aguayo, E., 2020. Establishing a preservation index for bone, dentin, and enamel bioapatite mineral using ATR-FTIR. J Archaeol Sci Rep 33, 102551. https://doi.org/10.1016/j.jasrep.2020.102551.
France, C.A.M., Zelanko, P.M., Kaufman, A.J., Holtz, T.R., 2007. Carbon and nitrogen isotopic analysis of Pleistocene mammals from the saltville quarry (Virginia, USA): implications for trophic relationships. Palaeogeogr. Palaeoclimatol. Palaeoecol. 249, 271–282. https://doi.org/10.1016/j.palaeo.2007.02.002.
Gorlova, R.N., 1982. Plant Macroremainder from Alimentary Canal of Mammoth from Urebey. Nauka, Moscow, pp. 19–29.
Grigoriev, S.E., Fisher, D.C., Obadà, T., Shirley, E.A., Rountrey, A.N., Savvinov, G.N., Garmaeva, D.K., Novgorodov, G.P., Cheprasov, M.Yu, Vasilev, S.E., Goncharov, A.E., Masharskiy, A., Egorova, V.E., Petrova, P.P., Egorova, E.E., Akhremenko, Y.A., van der Plicht, J., Galanin, A.A., Fedorov, S.E., Ivanov, E.V., Tikhonov, A.N., 2017. A woolly mammoth (Mammuthus primigeniu) carcass from Maly Lyakhovsky island (New Siberian Islands, Russian Federation). Quat. Int. 445, 89–103. https://doi.org/10.1016/j.quaint.2017.01.007.
Gröcke, D.R., Bocherens, H., Mariotti, A., 1997. Annual rainfall and nitrogen-isotope correlation in macropod collagen: application as a palaeoprecipitation indicator. Earth Planet Sci. Lett. 153, 279–285. https://doi.org/10.1016/S0012-821X(97)00189-1.
Guiry, E.J., Szpak, P., 2021. Improved quality control criteria for stable carbon and nitrogen isotope measurements of ancient bone collagen. J. Archaeol. Sci. 132, 105416. https://doi.org/10.1016/j.jas.2021.105416.
Guthrie, R.D., 1968. Paleoecology of the large-mammal community in interior Alaska during the late Pleistocene. Am. Midl. Nat. 79, 346. https://doi.org/10.2307/2423182.
Hartman, G., 2011. Are elevated δ 15 N values in herbivores in hot and arid environments caused by diet or animal physiology? Funct. Ecol. 25, 122–131. https://doi.org/10.1111/j.1365-2435.2010.01782.x.
Heaton, T.H.E., 1987. The 15N/14N ratios of plants in South Africa and Namibia: relationship to climate and coastal/saline environments. Oecologia 74, 236–246. https://doi.org/10.1007/BF00379365.
Hibbert, D., 1982. History OF the steppe-tundra CONCEPT. In: Paleoecology of Beringia. Elsevier, pp. 153–156. https://doi.org/10.1016/B978-0-12-355860-2.50017-X.
Hughes, P.D., Gibbard, P.L., 2015. A stratigraphical basis for the Last Glacial Maximum (LGM). Quat. Int. 383, 174–185. https://doi.org/10.1016/j.quaint.2014.06.006.
Iacumin, P., Di Matteo, A., Nikolaev, V., Kuznetsova, T.V., 2010. Climate information from C, N and O stable isotope analyses of mammoth bones from northern Siberia. Quat. Int. 212, 206–212. https://doi.org/10.1016/j.quaint.2009.10.009.
Iacumin, P., Nikolaev, V., Ramigni, M., 2000. C and N stable isotope measurements on Eurasian fossil mammals, 40 000 to 10 000 years BP: herbivore physiologies and palaeoenvironmental reconstruction. Palaeogeogr. Palaeoclimatol. Palaeoecol. 163, 33–47. https://doi.org/10.1016/S0031-0182(00)00141-3.
Iva Analysentechnik, 2025. WWW Document. https://www.iva-analysentechnik.de/en/.
Kahlke, R.-D., 2014. The origin of Eurasian mammoth faunas (Mammuthus–Coelodonta faunal complex). Quat. Sci. Rev. 96, 32–49. https://doi.org/10.1016/j.quascirev.2013.01.012.
Kirillova, I.V., Markova, E.A., Panin, A.V., Van der Plicht, J., Titov, V.V., 2023. ON small continental mammoths and dwarfism. Zoological journal 102, 1280–1300. https://doi.org/10.31857/S0044513423100045 (in Russian).
Koch, P.L., Barnosky, A.D., 2006. Late Quaternary extinctions: state of the debate. Annu. Rev. Ecol. Evol. Syst. 37, 215–250. https://doi.org/10.1146/annurev.ecolsys.34.011802.132415.
Kohn, M.J., 2010. Carbon Isotope Compositions of Terrestrial C3 Plants as Indicators of (Paleo)Ecology and (Paleo)Climate, 107. Proceedings of the National Academy of Sciences, pp. 19691–19695. https://doi.org/10.1073/pnas.1004933107.
Kohn, M.J., Cerling, T.E., 2002. Stable isotope compositions of biological apatite. Rev. Mineral. Geochem. 48, 455–488. https://doi.org/10.2138/rmg.2002.48.12.
Körner, Ch, Farquhar, G.D., Wong, S.C., 1991. Carbon isotope discrimination by plants follows latitudinal and altitudinal trends. Oecologia 88, 30–40. https://doi.org/10.1007/BF00328400.
Krivokorin, I., Amon, L., Leshchinskiy, S.V., Arppe, L., 2024. Oxygen isotope studies of the largest West Siberian mammoth sites and implications for last glacial maximum

climate reconstruction. Quat. Sci. Rev. 343, 108938. https://doi.org/10.1016/j.quascirev.2024.108938.
Krzemińska, A., Wędzicha, S., 2015. Pathological changes on the ribs of woolly mammoths (Mammuthus primigenius). Quat. Int. 359–360, 186–194. https://doi.org/10.1016/j.quaint.2014.04.059.
Kubiak, H., 1982. Morphological characters of the mammoth: an adaptation to the arctic-steppe environment. In: Paleoecology of Beringia. Elsevier, pp. 281–289. https://doi.org/10.1016/B978-0-12-355860-2.50028-4.
Kuitems, M., van Kolfschoten, T., van der Plicht, J., 2015. Elevated δ15N values in mammoths: a comparison with modern elephants. Archaeol. Anthropol. Sci. 7, 289–295. https://doi.org/10.1007/s12520-012-0095-2.
Kuzmin, Y.V., Leshchinskiy, S.V., Zenin, V.N., Burkanova, E.M., Zazovskaya, E.P., Samandrosova, A.S., 2023. Chronology of the volchia griva megafaunal locality and paleolithic site (Western Siberia) and the issue OF human occupation of Siberia at the last glacial maximum. Radiocarbon 1–13. https://doi.org/10.1017/RDC.2023.82.
Lazarev, S., Leshchinskiy, S.V., 2011. Preliminary results of drilling activity on the Krasnoyarskaya Kurya mammoth site. Trudy TSU 280, 232–235.
Leshchinskiy, S., 2015. Enzootic diseases and extinction of mammoths as a reflection of deep geochemical changes in ecosystems of Northern Eurasia. Archaeol. Anthropol. Sci. 7, 297–317. https://doi.org/10.1007/s12520-014-0205-4.
Leshchinskiy, S., Burkanova, E., Polumogina, Y., Lazarev, S., Zenin, V., 2014. Last glacial maximum mammoth fauna of the Krasnoyarskaya Kurya site (southeastern part of the West Siberian Plain). SCIENTIFIC ANNALS OF THE SCHOOL OF GEOLOGY 105.
Leshchinskiy, S.V., 2018. Results of latest paleontological, stratigraphic and geoarchaeological research of the Volchia Griva mammoth fauna site. Proceedings of the Zoological Institute RAS 322, 315–384. https://doi.org/10.31610/trudyzin/2018.322.3.315.
Leshchinskiy, S.V., 2017. Strong evidence for dietary mineral imbalance as the cause of osteodystrophy in late glacial woolly mammoths at the Berelyokh site (Northern Yakutia, Russia). Quat. Int. 445, 146–170. https://doi.org/10.1016/j.quaint.2017.02.036.
Leshchinskiy, S.V., 2012. Paleoecological investigation of mammoth remains from the Kraków Spadzista Street (B) site. Quat. Int. 276–277, 155–169. https://doi.org/10.1016/j.quaint.2012.05.025.
Leshchinskiy, S.V., 2006. Lugovskoye: environment, taphonomy, and origin of a paleofaunal site. Archaeol. Ethnol. Anthropol. Eurasia 25, 33–40. https://doi.org/10.1134/S1563011006010026.
Leshchinskiy, S.V., Burkanova, E.M., 2022. The Volchia Griva mineral oasis as unique locus for research of the mammoth fauna and the late Pleistocene environment in Northern Eurasia. Quat. Res. 109, 157–182. https://doi.org/10.1017/qua.2022.8.
Leshchinskiy, S.V., Zenin, V.N., Burkanova, E.M., Kuzmin, Y.V., 2023. The unique late Paleolithic artifactual bone assemblage from the Volchia Griva site, Western Siberia. Quat. Res. 114, 93–113. https://doi.org/10.1017/qua.2023.4.
Mann, D.H., Groves, P., Kunz, M.L., Reanier, R.E., Gaglioti, B.V., 2013. Ice-age megafauna in Arctic Alaska: extinction, invasion, survival. Quat. Sci. Rev. 70, 91–108. https://doi.org/10.1016/j.quascirev.2013.03.015.
Männel, T.T., Auerswald, K., Schnyder, H., 2007. Altitudinal gradients of grassland carbon and nitrogen isotope composition are recorded in the hair of grazers. Global Ecol. Biogeogr. 16, 583–592. https://doi.org/10.1111/j.1466-8238.2007.00322.x.
Maschenko, E.N., 2010. Age Profile and Morphology of Mammoth from the Chulym River (Teguldet Locality, Tomsk Region, Russia). Lazarev PA. Proc 4th Int Mammoth Conf, Yakutsk, pp. 41–53.
Metcalfe, J.Z., Longstaffe, F.J., Jass, C.N., Zazula, G.D., Keddie, G., 2016. Taxonomy, location of origin and health status of proboscideans from Western Canada investigated using stable isotope analysis. J. Quat. Sci. 31, 126–142. https://doi.org/10.1002/jqs.2849.
Olivier, R.C.D., 1982. Ecology and of living elephants: bases for assumptions concerning the extinct woolly mammoths. In: Paleoecology of Beringia. Elsevier, pp. 291–305. https://doi.org/10.1016/B978-0-12-355860-2.50029-6.
Orlova, L.A., Kuzmin, Y.V., Dementiev, V.N., 2004. A review of the evidence for extinction chronologies for five species of upper Pleistocene megafauna in Siberia. Radiocarbon 46, 301–314. https://doi.org/10.1017/S0033822200039618.
Rakhmankulova, Z.F., Shuyskaya, E.V., Voronin, P.Yu, Usmanov, I.Yu, 2019. Comparative study on resistance of C3 and C4 xerohalophytes of the genus atriplex to water deficit and salinity. Russ. J. Plant Physiol. 66, 250–258. https://doi.org/10.1134/S1021443719020109.
Reimer, P.J., Austin, W.E.N., Bard, E., Bayliss, A., Blackwell, P.G., Bronk Ramsey, C., Butzin, M., Cheng, H., Edwards, R.L., Friedrich, M., Grootes, P.M., Guilderson, T.P., Hajdas, I., Heaton, T.J., Hogg, A.G., Hughen, K.A., Kromer, B., Manning, S.W., Muscheler, R., Palmer, J.G., Pearson, C., van der Plicht, J., Reimer, R.W., Richards, D.A., Scott, E.M., Southon, J.R., Turney, C.S.M., Wacker, L., Adolphi, F., Büntgen, U., Capano, M., Fahrni, S.M., Fogtmann-Schulz, A., Friedrich, R., Köhler, P., Kudsk, S., Miyake, F., Olsen, J., Reinig, F., Sakamoto, M., Sookdeo, A., Talamo, S., 2020. The IntCal20 Northern hemisphere radiocarbon age calibration curve (0–55 cal kBP). Radiocarbon 62, 725–757. https://doi.org/10.1017/RDC.2020.41.
Sah, S.P., Brumme, R., 2003. Altitudinal gradients of natural abundance of stable isotopes of nitrogen and carbon in the needles and soil of a pine forest in Nepal. J. Sci. 49, 19–26. https://doi.org/10.17221/4673-JFS.
Schenk, H.J., Jackson, R.B., 2002. Rooting depths, lateral root spreads and below-ground/above-ground allometries of plants in water-limited ecosystems. J. Ecol. 90, 480–494. https://doi.org/10.1046/j.1365-2745.2002.00682.x.
Schirrmeister, L., Siegert, C., Kuznetsova, T., Kuzmina, S., Andreev, A., Kienast, F., Meyer, H., Bobrov, A., 2002. Paleoenvironmental and paleoclimatic records from permafrost deposits in the arctic region of Northern Siberia. Quat. Int. 89, 97–118. https://doi.org/10.1016/S1040-6182(01)00083-0.
Schoeninger, M.J., DeNiro, M.J., 1984. Nitrogen and carbon isotopic composition of bone collagen from marine and terrestrial animals. Geochem. Cosmochim. Acta 48, 625–639. https://doi.org/10.1016/0016-7037(84)90091-7.
Schweger, C.E., 1982. Late pleistocene vegetation of Eastern Beringia: pollen analysis of dated Alluvium. In: Paleoecology of Beringia. Elsevier, pp. 95–112. https://doi.org/10.1016/B978-0-12-355860-2.50013-2.
Sealy, J., Johnson, M., Richards, M., Nehlich, O., 2014. Comparison of two methods of extracting bone collagen for stable carbon and nitrogen isotope analysis: comparing whole bone demineralization with gelatinization and ultrafiltration. J. Archaeol. Sci. 47, 64–69. https://doi.org/10.1016/j.jas.2014.04.011.
Sealy, J.C., van der Merwe, N.J., Thorp, J.A.L., Lanham, J.L., 1987. Nitrogen isotopic ecology in southern Africa: implications for environmental and dietary tracing. Geochem. Cosmochim. Acta 51, 2707–2717. https://doi.org/10.1016/0016-7037(87)90151-7.
Seuru, S., Leshchinskiy, S., Auguste, P., Fedyaev, N., 2017. Woolly mammoth and man at krasnoyarskaya kurya site, West Siberian Plain, Russia (excavation results of 2014). Bull. Soc. Geol. Fr. 188, 4. https://doi.org/10.1051/bsgf/2017005.
Sher, A.V., Kuzmina, S.A., Kuznetsova, T.V., Sulerzhitsky, L.D., 2005. New insights into the Weichselian environment and climate of the East Siberian Arctic, derived from fossil insects, plants, and mammals. Quat. Sci. Rev. 24, 533–569. https://doi.org/10.1016/j.quascirev.2004.09.007.
Sponheimer, M., Robinson, T., Ayliffe, L., Roeder, B., Hammer, J., Passey, B., West, A., Cerling, T., Dearing, D., Ehleringer, J., 2003. Nitrogen isotopes in mammalian herbivores: hair δ^{15}N values from a controlled feeding study. Int. J. Osteoarchaeol. 13, 80–87. https://doi.org/10.1002/oa.655.
Stuart, A.J., 2005. The extinction of woolly mammoth (Mammuthus primigenius) and straight-tusked elephant (Palaeoloxodon antiquus) in Europe. Quat. Int. 126–128, 171–177. https://doi.org/10.1016/j.quaint.2004.04.021.
Stuart, A.J., 2015. Late Quaternary megafaunal extinctions on the continents: a short review. Geol. J. 50, 338–363. https://doi.org/10.1002/gj.2633.
Stuiver, M., Braziunas, T.F., 1987. Tree cellulose 13C/12C isotope ratios and climatic change. Nature 328, 58–60. https://doi.org/10.1038/328058a0.
Sukhorukov, A.P., Kushunina, M., Sennikov, A.N., 2022. A new classification of C4-Atriplex species in Russia, with the first alien record of Atriplex flabellum (Chenopodiaceae, Amaranthaceae) from North Siberia. PhytoKeys 202, 59–72. https://doi.org/10.3897/phytokeys.202.87306.
Szpak, P., 2014. Complexities of nitrogen isotope biogeochemistry in plant-soil systems: implications for the study of ancient agricultural and animal management practices. Front. Plant Sci. 5. https://doi.org/10.3389/fpls.2014.00288.
Szpak, P., Gröcke, D.R., Debruyne, R., MacPhee, R.D.E., Guthrie, R.D., Froese, D., Zazula, G.D., Patterson, W.P., Poinar, H.N., 2010. Regional differences in bone collagen δ13C and δ15N of Pleistocene mammoths: implications for paleoecology of the mammoth steppe. Palaeogeogr. Palaeoclimatol. Palaeoecol. 286, 88–96. https://doi.org/10.1016/j.palaeo.2009.12.009.
van der Merwe, N.J., 1982. Carbon isotopes, photosynthesis, and archaeology: different pathways of photosynthesis cause characteristic changes in carbon isotope ratios that make possible the study of prehistoric human diets. Am. Sci. 70, 596–606.
van Geel, B., Aptroot, A., Baittinger, C., Birks, H.H., Bull, I.D., Cross, H.B., Evershed, R.P., Gravendeel, B., Kompanje, E.J.O., Kuperus, P., Mol, D., Nierop, K.G.J., Pals, J.P., Tikhonov, A.N., van Reenen, G., van Tienderen, P.H., 2008. The Ecological implications of a Yakutian mammoth's last meal. Quat. Res. 69, 361–376. https://doi.org/10.1016/j.yqres.2008.02.004.
van Geel, B., Guthrie, R.D., Altmann, J.G., Broekens, P., Bull, I.D., Gill, F.L., Jansen, B., Nieman, A.M., Gravendeel, B., 2011. Mycological evidence of coprophagy from the feces of an Alaskan late glacial mammoth. Quat. Sci. Rev. 30, 2289–2303. https://doi.org/10.1016/j.quascirev.2010.03.008.
van Groenigen, J.-W., van Kessel, C., 2002. Salinity-induced patterns of natural abundance Carbon-13 and Nitrogen-15 in plant and soil. Soil Sci. Soc. Am. J. 66, 489–498. https://doi.org/10.2136/sssaj2002.4890.
van Klinken, G.J., 1999. Bone collagen quality indicators for palaeodietary and radiocarbon measurements. J. Archaeol. Sci. 26, 687–695. https://doi.org/10.1006/jasc.1998.0385.
Van Klinken, G.J., van der Plicht, H., Hedges, R.E.M., 1994. Bond ^{13}C/^{12}C ratios reflect (palaeo-)climatic variations. Geophys. Res. Lett. 21, 445–448. https://doi.org/10.1029/94GL00177.
Vandenberghe, J., French, H.M., Gorbunov, A., Marchenko, S., Velichko, A.A., Jin, H., Cui, Z., Zhang, T., Wan, X., 2014. The Last Permafrost Maximum (LPM) map of the Northern Hemisphere: permafrost extent and mean annual air temperatures, 25–17 ka BP. Boreas 43, 652–666. https://doi.org/10.1111/bor.12070.
Vereshchagin, N.K., Baryshnikov, G.F., 1982. Paleoecology of the mammoth fauna in the eurasian arctic. In: Paleoecology of Beringia. Elsevier, pp. 267–279. https://doi.org/10.1016/B978-0-12-355860-2.50027-2.
Wang, Y., Pedersen, M.W., Alsos, I.G., De Sanctis, B., Racimo, F., Prohaska, A., Coissac, E., Owens, H.L., Merkel, M.K.F., Fernandez-Guerra, A., Rouillard, A., Lammers, Y., Alberti, A., Denoeud, F., Money, D., Ruter, A.H., McColl, H., Larsen, N. K., Cherezova, A.A., Edwards, M.E., Fedorov, G.B., Haile, J., Orlando, L., Vinner, L., Korneliussen, T.S., Beilman, D.W., Bjørk, A.A., Cao, J., Dockter, C., Esdale, J., Gusarova, G., Kjeldsen, K.K., Mangerud, J., Rasic, J.T., Skadhauge, B., Svendsen, J.I., Tikhonov, A., Wincker, P., Xing, Y., Zhang, Y., Froese, D.G., Rahbek, C., Bravo, D.N., Holden, P.B., Edwards, N.R., Durbin, R., Meltzer, D.J., Kjær, K.H., Möller, P., Willerslev, E., 2021. Late Quaternary dynamics of arctic biota from ancient environmental genomics. Nature 600, 86–92. https://doi.org/10.1038/s41586-021-04016-x.
Wojtal, P., 2004. New excavations at Kraków Spadzista street (B).

Wojtal, P., Sobczyk, K., 2005. Man and woolly mammoth at the Kraków Spadzista Street (B) – taphonomy of the site. J. Archaeol. Sci. 32, 193–206. https://doi.org/10.1016/j.jas.2004.08.005.

Wooller, M.J., Bataille, C., Druckenmiller, P., Erickson, G.M., Groves, P., Haubenstock, N., Howe, T., Irrgeher, J., Mann, D., Moon, K., Potter, B.A., Prohaska, T., Rasic, J., Reuther, J., Shapiro, B., Spaleta, K.J., Willis, A.D., 2021. Lifetime mobility of an Arctic woolly mammoth. Science 373, 806–808. https://doi.org/10.1126/science.abg1134.

Zech, M., Bimüller, C., Hemp, A., Samimi, C., Broesike, C., Hörold, C., Zech, W., 2011. Human and climate impact on ^{15} N natural abundance of plants and soils in high-mountain ecosystems: a short review and two examples from the Eastern Pamirs and mt. Kilimanjaro. Isotopes. Environ Health Stud 47, 286–296. https://doi.org/10.1080/10256016.2011.596277.

Zimov, S.A., Zimov, N.S., Tikhonov, A.N., Chapin, F.S., 2012. Mammoth steppe: a high-productivity phenomenon. Quat. Sci. Rev. 57, 26–45. https://doi.org/10.1016/j.quascirev.2012.10.005.

Curriculum vitae

Personal data

Name:	Ivan Krivokorin
Date of birth:	28.04.1997
Place of birth:	Moscow, Russia
Citizenship:	Russian Federation

Contact data

E-mail:	ivansmail97@gmail.com

Education

2021–2025	Tallinn University of Technology, PhD
2019–2020	University of Reading, MA
2015–2019	Moscow State University, BSc
2012–2015	Lyceum 1535, High school

Language competence

English	C2
Russian	native
Estonian	B1
French	A2

Professional employment

2021–2025	Tallinn University of Technology
2017–2019	Moscow State University

Elulookirjeldus

Isikuandmed

Nimi:	Ivan Krivokorin
Sünniaeg:	28.04.1997
Sünnikoht:	Moskva, Venemaa
Kodakondsus:	Venemaa

Kontaktandmed

E-post:	ivansmail97@gmail.com

Hariduskäik

2021–2025	Tallinna Tehnikaülikool, PhD
2019–2020	Reading Ülikool, MA
2015–2019	Moskva Riiklik Ülikool, BSc
2012–2015	Lyceum 1535, Keskharidus

Keelteoskus

Inglise keel	C2
Vene keel	emakeel
Eesti keel	B1
Prantsuse keel	A2

Teenistuskäik

2021–2025	Tallinna Tehnikaülikool
2017–2019	Moskva Riiklik Ülikool